

AD-A051 532

HARRIS CORP MELBOURNE FL ELECTRO-OPTICS DEPT  
MICRO-REDUCTION AND ENLARGEMENT OF GRAPHIC INFORMATION STUDY (M--ETC(U).  
DEC 77 R G ZECH, L M RALSTON, B R REDDERSEN DAA653-75-C-0155  
HESD/EOD-1624-F ETL-0063 NL

UNCLASSIFIED

1 OF 5  
AD  
A051 532





AD A051532

DDC FILE COPY

89136

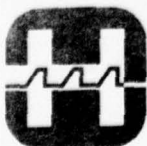
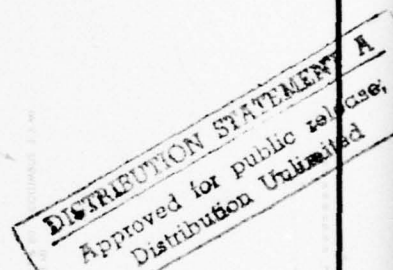
# MICRO-REDUCTION AND ENLARGEMENT OF GRAPHIC INFORMATION STUDY

## MEGIS FINAL TECHNICAL REPORT ETL-0063

PREPARED FOR  
U.S. ARMY ENGINEER TOPOGRAPHIC LABORATORIES  
DEPARTMENT OF THE ARMY  
FORT BELVOIR, VIRGINIA  
CONTRACT NO. DAAG-53-75-C-0155

DECEMBER 1977

PREPARED BY  
ELECTRO-OPTICS DEPARTMENT



**HARRIS**  
COMMUNICATIONS AND  
INFORMATION HANDLING

HARRIS CORPORATION Electronic Systems Division  
P.O. Box 37, Melbourne, Florida 32901 305 / 727-4000

DESTROY THIS REPORT WHEN NO LONGER NEEDED.  
DO NOT RETURN IT TO THE ORIGINATOR.

---

THE FINDINGS IN THIS REPORT ARE NOT TO BE  
CONSTRUED AS AN OFFICIAL DEPARTMENT OF  
THE ARMY POSITION UNLESS SO DESIGNATED BY  
OTHER AUTHORIZED DOCUMENTS.

---

THE CITATION IN THIS REPORT OF TRADE NAMES  
OF COMMERCIALY AVAILABLE PRODUCTS DOES  
NOT CONSTITUTE OFFICIAL ENDORSEMENT OR  
APPROVAL OF THE USE OF SUCH PRODUCTS.

12

**MICRO-REDUCTION AND ENLARGEMENT  
OF GRAPHIC INFORMATION STUDY**

**MEGIS**  
**FINAL TECHNICAL REPORT**  
**ETL-0063**

**PREPARED FOR**  
**U.S. ARMY ENGINEER TOPOGRAPHIC LABORATORIES**  
**DEPARTMENT OF THE ARMY**  
**FORT BELVOIR, VIRGINIA**  
**CONTRACT NO. DAAG-53-75-C-0155**

**DECEMBER 1977**

**PREPARED BY**  
**ELECTRO-OPTICS DEPARTMENT**

UNCLASSIFIED

SECURITY CLASSIFICATION OF THIS PAGE (When Data Entered)

19 REPORT DOCUMENTATION PAGE		READ INSTRUCTIONS BEFORE COMPLETING FORM
18 1. REPORT NUMBER ETL-0063	2. GOVT ACCESSION NO.	3. RECIPIENT'S CATALOG NUMBER
6 4. TITLE (and Subtitle) Microreduction and Enlargement of Graphic Information Study (MEGIS)	9 5. TYPE OF REPORT & PERIOD COVERED Final Technical Report, March 1975 to December 1977	14 6. PERFORMING ORG. REPORT NUMBER HESD/EOD-1624-F
10 7. AUTHOR(s) R. G. Zech, L. M. Ralston, B. R. Reddersen and H. N. Roberts	8. CONTRACT OR GRANT NUMBER(s) DAAG53-75-C-0155	15 10. PROGRAM ELEMENT, PROJECT, TASK AREA & WORK UNIT NUMBERS
9. PERFORMING ORGANIZATION NAME AND ADDRESS Electronic Systems Division Harris Corporation Melbourne, Florida 32901	11 12. REPORT DATE December 1977	12 13. NUMBER OF PAGES 397
11. CONTROLLING OFFICE NAME AND ADDRESS U.S. Army Engineer Topographic Laboratories Fort Belvoir, Virginia 22060	15. SECURITY CLASS. (of this report) UNCLASSIFIED	15a. DECLASSIFICATION/DOWNGRADING SCHEDULE
14. MONITORING AGENCY NAME & ADDRESS (if different from Controlling Office)		
16. DISTRIBUTION STATEMENT (of this Report) Approved for Public Release; Distribution Unlimited		
17. DISTRIBUTION STATEMENT (of the abstract entered in Block 20, if different from Report)		
18. SUPPLEMENTARY NOTES		
19. KEY WORDS (Continue on reverse side if necessary and identify by block number) Microstorage and Retrieval, Holography, Cartography, Recording Media, Laser Recording, Micrographics, Archival Storage		
20. ABSTRACT (Continue on reverse side if necessary and identify by block number) The microreduction and enlargement of high-resolution graphic data such as map separations was investigated. Original graphics were photoreduced to 70 mm film trans- parencies and stored as 20 x 20 mm phase-randomized Fourier-transform holograms. Experimental data show that enlargement to full size produces only minimal distortion. Image brightness and brightness uniformity were adequate for reproduction. However, resolution and line quality did not meet current standards for cartographic production. Holography is judged to be a promising approach to high-density microstorage only if → next page		

DD FORM 1 JAN 73 1473 EDITION OF 1 NOV 65 IS OBSOLETE

UNCLASSIFIED

SECURITY CLASSIFICATION OF THIS PAGE (When Data Entered)

392 092



UNCLASSIFIED

SECURITY CLASSIFICATION OF THIS PAGE(When Data Entered)

20.

several fundamental problems can be solved.

ACCESSION For	
NTIS	White Section <input checked="" type="checkbox"/>
ODC	Buff Section <input type="checkbox"/>
EXAMINED	<input type="checkbox"/>
JUSTIFICATION.....	
BY.....	
DISTRIBUTION/AVAILABILITY CODES	
Dist.	AVAIL. and/or SPECIAL
A	

UNCLASSIFIED

SECURITY CLASSIFICATION OF THIS PAGE(When Data Entered)

## INSTRUCTIONS FOR PREPARATION OF REPORT DOCUMENTATION PAGE

**RESPONSIBILITY.** The controlling DoD office will be responsible for completion of the Report Documentation Page, DD Form 1473, in all technical reports prepared by or for DoD organizations.

**CLASSIFICATION.** Since this Report Documentation Page, DD Form 1473, is used in preparing announcements, bibliographies, and data banks, it should be unclassified if possible. If a classification is required, identify the classified items on the page by the appropriate symbol.

### COMPLETION GUIDE

**General.** Make Blocks 1, 4, 5, 6, 7, 11, 13, 15, and 16 agree with the corresponding information on the report cover. Leave Blocks 2 and 3 blank.

**Block 1.** Report Number. Enter the unique alphanumeric report number shown on the cover.

**Block 2.** Government Accession No. Leave Blank. This space is for use by the Defense Documentation Center.

**Block 3.** Recipient's Catalog Number. Leave blank. This space is for the use of the report recipient to assist in future retrieval of the document.

**Block 4.** Title and Subtitle. Enter the title in all capital letters exactly as it appears on the publication. Titles should be unclassified whenever possible. Write out the English equivalent for Greek letters and mathematical symbols in the title (see "Abstracting Scientific and Technical Reports of Defense-sponsored RDT/E," AD-667 000). If the report has a subtitle, this subtitle should follow the main title, be separated by a comma or semicolon if appropriate, and be initially capitalized. If a publication has a title in a foreign language, translate the title into English and follow the English translation with the title in the original language. Make every effort to simplify the title before publication.

**Block 5.** Type of Report and Period Covered. Indicate here whether report is interim, final, etc., and, if applicable, inclusive dates of period covered, such as the life of a contract covered in a final contractor report.

**Block 6.** Performing Organization Report Number. Only numbers other than the official report number shown in Block 1, such as series numbers for in-house reports or a contractor/grantee number assigned by him, will be placed in this space. If no such numbers are used, leave this space blank.

**Block 7.** Author(s). Include corresponding information from the report cover. Give the name(s) of the author(s) in conventional order (for example, John R. Doe or, if author prefers, J. Robert Doe). In addition, list the affiliation of an author if it differs from that of the performing organization.

**Block 8.** Contract or Grant Number(s). For a contractor or grantee report, enter the complete contract or grant number(s) under which the work reported was accomplished. Leave blank in in-house reports.

**Block 9.** Performing Organization Name and Address. For in-house reports enter the name and address, including office symbol, of the performing activity. For contractor or grantee reports enter the name and address of the contractor or grantee who prepared the report and identify the appropriate corporate division, school, laboratory, etc., of the author. List city, state, and ZIP Code.

**Block 10.** Program Element, Project, Task Area, and Work Unit Numbers. Enter here the number code from the applicable Department of Defense form, such as the DD Form 1498, "Research and Technology Work Unit Summary" or the DD Form 1634, "Research and Development Planning Summary," which identifies the program element, project, task area, and work unit or equivalent under which the work was authorized.

**Block 11.** Controlling Office Name and Address. Enter the full, official name and address, including office symbol, of the controlling office. (Equates to funding/sponsoring agency. For definition see DoD Directive 5200.20, "Distribution Statements on Technical Documents.")

**Block 12.** Report Date. Enter here the day, month, and year or month and year as shown on the cover.

**Block 13.** Number of Pages. Enter the total number of pages.

**Block 14.** Monitoring Agency Name and Address (if different from Controlling Office). For use when the controlling or funding office does not directly administer a project, contract, or grant, but delegates the administrative responsibility to another organization.

**Blocks 15 & 15a.** Security Classification of the Report: Declassification/Downgrading Schedule of the Report. Enter in 15 the highest classification of the report. If appropriate, enter in 15a the declassification/downgrading schedule of the report, using the abbreviations for declassification/downgrading schedules listed in paragraph 4-207 of DoD 5200.1-R.

**Block 16.** Distribution Statement of the Report. Insert here the applicable distribution statement of the report from DoD Directive 5200.20, "Distribution Statements on Technical Documents."

**Block 17.** Distribution Statement (of the abstract entered in Block 20, if different from the distribution statement of the report). Insert here the applicable distribution statement of the abstract from DoD Directive 5200.20, "Distribution Statements on Technical Documents."

**Block 18.** Supplementary Notes. Enter information not included elsewhere but useful, such as: Prepared in cooperation with . . . Translation of (or by) . . . Presented at conference of . . . To be published in . . .

**Block 19.** Key Words. Select terms or short phrases that identify the principal subjects covered in the report, and are sufficiently specific and precise to be used as index entries for cataloging, conforming to standard terminology. The DoD "Thesaurus of Engineering and Scientific Terms" (TEST), AD-672 000, can be helpful.

**Block 20.** Abstract. The abstract should be a brief (not to exceed 200 words) factual summary of the most significant information contained in the report. If possible, the abstract of a classified report should be unclassified and the abstract to an unclassified report should consist of publicly-releasable information. If the report contains a significant bibliography or literature survey, mention it here. For information on preparing abstracts see "Abstracting Scientific and Technical Reports of Defense-Sponsored RDT&E," AD-667 000.



# TABLE OF CONTENTS

<u>Paragraph</u>	<u>Title</u>	<u>Page</u>
	SUMMARY .....	x
	FOREWORD .....	xi
	ACKNOWLEDGEMENTS .....	xii
SECTION I INTRODUCTION		
1.1	SCOPE AND APPROACH .....	1-3
1.2	TECHNOLOGY CONTENT AND MAJOR ACTIVITIES .....	1-6
1.3	REPORT ORGANIZATION .....	1-9
1.4	GENERAL REFERENCES .....	1-9
SECTION II ANALYSIS AND DESIGN		
2.1	COMPARISON OF CONVENTIONAL AND HOLOGRAPHIC MICROSTORAGE AND RETRIEVAL .....	2-4
2.2	FOURIER-TRANSFORM HOLOGRAPHIC RECORDER/REPRODUCER .....	2-10
2.2.1	Recorder Design and Analysis .....	2-17
2.2.1.1	Initial Considerations .....	2-17
2.2.1.2	Hologram Recording Parameters .....	2-24
2.2.1.3	Hologram Exposure Requirement .....	2-31
2.2.1.4	Image Resolution .....	2-33
2.2.2	Reproducer Design and Analysis .....	2-36
2.2.2.1	Diffraction Efficiency .....	2-37
2.2.2.2	Signal-to-Noise Ratio .....	2-40
2.2.2.3	Image Luminance .....	2-45
2.2.2.3.1	Direct Projection Image Luminance .....	2-46
2.2.2.3.2	Holographic Image Luminance .....	2-49
2.2.2.4	Hardcopy Reproduction .....	2-52
2.2.3	Problem Areas .....	2-56
2.3	ALTERNATIVE RECORDER/REPRODUCER CONCEPTS .....	2-58
2.3.1	Fresnel Holography .....	2-58
2.3.2	Direct Laser Projection Recorder/Reproducer .....	2-62
2.3.3	Kohler-TIR Holography .....	2-69
2.3.4	Space-Invariant Holography .....	2-73
2.4	SPECIAL CONSIDERATIONS .....	2-76
2.4.1	Film Chips .....	2-76
2.4.2	Aberrations .....	2-77
2.4.3	Lasers for Cartographic Storage and Displays .....	2-79
2.4.4	Optics .....	2-88
2.5	VISUAL DISPLAYS .....	2-97
2.5.1	Basic Considerations .....	2-97
2.5.2	Screen Types .....	2-103
2.6	REFERENCES AND NOTES .....	2-109

## TABLE OF CONTENTS (Continued)

<u>Paragraph</u>	<u>Title</u>	<u>Page</u>
SECTION III RECORDING MATERIALS		
3.1	BASIC CONCEPTS .....	3-3
3.1.1	Storage Mechanisms .....	3-5
3.1.2	Definitions and Special Terms .....	3-6
3.1.2.1	Performance Parameters .....	3-6
3.1.2.2	Experimental Characterization .....	3-9
3.1.2.3	Physical and Chemical Properties .....	3-13
3.1.2.4	Anomalous Effects .....	3-16
3.2	MICROREDUCTION FILMS .....	3-20
3.3	HOLOGRAPHIC FILMS .....	3-26
3.4	HARDCOPY FILMS .....	3-34
3.5	PRESSPLATE MATERIALS .....	3-38
3.5.1	Current Pressplate Technology .....	3-38
3.5.2	Candidate Direct Pressplate Materials .....	3-39
3.6	SUMMARY AND COMMENTS .....	3-40
3.7	NOTES AND REFERENCES .....	3-50
SECTION IV BREADBOARD EXPERIMENTS		
4.1	FILM CHIP EVALUATION .....	4-2
4.2	HOE FABRICATION .....	4-8
4.3	PHASE RANDOMIZER FABRICATION .....	4-15
4.4	DIRECT PROJECTION STUDY .....	4-17
4.5	WRAY MICRO LENS EVALUATION .....	4-28
4.6	SYSTEM COMPONENTS .....	4-29
4.6.1	Liquid Gates .....	4-29
4.6.2	Film Holders .....	4-32
4.6.3	Special Components .....	4-34
4.7	RECORDER/REPRODUCER PERFORMANCE .....	4-34
4.7.1	Direct Projection (Micrographic) System .....	4-36
4.7.2	Holographic Recorder/Reproducer .....	4-39
4.8	SPECKLE REDUCTION .....	4-65
4.8.1	Phase Randomizers .....	4-65
4.8.2	Multiple Signal Beams .....	4-70
4.8.3	Holographic Recording Techniques .....	4-72
4.8.4	Hologram Readout Techniques .....	4-76
4.8.5	Hardcopy Exposure and Processing .....	4-78
4.8.6	Incoherent Addition of Holograms .....	4-81
4.8.7	Summary and Conclusions .....	4-89
4.9	SPACE-INVARIANT INTERFEROMETER .....	4-89
4.9.1	Experimental System .....	4-90
4.9.2	Experimental Results .....	4-93
4.9.3	Summary and Conclusions .....	4-93
4.10	NOTES AND REFERENCES .....	4-93

## TABLE OF CONTENTS (Continued)

<u>Paragraph</u>	<u>Title</u>	<u>Page</u>
SECTION V HARDCOPY REPRODUCTION		
5.1	A DEFINITION OF DISTORTION .....	5-2
5.2	SOURCES OF DISTORTION .....	5-5
5.2.1	Mechanical Distortions .....	5-5
5.2.2	Holographic Distortions .....	5-14
5.2.3	Other Optical Distortions .....	5-14
5.2.4	Hardcopy Film Distortions .....	5-23
5.3	THE BORROWDALE FILM HOLDER .....	5-23
5.4	MOIRE ALIGNMENT METHOD .....	5-26
5.5	ITERATION .....	5-33
5.6	RESULTS .....	5-40
5.7	EXPERIMENTAL WORK ON HARDCOPY MATERIALS .....	5-44
5.8	REFERENCES .....	5-47
SECTION VI SYSTEMS CONSIDERATIONS		
6.1	INPUT PRODUCTS AND PROCEDURES .....	6-4
6.2	QUALITY ASSESSMENT .....	6-5
6.3	MICROREDUCTION .....	6-6
6.4	CENTRAL CONTROLLER .....	6-7
6.5	STORAGE AND RETRIEVAL .....	6-8
6.6	BLOWBACK .....	6-10
6.7	OVERVIEW .....	6-11
SECTION VII CONCLUSIONS AND RECOMMENDATIONS		
APPENDICES		
A	EQUIPMENT TEST PLAN	
B	SELECTED TECHNICAL REFERENCES	
	Design Relationships for Holographic Memories .....	B-2
	Packing Density in Holographic Systems .....	B-13



# LIST OF ILLUSTRATIONS

<u>Figure</u>	<u>Title</u>	<u>Page</u>
2-1a, b	Conceptual Fourier-Transform Holographic Recorder/Reproducer .....	2-6
2-2	Schematic Diagram of a Fourier-Transform Holographic Recorder/Reproducer .....	2-13
2-3	Alternative Signal Beam Implementation for a Fourier-Transform Holographic Recorder/Reproducer .....	2-16
2-4	Basic Geometry of a Fourier-Transform Holographic Recorder/Reproducer .....	2-18
2-5	Scaled Ray Diagram Showing the Effect of the Hologram Aperture on Field and Resolution for Several Object Points .....	2-35
2-6	Schematic Layout of a Fresnel Hologram Recorder/Reproducer .....	2-60
2-7	Schematic Layout of a Direct Projection Recorder/Reproducer .....	2-65
2-8	Basic Concepts of Kohler-TIR Holography .....	2-70
2-9	Schematic Layout of a Space-Invariant Holographic Recorder/Reproducer .....	2-74
2-10	Film Chip Illumination Methods .....	2-89
2-11	Special Optical Problems: Nonuniform Fourier-Transform and $\cos^4$ Falloff .....	2-91
2-12	Optical Transfer Function Curve for the Wray Micro Lens ...	2-94
2-13	Screen Gain as a Function of Viewing Angle for Several Commercial Display Screens .....	2-107
4-1	Enlargement With Incoherent Light of a Silk Screen Test Target at 20X Magnification Using Kohler Projection System .....	4-4
4-2	Enlargement With Incoherent Light of a 20X Reduced Film Chip Using a Kohler Projection System .....	4-5
4-3	Resolution of Film Chip Target Arrays After Imaging to Full-Scale Using a Kohler Projection System .....	4-7
4-4	Experimental Geometry Used to Record Holographic Optical Elements .....	4-13
4-5	Image Resolution as a Function of Aperture Diameter With the Type of Object Illumination as a Parameter .....	4-19
4-6	Direct Projection Image of a Resolution Target, Illuminated With Specular Coherent Light, Showing Noise Effects .....	4-22
4-7	Direct Projection Image of a UTM Grid Film Chip, Illuminated With Specular Coherent Light, Which Was Reproduced With Optimum Hardcopy Exposure .....	4-23
4-8	Direct Projection Image of a Vegetation Film Chip, Illuminated With Specular Coherent Light, Which Was Reproduced With Optimum Hardcopy Exposure .....	4-24
4-9	Direct Projection Image of a Resolution Target Illuminated With Diffuse Multiwavelength Coherent Light .....	4-25

# LIST OF ILLUSTRATIONS (Continued)

<u>Figure</u>	<u>Title</u>	<u>Page</u>
4-10	Schematic of the Geometrical Optics Equivalent of the Wray Micro Lens .....	4-30
4-11	Wray Micro Lens Layout Supplied by Rank Optics .....	4-31
4-12	Wray Micro Lens Mount and Transport System .....	4-35
4-13	Hardcopy Image of a Contour Map Separation Film Chip, Illuminated With Incoherent Multiwavelength Laser Light in the Kohler Projection Mode .....	4-38
4-14	Holographic Recorder System Using a Holographic Optical Element as the Fourier-Transform Lens .....	4-41
4-15	Diffraction Efficiency and Signal-to-Noise Ratio as a Function of Exposure with K-Ratio as a Parameter .....	4-42
4-16	Diffraction Efficiency and Signal-to-Noise Ratio as a Function of Exposure for $K = 10$ .....	4-43
4-17	Comparison of Throughput Image and Holographic Reconstruction for a Culture Sheet Film Chip .....	4-45
4-18	Comparison of Throughput Image and Holographic Reconstruction of a Contour Sheet Film Chip .....	4-46
4-19	Two Wavelength Kohler Holographic Recorder/Reproducers ....	4-48
4-20	DE and SNR as Functions of Exposure for Two Wavelength Amplitude Holograms Recorded With the Holographic Kohler Breadboard .....	4-50
4-21	DE and SNR as Functions of Exposure for Two Wavelength Bleached Holograms Recorded With the Holographic Kohler Breadboard .....	4-51
4-22	Single-Wavelength Reconstruction of a Two-Wavelength Amplitude Hologram .....	4-54
4-23	Direct Projection of a Resolution Target Illuminated With Diffuse Coherent Light in the Holographic Kohler Mode .....	4-55
4-24	Single-Wavelength Holographic Reconstruction of a Resolution Target Using the Holographic Kohler Breadboard .....	4-56
4-25	Direct Projection of a Resolution Target, Illuminated With Incoherent Laser Light, Using the Holographic Kohler Breadboard .....	4-57
4-26	Single-Wavelength Reconstruction of a Two-Wavelength Hologram Recorded in the Holographic Kohler Breadboard ..	4-58
4-27	Two-Wavelength Reconstruction of a Two-Wavelength Hologram Recorded in the Holographic Kohler Breadboard .....	4-59
4-28	Direct Projection, With Single-Wavelength Diffuse Coherent Light, Using the Holographic Kohler Breadboard .....	4-60
4-29	Direct Projection, With Two-Wavelength Diffuse Coherent Light, Using the Holographic Kohler Breadboard .....	4-61
4-30	Direct Projection, With Specular Coherent Light, Using the Holographic Kohler Breadboard .....	4-62

# LIST OF ILLUSTRATIONS (Continued)

<u>Figure</u>	<u>Title</u>	<u>Page</u>
4-31	Direct Projection, With Incoherent Light, Using the Holographic Kohler Breadboard .....	4-63
4-32	The Effect of Diffuser Position on Speckle .....	4-71
4-33	The Effect of Self-Imaging Gratings on Speckle .....	4-73
4-34	The Effect of a Combination of Diffuser and Grating on Speckle .....	4-74
4-35	The Effect of Dithering the Reconstruction Beam on Speckle .....	4-79
4-36	The Effect of Hardcopy Exposure on Speckle .....	4-80
4-37	The Effect of Reversal Processing on Speckle .....	4-82
4-38	The Effect of Simulated Incoherent Addition on Speckle ....	4-84
4-39	The Effect of Simulating 100 Incoherent Additions on Speckle .....	4-85
4-40	Holographic Projection of a Contour Separation Film Chip Illuminated With Two Wavelength Diffuse Coherent Light ..	4-86
4-41	Holographic Projection of a Culture Separation Film Chip Illuminated With Two Wavelength Diffuse Coherent Light ..	4-87
4-42	Direct Projection of a Culture Separation Film Chip Illuminated With Two Wavelength Diffuse Coherent Light ..	4-88
4-43	Experiment Breadboard Version of a Space-Invariant Interferometer .....	4-91
5-1	Pincushion and Barrel Distortion .....	5-4
5-2	The Effect of Hologram or Film Chip Rotations .....	5-6
5-3	The Effect of Hologram or Film Chip Translations Normal to the Optical Axis .....	5-7
5-4	The Effect of Hologram or Film Chip Translations Along the Optical Axis .....	5-9
5-5	Focus and Magnification Errors as a Function of Hologram or Film Chip Axial Misalignments .....	5-10
5-6	Experimental Verification of Curve of Magnification Error .....	5-12
5-7	The Effect of Hologram or Film Chip Tilts .....	5-13
5-8	Hologram Emulsion Shrinkage .....	5-15
5-9	Longitudinal Spherical Aberration of Glass Plates as Functions of the Illuminating Cone Half-Angle and Plate Thickness .....	5-17
5-10	Longitudinal Spherical Aberrations of Polyester Film Base as Functions of the Illuminating Cone Half-Angle and Film Base Thickness .....	5-18
5-11	Astigmatism in Optical Systems .....	5-20
5-12	Astigmatism of 0.25 Inch Glass Plates as a Function of Plate Tilt Angle .....	5-21
5-13	The 4 x 5 Foot Overhead Hardcopy Easel .....	5-25
5-14	The Moiré Alignment Techniques .....	5-27



# LIST OF ILLUSTRATIONS (Continued)

<u>Figure</u>	<u>Title</u>	<u>Page</u>
5-15	The Effect of Translation and Scaling on Moiré Target Fringes .....	5-29
5-16	The Moiré Target .....	5-31
5-17	The Grid Measurement Layout .....	5-34
5-18	Distortion Analysis Program A .....	5-35
5-19	A Typical Printout From Distortion Analysis Program A ....	5-37
5-20	Distortion Analysis Program B .....	5-38
5-21	A Typical Printout From Distortion Analysis Program B ....	5-39
5-22	Hardcopy Reproduction Flow Chart .....	5-41
5-23	The Number of Grid Coordinate Measurements Within +0.002 Inch of the Mean Distance Error as a Function of the Calculated Standard Deviation From Mean .....	5-42
6-1	Storage and Retrieval Carousel Unit .....	6-9
A-1	Resolution Target Numbering Diagram .....	A-32

# LIST OF TABLES

<u>Table</u>	<u>Title</u>	<u>Page</u>
1-1	Best Performance of a Holographic Recorder/Reproducer (22 x 30 Inch Repromats) .....	1-5
1-2	Best Performance of a Direct Laser Recorder/Reproducer (22 x 30 Inch Repromats) .....	1-7
2-1	Motivation for Selecting Fourier-Transform Holography as the Baseline MEGIS Approach .....	2-11
2-2	Holographic Recorder Design Parameters: Constant 16X Reduction ( $d_1 = 4250$ mm and $d_2 = 266$ mm) .....	2-21
2-3	Holographic Recorder Design Parameters: Variable Reduction Ratio (Constant 70 mm x 100 mm Film Chip Format) .....	2-21
2-4	Holographic Recorder Design Parameters: (Constant 70 mm x 100 mm Film Chip Format with $d_2 = 266$ mm) .....	2-21
2-5	Summary of Design Parameter For a Holographic Recorder ...	2-23
2-6	Photopic Eye Response for Several Commercial Lasers .....	2-47
2-7	Fresnel Holography Recorder/Reproducer Specifications ....	2-63
2-8	Best Performance of a Direct Laser Recorder/ Reproducer (22 x 30 Inch Repromats) .....	2-67
2-9	Projected Direct Laser Recorder/Reproducer Performance ...	2-69
2-10	Typical Laser Parameters .....	2-81
2-11	Representative Argon-Ion Lasers .....	2-83
2-12	Representative Krypton-Ion Lasers .....	2-84
2-13	Helium-Cadmium Lasers .....	2-86
2-14	Typical Dye Laser Parameters .....	2-87
2-15	10X and 20X Low-Distortion Microreduction Lenses .....	2-96
2-16	Visual Display Requirements .....	2-98
2-17	Front-Projection Display Screens .....	2-104
2-18	Rear-Projection Display Screens .....	2-105
3-1	Specifications for Microreduction Films .....	3-22
3-2	Microreduction Films .....	3-24
3-3	Specifications for Holographic Films .....	3-30
3-4	Photographic Films for Holographic Recording .....	3-32
3-5	Comparison of SO-343 Photographic Film With Nonconventional Recording Materials .....	3-33
3-6	Specifications for Hardcopy Films .....	3-35
3-7	Hardcopy Films .....	3-37
3-8	Major Pressplate Considerations .....	3-41
3-9	Specifications for Direct Offset Pressplate Materials ....	3-42
3-10	Pressplate Recording Materials .....	3-44
3-11	Features of Preferred Pressplate Media .....	3-45
3-12	Photographic Considerations .....	3-46
3-13	Data Storage Considerations .....	3-47
3-14	Systems Considerations .....	3-48

# LIST OF TABLES (Continued)

<u>Table</u>	<u>Title</u>	<u>Page</u>
4-1	Candidate HOE Recording Media .....	4-10
4-2	Advantages and Disadvantages of HOE Recording Materials ..	4-11
4-3	Advantages and Disadvantages of Candidate Bleaches .....	4-11
4-4	Resolution Transfer Obtained for Different Film Support Techniques .....	4-21
4-5	Resolution and Image Quality Performance for Holographic and Direct Kohler Projection .....	4-27
4-6	Contrast Performance of a Direct Laser Projection System .....	4-37
4-7	Holographic Storage and Retrieval at 38X Reduction for 22 x 30 Inch Repromats .....	4-44
4-8	Performance of a Holographic Kohler Recorder/Reproducer ...	4-52
4-9	Hardcopy Reproduction Characteristics for Direct and Holographic Laser Recorder/Reproducers .....	4-66
4-10	Performance of Photographic Phase Randomizers .....	4-67
4-11	Phase Randomizer Characteristics .....	4-69
5-1	Summary of Distortion Measurements .....	5-43
A-1	Holographic Grid Blowback Coordinate Measurements .....	A-22
A-2	Resolution Target Measurements .....	A-25
A-3	Additional Resolution Target Measurements .....	A-27
A-4	Luminance Measurements .....	A-29
A-5	Relative Intensities .....	A-31



## SUMMARY

This report summarizes the results of an analytical and experimental Microreduction and Enlargement of Graphic Information Study (MEGIS) using both direct imaging and holographic techniques. Several breadboard recorder/reproducers were fabricated and used for the microreduction and enlargement of topographic map separations (repromats). The related problems of hardcopy reproduction and recording materials were studied in detail. The overall objective of the study was to demonstrate the feasibility of projecting full-scale map separations for both visual display and hardcopy reproduction from a 20 mm x 20 mm microstorage format that had the following characteristics: resolution sufficient to reproduce well-defined 3-mil line widths, full-scale distortion of less than  $\pm 2$  mils rms, a display luminance level of 35 fL, and luminance variations of less than 25 percent over the full-scale display.

Based upon the analytical and experimental results of this study we conclude that:

- The suitability of the baseline Fourier-transform holographic approach was not demonstrated. Other forms of holography are promising, but must be evaluated more fully experimentally.
- A direct laser projection recorder/reproducer using a 70 mm storage format was experimentally shown to satisfy all ETL requirements (except for storage format size) for storing, retrieving, and reproducing graphic information.
- The  $\pm 2$ -mil rms distortion goal appears achievable. The distortion caused by optical microreduction and enlargement is negligible when compared to the distortion introduced by dimensional changes of the recording materials polyester film base.
- All recording materials required for producing film chips, holograms, repromats, and pressplates are or will be available in the near future. Pressplate materials for direct projection imaging are an area of possible concern; however, the evolution of high quality projection speed electrophotographic pressplates will minimize this problem. An area of concern for holographic recording is the phase noise of commercial polyester film base materials; this may be a fundamental problem.

## FOREWORD

This report summarizes the results of analysis and experimental work designed to explore the general feasibility of optical storage, primarily holographic, of graphic information. The primary emphasis of the effort was an investigation of holographic techniques for the microreduction and enlargement of topographic map separations (repromats). The study was motivated in part by the growing volume of repromats (over 3 million) and by the costs of reproduction and storage within map and chart production centers.

This report was prepared by the Electro-Optics Department of the Electronic Systems Division of Harris Corporation in Melbourne, Florida. It documents technical work completed between 25 March 1975 and 9 May 1976 for Contract No. DAAG53-75-C-0155, United States Army Engineering Topographic Laboratories. R. K. Brooke, Jr., A. C. Gunther, W. R. Graver, and J. Odell served, successively, as project engineer and COTR.

The principal investigator and program manager was Dr. R. G. Zech. Principal task leaders were L. M. Ralston and B. R. Reddersen. Important experimental contributions were made by J. E. Holmes and M. W. Shareck. Contributors to this report are D. C. Bailey, L. M. Ralston, B. R. Reddersen, Dr. H. N. Roberts, M. W. Shareck, and Dr. R. G. Zech. Dr. Zech is the technical editor, and is responsible for the content and format of the report.

Technical direction and R&D personnel were provided by the Optical Processing and Storage Section, headed by Dr. H. N. Roberts. The Electro-Optics Department is under the general direction of Dr. A. VanderLugt.

The completion date of this report is September 1976. The publication date is December 1977.

## ACKNOWLEDGEMENTS

We are pleased to acknowledge the cooperation, advice and insight provided by the following individuals:

- Col. M. K. Kurtz, Ph.D., Director (retired)

Dr. Robert Leighty

Mr. John Odell

Mr. Henry Weiner

United States Army Engineering Topographic Laboratories

Fort Belvoir, VA

The technical discussions and advice of W. R. Graver of the Research Institute of USA ETL merit special recognition and thanks.

- Mr. Jon Maxwell

Rank Optics

Leeds, England

- Mr. Stan Pentacost

R. W. Borrowdale Company

Chicago, IL



SECTION I  
INTRODUCTION

## SECTION I

### INTRODUCTION

The analytical and experimental work summarized in this final technical report was performed in support of the following contract:

#### MICROREDUCTION AND ENLARGEMENT OF GRAPHIC INFORMATION STUDY (MEGIS)

Contract No. DAAG53-75-C-0155  
United States Army Engineering Topographic Laboratories

#### PURPOSE

- To investigate the storage, at high packing densities, and the retrieval, with high fidelity, of color separations (repromats) used for the production of maps and charts

#### OBJECTIVES

- To demonstrate the feasibility and value of holographic and alternative optical storage and retrieval techniques for the display and hardcopy reproduction of graphic information
- To generate baseline specifications and design criteria for an engineering prototype optical storage and retrieval system

#### TECHNICAL APPROACH

- Up to 24 phase-randomized, Fourier-transform holograms separately recorded on 105 mm x 148 mm film chips (microfiche format) with direct storage and enlargement from 70 mm transparencies the principal alternative approach

#### SCOPE OF WORK GOALS

- Holograms smaller than 20 mm x 20 mm in size; up to 24 holograms per unit record

- Hologram readout with 10 percent efficiency and 15 dB contrast ratio
- Full scale hardcopy with a metric distortion of less than  $\pm 2$ -mils rms
- Resolution sufficient to reproduce well-defined 3-mil lines (125 cycles/mm minimum) in full-scale hardcopy
- Display luminance of 35 fL with less than 10 percent center-to-edge luminance variation

#### 1.1 SCOPE AND APPROACH

The Microreduction and Enlargement of Graphic Information Study (MEGIS Program) applied new technology to the solution of problems related to the storage, retrieval, projection, and hardcopy reproduction of cartographic data. Originally, the emphasis of the effort was directed toward high quality visual displays, especially for tactical applications. A careful analysis of near-term storage and retrieval requirements of DMA cartographic production centers refocused the direction of the program toward hardcopy reproduction and associated problem areas. The key objective of the program was to provide new techniques for storing large film map separations, or repromats, and other graphics at high reductions and for later projecting the data at full scale, with negligible distortion, for hardcopy reproduction.

The baseline approach of the MEGIS Program was holographic storage and retrieval. Original graphics (or repromats) were reduced 10 to 20 times to generate 70 mm transparencies (film chips) using a high precision Wray microreduction lens. The transparencies provided the input for a Fourier-transform hologram recording breadboard. Each transparency was stored in the form of a phase randomized hologram, which was generally 20 mm on a side. Using a step-and-record method, a matrix of holograms was generated on a unit

record of film that was similar to a conventional 105 mm x 148 mm microfiche. Ideally, the film unit record contains all the graphic information needed to reproduce a complete map, i.e., contains a full set of repromats, plus several test patterns (resolution target arrays and moire' figures). Data recovery was achieved by readout of the holograms. Each hologram produced a virtual image of the graphic data it represented; this virtual image was enlarged or projected at full scale. Key advantages of this approach are compact storage (up to 80X linear reduction), very high image luminance, excellent center-to-edge luminance uniformity, a high degree of scratch and dust immunity (redundant recording), and negligible metric distortion. Major problem areas are image resolution and laser speckle noise. The best measured performance parameters of a holographic recorder/reproducer are summarized in Table 1-1.

An alternative approach of the MEGIS Program was direct storage and retrieval by microimaging. Original graphics, or repromats, were again reduced 10 to 20 times to form 70 mm film chips. (A second microreduction step to a 35 mm format appears feasible, but was not attempted as part of this program.) These steps constituted the storage operation. The graphic information was retrieved by projecting the film chip with the same lens used for microreduction to generate either a full scale display or hardcopy. An argon laser operating  $TEM_{00}$  in an all-line, all-temporal mode was the projection light source. The film chip was illuminated with laser light that was dispersed and uniformized by the combination of rotating and stationary diffusers; the latter was imaged so that the Kohler projection condition was satisfied. The combination of all these factors provided visual displays and hardcopy characterized by relatively high image luminance, excellent



Table 1-1. Best Performance of a Holographic Recorder/Reproducer\*  
(22 x 30 Inch Repromats)

Parameter	Goal	Actual	Comments
Size	20 mm x 20 mm	20 mm x 20 mm	Larger size would improve resolution
Efficiency	10%	2-12%	Varies with information content of repromat
Contrast	15 dB	10-15 dB	Sufficient for hardcopy reproduction
Resolution	125 cycles/mm	64 cycles/mm	Fundamental problem area; caused by film base phase errors
Distortion	<2-mil rms	<1.5-mil rms	Typical; relative to film base dimensional changes
Uniformity	>10%	>10%	Improvement possible
Luminance	35 fL	20-180 fL	For 1 watt of input laser power; varies with information content of repromat
Image Quality	No image defects	Not acceptable	Speckle noise decreases resolution and causes mottled line structure. Suitable for visual displays, but not for hardcopy

\*Phase-randomized Fourier-transform holograms recorded on Kodak SO-343 film and bleached with bromine vapor.

center-to-edge luminance uniformity and cosmetic quality, high contrast and resolution, and negligible metric distortion for both binary and continuous tone graphic inputs. Major problem areas are low image luminance level (not important for hardcopy reproduction) and nonredundant recording. The best performance parameters of a direct recorder/reproducer are summarized in Table 1-2.

#### 1.2 TECHNOLOGY CONTENT AND MAJOR ACTIVITIES

The activities in support of the goals of the MEGIS Program were wide ranging and required in some cases the development of at least baseline expertise in several new, but relevant, disciplines. Among the most important technologies involved were holography, graphic arts, conventional micrographic storage and retrieval, visual displays, lithographic and pressplate recording materials, cartography, printing, projection optical systems design, and precision alignment, measurement, and translation techniques to aid distortion analysis and compensation. The interlacing of these technologies has proved beneficial toward a more complete understanding of the implementation requirements of a cartographic storage and retrieval system. Specific activities included:

1. Evaluation of Government-supplied transparencies of graphic materials in terms of resolution, density uniformity, and cosmetic quality
2. Evaluation of the performance of the Government-supplied Wray microreduction lens and the generation of an equivalent optical diagram showing principal planes, focal planes, nodal points, and the location of the internal limiting aperture
3. Baseline analysis and experimental study of holographic parameters affecting recorder/reproducer performance



Table 1-2. Best Performance of a Direct Laser Recorder/Reproducer  
(22 x 30 Inch Repromats)

Parameter	Goal	Actual	Comments
Size	20 mm x 20 mm	66 mm x 82.5 mm	Conventional microreduction to a 35 mm format is feasible
Efficiency	10%	< 1%	Improvement possible
Contrast	15 dB	20 db	Provides excellent hard-copy and displays
Resolution	125 cycles/mm	> 228 cycles/mm	Limited only by resolution of transparency
Distortion	< 2-mil rms	< 1-mil rms	Typical; relative to film base dimensional changes
Uniformity	> 10%	~ 5%	
Luminance	35 fL	~ 2 fL	For 1 watt of input laser power; more than 20 fL feasible; not dependent on information content
Image Quality	No image defects	No image defects	Suitable for both displays and hardcopy reproduction

4. Design and fabrication of critical breadboard components for holding, transporting, and positioning film chips, holograms, and the microreduction lens
5. Design, fabrication, and testing of holographic optical elements for use as low f/number Fourier-transform lens
6. Analysis and experimental verification of the effect of liquid gates on breadboard storage and retrieval performance
7. Fabrication and testing of several classes of optical phase randomizers
8. Design and fabrication of several recorder/reproducers suitable for the microreduction and enlargement of graphic materials in the 22 x 30 inch to 48 x 60 inch size range
9. Investigation of the feasibility of reconstruction beam jittering as a method of eliminating laser speckle
10. Investigation of factors affecting system resolution
11. Analysis and development of techniques to minimize metric distortion
12. Development of a method using moiré patterns for sizing film chip enlargements to aid distortion minimization
13. Design and testing of a precision electrostatic film holder suitable for microreduction (as a copy easel) and enlargement (as a film holder) of standard repromats up to 48 x 60 inches in size
14. Study of the problems related to the use of lithographic materials for hardcopy reproduction (repromat generation)

15. Evaluation of the potential of laser pressplates and electrophotographic materials for hardcopy reproduction and quick reaction maps and charts

### 1.3 REPORT ORGANIZATION

The final technical report is organized to reflect the major research and development activities of the MEGIS Program. Section II is a summary of analytical considerations relevant to holography and conventional microstorage and retrieval. Section III is dedicated to a thorough exposition of candidate recording materials and recording materials considerations, as they relate to film chips, holograms, repromats, and pressplates. Experimental data are discussed and summarized in Section IV. In Section V hardcopy reproduction is analyzed with special emphasis on metric distortion. Section VI is a discussion of some baseline systems considerations, and Section VII outlines our conclusions and recommendations. Finally, the MEGIS Equipment Test Plan (ETP) is documented in Appendix A and selected reprints are collected in Appendix B in technical support of Section II.

### 1.4 GENERAL REFERENCES

There are a number of excellent technical reports discussing holography and microstorage and retrieval as it relates to graphic information. The most relevant of these are the following:

1. "Laser-Hologram Multicolor Moving Map Display System," G. T. Burton, B. R. Clay, Croce, and D. A. Gore, RCA Advanced Technology Laboratories (Burlington, MA), Final Technical Report, Contract No. N62269-70-C-0080, Naval Air Development Center, November 1970.
2. "Study of Potential Applications of Holographic Techniques to Mapping," M. K. Kurtz, Jr., N. Balasubramanian, E. M. Mikhail,



W. H. Stevenson, Purdue Research Foundation, Purdue University (Lafayette, Indiana), Final Technical Report, Contract No. DAAK-02-69-C-0563, USA Engineering Topographic Laboratories, October 1971.

3. "Micromap Camera for Display Systems," E. K. Woods, USA Engineering Topographic Laboratories (Fort Belvoir, VA), Final Technical Report ETL-ETR-71-5, Task 4A663712D85508, October 1971.
4. "Prototype Lithographic Enlarging Projection Platemaker," H. Wiener, USA Engineering Topographic Laboratories (Fort Belvoir, VA), Final Technical Report ETL-ETR-4, Task 4A663712D85508, August 1972.
5. "Study of the Characteristics of the Holographic Stereomodel for Application in Mensuration and Mapping," T. F. Kellie and W. H. Stevenson, Purdue Research Foundation, Purdue University (Lafayette, Indiana), Final Technical Report, Contract No. DAAK-02-72-C-0063, USA Engineering Topographic Laboratories, October 1973.

Much of the background required for a complete understanding of the data presented in this report will be found in these documents.

SECTION II  
ANALYSIS AND DESIGN

## SECTION II

### ANALYSIS AND DESIGN

The storage and retrieval of maps, charts, documents, graphical data, engineering drawings, and so forth have become increasingly difficult and costly because large amounts of information are generated by modern technology. In many applications, microfilm is a cost-effective solution to this problem since it provides a relatively inexpensive means of reducing storage requirements and for facilitating retrieval. However, as the requirements for storage capacity increase and the need for storage at higher densities become important, the limitations of conventional micrographic storage and retrieval become evident. These include requirements for well-corrected microreduction lenses, for great precision in the alignment of readout optics, for storage materials with virtually no defects, and for careful handling of the stored data since dust and scratches can easily obscure or destroy portions of the recorded information. Furthermore, duplication of very high density microfilm is complex and costly. These limitations have generally hindered the application of conventional micrographic techniques in high density storage and retrieval systems.

Holographic storage and retrieval techniques, on the other hand, make it possible in principle, to store graphics at high densities and to index, retrieve, and view them with fewer of the problems stated above. High-density holographic document storage and retrieval systems have been developed that use recording media such as high-resolution photographic emulsions and photoresists.<sup>1</sup> When using holographic techniques, it is found that storage capacity and image quality in certain cases surpass that which can



be achieved with highly sophisticated microfilm units. The use of volume recording materials,<sup>2</sup> which offer the possibility of further increasing the storage capacity of a holographic system, has also been investigated.

Although the use of holographic methods for microstorage often leads to a more complex and costly system, they permit much larger quantities of data to be stored more densely and securely and to be retrieved more conveniently than is possible with conventional microreduction approaches.

Harris Electro-Optics has used the principles of holography in several related types of data storage and retrieval systems. The first system is a block-oriented, random-access read/write memory;<sup>3</sup> the second is a mass memory having archival properties (read-only);<sup>4</sup> the third is a very high speed holographic recorder for storing and retrieving wide bandwidth data.<sup>5</sup> In each of these systems the stored data originates as an electrical bit stream that is stored holographically and retrieved by reading out the stored bit pattern onto a photodetector array, which then regenerates the original bit stream.

Some of the advantages of holography that make these systems attractive, e.g., high packing densities, natural encoding, insensitivity to readout parameter variations and so forth, can also be cited for the storage and retrieval of graphic information. The basic techniques are similar to those used in the memories cited above; the major difference is that the data is a two-dimensional topographic map separation or other graphic that is stored holographically and played back in an image format. Thus, the microreduction and enlargement (or microstorage and retrieval) of cartographic information clearly involves many of the considerations relevant to read-only optical memories.

## 2.1 COMPARISON OF CONVENTIONAL AND HOLOGRAPHIC MICROSTORAGE AND RETRIEVAL

Although the microstorage and retrieval techniques described here can be applied to documents, engineering drawings and specifications, and other types of graphic information, the primary application interest is in charts and maps. We refer to this class of data as "graphics." It is assumed that the graphics originate as images on either film transparencies (e.g., a map separation) or paper with typical dimensions of 22 x 30 inches, 32 x 48 inches, and 48 x 60 inches. The smallest spatial detail (resolution element) for all graphic formats is assumed to be 3 mils (about  $76\text{ }\mu\text{m}$ ).

Conventional micrographic techniques can be used to reduce the existing and anticipated volume of data. But to achieve the desired reduction to a 20 mm x 20 mm area, a reduction ratio of 76X is required for the largest size graphic. As the resolution of the source document is assumed to be about  $76\text{ }\mu\text{m}$ , the resolution to be maintained in the microreduced image is about  $1\text{ }\mu\text{m}$  (equivalent to 1000 cycles/mm ). By way of comparison, at the highest reduction ratios, commercial microfilm equipment does not generally record spatial detail of less than  $2.5\text{ }\mu\text{m}$ . Hence, conventional micrographic techniques by themselves generally cannot achieve the desired reduction ratios.

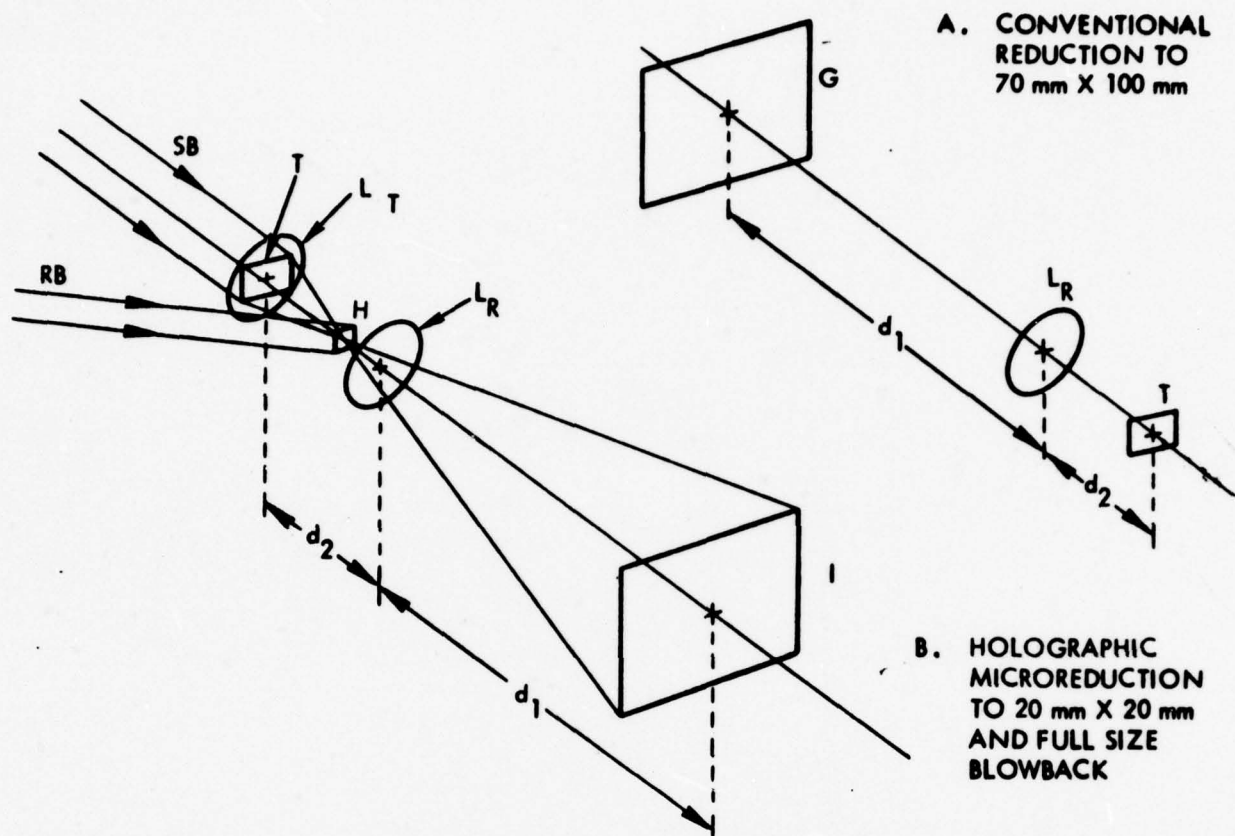
A second disadvantage of conventional micrographics is that the depth of focus at extreme reduction ratios is extremely difficult to maintain both in the recording and retrieval steps. Even in a controlled environment, precise control of the position of both the graphic and the film relative to the lens is difficult to achieve. Vibrations and relative humidity and temperature variations may introduce additional problems in the retrieval process, making depth of focus even more difficult to maintain.

Holographic techniques, in principle, offer an attractive and practical solution to these problems. Suppose that we first reduce a 22 x 30 inch graphic (the most common map separation size) approximately 10X to form a 70 mm x 100 mm film chip, using conventional micrographic techniques as shown in Figure 2-1a. Other reduction ratios are possible for this microreduction step; the ratio used does not significantly affect the following discussion (i.e., packing density, signal-to-noise ratio, diffraction efficiency, and so forth, are independent of the initial photoreduction ratio). The 70 mm negative transparency will contain detail down to about  $7.6\ \mu\text{m}$  if the original graphical data has  $76\ \mu\text{m}$  resolution.

The negative transparency is then placed in a holographic recording system, as shown in Figure 2-1b, and illuminated with a beam of coherent light. Light transmitted and diffracted by the transparency is collected by an imaging lens which projects a full scale image onto a viewing screen. If the imaging lens is the same one used in the initial microreduction step (symmetry) and if the overall magnification is unity, the resultant image is free of distortion. This follows from basic optical design theory from which it can be shown that any telecentric system is free from distortion.<sup>6</sup>

Suppose that we now place a photographic film at the back focal plane of the lens  $L_T$  as shown in Figure 2-1b and record the irradiance distribution at that plane, having added an off-axis reference beam. The reference beam interferes with the signal beam so that both the amplitude and phase of the signal beam are recorded as a nonnegative function on photographic film. After a set of exposures is made, for example, on a typical 105 mm x 148 mm fiche (one hologram per graphic), the film can be developed in the usual way and placed in a storage and retrieval unit.





- G : FULL SIZE INPUT GRAPHIC
- I : FULL SIZE OUTPUT IMAGE
- $L_R$  : REDUCTION/REPRODUCTION LENS
- $L_T$  : FOURIER TRANSFORMING LENS
- T : 70 mm X 100 mm TRANSPARENCY
- H : HOLOGRAM
- SB : COHERENT SIGNAL BEAM
- RB : REFERENCE/READOUT BEAM
- $d_1$  : DISTANCE TO G AND GI FROM  $L_R$
- $d_2$  : DISTANCE TO T AND VIRTUAL IMAGE OF T DURING READOUT FROM  $L_R$

89465-1

Figure 2-1a and b. Conceptual Fourier-Transform Holographic Recorder/Reproducer

Figure 2-1b also shows the basic retrieval process. This system is particularly simple because only the single lens  $L_R$  is required to readout the image of the graphic on the viewing screen. Any hologram could be selected from the 105 mm x 148 mm fiche by means of an x-y mechanism and illuminated by the readout beam (a replica of the reference beam). The original signal wavefront is thereby recreated, and it propagates as though it had never been stored in the film in the form of a hologram. This wavefront includes the distortion compensation term that ideally ensures that the reconstructed image is free from distortion.

The type of holographic storage just described is called Fourier-transform holography, and is the baseline approach used for the MEGIS Program. We selected Fourier-transform holograms for map separation (repmat) storage because this type of hologram has a natural distributive coding, provides a maximum packing density format (see Appendix B), and is least sensitive to variations of readout parameters. Depending upon the graphic to be stored, the hologram is sometimes recorded in a plane in the neighborhood of the Fourier transform plane. This type of hologram is called a near - Fourier transform hologram. It has most of the advantages of an exact Fourier transform hologram, but has the additional advantage of partially smoothing the spatial frequency spectrum of the graphic information, which therefore reduces the dynamic range requirement on the recording material. To eliminate the dynamic range problems and to minimize coherent noise, the signal can be phase randomized; this type of hologram recording is called phase-randomized Fourier-transform. Unfortunately, if a diffuse phase randomizer must be used, speckle noise is generated.<sup>7</sup> The trade-offs are generally not favorable.

Other forms of holography are possible. For example, Fresnel holograms<sup>8</sup> were considered, but excluded initially because this type of holography did not provide maximum packing density or adequate encoding without the use of diffuse illumination which causes the reformat image to have a coarse, granular appearance. This is true, of course, only when the 20 mm x 20 mm storage format constraint is applied. We show later, however, that with the size constraint modified Fresnel holography becomes a more attractive approach. Image plane holograms<sup>9</sup> might also appear to have some advantages. However, it is clear that the same storage format constraint that limits conventional micrographics also applies to image plane holograms: the microreduced image must contain detail of about 1  $\mu$ m. Moreover, the image plane holographic approach is highly sensitive to defects on the surface of the recording medium. The main advantage of an image plane hologram is its inherently low dispersion which permits readout with a chromatic (non-laser) light source. Because of unavoidable aberrations, this approach is not desirable for precision map and chart reproduction. Other forms of holographic storage are discussed later.

It is worthwhile at this point to note that for Fourier-transform holographic storage the maximum throughput resolution demand placed on the optics will not exceed about 4  $\mu$ m when a 70 mm film chip is used as an input. This is easily handled by the microreduction lenses typically used to provide the initial reduction of the full scale graphics. The holographic recording material, however, must have at least 50 percent spatial frequency response at 1500 cycles/mm. However, for most Lippmann emulsions (e.g., Kodak SO-343) this is not a problem because their spatial frequency response is generally flat to about 2000 cycles/mm.



Compared to conventional micrographic techniques, a Fourier or near-Fourier transform holographic storage and retrieval system has several valuable features:

1. Each resolution element (pixel) of the graphic contributes light to every part of the hologram. This natural encoding phenomenon gives partial immunity to dust, scratches or blemishes which might obscure significant areas of a micrographic image.
2. The axial position tolerances of the hologram, both in recording and retrieval, are much greater. Instead of a need to maintain a depth of focus adequate to record or reproduce a  $1\text{ }\mu\text{m}$  spot (equivalent to a diffraction-limited  $f/1.6$  lens system), the hologram need only be positioned to an axial tolerance equivalent to an  $f/120$  lens. Since the depth of focus is proportional to the square of the  $f$ /number, the holographic system has a tolerance that is more than 5000 times less stringent (for an equivalent reduction ratio) than a conventional micrographic system. This does not imply an immunity to the scale changes which will occur for any axial translation. However, the scale changes can be compensated by refocusing.
3. A large reduction of the lateral positional tolerance of the hologram is possible. In conventional systems operating at a magnification of 76X, a 0.05 inch movement of the film results in a 3.8 inch image movement. Such systems are, therefore, sensitive to vibrations and thermal variations, and require

accurate x-y selection mechanisms. A hologram recorded in the Fourier transform plane can be moved small distances (as long as it is almost fully illuminated) without introducing any image motion or resolution loss. For reasons noted earlier, it is often better to record in a near Fourier transform plane; even then the sensitivity to motion is significantly reduced. The distance that the image moves is, at worst, the same distance that the hologram moves. But in any practical system, the image motion will be approximately 1 percent of the hologram motion. Thus, if the hologram moves 100 mils, the image will not move more than 1 mil.

4. Holograms can be duplicated, if required, because the stored wavefronts can be released from a master hologram and recorded on a duplicate placed a small distance away. Contact between the master copy and the duplicate is not necessary. In conventional micrographics, contact copying is extremely difficult at reductions that require the retention of spatial detail smaller than about 5  $\mu\text{m}$ .

## 2.2 FOURIER-TRANSFORM HOLOGRAPHIC RECORDER/REPRODUCER

The baseline approach of the MEGIS Program is Fourier-transform holography. Our motivation for this choice of techniques is summarized in Table 2-1. Briefly, maps and other graphics can be most efficiently stored and read out using Fourier or near-Fourier transform holograms. Holograms of this type have several important advantages, e.g., a natural distributive coding, partial immunity to information loss due to dirt, scratches and artifacts, and insensitivity of readout to lateral movement. These holograms

Table 2-1. Motivation for Selecting Fourier-Transform Holography as the Baseline MEGIS Approach

- Natural distributive coding; this prevents information loss if the hologram is scratched, abraded, or partially covered by dust or other particulate matter.
- Maximum information packing density, i.e., this form of holography yields a maximum overall reduction ratio.
- Lateral translation invariance, i.e., the holographic image remains stationary when the hologram is shifted perpendicular to its axis.
- High axial positioning tolerances for both storage and retrieval; axial positioning for recording is arbitrary since no focussing is involved, while axial shifts generally cause a scale change that can be compensated by refocussing.
- High diffraction efficiency and signal-to-noise ratio capability which yields, in principle, full-scale images with high brightness and contrast.
- General compatibility with the micrographic approaches being tested and evaluated at ETL.
- Prior success in applications requiring the storage and retrieval of digital and alphanumeric data.

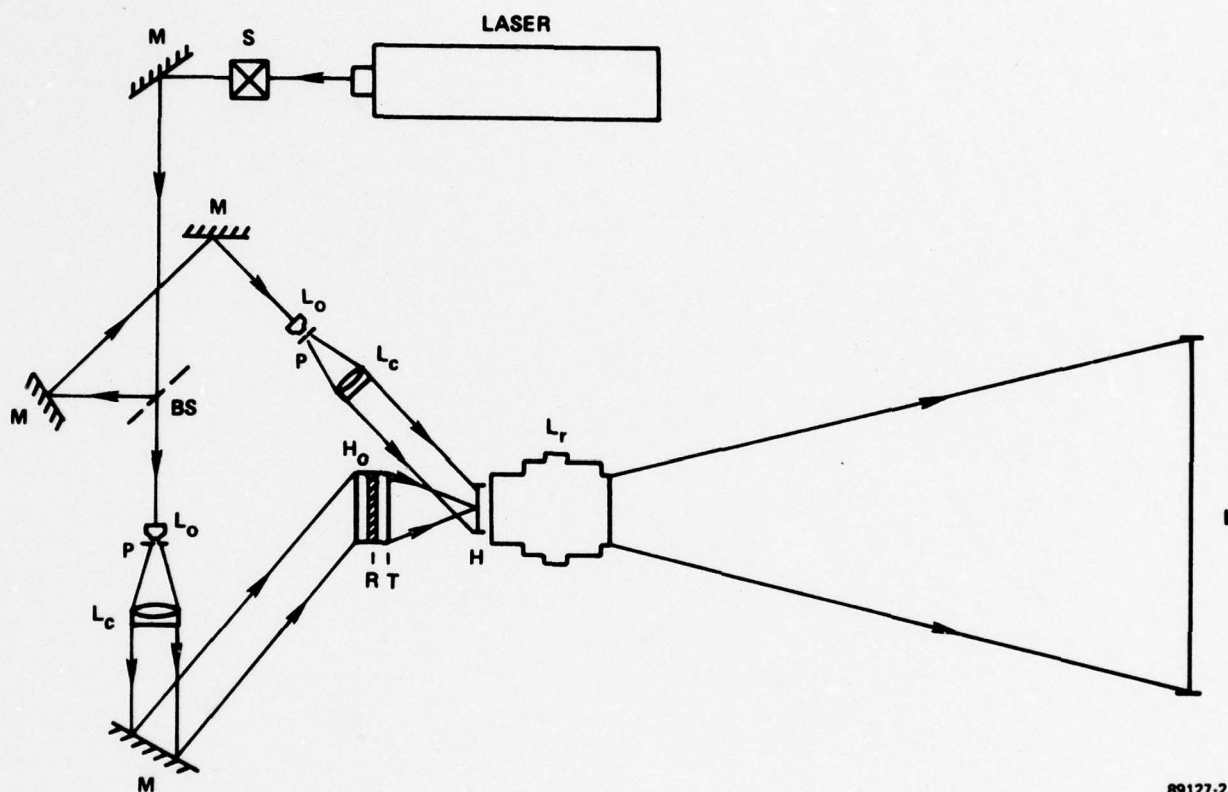


are ideal for systems applications, such as map separation storage, because information packing density is maximized. This permits a large number of holograms to be stored in a small area.

Important theoretical aspects of holographic information storage in these formats can be found in Appendix B. In Appendix B, the question of how to maximize the packing density (or minimize the recording area needed to provide the specified image resolution) is addressed and these techniques are compared with conventional micrographic reduction techniques. In this section, we outline the design and analysis of a holographic recorder/reproducer for the compact storage of map separations and other graphics. Key parameters are defined, and their impact on storage performance is discussed.

The basic construction and method of operation of a Fourier-transform hologram recorder/reproducer can be explained with the aid of Figure 2-2. We shall assume that the full scale input graphic has been reduced to a 70 mm film chip. The recorder subsystem includes a laser, appropriate optics, the film chip, and the hologram recording hardware. The reproducer subsystem includes a laser, beam forming optics, the hologram, the enlargement lens (which will always be the same as the microreduction lens), and the full-scale image film holder. A more detailed description of the operation of these subsystems follows.

In the recorder subsystem an unexpanded argon laser beam ( $\lambda = 514.5 \text{ nm}$ ) passes through a shutter S and is directed by mirror M toward a variable beam splitter BS', i.e., one whose transmittance (or reflectance) can be varied between 0 and 100 percent. The transmitted part of the laser beam is expanded with a microscope objective  $L_0$ , spatially filtered with a pinhole P, and collimated with a planoconvex lens  $L_C$ . Another mirror M



89127-2

Figure 2-2. Schematic Diagram of a Fourier-Transform Holographic Recorder/Reproducer

directs the expanded and collimated beam to a holographic optical element (HOE)  $H_0$ . The HOE  $H_0$  (see Section IV for details of construction) functions as a low f/number, low-aberration Fourier-transform lens, whose format is matched to that of the 70 mm film chip. The converging cone of light diffracted by the HOE is partially diffused and scattered by the phase randomizer R (see Section IV for details of construction) and is used to illuminate the film chip T. The light modulated by T, which we shall call the signal beam, comes to focus in the hologram recording plane H. With the proper design and fabrication of R, most of the light incident on H just fills an area equal to the hologram size. The reflected part of the laser beam is directed by mirror M to a microscope objective  $L_0$ , pinhole P, and collimating lens  $L_c$ , which produce a uniform collimated reference beam. The reference beam is incident on the hologram recording plane H at an angle  $\theta$  (the offset angle), where it interferes with the signal beam. The resultant interference pattern is recorded on a high-resolution photographic emulsion (Kodak SO-343 film) and is subsequently chemically processed to form a hologram. In one possible operational mode, a set of film chips and a step-and-record technique are used to generate a matrix of 24 holograms in a 105 mm x 148 mm microfiche format.

In the reproducer subsystem the unexpanded argon laser beam passes through the shutter S and is again directed to the variable beam splitter BS'. Now, however, BS' is adjusted to be 100 percent reflecting; that is, all of the laser light is "dumped" into the reference beam path. The optics of the reference beam path is unchanged; hence, all holograms are illuminated with an exact replica of the original reference beam (a plane wave incident at H at an angle  $\theta$ ), which is now called the readout beam. The hologram

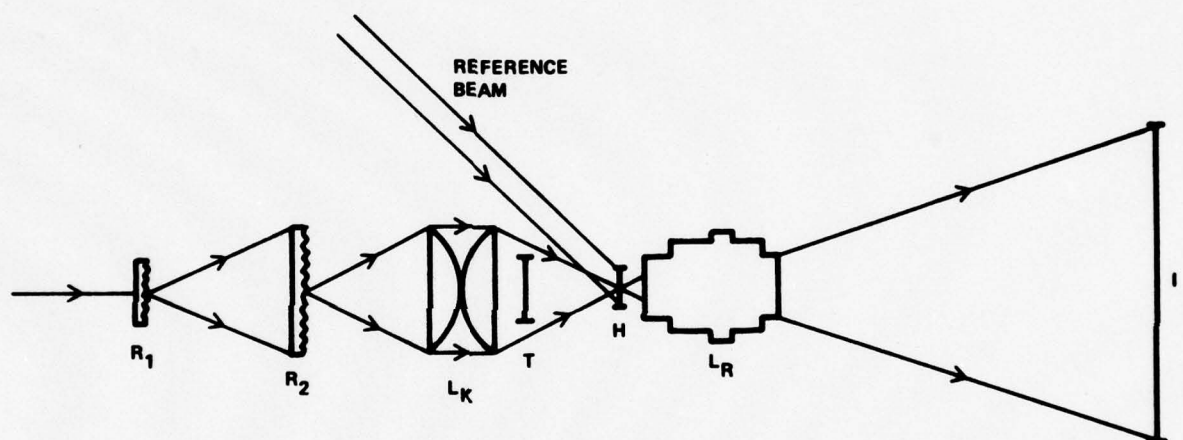


diffracts the readout beam along the axis of the enlargement lens. The light diffracted by the hologram forms a virtual image of the original film chip. This image is reimaged by the enlargement lens to form a full scale image of the reprostat or other graphic data contained in the film chip at the hardcopy film holder plane I (see Section V for a description of this device). At I, the image of the map separation is available for both visual display and hardcopy generation.

An alternative signal beam implementation is shown in Figure 2-3. Here, the unexpanded argon laser beam is doubly diffused by phase randomizers  $R_1$  and  $R_2$ .  $R_2$  is imaged by the condenser lens system  $L_k$  onto the hologram recording plane H. Since the clear aperture of H is the entrance pupil of the overall optical system, the Kohler illumination condition is satisfied relative to the hologram, but not to the projection lens. As discussed later, this did not improve the performance of the holographic recorder/reproducer. This signal beam implementation has the advantages of not requiring a HOE Fourier-transform lens and of greater simplicity and lower cost. We found, however, that optimum signal beam implementation was obtained with a HOE, as shown in Figure 2-2.

In succeeding paragraphs, we address important specific considerations related to the design and performance of the Fourier-transform recorder/reproducer. There are a number of important relationships between holographic parameters and the quality of displayed or hardcopy reproductions of cartographic imagery. For example, image brightness and diffraction efficiency, image contrast and signal-to-noise ratio, compactness of storage and hologram size, and so forth. These ideas are integrated into a discussion





00136-30

Figure 2-3. Alternative Signal Beam Implementation for a Fourier-Transform Holographic Recorder/Reproducer

of holographic recorder/reproducer analysis and design considerations for the microstorage and retrieval of cartographic data, specifically (color) map separations, or repromats. For convenience, the various recorder and reproducer considerations are discussed separately.

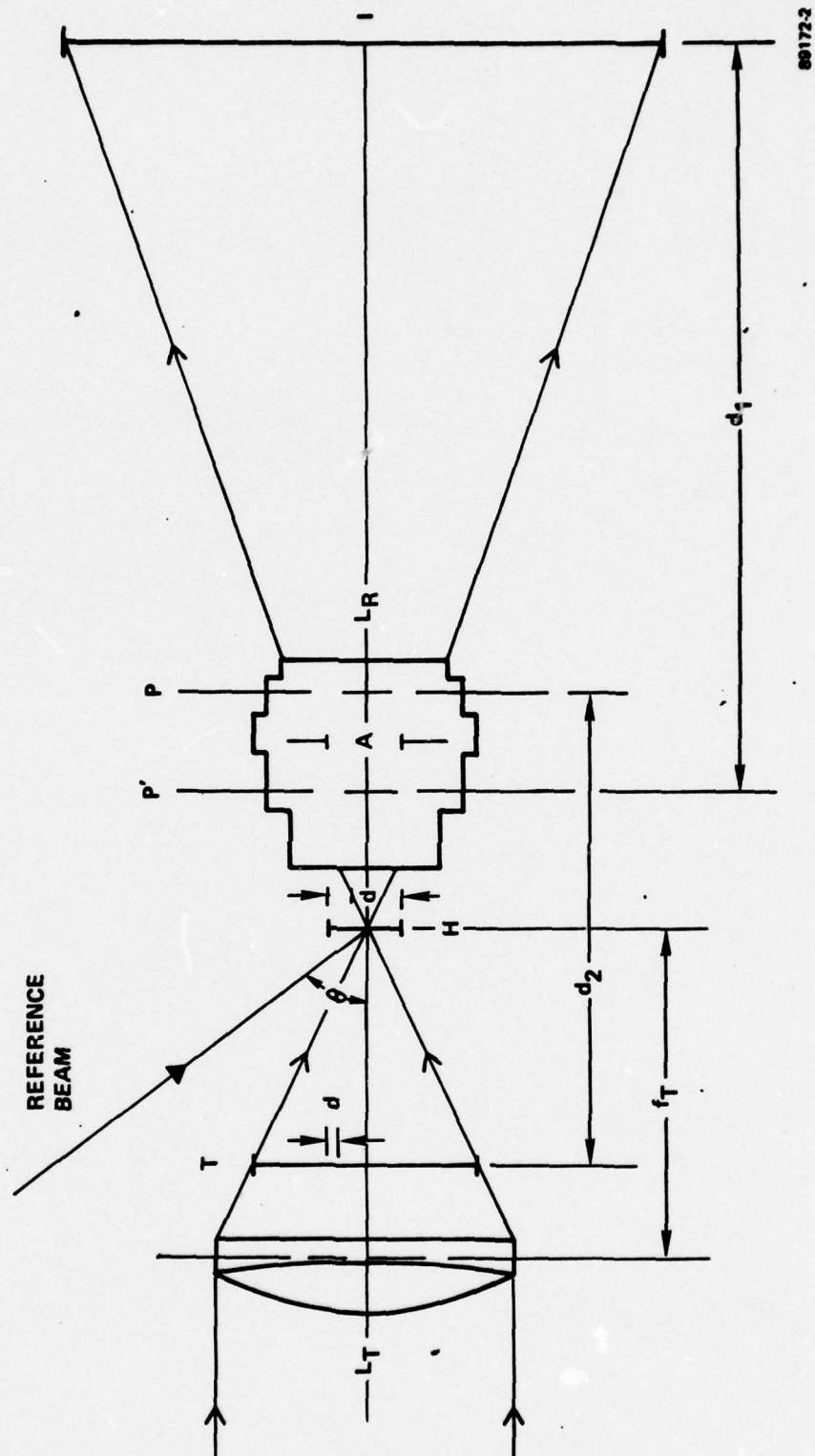
### 2.2.1 Recorder Design and Analysis

An attractive feature of high-density holographic storage of cartographic information is the relative simplicity of the optics and other hardware needed for recording and playback. Figure 2-4 shows the essential details of a Fourier-transform holographic recorder. It is comprised of a diffraction-limited collimator  $L_T$  that forms the Fourier-transform of a microreduced map separation (film chip)  $T$  near the holographic recording plane  $H$ , the original microreduction lens  $L_R$  which collects the light diffracted by the cartographic information and reproduces a full scale image on the display screen  $I$  and the reference beam which is incident at an angle  $\theta$  to the plane  $H$ . Note that this schematic of the recording breadboard is a plan view of Figure 2-1b.

#### 2.2.1.1 Initial Considerations

The minimum resolvable detail in the microreduced repromat is  $d$  and the hologram is assumed to have a square format with side  $\bar{d}$ . Coherent light of wavelength  $\lambda$  is used for recording and playing back the hologram. The transform lens  $L_T$  has a focal length  $f_T$  and the microreduction lens  $L_R$  has a focal length of  $f_R$ .

As an aid to analysis, a number of useful relationships are summarized. Let  $M$  be the demagnification of the original map or graphic. Then using the quantities defined in Figure 2-4,



89172-2

Figure 2-4. Basic Geometry of a Fourier-Transform Holographic Recorder/Reproducer



$$M = - \frac{d_2}{d_1} \quad (2.1)$$

$$d_1 = \left(1 - \frac{1}{M}\right) f_R$$

$$d_2 = (1 - M) f_R$$

Note that  $d_1$  and  $d_2$  are measured from the principal planes of  $L_R$ . The hologram size  $d$  required to resolve the smallest spatial detail (minimum resolution element or pixel)  $d$  is given by<sup>10</sup>

$$\bar{d} = \lambda f_T / d \quad (2.2)$$

The maximum value of  $\bar{d}$  is specified as less than or equal to 20 mm.

To obtain estimates of breadboard dimensions and optical parameters, we consider several microreduction schemes. For this discussion we assume that the microreduction lens is an f/5.6, 10-inch Wray Micro Lens, which is specified as being diffraction-limited at f/5.6 in both the sagittal and tangential planes over a  $12^\circ$  semiangular field. This is one type of microreduction lens currently used at ETL to generate 70 mm x 100 mm film chips. We also assume a recording wavelength of 514.5 nm, and that all map separations have 3-mil full scale resolution, regardless of format.

We consider first the case in which the reduction ratio is fixed and, hence, so are  $d_1$  and  $d_2$ . This microreduction arrangement is characteristic of flatbed planetary type microfilm cameras. To ensure that the largest map separation does not overfill a 70 mm x 100 mm film chip, a reduction of 16X is required. This makes  $d_1 = 4250$  mm and  $d_2 = 266$  mm. The lens must resolve about 4.8  $\mu$ m at the 70 mm film chip plane.<sup>11</sup>

The maximum focal length of the Fourier-transform lens is thus given by

$$f_T = \frac{d\bar{d}}{\lambda} = \frac{4.8 \mu\text{m} \times 20 \text{ mm}}{0.5145 \mu\text{m}} = 187 \text{ mm} \quad (2.3)$$

Since the diagonal of a 70 mm x 100 mm film chip is 122 mm, the  $f/\text{number}$  of this lens must be less than or equal to 1.53. A practical choice for the Fourier-transform lens might then be  $f_T = 175$  mm with a nominal speed of  $f/1.4$ . Table 2-2 summarizes relevant design data for this case. Note that the 70 mm x 100 mm format is filled only for the 48 x 60 inch map separation and that the number of map separations that can be stored on a 105 mm x 148 mm film chip is therefore limited to about 24. This disadvantage is compensated by the advantage of a fixed geometry for recording and playback.

An alternative approach is to use variable reduction ratios so as to always fill the 70 mm x 100 mm format. This means that  $d$ ,  $\bar{d}$ ,  $d_1$ , and  $d_2$  will vary with the size of the map separation. If we assume that a 175 mm,  $f/1.4$  Fourier-transform lens is used, the data in Table 2-3 are obtained. The data show that the recording and playback geometry change significantly as a function of the size of the map separation. Note, however, that the required hologram size is only 9.6 mm for the 22 x 30 inch graphics and 14.7 mm for the 32 x 48 inch graphics. This means that ideally about 96 and 54 map separations, respectively, could be stored on a 105 mm x 148 mm film chip. The variable reduction case with a constant 70 mm x 100 mm format indicates that significant storage density gains can be realized if the map separations are grouped with respect to size.

As a final case, we fix  $d_2$  and vary  $d_1$  and  $f_R$ . Again the 70 mm x 100 mm format is held constant. In this case, we obtain the data summarized in Table 2-4 for  $d_2 = 266$  mm. Note that the values for the reduction ratio and the hologram size are the same as for the previous case. The nominal values of  $f_R$  are also given, together with a correction lens of

Table 2-2. Holographic Recorder Design Parameters:  
Constant 16X Reduction ( $d_1 = 4250$  mm and  $d_2 = 266$  mm)

<u>Format</u>	<u>Reduction</u>	<u>Film Chip Size</u>	<u>d</u>	<u>min. <math>\bar{d}</math></u>
22" x 30"	16X	30 mm x 50 mm	4.8 $\mu$ m	20 mm
32" x 48"	16X	50 mm x 70 mm	4.8 $\mu$ m	20 mm
48" x 60"	16X	70 mm x 100 mm	4.8 $\mu$ m	20 mm

Table 2-3. Holographic Recorder Design Parameters:  
Variable Reduction Ratio (Constant 70 mm x 100 mm Film Chip Format)

<u>Format</u>	<u>Reduction</u>	<u>d</u>	<u>min. <math>\bar{d}</math></u>	<u><math>d_1</math></u>	<u><math>d_2</math></u>
22" x 30"	8X	9.5 $\mu$ m	9.6 mm	2250 mm	281 mm
32" x 48"	12X	6.4 $\mu$ m	14.7 mm	3250 mm	271 mm
48" x 60"	16X	4.8 $\mu$ m	19.6 mm	4250 mm	266 mm

Table 2-4. Holographic Recorder Design Parameters:  
(Constant 70 mm x 100 mm Film Chip Format with  $d_2 = 266$  mm)

<u>Format</u>	<u>Reduction</u>	<u><math>f_R</math></u>	<u><math>f_C</math></u>	<u><math>d_1</math></u>	<u>min. <math>\bar{d}</math></u>
22" x 30"	8X	236 mm	+4.2 m	2124 mm	9.6 mm
32" x 48"	12X	246 mm	+15.4 m	3198 mm	14.7 mm
48" x 60"	16X	250 mm	none	4250 mm	19.6 mm



focal length  $f_c$  that would permit  $f_R$  to remain constant at 250 mm if the two lenses were placed in contact. This approach is seen to be an ideal combination of the best features of the previous cases; it may not, however, be practical because of the MEGIS Program distortion specification.

Approach number two was selected for experimental work because map separation sizes are generally not mixed. That is, the various DMA production centers print different size maps. Thus, from a systems viewpoint, a recorder can be designed and optimized for a fixed reprostat size. However, for tactical applications, the first approach may be more satisfactory since it permits the display and reproduction of maps and charts in a fixed geometry system.

Several details are relevant to understanding some of the data presented in the remainder of the report. They are as follows:

1. Film chip size was nominally 70 mm x 100 mm; however, because of a framing limitation in the microreduction camera, the actual image area was 66.5 mm x 82.5 mm.
2. All Government-supplied film chips were microreductions of 22 x 30 inch and 48 x 60 inch map separations. No film chips produced from 32 x 48 inch map separations were supplied for experimental evaluation.
3. The 22 x 30 inch map separations were microreduced 10X in a single step using the Wray Micro Lens. The 48 x 60 inch map separations were microreduced 20X in two steps, one of which was not controlled well enough to establish a metric distortion baseline.

Using these data as a baseline, typical recorder parameters for the 22 x 30 inch and 48 x 60 inch map separations are summarized in Table 2.5.



Table 2.5. Summary of Design Parameter For a Holographic Recorder

<u>Parameter</u>	<u>Topo-Sheets</u>	<u>Hydro-Sheets</u>
Map Separation Size	22" x 30"	48" x 60"
Pixel Size	3-mil x 3-mil	3-mil x 3-mil
Film Chip Size (nominal)	70 mm x 100 mm	70 mm x 100 mm
Microreduction/Enlargement Lens	10", f/5.6 Wray Micro Lens	10", f/5.6 Wray Micro Lens
Reduction, M	1/10X	1/20X
Film Chip Resolution, d	7.6 $\mu$ m	3.8 $\mu$ m
Projection Distance, d <sub>1</sub>	2794 mm (9.17 f)	5334 mm (17.5 f)
Microreduction Image Distance, d <sub>2</sub>	279.4 mm	266.7 mm
Fourier-Transform Lens	f <sub>T</sub> = 148 mm f/no. = 1.2	f <sub>T</sub> = 148 mm f/no. = 1.2
Hologram Size, $\bar{d}$	10 mm x 10 mm	20 mm x 20 mm
Recording Wavelength	514.5 nm	514.5 nm
Reference Beam Angular Offset, $\theta$	45°	45°

The actual recorder parameters used to construct the experimental breadboard varied somewhat from these values for reasons discussed in Section IV. We mention, however, that the parameters of the Fourier-transform lens are in part dictated by the distance of the film chip from the back surface of the microreduction and enlargement lens. That is the f/number of the Fourier-transform lens must always satisfy the following inequality:

$$f/\text{number} \leq \frac{\text{Film Chip-to-Lens Distance}}{\text{Film Chip Diagonal}}$$

The nominal film chip diagonal is 122 mm; for M = 1/10X the film chip-to-lens distance is 150 mm, whereas for M = 1/20X, it is 136 mm. Therefore, f/number = 1.23 when M = 1/10X and f/number = 1.12 when M = 1/20X.

Fortunately, the actual diagonal of the film chip is about 106 mm; the f/number requirement in this case is 1.42 and 1.28 when  $M = 1/10X$  and  $M = 1/20X$ , respectively. Also, in both cases, these f/numbers are larger than the holographic requirement of f/1.2.

#### 2.2.1.2 Hologram Recording Parameters

Optimum design and performance of the recorder depends on the choice of hologram recording parameters. We have several degrees of freedom in the selection of some recording parameters, whereas others are fixed by explicit MEGIS Program specifications. In the subsequent discussions, we define principal recording parameters and their systems interactions.

##### 1. Film Chip Size

Film chip size is dictated by the size and resolution of original map separations, microreduction lens, microstorage format, and hologram size. For 3-mil resolution in a full scale repromat, direct microreductions 1/20X or smaller generally exceed the capabilities of state-of-the-art, low-distortion optics. In practice, this means that 22 x 30-inch repromats can be reduced to a format no smaller than about 35 mm. For the largest map separations used (48 x 60 inch and 48 x 72 inch), the minimum format is 70 mm. We have shown experimentally that a direct projection microstorage system based on film chips of this size could satisfy all reproduction specifications. We mention that for Fourier-transform holograms, the hologram size and film chip size scale inversely (smaller film chips require larger holograms).

## 2. Hologram Size

Hologram size is determined by the film chip resolution, Fourier-transform lens focal length, and recording wavelength; that is from  $\bar{d} = \lambda f_T / d$ . We emphasize that this is a minimum size based on the Rayleigh separation criterion (or Nyquist limit). (An important output of this study is that the hologram size must generally be large enough to transmit without vignetting the light bundle generated by Kohler projection of the film chip; this becomes apparent from reading Sections IV and V and the ETP Summary of Appendix A.) Band limiting the optical throughput with a hologram of this size causes considerable intensity rolloff in the projected image of narrow lines and other small spatial detail. We can relate resolution to hologram size by observing that<sup>12</sup>

$$\nu_M = \frac{1}{2\bar{d}} \text{ (cycles/mm)} \quad (2.5)$$

and hence,

$$\bar{d} \geq 2\nu_M \lambda f_T \quad (2.6)$$

These formulae for hologram size assume a diffraction-limited optical system. Aberrations and phase errors, in addition to field coverage requirements, will always force the selection of a larger hologram size.

## 3. Modulation Level (K-Ratio)

The hologram modulation  $M_0$  is determined by the ratio of average reference beam to average signal beam irradiance, or K-ratio:



$$M_0 = 2 \sqrt{K/(K+1)} \quad (2.7)$$

where

$$0 < M_0 \leq 1$$

The modulation parameter has an important impact on diffraction efficiency, which in turn determines image luminance and signal-to-noise ratio. Generally, a K-ratio in the 10 to 20 range, which yields  $M_0 \sim 0.5$ , is selected as a compromise between diffraction efficiency and signal-to-noise ratio requirements. For specular Fourier-transform holograms, a much higher K-ratio is required to accommodate the dynamic range of the signal spectrum. On the other hand, the large data content (much of which is, of course, redundant) of a diffuse phase-randomized Fourier-transform hologram is effective in reducing intermodulation noise, which in turn permits the use of lower K-ratios. We found in our experimental work that a K-ratio of about 5 provided maximum diffraction efficiency and signal-to-noise ratio. We mention that K-ratio varies with the information content of the film chip; that is, average signal strength is a function of the average transmittance of the film chip. This tends to equalize diffraction efficiency and signal-to-noise ratio performance, regardless of information content, so that these parameters are less signal dependent than they might appear.

#### 4. Spatial Carrier Frequency

The spatial carrier frequency  $\nu_c$  is a function of reference beam offset angle  $\theta$  and recording wavelength  $\lambda$ :



$$\nu_c = \frac{\sin \theta}{\lambda} \quad (2.8)$$

For the Fourier-transform holographic recorder,  $\theta$  is required to be large enough for the reference beam to reach the hologram recording plane without vignetting; this is a minimum requirement. In some cases there is an advantage to using higher offset angles to increase the effective thickness of the hologram, and to thus increase diffraction efficiency. However, this is generally not an attractive trade-off. We chose  $\theta \approx 45^\circ$ , which was close to a minimum value. Hence, with  $\lambda = 514.5 \text{ nm}$ ,  $\nu_c \approx 1375 \text{ cycles/mm}$ . As a rule, the high value of  $\nu_c$  forces the use of recording materials with resolving powers greater than 2000 cycles/mm.

##### 5. Recording Material

The recording material is the light-sensitive medium in which holograms are stored. We selected Kodak S0-343 High Resolution film as the MEGIS Program baseline recording material. It is an orthochromatic, Lippmann silver halide photographic emulsion coated on a 7-mil polyester base with a resolving power greater than 3000 cycles/mm and an exposure requirement at  $\lambda = 514.5 \text{ nm}$  of about  $1000 \text{ ergs/cm}^2$ . Experimental data show that this is the best orthochromatic film commercially available. We exposed and processed the S0-343 film in a conventional way and then bleached it to form volume phase holograms. Further background data on S0-343 and other recording material is given in Section III.

#### 6. Hologram Type

Hologram type is usually dictated by recording geometry, recording wavelength, and type and physical thickness of the recording material. As explained in Section III, information is stored in holograms as absorption or phase variation.

Holograms are considered planar or volume on the basis of sensitivity to Bragg effects (Kogelnik Q-factor). Since high image luminance is required for the visual display and reproduction of map separations, we chose to use volume phase holograms because of their high diffraction efficiency and relatively low insertion loss. Planar phase holograms have sufficient diffraction efficiency potential, but no visible-light sensitive recording materials (e.g., photoresists) have sufficient resolving power.

#### 7. Phase Randomization

Phase randomization is a means of minimizing and, in certain cases, eliminating coherent noise and smoothing the Fourier-spectrum of the map separation data. Unfortunately, phase randomization of any kind will create a granular structure in the reconstructed holographic image; for this reason it is generally avoided. Originally, we had planned to record near-Fourier transform, specular (unrandomized) holograms. However, scratches, dust, fingerprints, etc., on the Wray Micro Lens and on some of the film chips generated a significant amount of coherent noise and, cosmetically, the map separation displays and hardcopy reproductions were also

noisy. Because of this we were forced to use phase randomization, even though it seriously degraded the fine spatial detail in reconstructed map separation images. The impact on the program was significant, as we show later. We designed and fabricated several phase randomizers that produced smooth signal spectra and concentrated signal power in the hologram recording area. Experimental work with phase randomizers is described in Section IV.

#### 8. Information Packing Density (IPD)

Information packing density is defined as the number pixels  $N$  stored in hologram area  $A_H$ . If we call the reduction ratio  $M$ , the full scale image area  $A_T$ , and the full scale image pixel size  $d_0 \times d_0$  (which is specified as 3-mil x 3-mil), the IPD is

$$\begin{aligned} \text{IPD} &= \frac{N}{A_H} & (2.9) \\ &= \frac{A_T}{d_0^2 A_H} \text{ (pixels/unit area)} \end{aligned}$$

where

$$\begin{aligned} N &= \frac{A_T}{d_0^2} \text{ (space bandwidth product)} \\ &= \frac{\text{Film Chip Area (} A_c \text{)}}{\text{Film Chip Resolution (} d \text{)}} \end{aligned}$$

and where

$$\begin{aligned} d &= M d_0 \\ A_c &= M^2 A_T \end{aligned}$$

A typical map separation will not generally have 3-mil detail over its entire area. Also, repromats tend to have their information content displayed in clear areas of the film (negative format). This yields minimum redundancy. Thus, the IPD is generally less than  $N/A_H$  by a factor  $\alpha$ , which may be interpreted as either the ratio of clear area to total repromat area or as average film chip intensity transmittance. By way of example, suppose

$$\begin{aligned} A_H &= 20 \text{ mm} \times 20 \text{ mm} \\ A_T &= 5000 \text{ cm}^2 (\sim 22 \times 30 \text{ inches}) \\ M &= 1/10X \\ d_o &= 3 \text{ mils } (76 \text{ } \mu\text{m}) \\ \alpha &= 10^{-1} \text{ (10 percent clear area)} \end{aligned}$$

Then

$$\text{IPD} = 2.16 \times 10^5 \text{ pixels/mm}^2$$

This is a very high information packing density, which, of course, is the reason for using Fourier-transform holograms. Previous studies suggest that maximum signal-to-noise ratio per pixel will be in the range of 13 to 16 dB. Finally, we state an important interrelationship between IPD, diffraction efficiency, and signal-to-noise ratio for Fourier-transform holograms.<sup>13</sup>

$$\frac{(\text{Information Packing Density})(\text{Signal-to-Noise Ratio})}{(\text{Diffraction Efficiency})} = \text{CONSTANT (2.10)}$$



This relationship makes obvious the performance constraints on a Fourier-transform holographic recorder/reproducer. It is useful for interpreting the data in Section IV and in Appendix A.

#### 2.2.1.3 Hologram Exposure Requirement

The exposure required to record a hologram is a function of laser power, optical system efficiency, recording film speed, diffraction efficiency requirement, and K-ratio. We used an argon laser with single-frequency power output of about 500 mW at  $\lambda = 514.5$  nm. Optical system efficiency is determined, not only by the efficiency of individual optical components, but also by the efficiency of illumination of the film chip (which is dependent upon the image luminance uniformity specification). A high level of image luminance uniformity requires considerable expansion of the laser beam and subsequent loss of laser power. Generally, this is a more important consideration for direct projection systems. Recording film speed is an inherent property; it is a fortunate fact that some of the best holographic recording media are Lippmann silver halide emulsions which have very high exposure sensitivity by comparison with other light-sensitive materials. Diffraction efficiency is a factor related to hologram exposure because diffraction efficiency level, all other parameters fixed, is a function only of exposure; high diffraction efficiency generally requires high exposure. Finally, K-ratio is a variable because 1) a minimum value of K-ratio is needed to obtain a specified image signal-to-noise ratio and 2) the input laser power is constant and must be divided between reference and signal beams (by the variable beamsplitter BS' in Figure 2-2) to yield a specified K-ratio.

The hologram exposure  $E_H$  in  $\text{mJ/cm}^2$  is given by the following equation:<sup>14</sup>

$$E_H = (I_R + \bar{I}_S) \tau_H = (K + 1) \bar{I}_S \tau_H \quad (2.11)$$

Where

$I_R$  = reference beam irradiance (mW/cm<sup>2</sup>)

$\bar{I}_S$  = average signal beam irradiance (mW/cm<sup>2</sup>)

$\tau_H$  = exposure time (an independent variable determined by film speed)

$K$  = beam ratio

Now

$$I_R = r \epsilon_R P_O \cos \theta / A_H \quad (2.12)$$

and

$$\bar{I}_S = (1 - r) \epsilon_O \epsilon_U \alpha P_O / A_H \quad (2.13)$$

Where

$P_O$  = output laser power (mW)

$r$  = beamsplitter reflection coefficient

$\epsilon_R$  = efficiency of optics forming the reference beam

$\epsilon_O$  = efficiency of optics forming the signal beam

$\epsilon_U$  = efficiency of illumination (a function of the image luminance uniformity requirement)

$\alpha$  = film chip transmittance

$A_H$  = hologram area (cm<sup>2</sup>)

$\theta$  = reference beam offset angle ( $\cos \theta$  is an obliquity factor)

Therefore

$$\begin{aligned} E_H &= \left[ r \epsilon_R \cos \theta + (1 - r) \epsilon_O \epsilon_U \alpha \right] \left[ P_O \tau_H / A_H \right] \\ &= (K + 1) (1 - r) (\epsilon_O \epsilon_U \alpha) (P_O \tau_H / A_H) \end{aligned} \quad (2.14)$$

and

$$K = \left( \frac{r}{1 - r} \right) \left( \frac{\epsilon_R \cos \theta}{\epsilon_O \epsilon_U \alpha} \right) \quad (2.15)$$

By way of example, suppose

$$\epsilon_r = \epsilon_o \approx 1/2$$

$$\epsilon_u = 1/4$$

$$\cos \theta = \cos 45^\circ = 0.707$$

$$A_H = 4 \text{ cm}^2$$

$$K = 5$$

$$\alpha = 1/10$$

$$P_o = 500 \text{ mW}$$

Then,

$$K = 5 = \left( \frac{r}{1-r} \right) (28) \text{ , which implies that } r \approx 0.15$$

$$E_H = 8 \tau_H \text{ (mJ/cm}^2\text{)}$$

Since a film like SO-343 requires an exposure of about  $0.1 \text{ mJ/cm}^2$ , the required exposure time per hologram recording is:

$$\tau_H = \frac{0.1}{8} = 0.0125 \text{ second (12.5 msec)}$$

Thus, hologram exposure is much less than 1 second, which is an attractive feature relative to possible systems operation in a production environment.

#### 2.2.1.4 Image Resolution

Image resolution is determined by hologram size and recorder breadboard parameters. As we analyze the steps used for the storage of map separations in microreduced form, the factors affecting image resolution will become clear.

The full-scale repromat is assumed to have resolution specified in terms of  $d_o \times d_o$  pixels, where  $d_o = 3 \text{ mils}$ . A well-corrected microreduction lens is used to photoreduce the map separation by a factor  $M$ . As the pixel size is now  $Md_o$ , the lens and film used to make the film chip



must resolve  $\nu_M = 1/2Md_0$  (for example, if  $M = 1/10X$ ,  $\nu_M = 61$  cycles/mm, whereas if  $M = 1/20X$ ,  $\nu_M = 122$  cycles/mm).

The Wray Micro Lens, which is an exceptional imaging lens, has MTF values of  $\sim 0.75$  at 61 cycles/mm and  $\sim 0.55$  at 122 cycles/mm, when used at  $f/5.6$ . The microreduction film, for example, Kodak SO-141, has an MTF value close to unity for spatial frequencies less than 200 cycles/mm.

In the holographic recorder, the film chip is illuminated with a low  $f$ /number converging cone of laser light and reimaged back through the same microreduction lens which we used to make the film chip (now called the enlargement or projection lens). Ideally, the cone of laser light forms an image of the light source in the pupil (aperture stop) of the enlargement lens; this is the optimum projection mode (Kohler condition satisfied) and ensures maximum resolution transfer<sup>15</sup> (and also maximum image luminance and uniformity). In practice, the introduction of the relatively small hologram aperture near the back element of the enlargement lens severely restricts the field of view (FOV) and decreases image luminance uniformity. This is illustrated in Figure 2-5. The hologram aperture also becomes the system aperture stop. Thus, we must reimage the light source into the hologram plane to maintain a Kohler projection condition. Whereas previously (with no hologram aperture present) the enlargement lens controlled resolution and field, the hologram now determines these parameters. This is a major disadvantage of Fourier-transform holography, unless the hologram size is large enough to permit the Kohler projection condition to be satisfied relative to the enlargement lens.



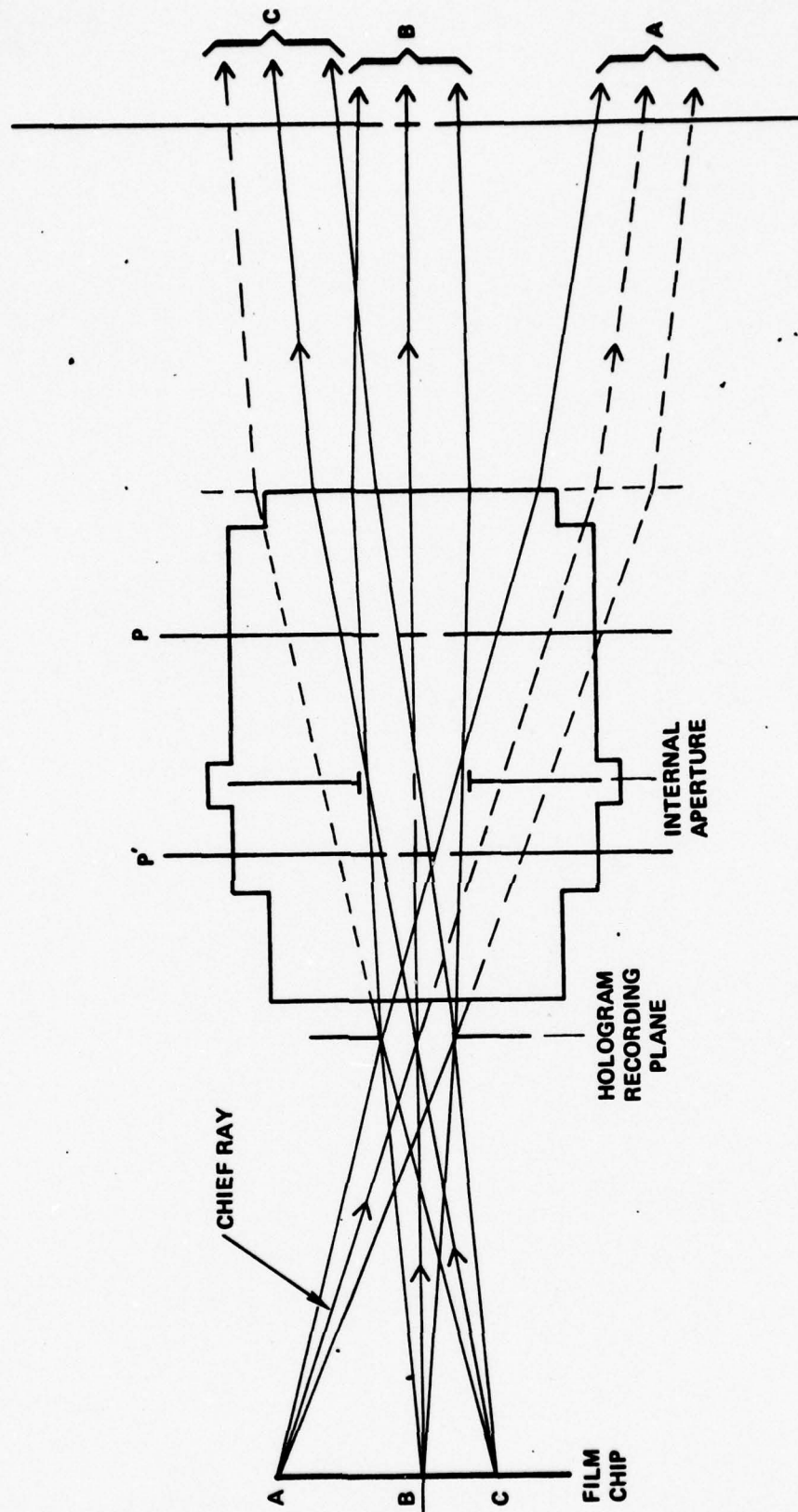


Figure 2-5. Scaled Ray Diagram Showing the Effect of the Hologram Aperture on Field and Resolution for Several Object Points

To complete our discussion, we note that the hologram itself can limit resolution not only because of its size, but also because of aberrations generated by angular misalignment, emulsion shrinkage, and film base phase errors. We learned experimentally (see Section IV) that angular misalignment can be eliminated and that emulsion shrinkage does not measurably reduce image resolution. However, the polyester film base proved to be the resolution-limiting element of the overall optical system. In terms of a diffusely-illuminated high-contrast 1951 AF tribar resolution target, the throughput resolution with a cleared piece of film base in the hologram aperture was only 64 cycles/mm. We found that acceptable imaging performance for hardcopy reproduction could be obtained with holographic storage only through the use of glass substrates and an index-matching gate. For visual displays, this problem was not as significant.

#### 2.2.2 Reproducer Design and Analysis

The holographic reproducer is comprised of a laser, a hologram transport, an enlargement lens (the microreduction lens), a hardcopy film platen, optics (mirrors, collimating lens, etc.), and control electronics. Its function is to retrieve, position, and read out holograms such that a full scale, distortion-free image of a map separation is formed on the hardcopy film platen. Although this study was not intended to provide a detailed engineering prototype design, we nevertheless designed, fabricated, and tested various reproducer components to verify that the retrieval process is possible in either a production or a tactical environment. The simplicity of the reproducer, as described earlier, together with the use of solid, but not massive, mechanical components allowed us to generate low-distortion reprints.

from both holographic and direct enlargement of microreduced map separations with good repeatability. Thus, here we focus our attention on reproduction parameters, and defer the discussion of components to Sections IV and V.

#### 2.2.2.1 Diffraction Efficiency

Diffraction efficiency is the key reproducer parameter. It has a major impact on readout laser power, signal-to-noise ratio, display brightness, and hardcopy film type and exposure time. A major advantage of a holographic system is the option of trading-off hologram exposure time for diffraction efficiency. That is, a low level of optical system efficiency can be tolerated in order to obtain an optimized throughput image because the holographic process will later produce a significantly brighter replica of the throughput image. Another important point is that the light diffracted by a hologram goes only into the information-bearing areas of the repromat. This provides an image luminance gain over direct projection proportional to  $1/\alpha$ ; this observation is discussed in more detail in Paragraph 2.2.2.3, in which image luminance is analyzed.

Diffraction efficiency (DE) is defined as the ratio of the average first-order holographic image irradiance to the readout beam irradiance (power and radiance ratios are also used). For Fourier-transform holograms of complex signals recorded in volume phase recording material, a formula for diffraction efficiency is:<sup>16</sup>

$$DE = \left[ \frac{2}{(1 + \nu_2)(1 + \sqrt{1 - \xi^2})} \right] \left[ \frac{\sin \beta L - \sin \phi \sin \phi \beta L}{1 - \phi^2} \right] \quad (2.16)$$

$$\text{Where } \beta = \frac{\pi \Delta n^M_0}{n \lambda \sqrt{\cos \theta_s \cos \theta_r}} (1 + \nu_2)^{\frac{1}{2}} \left( \frac{1 + \sqrt{1 - \xi^2}}{2} \right)^{\frac{1}{2}}$$



$L$  = hologram thickness

$\Delta n$  = average refractive index change of holographic recording material created by the recording exposure and processing

$n$  = average refractive index of holographic recording material

$\lambda$  = recording/readout wavelength

$\cos \theta_s, \cos \theta_r$  = direction cosines of signal and reference beams, respectively

$$M_0 = \frac{2\sqrt{K}}{K+1} \quad (\text{average modulation parameter})$$

$K$  = average reference beam irradiance to average signal beam irradiance ratio

$$\phi = \left[ \frac{1 - \sqrt{1 - \xi^2}}{1 + \sqrt{1 - \xi^2}} \right]^{\frac{1}{2}}$$

$$\xi = \frac{2\nu_1}{1 + \nu_2}$$

$$\nu_1 = \frac{\sigma^2(I_s)}{K I_s^2} = \frac{1}{K} \bullet \frac{\text{variance}(I_s)}{\text{mean square}(I_s)}$$

$I_s$  = signal beam irradiance

$$\nu_2 = \frac{\cos^2 \theta_s + \cos^2 \theta_r}{\cos \theta_s \cos \theta_r} \nu_1$$

This relatively complex formula takes into account the generally random nature of the signal beam and the interaction of linear and nonlinear field components created by the holographic recording and reconstruction process. The latter is a particularly appropriate concern for phase-randomized data readout at high DE levels. For the hologram recording parameters used for the storage of map separations, we can express DE as

$$DE \approx \left( \frac{K}{K+2} \right) \sin^2 \beta L \quad (2-17)$$

Where

$$\beta L \approx \frac{\pi \Delta n M_0}{n \lambda \sqrt{\cos \theta_s \cos \theta_r}} \left[ \frac{K+2}{K} \right]^{\frac{1}{2}} L$$

$$\xi \approx \frac{2}{K+2}$$

$$\phi \approx 0$$

$$\nu_1 \approx 1/K$$

This simplification is possible because of the high information content of the input signal and the use of  $K \gtrsim 5$ . It is of interest to note that even at the present level of approximation, the maximum value of DE is  $K/(K+2)$  instead of 1. Only for large values of  $K$  and phase modulation  $\beta L \approx \pi/2$  does  $DE \rightarrow 1$ ; this is a residual impact of the complex nature of the input signal.<sup>17</sup>

We have assumed that the hologram is lossless. In practice, this is seldom the case. For bleached photographic emulsions, the insertion loss can be relatively high, often approaching 50 percent of the incident light. The insertion loss is a function of prebleach density, as, unfortunately, is the average holographic refractive index change  $\Delta n$ . Thus, as prebleach density is increased to increase  $\Delta n$ , the insertion loss increases simultaneously. Moreover, since the magnitude of  $\Delta$  is proportional to the number of silver halide microcrystals per unit volume, scatter noise also increases.<sup>18</sup> The impact on signal-to-noise ratio is significant. Many other recording materials have a similar interrelationship between scatter noise, insertion loss, and DE.

#### 2.2.2.2 Signal-to-Noise Ratio

Signal-to-noise ratio (SNR) is defined as the ratio of average signal irradiance (power per unit area in the clear areas of a map separation) to average background noise. For binary map separations, SNR, as defined, and contrast ratio are the same. SNR is an important reproducer parameter because of its impact on image cosmetic quality, resolution, and hardcopy reproduction.

The signal-to-noise ratio of information stored and readout from a hologram is determined by several factors: contrast and cosmetic quality of the input, linearity and homogeneity of the recording material, diffraction efficiency level, storage density, and so forth. Since the holographic microstorage and retrieval of map separations must be relatively distortion free and of high resolution, we focus our attention on noise sources that degrade image quality. Also, because of the inherent high image brightness requirement for the present application, we shall discuss SNR in terms of volume phase holograms, the type used for the experimental phases of the MEGIS Program.

In recording and reproducing map separations from volume phase holograms, noise is generated in several ways.<sup>19</sup> First, the holographic process itself is inherently nonlinear. Even if the recording material response is ideally linear, the diffraction of the reconstructed signal by the low frequency bias of the holographic refractive index distribution produces signal distortion noise, which is a signal-dependent nonlinear noise. If the recording material is nonlinear or overmodulated, then signal-dependent intermodulation noise is also introduced into the reconstruction process. Second, the majority of recording materials are not microscopically homogeneous, i.e. they have scattering centers. This is especially true for



bleached photographic emulsions. Both the readout beam and the diffracted signal beam interact with the scattering centers to produce background noise. At very high diffraction efficiency levels, forward scattering by the reconstructed signal beam can seriously degrade SNR. Third, the surface of many recording materials is generally degraded by exposure and processing. Again this is especially true of bleached photographic emulsions. The effect is similar to that observed when a slightly diffuse phase plate is placed on the surface of an otherwise perfect hologram: the diffracted signal waves are distorted. Fourth, phase randomization of the input data with, for example, a ground glass diffuser causes speckle noise. A phase randomizer was required for recording Fourier-transform holograms because the cosmetic noise caused by scratches, dust particles, and other defects on the film chips and the micro-reduction and enlargement lens was unacceptable for the hardcopy reproduction of map separations. By diffusely illuminating the film chip, which is equivalent to modulating a white noise source, we gained immunity from coherent noise and also smoothed the signal spectrum in the Fourier-transform recording plane. However, because the optical system has a finite spatial bandwidth, the image of the map separation is broken up into phase-randomized resolution cells, or speckles. Since the hologram size was chosen to match the minimum spatial detail (or pixel size) of 3-mils in the map separation, the speckle and pixel sizes are equal in the full size image. As a result, there are both resolution loss and discontinuities in fine line structure. Fifth, we note that coherent noise introduced by the microreduction and enlargement lens places an upper bound on achievable image SNR. The cosmetic noise (Fresnel rings, streaks, etc.) in a map separation image caused by dust particles,

scratches, and small imperfections on the glass surfaces of the lens is, in practice, generally unavoidable when specular laser light is used for illumination of the film chip. Diffuse laser light solves this problem, but now each image point is corrupted by scatter noise from the entire area of each lens surface. Throughput measurements show that maximum signal-to-noise ratio is limited to about 15 dB for map separations with a large clear area and to 20 dB for those with a small clear area; experimental data are in agreement with these observations.

We point out that high SNR (or contrast) in the map separation image may not in certain cases be a necessary condition for good visual displays or hardcopy reproduction. In the case of visual displays the brightness and contrast accommodation of the eye can be exploited, whereas in the case of hardcopy reproduction the hard clipping nature of lithographic films used to make reprostats tends to threshold away a large fraction of background noise. We have found from observer reaction and from hardcopy reproduction experiments that a SNR greater than 10 is generally required. However, background noise and speckle often cause resolution loss because of fill in. Exposing the hardcopy reproduction film so as to eliminate this kind of noise invariably causes line breakup and loss of fine detail. Moreover, speckle noise cannot be eliminated by this procedure (the overall printing process does, however, smooth out speckle, but line edges are irregular). Thus, a relatively high SNR is needed to assure the reproduction of high resolution information and good image contrast.

An expression for signal-to-noise ratio which is valid for Fourier-transform holograms is<sup>20</sup>:

$$\text{SNR} = \frac{1}{\frac{1}{\text{SNR}_{\text{NL}}} + \frac{1}{\text{SNR}_{\text{SN}}}} \quad (2.18)$$

where

$$\text{SNR}_{\text{NL}} = \left[ \frac{\text{Average Signal}}{\text{Average Nonlinear Noise}} \right] - \text{Ratio}$$

and

$$\text{SNR}_{\text{SN}} = \left[ \frac{\text{Average Signal}}{\text{Average Scatter Noise}} \right] - \text{Ratio}$$

The magnitude of  $\text{SNR}_{\text{NL}}$  is determined principally by diffraction efficiency and signal distortion noise. The use of beam ratios  $K \geq 5$  and the large dimensionality of the signal beam help to minimize  $\text{SNR}_{\text{NL}}$ . A formula for  $\text{SNR}_{\text{NL}}$  is

$$\text{SNR}_{\text{NL}} = \frac{3}{2} (K + 2) \left[ \frac{\sin \beta L}{1 - \cos \beta L} \right]^2 \quad (2.19)$$

where  $K$  and  $\beta L$  are as defined in Paragraph 2.2.2.1. We recognize that  $\text{SNR}_{\text{NL}}$  implicitly depends on the diffraction efficiency level and observe that it is an explicit function only of  $K$ -ratio and average holographic phase modulation ( $\beta L$ ). In general, we can trade off diffraction efficiency for  $\text{SNR}_{\text{NL}}$ . A formula for  $\text{SNR}_{\text{SN}}$  is

$$\text{SNR}_{\text{SN}} = \frac{\text{DE}}{B_s \phi_n(\nu_c) [1 + q\text{DE}]} \quad (2.20)$$

where

$B_s$  = spatial bandwidth of the signal

$\phi_n(\nu_c)$  = value of normalized scatter noise power spectrum at the spatial carrier frequency  $\nu_c$

$q$  = ratio of average forward scatter noise to average reference beam scatter noise in the signal direction



The Wiener Spectrum  $\Phi_n(\nu)$  is a function of scattering from the recording material and from the microreduction and enlargement lens. The term  $qDE$ , which always decreases the value of  $SNR_{SN}$ , is a consequence of the forward propagation of the diffracted signal beam through the scattering centers in the volume of the hologram recording material. The parameter  $q$  is determined by the angular separation of the reference and signal beams and typically ranges in value from  $10^1$  to  $10^4$ . As in the case of  $SNR_{NL}$ , we can trade off  $SNR_{SN}$  and  $DE$ . An important observation is that the contribution to  $\Phi_n(\nu)$  from recording material scatter is often exposure dependent, and hence,  $DE$ -dependent. This observation is particularly relevant for silver halide photographic emulsions.

For the storage of map separations in bleached photographic emulsion holograms (Kodak SO-343 High Resolution Film) and for typical holographic recording parameters, the following data can be used to estimate  $SNR$ :

$$\begin{aligned} DE &= 0.1 \text{ (10 percent; design goal)} \\ K &= 8 \\ B_s &= 125 \text{ cycles/mm (20 mm hologram)} \\ q &= 1.25 \times 10^3 \\ B_s \Phi_n(\nu_c) &\approx 2.5 \times 10^{-5} \text{ at } \nu_c = 1400 \text{ cycles/mm} \end{aligned}$$

Therefore,

$$\begin{aligned} SNR_{NL} &\approx 450 \text{ (26.5 dB)} \\ SNR_{SN} &\approx 32 \text{ (15 dB)} \end{aligned}$$

and

$$\text{SNR} = \frac{1}{\frac{1}{450} + \frac{1}{32}} \approx 30 \text{ (14.8 dB)}$$

For these recording conditions, SNR is determined by scatter noise; nonlinear noise is almost negligible. Moreover, analysis of throughput data shows that the photographic emulsion contributes about twice as much scatter noise as the microreduction and enlargement lens for the assumed recording/readout parameters.

The considerations discussed here are typical. Recording materials with better scatter noise performance exist, e.g., photopolymers, dichromated gelatin, and photodegradable polymers, but they are usually of an experimental nature or not available as commercial products. In addition, most have exposure sensitivities many orders of magnitude lower than a high resolution photographic emulsion. All real optical components will produce both coherent and scatter noise. Some nonlinear noise is generally unavoidable, although it can be minimized by appropriate K-ratio selection. It should be clear, however, that high diffraction efficiency (and correspondingly high image luminance) and high contrast and SNR cannot, in general, be obtained simultaneously.

#### 2.2.2.3 Image Luminance<sup>21</sup>

Image luminance  $L$  (often called brightness) is the luminous flux  $\Phi$  per unit projected area  $A$  per unit solid angle  $\Omega$  reaching the eye of the viewer of a map display. It is an invariant in a lossless optical system. Mathematically, we can write:

$$L = \frac{\partial \Phi}{\partial A \partial \Omega \cos \psi} \quad (2.21)$$

where

$$\phi = 685 \int_{\lambda} \sum_n P_{on} V(\lambda_n) \delta(\lambda - \lambda_n) d\lambda \text{ (lumens)}$$

$P_{on}$  = laser power (watts) at wavelength  $\lambda_n$

$V(\lambda_n)$  = visibility function (photopic eye response)

$\delta(\lambda)$  = Dirac delta function

$dA \cos \psi$  = projected area ( $\text{cm}^2$ )

$d\Omega$  = element of solid angle (steradians)

A requirement of the MEGIS program is to demonstrate an image luminance of 35 foot-Lamberts (fL).

A practical way to compute image luminance is to determine the illuminance of the repromat image on the viewing screen, assume that the viewing screen is ideally Lambertian, and multiply by an appropriate gain function. If area is measured in square feet, and laser power is converted to luminous flux then image luminance is obtained directly in foot-Lamberts. A useful conversion factor is

$$1 \text{ fL} = [1/2 V(\lambda)] \mu\text{W}/\text{cm}^2/\text{sr} \quad (2.22)$$

We begin our discussion by first considering the image luminance of a direct projection system. Then the holographic case is analyzed. Several examples are used to illustrate the different performance capabilities of these approaches. We show that the advantage of holography over direct projection is related to several efficiency parameters and the film chip transmittance  $\alpha$ .

#### 2.2.2.3.1 Direct Projection Image Luminance

The average luminance for a single wavelength, direct laser projection system  $L_D$  (in fL) can be determined from the following equation:



$$L_D = 2 V(\lambda) G(\theta) \epsilon_0 \epsilon_U \epsilon_L \epsilon_S P_0/A_T \quad (2.23)$$

where

$V(\lambda)$  = photopic eye response function evaluated at  $\lambda$

$G(\theta)$  = luminance gain relative to a Lambertian viewing screen

$\theta$  = viewing angle measured from the viewing screen normal

$\epsilon_0$  = transmittance of the optics required to illuminate the film chip

$\epsilon_U$  = efficiency of illumination relative to a specified luminance uniformity level

$\epsilon_L$  = transmittance of the projection lens

$\epsilon_S$  = transmittance of the viewing screen

$P_0$  = laser output power ( $\mu W$ )

$A_T$  = area of full scale image ( $cm^2$ )

The value of  $L_D$  is directly proportional to laser power  $P_0$  and inversely proportional to the area (size) of the full scale display  $A_T$ . The human factor, as expressed by the photopic eye response function  $V(\lambda)$ , is also an important determinant of image luminance. The values of  $V(\lambda)$  for several commercial CW lasers are summarized in Table 2-6.

Table 2-6. Photopic Eye Response for Several Commercial Lasers

Laser	Typical Power (mW)	Wavelength $\lambda$	$V(\lambda)$
He-Cd	50	441.6 nm (violet)	0.026
Argon	1000	488 nm (blue)	0.191
	1000	514.5 nm (green)	0.608
He-Ne	50	632.8 nm (red)	0.235
Krypton	1000	647.1 nm (red)	0.125
	500	568.2 nm (yellow)	0.964

The sensitivity of image luminance to  $V(\lambda)$  is clear. Note that  $V(\lambda)$  is three times greater at 514.5 nm than it is at 488 nm: this explains our choice of 514.5 nm as the principal recording and display wavelength. A more subtle factor is the luminance uniformity efficiency  $\epsilon_U$ . As a rule, a high degree of luminance uniformity can be obtained only by overexpanding the illuminating laser beam. This is because the beam of most commercial lasers has a Gaussian intensity distribution. Analysis reveals that if center-to-edge uniformity is required to be  $\xi$ , then  $\epsilon_U \leq \xi$ . For example, if 10 percent center-to-edge uniformity is specified, then  $\epsilon_U \leq 0.1$ . This result suggests that laser projection is inherently inefficient. However, this is not the case, since there is no fundamental reason why Gaussian (fundamental mode) laser beams must be used. Greater uniformity is readily obtained by generating a laser beam comprised of several higher order spatial modes in addition to the  $TEM_{00}$  mode.

When the laser beam contains a number of wavelengths  $\lambda_n$ , the formula for image luminance is:

$$L_D = 2G(\theta) \epsilon_0 \epsilon_U \epsilon_L \epsilon_S \sum_n V(\lambda_n) P_0(\lambda_n) / A_T \quad (2.24)$$

where we have assumed that  $G$  and the  $\epsilon$ 's vary slowly with wavelength. By way of example suppose

$$\lambda_1 = 488 \text{ nm}$$

$$P(\lambda_1) = 0.5 \text{ W}$$

$$V(\lambda_1) = 0.191$$

$$\lambda_2 = 514.5 \text{ nm}$$

$$P(\lambda_2) = 0.5 \text{ W}$$

$$V(\lambda_2) = 0.608$$

$$G(\theta) = 1 \text{ (Lambertian screen)}$$

$$A_T = 5000 \text{ cm}^2 \text{ (~22 x 30 inches)}$$

and

$$\epsilon_0 \epsilon_U \epsilon_L \epsilon_S \approx 0.01 \text{ (5 percent luminance uniformity)}$$

then,

$$L_D = 1.6 \text{ fL}$$

Thus, in this example, 1 W of laser power evenly divided between the principal wavelengths of an Argon laser provides an image luminance of 1.6 fL.

Higher image luminance can be obtained by increasing laser power, improving optical and illumination efficiency (decreasing luminance uniformity), and using a high-gain viewing screen. A final, but important, point is that  $L_D$  does not vary with the clear area (a measure of information content) of the film chip used to form the full-scale map separation image. The opposite is true for holographic projection, as we show subsequently.

#### 2.2.2.3.2. Holographic Image Luminance

The average luminance  $L_H$  (in fL) for a single wavelength holographic projection system can be computed from the following equation:

$$L_H = 2 V(\lambda) G(\theta) \epsilon_R \epsilon_L \epsilon_S \eta P_0 / \alpha A_T \quad (2.25)$$

where

$V(\lambda)$  = photopic eye response function evaluated at  $\lambda$

$G(\theta)$  = luminance gain relative to a Lambertian viewing screen

$\theta$  = viewing angle measured from the viewing screen normal

$\epsilon_R$  = transmittance of reference/readout beam optics

$\epsilon_L$  = transmittance of the projection lens

$\epsilon_S$  = transmittance of the viewing screen

$P_0$  = laser output power ( $\mu W$ )

$A_T$  = area of full-scale image ( $cm^2$ )

$\eta$  = diffraction efficiency of the hologram

$\alpha$  = ratio of clear area to total area of the full-scale enlargement; also, average intensity transmittance of the film chip



The value of  $L_H$  is directly proportional to the laser power  $P_0$  and inversely proportional to the area of the full-scale display  $A_T$ . It is also directly proportional to the diffraction efficiency  $\eta$ , but unlike  $L_D$ , is independent of the luminance uniformity efficiency  $\epsilon_U$ . This is a major advantage of holography, since it allows luminance uniformity and hologram recording time to be traded off in a favorable way. In addition,  $L_H$  is inversely proportional to the fraction of active area in the full-scale display. This indirectly provides a signal-dependent luminance gain; that is, the luminance of a full-scale map separation of clear area  $\alpha A_T$  is greater by a factor of  $1/\alpha$  when compared with a uniform full-scale display of area  $A_T$ . In the direct projection case, the luminance of a full-scale display is independent of the active area of the display. We mention that, as the beam ratio  $K$  becomes large, the ratio  $\eta/\alpha$  becomes constant. This condition decouples image luminance from image active area, and permits constant hologram and hardcopy reproduction recording times. However, the overall level of image luminance becomes significantly smaller.

As in the direct projection case, when two or more laser wavelengths are used for recording and readout, the formula for image luminance becomes

$$L_H = 2G(\theta) \epsilon_R \epsilon_L \epsilon_S \sum_n \eta(\lambda_n) V(\lambda_n) P_0(\lambda_n) / \alpha A_T \quad (2.25)$$

We again assume that  $G$  and the  $\epsilon$ 's vary slowly with wavelength. The holograms corresponding to each  $\lambda_n$  are incoherently superimposed; this generally causes  $\eta(\lambda_n)$  to decrease in value by  $1/N^2$ , where  $N$  is the number of incoherent superpositions.<sup>22</sup> The net loss in image luminance goes as  $1/N$ , since there are  $N$  sources. Consider the previous example given for the direct projection case, but with several new parameters.

Suppose

$$\lambda_1 = 488 \text{ nm}$$

$$P(\lambda_1) = 0.5 \text{ W}$$

$$V(\lambda_1) = 0.191$$

$$\lambda_2 = 514.5 \text{ nm}$$

$$P(\lambda_2) = 0.5 \text{ W}$$

$$V(\lambda_2) = 0.608$$

$$G(\theta) = 1 \text{ (Lambertian screen)} \quad A_T = 5000 \text{ cm}^2 \text{ (22 x 30 inches)}$$

$$(\eta_1) = 0.1$$

$$\eta(\lambda_2) = 0.1$$

$$n = 2$$

and

$$\epsilon_R \epsilon_L \epsilon_S = 0.5 \text{ (five percent luminance uniformity)}$$

then,

$$L_H = 2/\alpha$$

Thus, 1 W of input laser power evenly divided between 488  $\mu\text{m}$  and 514.5  $\mu\text{m}$  provides  $2/\alpha$  fL of image luminance. When  $\alpha = 1$  (uniform display, no information content),  $L_H = 2$  fL; however, when  $\alpha = 0.1$ , which is more typical,  $L_H = 20$  fL.

Compare this with a single wavelength hologram for which  $n = 1$ ,  $\lambda = 514.5 \text{ nm}$  and  $P_0 = 1 \text{ W}$ . In this case

$$L_H = 12.2/\alpha$$

$$= \begin{cases} 1.2 \text{ fL for } \alpha = 1 \\ 122 \text{ fL for } \alpha = 0.1 \end{cases}$$

Clearly, single wavelength recording and readout with a high visibility laser wavelength is the best way to obtain high image luminance.

Finally, it is instructive to compute the ratio of  $L_H$  to  $L_D$ .

We find that

$$\frac{L_H}{L_D} = \frac{\epsilon_R \eta}{\alpha \epsilon_0 \epsilon_U} \quad (2.26)$$

This equation makes clear why holography generally provides higher image luminance. The value of  $L_H/L_D$  is inversely proportional to the signal

forming inefficiencies represented by  $\alpha$ ,  $\epsilon_0$ , and  $\epsilon_U$ . The ratio  $L_H/L_D$  is sometimes called the reconstruction ratio because it compares diffracted image luminance with throughput image luminance. Generally,  $\epsilon_R = \epsilon_0$  and  $\eta = \epsilon_U$ , and thus

$$L_H/L_D = 1/\alpha$$

and

$$1 \leq L_H/L_D < \infty$$

since  $1 \geq \alpha > 0$

In our experimental work  $\alpha$  ranged from 0.01 to 0.4 and hence,  $L_H/L_D$  ranged from 2.5 to 100.

#### 2.2.2.4 Hardcopy Reproduction

Hardcopy reproduction is discussed in detail in Section V. Here, we analyze several considerations relevant to this reproducer function. In particular, we provide background on recording time, recording materials, and the film platen.

The recording time required to reproduce a microstored repromat is a function of the optical efficiency of the reproducer and the type of recording material. In the preceding paragraph we discussed image luminance; the same considerations apply here. That is, the amount of light per unit area at the full scale image plane can be determined by analyzing in terms of diffraction efficiency, laser power, and so forth. Therefore, we can show that the average irradiance  $I_{RH}$  in  $\mu W/cm^2$  at the film platen for a holographic reproducer is:

$$I_{RH} = \epsilon_R \epsilon_L \eta P_0 / \alpha A_T \quad (2.27)$$

where  $\epsilon_R, \epsilon_L, \eta, P_0, \alpha$ , and  $A_T$  are as defined in Paragraph 2.2.2.3.2.

The exposure requirement  $E_{RH}$  in  $\mu J/cm^2$  to reproduce a full scale map separation is:



$$E_{RH} = I_{RH} \tau_{RH} \quad (2.28)$$

where  $\tau_{RH}$  is the exposure time.

As an example, suppose

$$\epsilon_R \epsilon_L = 0.5$$

$$P_O = 500 \text{ mW}$$

$$\eta = 0.1$$

$$\alpha = 0.1$$

$$A_T = 5000 \text{ cm}^2 (\sim 22 \times 30 \text{ inches})$$

and

$$E_{RH} \approx 10 \mu\text{J}/\text{cm}^2 \text{ (for Kodak SS7 Duplicating Film)}$$

then

$$I_{RH} = 50 \mu\text{W}/\text{cm}^2$$

and

$$\tau_{RH} = 0.2 \text{ second}$$

By way of comparison, in the direct projection case we can show that the average irradiance  $I_{RD}$  is:

$$I_{RD} = \epsilon_O \epsilon_U \epsilon_L P_O / A_T \quad (2.29)$$

and

$$E_{RD} = I_{RD} \tau_D \quad (2.30)$$

where

$\epsilon_O$ ,  $\epsilon_U$ ,  $\epsilon_L$ ,  $P_O$ , and  $A_T$  are as defined in Paragraph 2.2.2.3.1.

Suppose that

$$\epsilon_O \epsilon_U \epsilon_L = 0.02 \text{ (no screen; } \epsilon_S = 1)$$

$$P_O = 500 \text{ mW}$$

and

$$A_T = 5000 \text{ cm}^2$$

then

$$I_{RD} = 2 \text{ } \mu\text{W}/\text{cm}^2$$

and

$$\tau_{RD} = 5 \text{ seconds}$$

Thus, the holographic reproducer is capable of generating map separations considerably faster than a direct system. This has important implications for rapid map and chart generation in tactical environments.

We chose Kodak SS7 Duplicating Film for our example because it is the film used for hardcopy reproduction. From experimental measurement we found that SS7 film is a very high contrast, high-resolution graphics art film; it is also positive working, which is a natural requirement because of the polarity of the film chips. The exposure requirement for clearing SS7 film at  $\lambda = 514.5 \text{ nm}$  is about  $10 \text{ } \mu\text{J}/\text{cm}^2$ . There are faster graphic arts films suitable for reprostat production; thus, exposure times for silver halide films will generally be less than or equal to those of our examples.

A more challenging mode of reproduction is to expose a pressplate directly. There are two fundamental reasons why this is difficult. First, many pressplate materials are only sensitive to UV light; second, most pressplate materials have a low exposure sensitivity. The wipe-on and presensitized diazo pressplates currently used at DMA production centers are examples.

There are, however, several potential pressplate systems that have both visible light sensitivity and a low exposure requirement. The most promising of these are electrophotographic; several new photoresists and photopolymers are also candidates. The electrophotographic materials can have

panchromatic sensitivity and an exposure requirement of less than  $10 \mu\text{J}/\text{cm}^2$ . Photoresists and photopolymers can have orthochromatic sensitivity and an exposure requirement of  $10^3$  to  $10^5 \mu\text{J}/\text{cm}^2$ .

Consider a worst-case example. Suppose we use a photoresist that requires  $5 \times 10^4 \mu\text{J}/\text{cm}^2$  exposure at 514.5 nm. If we select the largest reliable commercial argon laser, we can obtain about 5 W of power<sup>23</sup> at  $\lambda = 514.5 \text{ nm}$ . With  $\epsilon_R \epsilon_L = 0.5$ ,  $\eta = 0.1$ ,  $\alpha = 0.1$ , and  $A_T = 5000 \text{ cm}^2$ , we obtain  $I_{RH} = 0.5 \times 10^3 \mu\text{W}/\text{cm}^2$  and  $\tau_{RH} = 100$  seconds.

If we take into account the fact that several map separations are generally overlayed to form the five color plates, then the exposure per map separation is even less. Clearly, the overall exposure will be less than 2 minutes. This compares favorably with the 3 to 6 minute exposure per map separation, using multikilowatt mercury or xenon arc lamps, required to expose wipe-on diazo pressplates.

Finally, the design, procurement, test, and integration of the hardcopy reproduction film platen, as discussed in Section V, represents a major achievement of the MEGIS Program. With this device, we were able to repeatably maintain image distortion relative to the film at the  $\pm 2$ -mil rms level. The device consists of a transparent electrostatic film platen mounted in a precision gimbaled frame, which in turn was mounted on overhead rails with up to 10 feet of translation to allow for different repro sizes. Angular rotations as fine as a few milliradians are possible on both the  $\theta$  and  $\phi$  axes; translation along the optic axis can be maintained with a precision of 2 to 3 mils. The film holder can also be used as a transparent copy easel. Hence, a single mechanical device can function as a microreduction camera, as a film platen, and as a display screen with a sheet of frosted



mylar added. As will be clear from the discussion of Section V, this subsystem is fully qualified for repromat production.

### 2.2.3 Problem Areas

We have alluded to several problem areas that have had a major impact on the results of the MEGIS Program. We now focus our attention specifically on these problem areas. Major problem areas are the following:

1. Scratches, dust, phase errors (for example, orange peel), and so forth on the film chips
2. Nonuniform density and resolution over the film chips
3. Coherent noise generated by dust, scratches, and other imperfections on the microreduction and enlargement lens (in this case the Wray Micro Lens)
4. Speckle noise caused by the use of a diffuse phase randomizer with which we had intended to minimize or eliminate problems 1 and 3
5. The optical mismatch between the imaging subsystem (10 inch Wray Micro Lens,  $f/5.6$ ) and the holographic subsystem (150 mm Fourier-transform lens,  $f/1.2$ )
6. The field-of-view limitation and nonoptimum Kohler projection condition that results when the hologram is recorded near the back surface of the projection lens
7. The phase errors and aberrations caused by the polyester film base which lead to significant resolution loss and broken line images

With the exception of the film base problem, the other problems have tenable solutions. Liquid gates can be used to eliminate phase errors.

Careful control over positioning, focus, exposure, and processing together with a clean-room type working environment should minimize problems caused by dust, scratches, and nonuniform resolution and density. Coherent noise generation by the projection lens can be reduced by designing a laser light equivalent of the Wray Micro Lens. With these changes, it may be possible to eliminate the diffuse phase randomizer, and with it, most of the speckle noise. The optical mismatch problem can be solved by either decreasing the film chip size or increasing the speed (lower  $f/\text{number}$ ) of the projection lens; practical considerations suggest that both steps are necessary. Decreasing film chip size, of course, forces a proportional increase in hologram size. But this is just the required solution to the limited field-of-view and nonoptimum Kohler projection condition. By appropriate choice of the various recorder parameters, we can simultaneously obtain optimum performance from both the optics and the hologram.

The film base problem is more fundamental. Although index matching in a liquid gate is helpful, it does not completely eliminate phase errors and aberrations. Moreover, a glass index matching cell of typical thickness (often 1 to 2 inches) placed in the path of a highly convergent beam causes astigmatism and spherical aberrations. (This and other resolution-limiting factors are discussed in parts of Sections IV and V.) Photographic emulsions on microflat glass substrates were used during several phases of the program both with and without index matching; this improved image resolution but is not a satisfactory solution, especially in a tactical environment. At this time, the film base problem does not have a completely satisfactory solution.

Neither the resources nor the direction of the MEGIS Program permitted implementation of the suggested problem solutions. It is recommended that any future effort provide sufficient latitude for the parameter trade-offs needed to optimize the optical system design. The Fourier-transform recorder/reproducer concept is still theoretically optimum. Successful future implementation may be possible with a relatively concentrated effort on reducing to practice the problem solutions suggested in this discussion.

### 2.3 ALTERNATIVE RECORDER/REPRODUCER CONCEPTS

In view of several fundamental problems associated with the Fourier-transform holographic recorder/reproducer concept, we analyzed several alternative concepts. Since the objective is to improve the state of the art of cartographic microstorage and retrieval, we include direct projection, which is nonholographic, as a candidate approach. In succeeding paragraphs, we discuss Fresnel, Kohler-TIR, and Space Invariant holographic recorder/reproducer concepts. We begin with a comparison of Fresnel and Holographic and Direct Projection systems, and then discuss the more novel Kohler-TIR and Space-Invariant approaches.

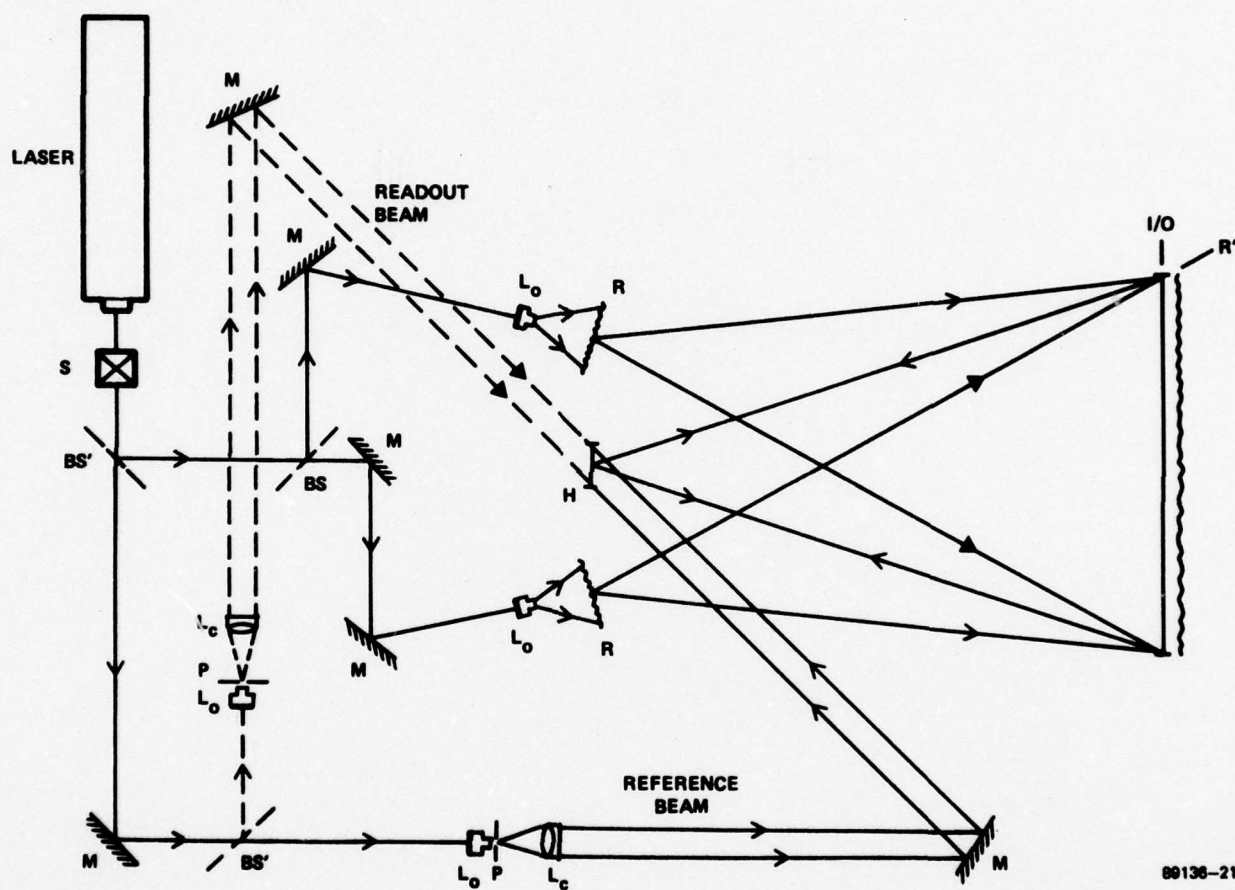
#### 2.3.1 Fresnel Holography

Fresnel holography is an elegant, though not completely satisfactory, approach to the storage of graphic information.<sup>24</sup> It has two advantages that merit special note. First, there are no intermediate steps; both storage and retrieval are direct without the need for film chips. Second, no lenses are required either for microreduction or enlargement. This is an especially important consideration for both tactical and production



center applications in which duplication of originating facilities and subsystems is not feasible. Of course, the redundant storage and high efficiency retrieval advantages of holograms are retained.

The principle of operation of the proposed Fresnel holography technique can be understood with the aid of Figure 2-6. For storage, the unexpanded beam of an argon laser is divided by a variable beam splitter BS' after passing through an electromechanical shutter S. The transmitted portion of the beam is directed by the mirror M to a second variable beam splitter BS' that is either completely transmitting for storage or completely reflecting for retrieval. After passing through BS', the laser beam is expanded with a microscope objective  $L_0$ , filtered with a pinhole P, and collimated with the lens  $L_c$ . This beam, which is the reference beam, is directed by a mirror M to the hologram recording plane H. The laser beam reflected by the first variable beam splitter is further divided into equal beams by a constant beam splitter BS to provide two illuminating beams. Each of these beams is directed by mirrors M to microscope objectives  $L_0$  which expand the beams; the expanding beams illuminate phase randomizers R. The light transmitted and distributed by each element R illuminates a Lambertian type reflecting and diffusing screen R'. The light reflected and diffused by R' is modulated by a full scale map separation T to form a signal beam at H, which then interferes with the reference beam. The interference pattern generated by mixing the signal and reference beams is recorded on a light-sensitive material, such as a photographic film, to form a hologram. For retrieval, the first variable beam splitter is made fully transmitting, while the second is adjusted to be fully reflective. A readout beam is formed in a manner exactly analogous to



89136-21

Figure 2-6. Schematic Layout of a Fresnel Hologram Recorder/Reproducer

that of the reference beam, and is shown by the dashed-line optical path in Figure 2-6. The symmetry of the reference and readout beam paths assures accurate realignment. When the hologram is illuminated with the readout beam, the conjugate of the original signal wave is reconstructed. This wave forms a full scale image of the original map separation at the graphic input/output plane. This image is available for either photographic or pressplate hardcopy reproduction, or for visual display.

From an implementation viewpoint the system illustrated in Figure 2-6 is both the recorder and reproducer. The entire system can be fabricated as a single unit, which enhances both controllability and repeatability. This format is particularly suitable for use in a map production environment. For tactical applications, a separate reproducer can be fabricated that incorporates only a laser, optics to form a collimated readout beam, a hologram storage unit, and a hardcopy reproduction film holder. The reproducer can be produced in a fixed-geometry, single-unit format. This feature greatly minimizes the possibility of misfocus and distortion.

There are several disadvantages to Fresnel holography that merit discussion. First, lateral translation invariance is no longer obtained. However, depth of focus is comparable to that of Fourier-transform holography. Second, speckle noise is present. For a 20 mm x 20 mm hologram, a speckle will be about 30  $\mu\text{m}$  in size; hence, a 3-mil pixel will have about 6 speckles/3-mil pixel. This is similar to the Fourier-transform hologram and is generally not acceptable. Increasing the hologram size to 40 mm x 40 mm reduces speckle size to 15  $\mu\text{m}$ , and results in 25 speckles/3-mil pixel. This is comparable to spatially coherent direct blowback using the Wray Micro Lens at  $f/4$  and  $\lambda = 514.5 \text{ nm}$ , which appears from experimental data to approach



the threshold of acceptability for cartographic printing. Increasing the hologram size to 75 mm x 75 mm yields 7.5  $\mu$ m speckles and 100 speckles/3-mil pixel. This speckle density is sufficient to render speckle noise negligible. An alternative to increasing hologram size to reduce speckle noise is the use of two recording wavelengths, e.g.  $\lambda = 488$  and 514.5 nm. The size and periodicity of the speckle patterns differ as a function of  $\lambda$ . The result is a fill-in effect that significantly smoothes the discontinuous speckle pattern.

Specifications for recorder/reproducer formats for storing and retrieving 22 x 30 inch and 48 x 60 inch map separations are summarized in Table 2-7. As an example, we have chosen a single wavelength, 20X reduction system. A 10 W cw argon laser is specified in order to obtain a relatively short hologram recording time. The laser power level is determined by the considerable inefficiency of the hologram recording process. That is, after obtaining single wavelength and single mode and single mode operation at 514.5 nm, only about 2.5 W of power is available. Of this amount, less than 1 part in 10,000 will be available in the signal beam at the hologram recording plane because of various system inefficiencies. Nonetheless, we estimate that with  $K = 4$  the exposure time on a film such as Kodak SO-343 will be less than 10 seconds for 22 x 30 inch map separation and less than 40 seconds for 48 x 60 inch map separations. All parameters listed in Table 2-7 except for the storage format, meet or exceed recent contract requirements.

### 2.3.2 Direct Laser Projection Recorder/Reproducer

A direct projection laser recorder/reproducer offers several advantages relative to a holographic system. Storage is accomplished with a single step to obtain a 70 mm or small film chip format for map separations

Table 2-7. Fresnel Holography Recorder/Reproducer Specifications

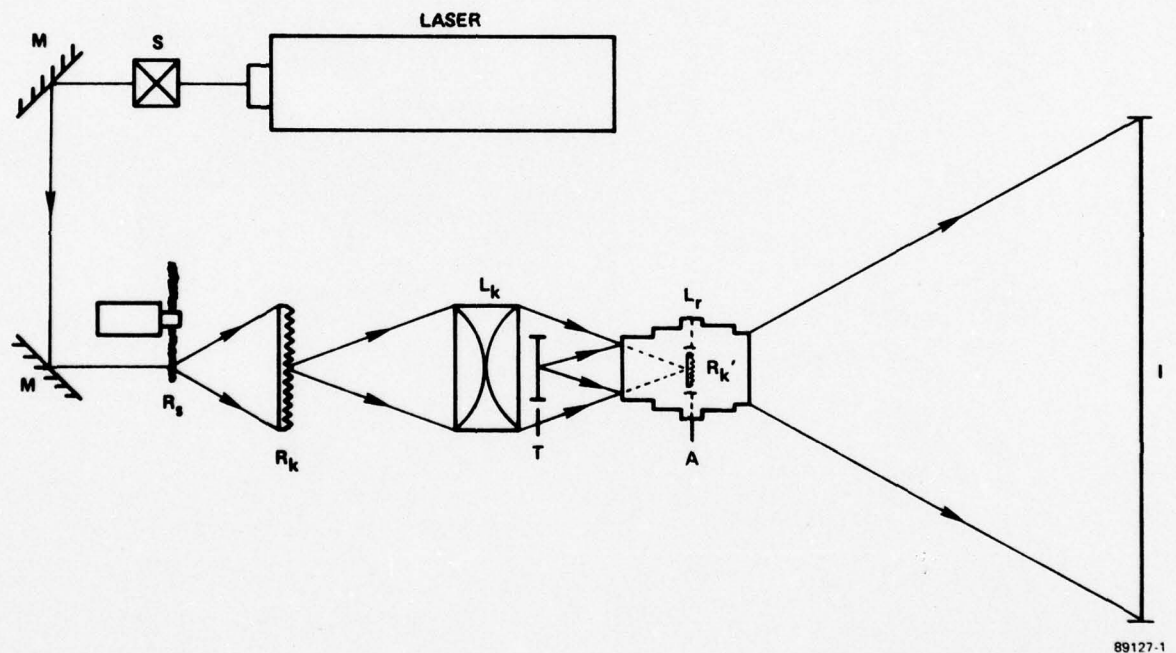
<u>Parameter</u>	<u>22 x 30 inch Map Separations</u>	<u>48 x 60 inch Map Separations</u>
Storage Format	40 mm x 40 mm	80 mm x 80 mm
Reduction	20X	20X
Laser	10 W cw argon $\lambda = 514.5 \text{ nm}$	10 W cw argon $\lambda = 514.5 \text{ nm}$
Hologram Recording Time	<10 sec	<40 sec
Diffraction Efficiency	>10%	>10%
Signal-to-Noise Ratio	>15 dB	>15 dB
Resolution (Full-Scale)	33 cyc/mm	33 cyc/mm
Distortion	< 2-mil rms	< 2-mil rms
Luminance Uniformity	$\geq 10\%$	$\geq 10\%$
Luminance	60 fL (Min) 120-600 fL (typical)	15 fL (Min) 40-150 fL (typical)
Image Irradiance	50 $\mu\text{W}/\text{cm}^2$ (min) 100-500 $\mu\text{W}/\text{cm}^2$ (typical)	12.5 $\mu\text{W}/\text{cm}^2$ (min) 25-125 $\mu\text{W}/\text{cm}^2$ (typical)
Speckle Size	$\sim 15 \mu\text{m}$	$\sim 15 \mu\text{m}$
Speckles/3-mil Pixel	25	25

ranging in size from 22 x 30 inches to 48 x 60 inches. A high degree of interferometric stability is not required, nor is a stable single-frequency laser.

Several disadvantages are worth noting. As mentioned in Paragraph 2.1, a 20 mm x 20 mm format does not appear feasible. Furthermore, to obtain a 35 fL luminance level, a relatively high-power argon laser is required. However, after we became better acquainted with DMA map and chart production requirements and some of the practical limitations of Fourier-transform holography, a reexamination of the direct laser projection approach was initiated, despite these apparent disadvantages. The result of the study was positive, provided a storage format greater than 20 mm x 20 mm is acceptable.

A breadboard laser projection system is shown schematically in Figure 2-7. The light source is an argon laser that is operating both multiline and multimode; most of the output power is obtained from the 488 nm and 514.5 nm wavelengths. The unexpanded laser beam passes through an electromechanical shutter  $S$ , is folded by the mirrors  $M$ , and finally, illuminates a rotating ground glass phase randomizer  $R_S$ . The rotation of  $R_S$  destroys the spatial coherence of the laser beam, and hence, eliminates the problem of speckle noise. The laser light transmitted by  $R_S$  in turn illuminates a stationary ground glass phase randomizer  $R_K$ , which serves as the apparent light source for the subsequent projection system. The condenser lens system  $L_K$  images  $R_K$  into the pupil  $A$  of the Wray microreduction and enlargement lens  $L_R$ ; this satisfies the Kohler projection condition. The film chip  $T$  is positioned so that it is imaged full scale by  $L_R$  at the graphic input/output plane  $I$ .





89127-1

Figure 2-7. Schematic Layout of a Direct Projection Recorder/Reproducer

This concept was experimentally investigated. No special components were required to fabricate the breadboard. A Spectra Physics Model 165 or Coherent Radiation CR2 argon laser (which is also suitable for holographic recording) was used unmodified as the light source. Actually, for this application there is considerable advantage in using a much less sophisticated laser. That is, an argon laser that is randomly polarized and that operates in more than the fundamental  $TEM_{00}$  spatial mode. These modifications yield both higher output power and a more uniform beam intensity profile. The phase randomizers were ground glass and the condenser lens systems one or more simple planoconvex lenses. The Wray Micro Lens is, of course, a lens of exceptional imaging quality though expensive. However, there are several commercial alternatives available, e.g., the Nikon 250 mm Ultra-Micro-Nikkor.

The performance of the breadboard system is summarized in Table 2-8. The data show that for a 70 mm storage format (10X reduction of a 22 x 30 inch map separation) we obtained 20 dB contrast, more than 228 cycles/mm resolution, rms distortion of less than 2-mils, about 5 percent luminance uniformity, approximately 2 fL image luminance for 1 watt of input laser power, and excellent image quality. (We mention that the projection of continuous tone information was characterized by similar imaging characteristics.) The projection of 70 mm film chips of 48 x 60 inch map and chart separations reduced 20 X was also studied. The level of performance was generally equal to that obtained for 22 x 30 inch map separations, but image luminance was reduced by about a factor of four because of the larger image area.

Table 2-8. Best Performance of a Direct Laser Recorder/Reproducer (22 x 30 Inch Repromats)

Parameter	Goal	Actual	Comments
Size	20 mm x 20 mm	66 mm x 82.5 mm	Conventional Micro-reduction to a 35 mm format is feasible
Efficiency	10%	<1%	Improvement possible
Contrast	15 dB	20 dB	Provides excellent hardcopy and displays
Resolution	125 cyc/mm	> 228 cyc/mm	Limited only by resolution of transparency
Distortion	<2-mil rms	<1-mil rms	Typical; relative to film base dimensional changes
Uniformity	>10%	~5%	
Luminance	35 fL	~2 fL	For 1 watt of input laser power; more than 20 fL feasible; not dependent on information content
Image Quality	No image defects	No image defects	Suitable for both visual displays and hardcopy reproduction

These results, while impressive, do not satisfy contract requirements for either storage format or image luminance. With regard to storage format size, we believe that storage formats as small as 35 mm (20X reduction) are feasible for 22 x 30 inch map separations. The Nikon 25 mm Ultra-Micro-Nikkor lens, which is designed for 20:1 microreductions at high resolution and with negligible distortion, is suitable for this purpose. A 70 mm storage format is the minimum size judged usable for 32 x 48 inch and 48 x 60 inch map separations. The image luminance problem can be solved by two



changes to the current breadboard: first, a more efficient optical system can be designed and second, a more powerful laser can be specified. Optical system efficiency improvements should provide a minimum image luminance increase of two; another factor of 10 is easily obtained by the use of a commercial 10 W argon laser. If 10 percent luminance uniformity is acceptable, then another luminance gain of two is possible. Scaling of the film chip does not affect luminance level, but may ease or increase the difficulty of obtaining a particular luminance uniformity level. In sum, increases in image luminance of between 20 and 40 times appear possible without new technology development.

With the suggested improvements a direct laser recorder/reproducer with specifications such as those summarized in Table 2-9 can be implemented. Although this system does not satisfy all current contract requirements, it nevertheless represents a workable and significant first step toward the microstorage of cartographic information. Overall performance of the system meets or exceeds the specifications on important parameters such as contrast, resolution, distortion, and cosmetic quality. Hardcopy reproduction to form repromats on films such as Kodak SS7 duplicating film or to directly expose electrophotographic pressplate materials can be accomplished with exposure times of less than 1 second. We mentioned that color proofs generated at ETL from map separations, produced on this program with a breadboard direct laser recorder/reproducer, were found to be comparable to those made by conventional techniques.

Finally, we note that a laser system enjoys several advantages over a conventional high pressure arc lamp system. First, there is no danger of heat distortion. Second, operation in the visible spectrum allows the use of

AD-A051 532

HARRIS CORP MELBOURNE FL ELECTRO-OPTICS DEPT

F/G 14/5

MICRO-REDUCTION AND ENLARGEMENT OF GRAPHIC INFORMATION STUDY (M--ETC(U)

DEC 77 R G ZECH, L M RALSTON, B R REDDERSEN

DAA653-75-C-0155

UNCLASSIFIED

HESD/EOD-1624-F

ETL-0063

NL

2 OF 5

AD  
A051 532



Table 2-9. Projected Direct Laser Recorder/Reproducer Performance

Parameter	22 inch x 30 inch Map Separations	48 inch x 60 inch Map Separations
Storage Format	32 mm x 38 mm	61 mm x 76 mm
Reduction	20X	20X
Laser	10 W cw multimode argon	10 W cw multimode argon
System Efficiency	~4%	~4%
Contrast	~20 dB	~20 dB
Resolution	>228 cyc/mm	>228 cyc/mm
Distortion	<1-mil rms	<1-mil rms
Luminance Uniformity	~10%	~10%
Luminance	~32-64 fL	~8-16 fL
Image Irradiance	~40-80 $\mu\text{W}/\text{cm}^2$	~10-20 $\mu\text{W}/\text{cm}^2$

the best available optics and coatings. Third, controllability and repeatability are significantly better. Finally, the use of visible light sensitive electrophotographic pressplates, e.g., those made by Azoplate, S.D. Warren and Coulter Information Systems, allow the rapid generation of color proofs and pressplates.

### 2.3.3 Kohler-TIR Holography

Kohler-TIR (total internal reflection) holography<sup>25</sup> combines features of holography, Kohler projection, and incoherent superposition in volume phase recording materials. Storage is achieved in two steps. First a repromat is microreduced to form a film chip of the graphic information. Then, as shown in Figure 2-8a, the film chip is stored in a TIR hologram.



# KOHLER-TIR HOLOGRAPHY

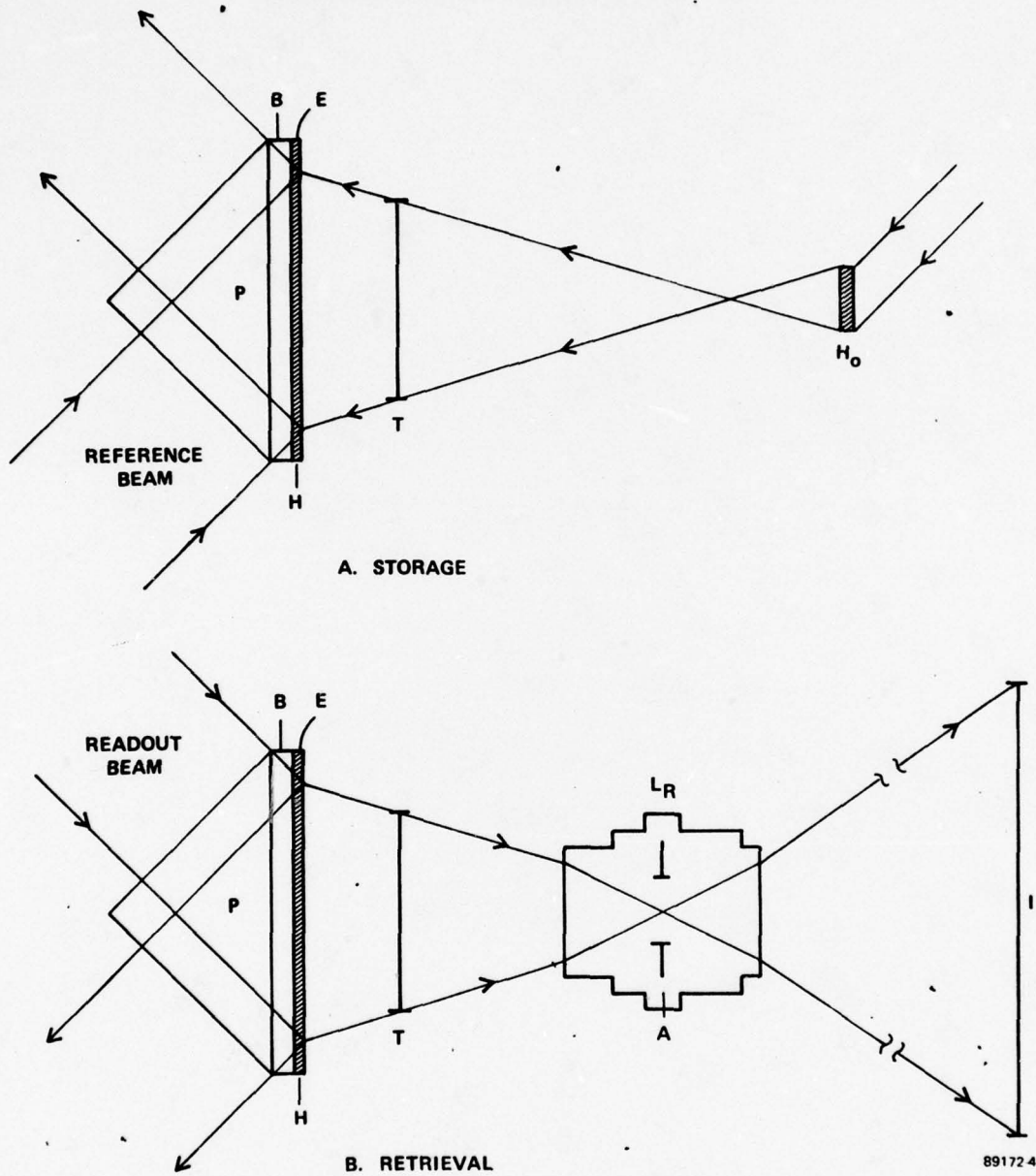


Figure 2-8. Basic Concepts of Kohler-TIR Holography

Finally, the TIR hologram is read out to form a real image of the film chip, as shown in Figure 2-8b, which is then projected by the enlargement lens to form a full scale map separation image.

Details of the storage process shown in Figure 2-8a are as follows. The film chip T is illuminated by a uniform, divergent wave diffracted by a holographic optical element  $H_0$ . Light transmitted and diffracted by the film chip is incident upon a light-sensitive surface E, which is coated on a plastic or glass substrate. The recording material substrate B is index matched to the base of an isosceles prism P. A plane wave of light enters the lower face of the prism, propagates to the surface of the recording material, and is reflected because of total internal reflection. The reflected plane wave, which functions as a reference beam, interferes in the light-sensitive layer with the light wave modulated by the film chip to form a transmission hologram (a reflection hologram is simultaneously formed, but can be eliminated by using laser light polarized parallel to the plane of incidence, i.e., the plane of the schematic drawing). If the light-sensitive layer is a phase medium about  $100\text{ }\mu\text{m}$  thick and if the angular orientation of the reference beam is variable to the extent of  $\pm 1^\circ$  around its initial position, a large number of film chips can be stored in the same volume of the recording material and later independently retrieved with excellent diffraction efficiency and signal-to-noise ratio. We mention that high image resolution is a general characteristic of TIR holograms; the full scale graphic images have resolution limited only by the enlargement lens (which is always assumed to be the microreduction lens or equivalent). Also, as 30 or more film chips (the largest number of color map

separations required for a single map is about 33; an average number is about 20) are stored in the same block of recording material, the information packing density is quite high.

The retrieval process shown in Figure 2-8b is straightforward. A plane wave of light enters the upper face of the prism, propagates to the interface of the light-sensitive layer where it is again totally reflected, and leaves the prism through its lower face. The incident plane wave, if it satisfies the Bragg condition, functions as a readout beam, since its propagation direction is the required conjugate to the original reference beam. It reconstructs a wave whose complex amplitude forms a converging real image of a film chip. Bragg angular orientation sensitivity suppresses the readout of other film chip holograms. The light rays (the dc part of the film chip image) converge in the pupil A of the enlargement lens  $L_R$ , and thus satisfy the Kohler projection condition. The enlargement lens, of course, forms a full-scale image of the film chip. These last details make evident the reason for calling this recorder/reproducer concept Kohler-TIR holography.

The Kohler-TIR concept eliminates or minimizes the problems associated with Fourier-transform holography. Resolution and field-of-view are no longer dependent on hologram size. The hologram is now behind the film chip, and thus cannot effect the imaging process. Film base scatter and phase errors have a negligible effect on contrast and resolution of the full scale image. Astigmatism and spherical aberrations because of the image light rays converging in the hologram or in a liquid gate are eliminated. There is no f/number mismatch between the holographic and imaging subsystem. Realization of the Kohler projection condition ensures maximum resolution, luminance, and



luminance uniformity in the projected map separation image. Moreover, the overall system is relatively simple, with a potential for stable operation in either a production or a tactical environment.

#### 2.3.4 Space-Invariant Holography

Space-invariant holography is another method for overcoming the limitation of film base phase errors and speckle and cosmetic noise. The basic idea is to record holograms with spatially incoherent light. In the present case, we are interested in laser light having several wavelengths, e.g., argon laser light. The holographic recorder utilizes gratings for both beam splitting and directing. The signal and reference beams travel separate paths, and every light ray in each of these beams travels an optical path whose length and form are a function only of its initial angular orientation, and not its initial position. Hence the name spatial invariance. The advantages of this method is that source coherence imposes no limit on object size, hologram size, or the number of fringes generated. Leith and Chang<sup>26</sup>, who developed the modern theory of space-invariant interferometers, have reduced to practice this method of recording holograms. Using tungsten or xenon arc lamps, they have produced high-contrast polychromatic interference fringes of exceptional quality (no speckle noise or Fresnel rings) with which both grating and holograms of phase objects were recorded. Since a high pressure Hg-arc lamp can be used, holographic images rich in UV light can be projected to expose conventional diazo pressplates.

A space-invariant holographic recorder/reproducer concept we propose is illustrated in Figure 2-9. The schematic diagram shows an unexpanded laser beam passing through the shutter S and being directed by the mirror M to the microscope objective  $L_0$ , pinhole P, and collimator  $L_c$ .

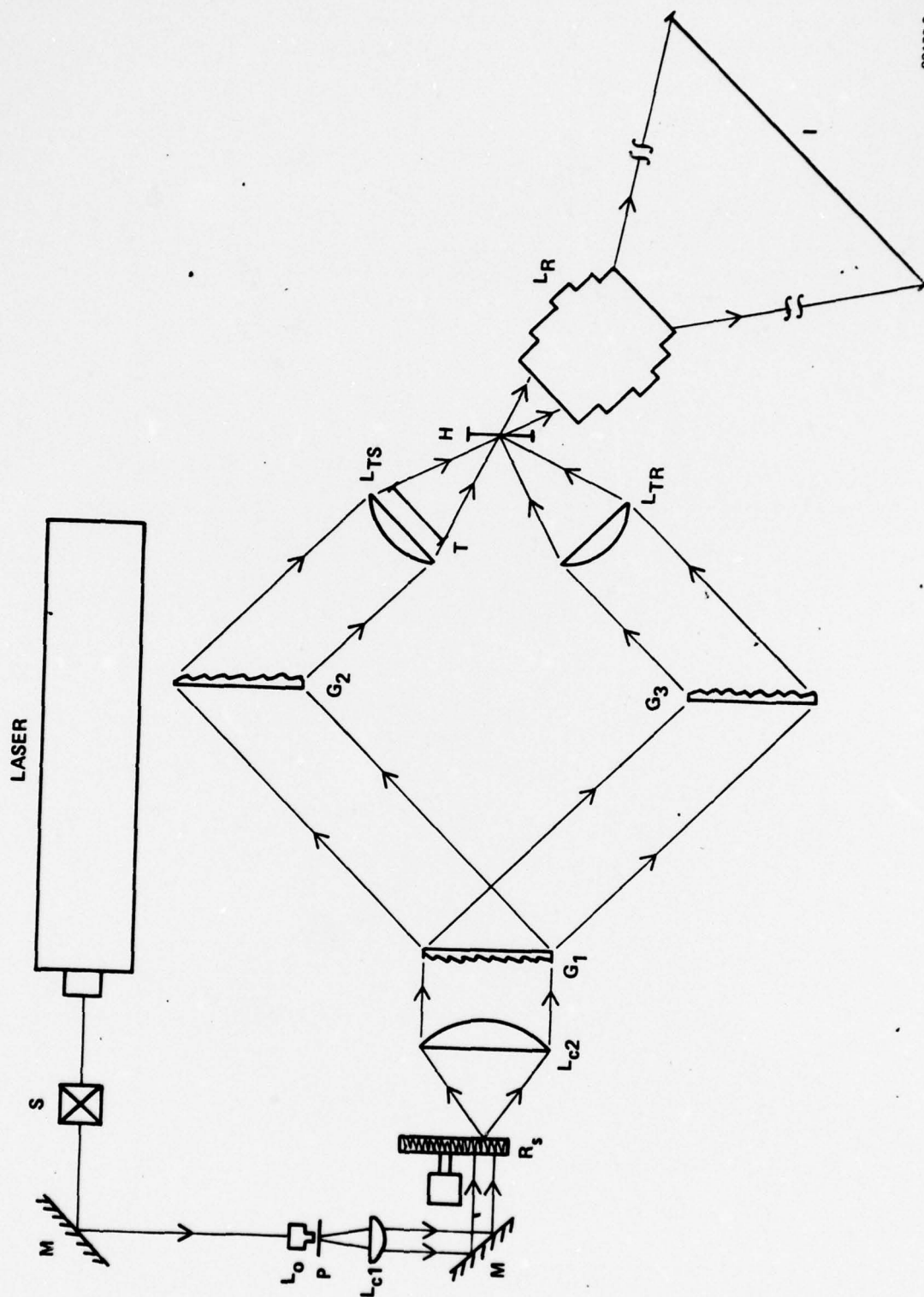


Figure 2-9. Schematic Layout of a Space-Invariant Holographic Recorder/Reproducer

where a spatially-filtered and collimated beam is formed. The collimated beam is directed by a second mirror M so that it illuminates a spinning ground glass diffuser  $R_S$ . This illuminated area of  $R_S$  acts like a monochromatic, but spatially incoherent, light source. The light transmitted by the diffuser is recollimated with the lens  $L_{C2}$ , and is used to illuminate the holographic grating  $G_1$ . The beams diffracted by  $G_1$  form the signal and reference beams, each of which is diffracted again by the holographic gratings  $G_2$  and  $G_3$ . The "Fourier-transform" lenses<sup>27</sup>  $L_{TS}$  and  $L_{TR}$  each image the incoherent source  $R_S$  onto the hologram recording plane, where the resultant interference pattern can be used to expose a holographic film. The storage of map separations takes place when the signal beam is modulated by film chips in the usual way. After processing, the hologram is illuminated with the reference beam to form a virtual image of T which is imaged full scale by the microreduction and enlargement lens  $L_R$ . Baseline experiments in support of this technique are discussed in Section IV.

The space-invariant recorder/reproducer is a holographic analog to the classical Mach-Zhender interferometer. As such, stability and high precision mechanical components are basic requirements. We found in our experimental work that these conditions are not difficult to meet if relatively massive components are used to mount the gratings. In view of the potential advantages of this approach, this may be acceptable for a system to be used in a production environment. For tactical environments the opposite is probably true.



## 2.4 SPECIAL CONSIDERATIONS

In this section we briefly discuss several considerations that are of key importance to the design, operation, and performance of either a holographic or direct recorder/reproducer. We chose film chips, aberrations, lasers, and optics for special discussion because of their impact on the outcome of the program. Other key considerations will be discussed in other parts of the report.

### 2.4.1 Film Chips

We used Government-supplied 70 mm x 100 mm positive transparencies (film chips) of map separations for holographic storage and playback. There were several reasons for this choice. First, a positive transparency generally is optimum for holographic storage because it provides a high level of redundancy removal, i.e., bandwidth compression. We assume, of course, that the original map separation has clear lines or annotations on an opaque (black) background or is binary with a relatively small clear area duty factor. Obviously the opaque regions contain no map details. Second, the use of a positive transparency serves to minimize the dynamic range requirement on the recording material and to improve signal-to-noise ratio in the reconstructed image. Moreover, less laser power is needed to maintain a specified image brightness level. Some relief of viewer eye fatigue and a general increase in viewer comfort is also obtained.

Map separations are microreduced in a precision optical system and recorded on photographic film. The resultant film chips must meet various baseline system requirements. For the present system concept, one requirement is that 10X to 20X reductions of 22 x 30 inches and 48 x 60 inches, respectively, map separations fit a common format; the 70 mm x 100 mm film chip

size satisfies this requirement. The film chip base material should be dimensionally stable to minimize distortion; this dictates the selection of a recording film with a polyester base as opposed to triacetate. The MTF of the film chip recording material must be 50 percent or greater at 125 cycles/mm. Image contrast must be high to maintain the binary nature of the reprostat. Careful exposure and processing are obvious requirements. More detailed consideration of recording materials for film chip production can be found in Section III. Since the microreduction camera uses mercury lamps with principal output at 546 nm for transilluminating the original, full-scale map separation, the film chip must be recorded on an orthochromatic film. Finally, because coherent light is used to illuminate the film chip in the optical recorder, scratches, orange peel, and other surface defects must be minimized. These and other considerations lead to the selection of Kodak S0-141 Holographic Recording Film as the primary recording material. Although S0-141 is negative working, several standard reversal processes are available to provide a positive imaging mode.

The film chips produced on S0-141 were adequate for projection to full scale with incoherent light. However, they were not satisfactory for coherent light projection or holography. Phase and scatter noise from the film chips were a primary reason for using a diffuse phase randomizer. Our experience on this program suggests that film chip production must be significantly improved.

#### 2.4.2 Aberrations

There are three potential sources of aberrations. Aberrations can be caused by the microreduction step, the holographic reconstruction process, or the substrate imperfections of the recording material. By microreducing

and later enlarging the stored cartographic information to full scale with the same lens, we eliminate this source of aberration from the storage and display process. The holographic reconstruction process can cause aberrations because a hologram behaves in some ways as a conventional optical element. Holographic aberrations arise as a consequence of angular misalignment, spectral shift, or distortion of the recording material (e.g., emulsion shrinkage). Since we record and read out with the same laser wavelength, no spectral shifts occur and only angular misalignment and emulsion shrinkage remain as possible causes of aberrations. However, critical angular alignment can be achieved experimentally by registering original and holographic reformat images. Misregistration is indicated by interference fringes; this is discussed in detail in Section V. Adequate alignment tolerances can be achieved in a practical system with precision mechanical devices, as was demonstrated on this program. Recording material distortion, such as shrinkage, can be compensated or avoided [see, for example, "Study of Potential Application of Holographic Techniques to Mapping," M. K. Kurtz, et al., ETL-CR-71-17, October (1971), page 51]. Actually, we were not able to detect holographic aberrations during any phase of experimental work. Finally, over a 20 mm area some aberrations may be generated because of nonuniformity of the recording material substrate (e.g., thickness variations in the photographic film base). This is correctable by use of an index matching gate or by means of protective post-exposure overcoats.

The type of aberration of greatest concern is distortion. From fundamental principles of geometrical optics<sup>28</sup>, we know that distortion can ideally be eliminated and, even in practice, greatly minimized by using telecentric optical systems. We add that for off-axis holograms astigmatism



is by far the dominant type of aberration when these aberrations do occur; distortion is generally negligible [see, for example, "Investigations of Uses of Holographic Optical Elements," R. G. Zech and J. Latta, NASA Final Technical Report, Contract No. NAS 8-28949, May (1973), Appendix A ].

Nevertheless, it was necessary, because of the reproduction requirements for map and other graphics, to measure distortion carefully in order to verify that it was less than the specified limit of  $\pm 2$  mils rms. We used several precision measurement devices (e.g., a Haag-Streit AG, Model A-1 coordinatograph) to measure distortion and to show that the principal contributor to distortion is film shrinkage. Details are given in Section V.

It is not our intention to minimize the potential impact of aberrations on system performance. Clearly, when aberrations are present metric fidelity cannot be maintained, and there will be resolution loss. However, we have determined through experimentation that when a well-designed microreduction and enlargement lens, such as the Wray Micro Lens or Nikon Ultra-Micro Nikkor, is used, together with high-resolution precision mechanical positioning devices, distortion and other aberrations, relative to film shrinkage, are negligible. This was an important initial systems consideration. As the data in Section V show, aberrations need not limit system performance.

#### 2.4.3 Lasers for Cartographic Storage and Displays

Wavelength is important in selecting a laser for the storage of graphic data. It must be compatible both with the limitations of present optical systems, as well as the range of sensitivities of photographic emulsions in general and pressplate materials in particular. This eliminates high-power infrared lasers from consideration because few photographic

materials and no pressplate materials have IR sensitivity. To ensure an image with good tonal qualities, both power stability and low noise become additional factors to consider. Further, since the laser is part of an engineering system, dependability in the form of long operation lifetime, ease of maintenance and minimal repair costs become important. Considered together, these criteria dictate that continuous wave lasers with industrially-proven capabilities be used. Of the varieties commercially available, the lasers which best fit these conditions are Helium-Neon, Argon-Ion, Krypton-Ion, Helium-Cadmium, whose general characteristics are given in Table 2-10, and, to a lesser extent, Helium-Selenium and certain dye lasers.

Helium-Neon lasers are stable, highly reliable, long-lived, inexpensive to purchase, as well as to maintain, require little power to operate, air cooled, and presently mass-produced for industry. One major graphic arts application where the Helium-Neon laser has proved successful is the facsimile-transmission field. Unfortunately for most applications, however, this laser has a relatively low power output, which is available only in the red and infrared; 100 mW at 632.8 nm is about the present state of the art limit. Furthermore, most precision microreduction and enlargement camera lenses are designed for use with the 546 nm Hg line, so wavelength shift aberrations would undoubtedly occur if He-Ne lasers were used. Nevertheless, because of their many advantages over other lasers, they should be considered a strong possibility for use where photographic emulsions with red sensitivity and color-corrected process lenses.

Argon-Ion lasers are the most powerful light sources for UV and blue wavelength graphic arts work available at the present time. One manufacturer, Spectra-Physics, offers a Model 921 laser with a guaranteed

Table 2-10. Typical Laser Parameters

Laser Parameter	Helium-Neon	Helium-Cadmium	Argon-Ion	Krypton-Ion
Wavelengths Available	632.8 nm 1150 nm 3390 nm	325.0 nm 441.6 nm	333.6-528.7 nm	350.7-799.3 nm
Range of Output Power per Line (mW)	0.1-100 1-3 1-10	1-3 1-75	10 50,000	10 2,500
RMS Power Stability	1% to 5%	2% to 10%	0.5% to 10%	0.5% to 10%
RMS Noise	0.1% to 5%	1% to 10%	0.5% to 2%	0.5% to 2%
Size (inches) (L x W x H)	12 x 3 x 2 to 74 x 7 x 9	18 x 4 x 3 to 74 x 6 x 9	18 x 6 x 6 to 86 x 6 x 6	18 x 6 x 6 to 86 x 6 x 6
Power Consumption (watts)	22 to 450	200 to 1,200	500 to >38,000	500 to >38,000
Lifetime (hours)	8,000 to 50,000	700 to 2,000	2,000 to 6,000	~1,000
Repair Cost (\$)	200	1,000	~4,000 w/ UV ~2,500 wo/ UV	~4,000 w/ UV ~2,500 wo/ UV
Price Range (\$)	80 to 5,000	1,800 to 8,000	4,500 to 32,000	5,000 to 20,000
Some Manufacturers	Coherent Radiation Spectra-Physics Hughes Liconix Jodon CW Radiation	Liconix RCA Spectra-Physics	Coherent Radiation Lexel Spectra-Physics Control Laser	Coherent Radiation Lexel Spectra-Physics Control Laser



40 watt all lines output, plus 15 watts at 514.5 nm and 14 watts at 488.0 nm. This much output power is obtained only with the addition of several problem areas of which the more obvious is the large electrical power requirement (in excess of 38,000 watts for some of the larger lasers) and the large size (the laser head for the 18 to 20 watt group ranges up to 86 x 6 x 6 inches and the total weight of the power supply plus laser head is over 600 pounds). A more subtle problem is that high power UV radiation can form color centers on the Brewster windows in these lasers, adding noise and instability while attenuating output power. Coherent Radiation claims it has solved this problem through the production of a new Brewster window material to replace the more common fused silica windows. Noise and power stability are generally very good (typically 0.5 percent rms noise and 0.5-1 percent rms power ripple with light regulation), but mechanical instability of the system is a problem. Lexel uses Invar structural members for thermal stability and Spectra-Physics uses quartz rod resonator supports for mechanical stability. Cooling demands add to the difficulties: the CR-18 requires a minimum of 6 gallons per minute flow to maintain power supply and laser head temperatures. Finally, Argon-Ion lasers are relatively expensive, an important factor for any graphic storage and reproduction system. The characteristics of typical Argon-Ion lasers are summarized in Table 2-11.

Krypton-Ion lasers are very similar to Argon-Ion lasers, and some Argon-Ion lasers can be converted to Krypton-Ion lasers, and vice-versa, simply by changing the gas fill and bore magnetic field. As a result, many of the advantages and disadvantages are the same, as the summary of typical laser parameters in Table 2-12 indicates. Where data was not available, because of similarities between the two types, Krypton-Ion data can be assumed similar

Table 2-11. Representative Argon-Ion Lasers  
(Power in watts at  $\lambda$  in nm)

Manufacturer	514.5	488.0	476.5	457.9	351.1/ 363.8	Price (\$)
Control Laser Model 559U	7.8	6.0	1.92	1.20	3.00	19,750
Spectra-Physics Model 170-03	6.0	5.0	1.50	1.20	0.74	23,100
Model 170-00	4.0	3.2	1.00	0.80	0.14	17,900
Model 162	0.005		0.010			4,750
Coherent Radiation Model CR-18	7.5	6.0	2.20	1.50	2.50	31,950
Model CR-12	5.0	4.0	1.50	1.00	1.50	24,850
Model CR-8	3.2	2.30	0.90	0.50	0.20	16,780
Model CR-5	2.0	1.50	0.60	0.350	0.15	14,380
Model CR-3	1.4	1.0	0.450	0.200	0.10	11,670
Model CR-2	0.8	0.70	0.300	0.150	0.075	10,470
Lexel Model 96	1.4	1.30	0.500	0.250	N. Av.	11,450
Visible					UV	

N. Av. = Data not available

Table 2-12. Representative Krypton-Ion Lasers

(Power in watts at  $\lambda$  in nm)

Manufacturer	647.1	568.2	530.9	520.8	482.5	476.2	350.7 356.4	Price (\$)
Control Laser Model 559K	2.400	0.900	1.200	0.420	0.180	0.300	1.500	19,750
Coherent Radiation Model CR-500K	0.500	0.150	0.200	0.070	0.030	0.005	0.100	9,700
Model CR-750K	0.750	0.200	0.250	0.150	0.075	0.010	0.250	14,950
Spectra-Physics Model 165-01	0.500	0.150	0.200	0.070	0.030	0.050	0.040	12,850
Model 170/171	2.000	0.500	0.600	0.300	0.300	0.300	0.300	23,000
Lexel Model 95K	0.300	N. Av.	N. Av.	N. Av.	N. Av.	N. Av.	N. Av.	10,700
	Red	Yellow		Green		Blue	UV	

. Av. = Data Not Available



to Argon-Ion data in the column next to it. The spectral range of Krypton-Ion lasers is greater than that of Argon-Ion lasers, which makes them good candidates for a color display system (such as proposed direct and holographic displays). But they are also relatively expensive in terms of available power. Moreover, about two-thirds of a Krypton-Ion laser's output is at wavelengths longer than the typical blue sensitivity region of most graphic arts photographic materials.

Helium-Cadmium lasers provide an efficient and relatively inexpensive source of coherent radiation at either 441.5 nm or 325.0 nm. Unfortunately, the maximum power output is low (3 mW maximum at 325 nm and 75 mW maximum at 441.6 nm), and both noise and power instability are high. This is because cadmium's 9 eV ionization potential is very low; as a comparison, helium ionizes at 25 eV. The effect is that the Helium-Cadmium laser is extremely sensitive to impurities, which in turn limits its lifetime to one of the shortest of the lasers being considered (less than 2,000 hours). Noise is a primary problem, but solutions appear to be available. Spectra-Physics Model 185 has 6 percent rms noise, whereas one of Liconix's models, the 410 V operating at 441.6 nm, specifies only 0.5 percent rms noise. Power is, nevertheless, quite low. However, if low cost is important and blue laser light is acceptable, Helium-Cadmium has some potential for small tactical reproduction systems. Typical He-Cd laser data are summarized in Table 2-13. Helium-Selenium lasers, which are similar to Helium-Cadmium lasers in design, are at present manufactured only by Liconix and El Don, USA. Their chief advantage is a uniform spectral output and relatively low price. They have no power output in the UV region, but where a full-color display is desired, their spectral distribution makes Helium-Selenium lasers very attractive candidates for color displays.

Table 2-13. Helium-Cadmium Lasers

Power in mW at $\lambda$ in nm				
Manufacturer	Laser Type	325.0	441.6	Price
Liconix				
Model 301	He-Cd UV	1.5		\$2,190
Model 302	He-Cd UV	5.0		\$3,750
Model 303	He-Cd UV	2.5		\$2,550
Model 401	He-Cd		10	\$1,990
Model 402	He-Cd		18	\$3,250
Model 405	He-Cd		40	\$4,750
Model 401 V	He-Cd		8	\$4,000
RCA				
UV-LD2148	He-Cd UV	3.0		\$4,515
UV-LD2148	He-Cd		20	\$4,095
Spectra-Physics				
Model 185-04	He-Cd		75	\$7,400
Model 185-05	He-Cd UV	15		\$7,650

Dye lasers, whose characteristics are summarized in Table 2-14, are much different than conventional ion and gas lasers of the types discussed previously, and for this reason they are harder to compare to those lasers. Since their operation depends on optical stimulation of a strongly fluorescent organic compound dissolved in a solvent, the output power depends both on the optical pumping method selected as well as the chosen dye. They are continuously tunable over a large range of wavelengths, and with proper care can deliver extremely high pulse power, making them a good choice where a high

Table 2-14. Typical Dye Laser Parameters

1.	Wavelength	3400-11,750 Å
2.	Spectral Bandwidth:	
	a. With broadband mirrors	15-150 Å
	b. With grating in cavity	~0.5 Å
	c. With grating plus etalon	~0.01 Å
3.	Output Power:	
	a. Total energy, peak	2 J
	b. Total energy, typical	0.1 J
	c. Power with 20 MW pump	~ 2 MW
	d. Power with flashlamp pump	0.75-2.0 MW
	e. Power with laser pumping	1 μW-7 KW
4.	Pulse Characteristics:	
	a. Pulse duration, flashlamp pumped	0.5 μs
	b. Pulse duration, laser pumped	20 ns
	c. Pulse duration, flashlamp pumped With intercavity saturable absorber	<1 ns
	d. Pulse duration, mode-locked pump	<10 <sup>-11</sup>
	e. Repetition rate, annular flashlamp	1 pps
	f. Repetition rate, linear flashlamp	20-50 pps
	g. Repetition rate, laser pumped	Up to 200 pps
	h. Repetition rate, laser pumped for small cavity	Continuous
5.	Operating Efficiency:	
	a. Flashlamp pumped	~0.4%
	b. Laser pumped	Up to 25%
6.	Power Stability, RMS	3%
7.	Noise, RMS from 10 Hz to 100 KHz	1%
8.	Price Range	\$2600-\$30,000

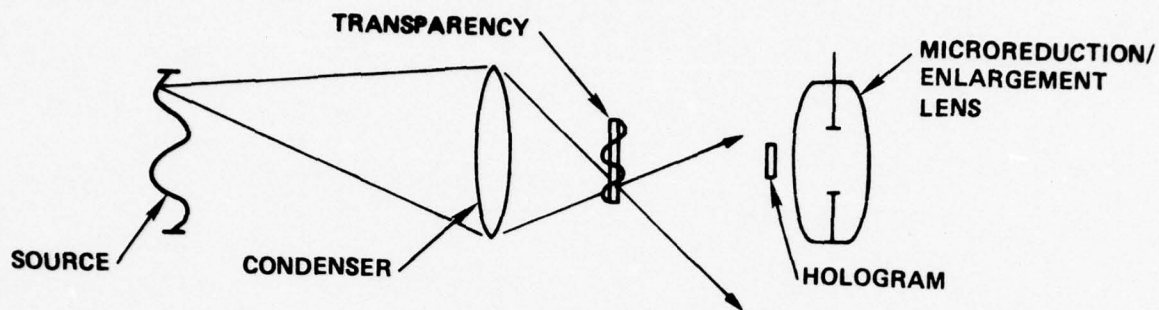


readout power is desired. Noise and power stability are comparable to that for Argon-Ion lasers, but dye lasers have less temporal coherence. As Table 2-14 shows, it is necessary to use gratings and etalons to ensure minimum spectral bandwidth, and therefore maximum coherence length. Further, dye lasers are generally more complicated than other lasers, and because of this they are far from industrially proven in graphic arts applications. Despite their ability to provide high pulse power, an important consideration for direct pressplate generation is their large and continuously tunable range of wavelengths, highly desirable for color work. Further testing of dye lasers is required before they can be considered qualified for use in a non-experimental system.

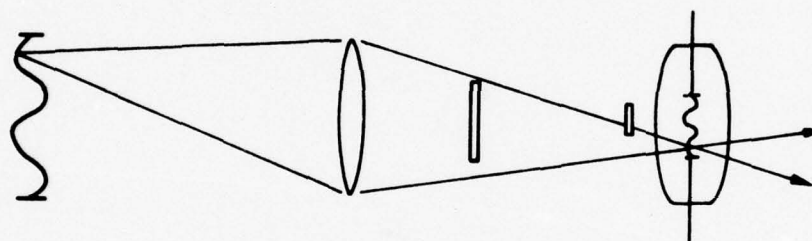
#### 2.4.4 Optics

One of several optical design challenges presented by the map separation storage problem was to illuminate the film chip in such a way that the full-scale repromat image appears to be a uniformly illuminated and magnified image of the film chip.

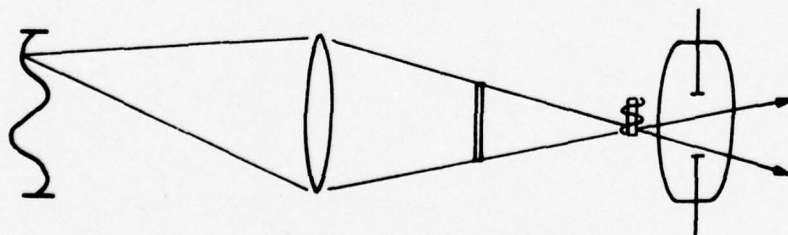
In Figure 2-10 the first and easiest method of illumination, Abbe illumination, is sketched. In this case the light source, a back-illuminated diffuse phase randomizer in the present system, is imaged directly onto the film chip. A variation of this is to place a diffuser directly in contact with the film chip. Since the elimination of coherent speckle noise is extremely important to coherent high-resolution imaging, the ability to image a diffuser so that the diffuser speckle is of minimum size is attractive. Of course, the hologram size (effective aperture) and/or the microreduction lens f/number limits the minimum speckle size regardless. Since Abbe illumination does not solve the problems of obtaining uniform illumination, an alternative method was investigated.



a. ABBE ILLUMINATION



b. KÖHLER ILLUMINATION FOR DIRECT BLOWBACK



c. KÖHLER ILLUMINATION FOR HOLOGRAPHY

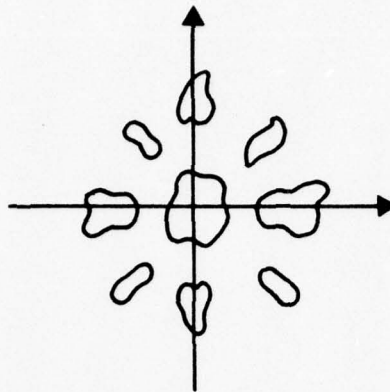
89136-5

Figure 2-10. Film Chip Illumination Methods

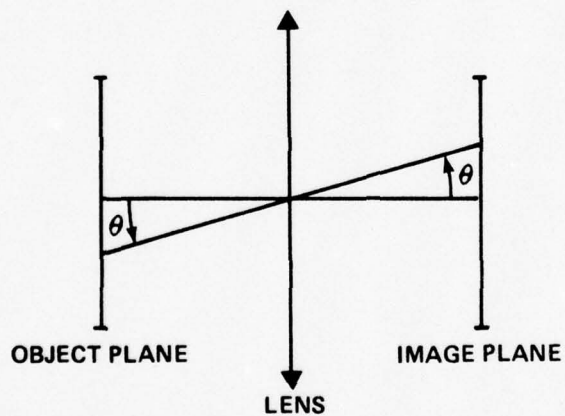
A second method, Kohler illumination, requires imaging the diffuser directly into the hologram aperture for Fourier-transform holograms or the aperture stop of the microreduction lens for the direct blowback. Kohler illumination provides the most uniform possible image irradiance in the case of direct projection. This is because the condenser lens design passes all direct and marginal image rays through the effective aperture stop. In addition, because the source is imaged into the lens, it will not be focussed at the image plane as would be the case for Abbe illumination. For holography, however, the hologram's 20 mm x 20 mm aperture acts as an external stop for the lens, and the Kohler illumination condition must be modified so that the diffuser remains imaged on the aperture stop of the system, which in this case is the clear aperture of hologram recording plane. In either case, the lens system must pass all extreme illumination rays from the film chip in order to provide uniform image illumination and to avoid resolution loss at the corners of the image field. We mention that a holographic Kohler system does not generally satisfy these requirements for a 20 mm x 20 mm hologram; this is a major problem area.

Because of the nature of the imaging process itself, it should be remembered that any illumination method results in a minimum illumination falloff away from the optic axis that is proportional to  $\cos^4 \theta$  times the illumination on-axis, where  $\theta$  is the field angle of the image. This is illustrated in Figure 2-11. This is because the illumination at any image point is directly proportional to the solid angle subtended by the lens exit pupil at that point, and thus is a consequence of the basic principles of geometric optics<sup>29</sup>. For the present system,  $\theta$  is a maximum of  $12^\circ$  for the Wray microreduction lens. This means that any conventional projection





a. A NONUNIFORM FOURIER TRANSFORM



b. THE  $\cos^4 \theta$  FALLOFF

89136-2

Figure 2-11. Special Optical Problems: Nonuniform Fourier-Transform and  $\cos^4 \theta$  Falloff

system with completely uniform input illumination at the film chip will have a minimum image irradiance rolloff from the center of the image to the edge of ~8.5 percent; this is fortunately less than the 10 percent design goal of the MEGIS Program.

In any illumination system the condenser lenses need only be of sufficiently high quality to avoid significant distortions of the illumination cone, since these lenses take no part in the imaging process itself. For this reason, large diameter and low f/number plano-convex lenses, Fresnel lenses, and holographic optical elements especially designed to image a low f/number light cone can be used to focus the light source into the hologram aperture (or into the microreduction lens aperture in the case of direct projection). The important considerations to note here are that multiwavelength projection may require attention to condenser chromatic aberrations and that the condenser must be free of internal flaws and bubbles. Otherwise, local non-uniformities may appear in the image because of diffraction caused by these flaws. Fresnel lenses, in particular, must be used with care to avoid reimaging their ruled concentric circle lens structure in the image plane.

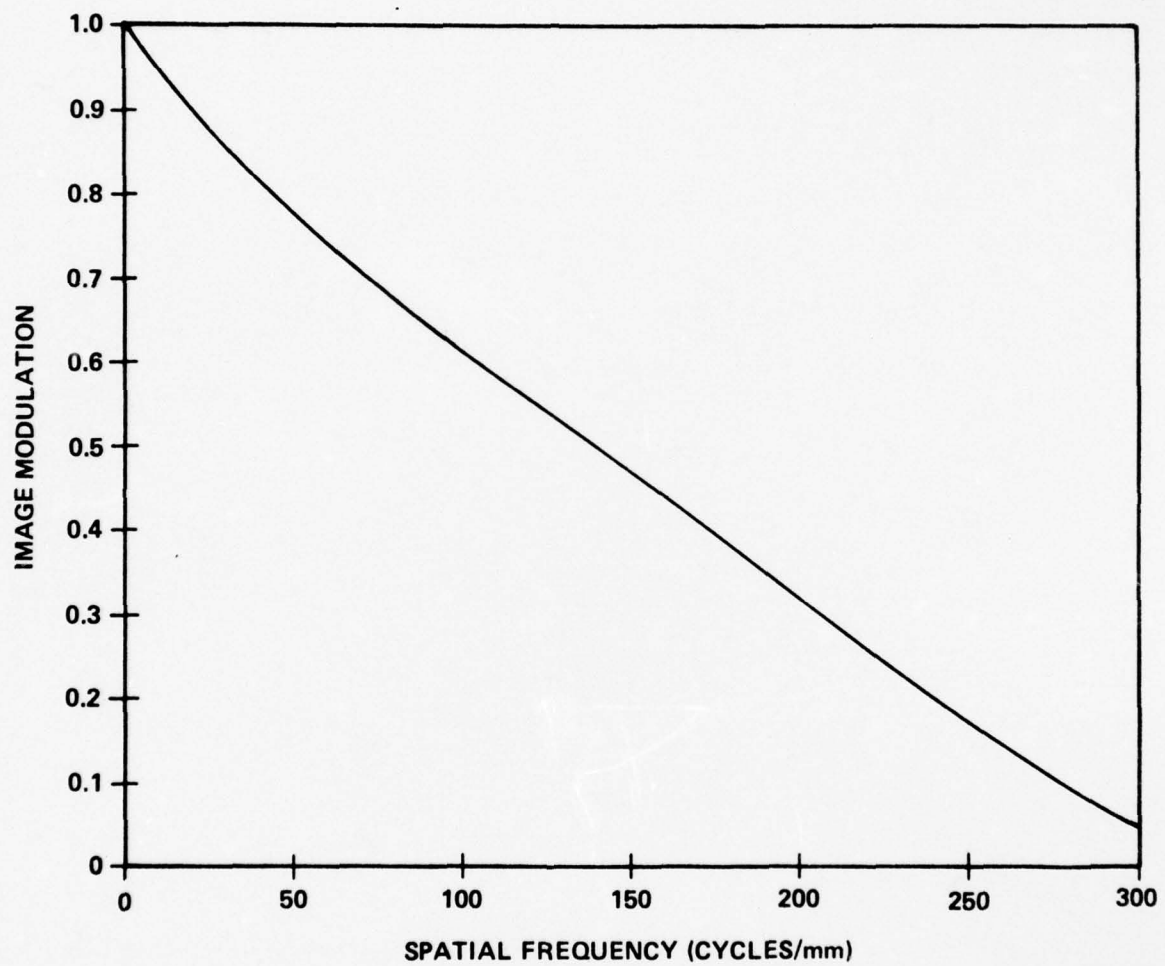
The microreduction and enlargement lens, in contrast to the condenser lens, must be a precision instrument. It must be designed for the reduction ratios anticipated, the resolution requirement, and the distortion specification. For the MEGIS Program, 10X and 20X reductions and image resolution at the film chip of 125 cycles/mm are required. Furthermore, the distortion of a full-scale reproduction from a film chip made with the lens must be such that the distance between any two points on the reproduction is within  $\pm 2$  mils rms of the distance on the original repromat used to record the film chip. For the maximum 48 x 60 inch enlargement (corresponding to the

20X reduction case), this corresponds to  $\pm 0.0033$  percent distortion over the 5-foot dimension. The microreduction and enlargement lens must also be chromatically-corrected for the wavelengths used for recording and playback, in this case 488 nm and 514.5 nm which are the two primary Argon-Ion laser wavelengths. Finally, it must cover the specified image field.

The Wray 250 mm, f/4, 10:1 Reduction Ratio Special Copy Lens (abbreviated simply as the Wray Micro Lens) satisfies these requirements within the limits of present measurement capabilities. The optical transfer function curve shown in Figure 2-12 was verified in experimental work. Coherent illumination produced a cutoff at approximately 128 cycles/mm, which falls close to the predicted 50 percent modulation point on the curve.<sup>30</sup> Lens distortion, as discussed in Section V, has been measured down to at least  $\pm 5$  mils; however, this datum includes the effects of two photographic processing steps in its evaluation and one can infer that the distortion of the lens is actually much lower. Resolution tests with 488 nm and 514.5 nm laser light indicate that the color correction of the lens extends beyond the 546 nm wavelength for which the lens design was optimized. Overall, we judge the Wray Micro Lens to be exceptionally well-qualified for precision microreduction and enlargement applications.

The Wray Micro Lens is not available as an off-the-shelf component. Its lens design is on file with Rank Optics of England, the present owners of the Wray Optics Group. It is believed that the cost of fabricating lenses of similar design might be comparable to that for both custom design and fabrication; an estimate of that cost is about \$25,000. For this reason, a survey of lens manufacturers was completed to determine the availability of lower quality, but off-the-shelf lenses, designed for microreduction and enlargement.





89136-19

Figure 2-12. Optical Transfer Function Curve for the Wray Micro Lens

The results of the survey are summarized in Table 2-15, and include the best results available relative to low distortion and high resolution. Ehrenreich Photo Technical Products, the U.S. branch of the Nikon Lens Design Group, has the closest off-the-shelf alternatives for anticipated reduction ratio requirements. The first of these, the 10X Fax-Ortho-Nikkor, was designed to handle large image fields for the projection of precision cutting templates onto steel plates coated with photoresist. As the data shows, it adequately meets all specifications at low cost except the distortion specification. The resolution, though unmentioned in the product literature, was measured by A. C. Gunther of the US Army Engineering Topographic Laboratories. The second lens, the Ultra-Micro-Nikkor, is one of a series of microreduction lenses designed for the production of high-quality photomasks. It appears qualified to meet the demands of the 20X reduction of 48 x 60 inch map separations except again for the distortion requirement. The final lens, a custom design described by Charles Teyssier of Tropel, Inc., is an estimate of the performance potential of a custom-designed lens. The lens would meet all system specifications, as well as providing a matched set of lenses to assure interchangeability of film chips from one projection system to another. Without this capability, additional distortion could be introduced during enlargement with a different lens than that used to record the film chip. The cost estimates are only approximate, but they do indicate the magnitude of a custom design cost based on modifications to available products.

Since custom design is a possibility, other discussions with lens manufacturers focused on the problem of a limiting optical system pupil caused by hologram recording at the back surface of the Wray Micro Lens. Regardless of the optical system design, limiting the entrance pupil of a precision lens

Table 2-15. 10X and 20X Low-Distortion Microreduction Lenses

Characteristic	Desired Value	250 mm, f/4 Wray Special Copy Lens	250 mm, f/5.6 Fax-Ortho-Nikkor	250 mm, f/4 Ultra-Micro-Nikkor	10X Custom Design
Manufacturer		Rank Optics	Ehrenreich Photo Technical Products	Ehrenreich Photo Technical Products	Tropel
Availability	Stock	Custom Fabrication	Stock	Stock	Custom Design and Fabrication
Reduction Ratio	10:1 and 20:1	10:1	10:1	20:1	10:1
Wavelength Range	514.5 nm and 488.0 nm	Designed for 546 nm	350 nm - 700 nm	546.1 nm	514.5 nm and 488.0 nm
Image Size	66 mm x 86 mm	75 mm x 75 mm * 66 mm x 86 mm *	200 mm x 200 mm at f/5.6	110 mm x 110 mm at f/5.6 80 mm x 80 mm at f/4	66 mm x 86 mm
Resolution	125 cycles/mm	200 cycles/mm * 285 cycles/mm *	180 cycles/mm on axis ** 130 cycles/mm off axis **	180 cycles/mm at 110 mm 320 cycles/mm at 80 mm	125 cycles/mm
Distortion	+0.002" or -0.0033%	+0.005" **	0.0%	0.00% at 110 mm +0.03% at 80 mm	+0.002"
Cost one	\$10,000	\$8,000 (new)	\$1,600	\$10,600	\$27,500 ea. for \$13,000 ea. for
50					

\* = Guaranteed value

\*\* = Measured Value



with an external stop which is much smaller than its entrance pupil clearly reduces system resolution and field coverage. One solution to this problem would be to split the reduction lens into two parts with the aperture stop between them and separated far enough apart so that a 20 mm x 20 mm reference beam could be introduced on the aperture stop at  $45^{\circ}$  to the optical axis. In this case, microreduction could be accomplished in the usual way. The holographic recording plane would be at the lens aperture stop, which is the optimum location. Another possibility would be to design a special lens with an external aperture stop for recording holograms. Conventional profile projection lenses are ordinarily designed in this way, but a major modification would be necessary to adapt the design to fit the current lens specifications.

## 2.5 VISUAL DISPLAYS

Graphic information for use in tactical environments or for the editing of cartographic data is often required in the visual display mode. Here, we address several relevant aspects of graphic information visual displays as they affect the goals of the MEGIS Program.

### 2.5.1 Basic Considerations

As a means of rapid access to information in a cartographic storage system, visual displays are optimum. However, if the visual displays are to accurately represent the graphic information as it appears in hardcopy form, several factors must be considered. In particular, because the human eye is the photodetector, the full-scale image of the graphic information must have certain characteristics which are different for visual displays than for hardcopy reproduction. Moreover, since an observer must study a displayed image from a distance, there must be something upon which the full-scale image is projected, i.e., a front-projection or rear-projection display screen. The

replacement of the photographic emulsion used for hardcopy reproduction with an eye-screen combination modifies system requirements.

The primary considerations for the visual display mode of map reproduction are outlined in Table 2-16, and discussed subsequently.

Table 2-16. Visual Display Requirements

Performance Specifications

- Luminance: 35 footlamberts
- Contrast:  
10:1 for clear lines on an opaque background  
to  
25:1 for opaque lines on a clear background
- Resolution: 12.5 cycles/mm
- Uniformity: Less than 25% decrease in luminance  
from center to edge; 10% desired

Other Considerations

- Ambient Illumination
- Speckle
- Gain
- Color

1. Luminance: Luminance is defined as  $L = dI / (dA \times \cos \theta)$ , which is the luminous intensity of a light source per projected area normal to the line of observation. For MEGIS, the specified luminance of the image is 35 footlamberts. This corresponds to the image luminance required for a visual resolving power of 0.6 minute of arc, which is close to the maximum unaided

resolving power of the human eye which is 0.52 minute of arc. Since 1 minute of arc =  $3 \times 10^{-4}$  radians, the smallest resolvable detail for an unaided eye at the visual rear point viewing distance of 10 inches (25 cm) with 35 footlamberts of luminance is  $1.8 \times 10^{-3}$  inches. When compared to the requirement that the system resolve  $3 \times 10^{-3}$  inches in the full-scale image, one may infer that a luminance of 35 footlamberts allows the eye to distinguish the smallest cartographic resolution element. If the luminance level is decreased to 10 footlamberts, however, the effect on visual acuity is not serious. In that case, the eye's resolving power becomes  $\sim 0.65$  minute of arc, corresponding to a resolution of  $1.9 \times 10^{-3}$  inches. Although luminance is important to visual acuity, it is clear that substantial latitude in the level of luminance exists if ambient illumination is minimal.

2. Contrast: For high contrast graphics, there may be two image formats to be displayed. The first kind has opaque lines on a clear background. Because of the substantial clear area commonly present in this kind of data, the eye picks up a large amount of background light while trying to observe the opaque information; the result is that a fairly high signal-to-noise ratio, a minimum of 25:1, is necessary to resolve minimum image detail. The second kind of image has clear lines on an opaque background. In this case the light from the clear signal lines is ordinarily concentrated in details close to the resolution limit of the eye, and these details are equivalent to



individual point sources of illumination if the signal-to-noise ratio is too high. In laser-illuminated displays this "dazzle" effect is especially evident, especially when coherent speckle adds to the problem. To minimize this effect, a signal-to-noise ratio of from 5:1 to 10:1 is specified for this type of visual display. Since cartographic materials can be a mixture of these two graphic formats, some compromise is needed to provide optimum viewing conditions. For this reason, we recommend that the image signal-to-noise ratio be in the range of 15:1 to 20:1 for most graphics.

3. Resolution: The full-scale image is required to be characterized by resolution sufficient to produce well-defined 3-mil lines in the display mode. This resolution, as the discussion of luminance noted, is near the resolution limit of the eye,  $\sim 1.6 \times 10^{-3}$  inches, for the 10-inch visual near-point distance. This means that if cartographic materials should have detail smaller than 3 mils wide, it must be studied with magnification. The magnitude of image luminance and image contrast also affect the visual resolving power, as described previously. Finally, the viewing screen itself must be sufficiently fine-grained to resolve detail on the order of 3 mils. Fortunately, the resolution of several common display screens is greater than 30 cycles/mm, and thus is not a problem for conventional graphic displays.
4. Ambient Illumination: When a large amount of stray light falls on a visual display and is scattered and reflected back to the

observer, the effect is to raise the noise level of the image. Since image contrast is important and since increasing image luminance requires more input power and possible overheating of the film chip, decreasing the amount of light scattered and reflected back to an observer is the best solution to this problem. Clearly, a first step is to eliminate the ambient light falling directly on the display. A second step is to vary the diffusivity of the viewing screen. However, decreasing the diffusivity of the screen narrows the field of view. A better solution is to either add a dark pigment to the diffusing material or to overcoat a rear-projection screen's diffuse surface with a dark pigment so that while the image light passes through the absorber once, the ambient light has to pass through it twice (once to reach the reflecting surface and once to pass back to the observer). In either case, the dark pigment will cause the image luminance to decrease slightly while minimizing the effect of ambient illumination.

5. Uniformity: The luminance measured at the edges of the image field of a visual display will generally decrease to a value less than that measured at the center of the image. This has the primary impact of varying the image contrast across the full-scale image if the luminance uniformity specification is not satisfied. Then the visual resolving power of the eye also varies across the image as well. A way to minimize this problem is to use the Kohler illumination method discussed in Paragraph 2.4.4.

6. Speckle: When a film chip is illuminated with coherent light and imaged through a bandlimited optical system, the resulting image will have speckle noise. Speckle noise together with the "dazzle" effect degrades contrast and lowers the edge resolution of the lines. In addition, the projected image has a definite granular characteristic. Any laser display (direct or holographic) method will suffer from this fundamental limitation.
7. Color: A color display requires a well-defined distribution of illumination wavelengths in order to match the nonuniform color response of the eye. A common method for doing this is to mix at different luminances the color primaries of red, green, and blue to form an additive color display. One possible combination uses wavelengths of 610 nm, 530 nm, and 460 nm, and relative luminances of approximately 0.80, 0.55, and 0.77, respectively. In a laser display system, a similar color balance could be achieved using a Krypton laser for the 647.1 nm red line, a Krypton laser for the 530.9 nm or an Argon laser for the 514.5 nm green line, and an Argon laser for the 488.0 nm blue line. The specific selection of wavelengths depends on the range of color information in the graphic material to be displayed. However, the suggested primaries are suited for most full-color visual displays. Krypton-Argon mixed-gas lasers could be used to provide all lines in one package, but the optimum color distribution requires the ability to individually tune the amount of power in each wavelength while maintaining the maximum power output possible for the display.



For this reason three lasers, either one Argon and two Krypton or two Argon and one Krypton, are required.

#### 2.5.2 Screen Types

The first decision in the selection of a display screen is whether to use a front-projection or rear-projection screen. Front-projection, as Table 2-17 demonstrates, is a well-developed method of displaying graphics. Front-projection screen types include the conventional white matte, beaded, and aluminized screens, the versatile lenticular screens, and two "active" screen types, i.e., fluorescent and phosphorescent varieties. These last two screen types eliminate speckle noise in coherent imaging because the effective light source is the radiant output from the fluorescent or phosphorescent materials in the screen, rather than the (coherent) laser source. The major problem is that the type of information contained in map separations often requires close examination of the display and often with the aid of magnification. If the observer stands close enough to the image to do this, however, he physically blocks the image. Only phosphorescent screens, of all the kinds listed, would allow this, but they are generally quite expensive to purchase and maintain. Thus, because of the projected need for close examination of the map display, the rear-projection screens listed in Table 2-18 provide a better display surface, though their technology is not as well developed as that of front-projection screens.

To compare screens, however, we need to introduce the concept of gain. Screen gain is defined as the ratio of image luminance at a given observation angle to that at the same angle for an ideal Lambertian screen.<sup>31</sup> A "perfect" diffuser of the Lambertian type, i.e., one with a gain of 1.0 independent of viewing angle, is one for which the actual

Table 2-17. Front-Projection Display Screens

<u>Type</u>	<u>Description</u>	<u>Peak Gain</u>	<u>Viewing Angle for Gain = 1.0</u>	<u>Comments</u>
White Matte	Nonglossy, dull white finish	0.85-0.90	Not possible	Has uniform gain. Image contrast is destroyed by ambient light.
White Semigloss	White with semigloss finish with sandy texture	1.50	Varies	Contrast is destroyed by ambient light. This screen cannot be curved.
White Pearlescent	White with pearlescent flakes for semigloss finish	2.5	Varies	Gain peak is extremely narrow, and hot spots are common at gain 1.5. Ambient light is a problem.
Aluminized, smooth	Leafing type aluminum paint on a smooth flat backing	12.0	25° to 28°	Good contrast performance despite strong ambient light. Screen should be stretched in a curved frame.
Aluminized, textured	Leafing type aluminum paint on a textured backing	8.0	28° to 30°	Good contrast despite ambient light. Screen should be stretched in a curved frame.
Semilenticular	Surface is embossed with vertical ribs and coating with leafing type aluminum paint	2.0	Varies	Good contrast. Screen does not require curvature.
Fully lenticulated	Miniature reflective lens shapes are embossed on a plastic base. Coating can be leafing type aluminum paint, pearlescent paint, or vapor-deposited aluminum	2.0	Varies; occurs at the cutoff angle of the lenticule	Can provide almost any desired illumination distribution and ambient illumination resistance. Can also be adapted to compensate for off-normal projection.
Beaded	Miniature beads deposited on a surface	3.0	30°	Efficiency better than for aluminized screens, but more sensitive to ambient illumination.
Fluorescent	Fluorescent paint on a surface	Varies	Varies	Unsuitable for color systems. Reduces speckle in coherent imaging. Extremely sensitive to ambient illumination.
Phosphorescent	Phosphorescent paint on a surface	Varies	Varies	Unsuitable for color systems. Reduces speckle in coherent imaging. Stores the picture so that microscopic examination is possible.

Table 2-18. Rear-Projection Display Screens

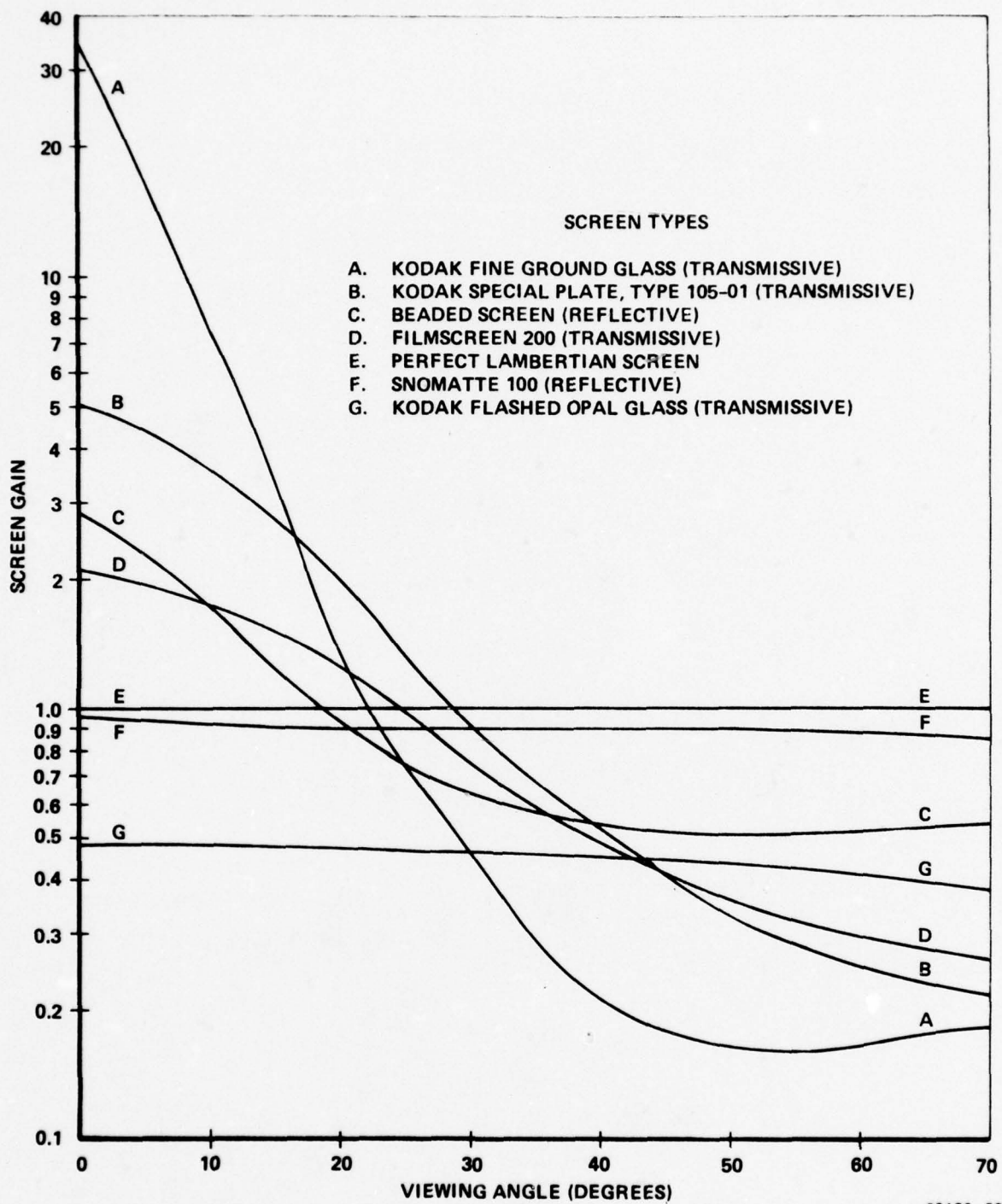
<u>Type</u>	<u>Description</u>	<u>Peak Gain</u>	<u>Viewing Angle for Gain = 1.0</u>	<u>Comments</u>
Ground Glass	Glass polished with coarse grit	100	10° - 30°	Gain is a function of coarseness of the glass. Image contrast is destroyed by ambient light.
Matte-Finished Mylar	Mylar with a ground-glass-like surface embossed on it	Varies	Varies	Similar to ground glass.
Photographic Plates with diffusion layers	Sensitized emulsion and a diffusing layer combined on one surface of the plate.	5-7	28°	When suitably exposed and processed, it provides a high-contrast photographic image on a diffuse, translucent background. It is especially useful when a blowback image is to be compared with a photographic image on the plate.
Coated Glass or Mylar	Plastic or paint diffusion layer coated on surface	10	15° - 35°	Similar to ground glass. Black pigments can reduce the effect of ambient light when added to the diffusing material.



observed light intensity a given distance away from the screen is constant regardless of the viewing angle (measured from the screen normal). Screens which do not diffuse the light in as uniform a manner will, therefore, have a gain greater than one in some regions and less than one in others.

The curves in Figure 2-13 illustrate the effect of gain in commercially-available diffusers and reflection screens. In the reflective category, Stuart Filmscreen's Snomatte 100 demonstrates how close reflective technology has approached the Lambertian standard: its gain is within 10 percent of unity at viewing angles out to beyond  $50^\circ$  from the surface normal. In contrast, the only transmissive screen which has a relatively flat response is opal glass. Unfortunately, opal glass is such an efficient diffuser that most of the image energy is lost by the time the light has passed through the material. Conventional ground glass is useful only for fairly narrow viewing angles. The best rear-projection screens are somewhere between these two extremes, with a peak gain from 2.0 to 3.0 and a fairly flat gain curve. The Filmscreen 200 is typical of this better group of rear-projection screens.

To relate the concept of gain to the present study, first consider the range of illumination angles available at the image plane. For a 24 x 36 inch image at a 10X magnification, for example, the image diagonal is 43.3 inches at a distance of 110 inches for a 10-inch microreduction lens focal length. This corresponds to a screen viewing angle of  $11.1^\circ$  for an observer looking perpendicular to the screen at an extreme corner of the screen. A 20X magnification with a 48 x 60 inch image has a corresponding  $10.4^\circ$  maximum viewing angle. If a few degrees of observer motion are allowed relative to the screen normal, then an acceptable screen must have a flat gain over a  $\pm 15^\circ$  field. A screen similar to Filmscreen 200 is



89136-23

Figure 2-13. Screen Gain as a Function of Viewing Angle  
for Several Commercial Display Screens

recommended for this purpose. However, a matte-finished Mylar is suitable despite its narrow scattering range. The Mylar also has an advantage in that it can readily be held on an electrostatic reproduction film easel of the sort specified for holding photographic film in Section V. Finally, a note on materials such as Kodak's 105-01 plate is necessary. This type of diffuser has a photographic emulsion coated on the diffuser and is used for the recording of graphic data for comparison with full-scale map separation images. For map study, standard 2-cm cartesian grids on this material could be used to provide quick measurements of stored data coordinates. In addition, alignment targets such as the moire alignment circles discussed in Section V could be permanently recorded on the reproduction film easel even before microreductions were made. Then the targets used to align the easel for low distortion would automatically be recorded into every film chip produced. Since the gain curve for 105-01 is better than that for ground glass, it is expected that there are other applications for this material where the gain of ground glass has proven acceptable.



## 2.6 REFERENCES AND NOTES

1. McMahon, D. H., Applied Optics 11, 798, 1972.  
Gale, M. T., and K. Knop, Applied Optics 15, 2189, 1976.
2. Zech, R. G., "Data Storage in Volume Holograms," Ph.D. Thesis, U. of Michigan, May 1974.
3. A  $10^{12}$  bit, space-deployable write/read/erase memory based on volume phase holography, developed by Harris Corporation for NASA Marshall Space Flight Center. See "Optical Read/Write Memory Techniques," Final Report, NASA CR-102973 and N71-15136, October 1971.
4. A human-read/machine-read microfiche mass storage system, based on one-dimensional computer-generated holograms, developed by Harris Corporation for Rome Air Development Center. See R. P. Guzik, "Optical Data Recording: Frontiers and the Manifest Destiny," EO System Design, June 1974, pp 22 -29.
5. A 1 Gb/s digital recorder/reproducer concept, based on one-dimensional Fourier-transform holograms, developed by Harris Corporation for Rome Air Development Center. See A. M. Bardos, Applied Optics 13, 832, 1974.
6. Smith, W. J., Modern Optical Engineering, McGraw Hill, New York 1966, p. 333.
7. For a discussion of speckle phenomena at a basic level see: N. George, "Speckle," Optics News, January 1976. For a complete discussion of speckle phenomena and applications see: "Speckle in Optics" (special issue), JOSA 66, November 1976.
8. Collier, R. J., C. B. Burckhardt and L. H. Lin, Optical Holography, Academic Press, New York 1971, p. 204.
9. An image plane hologram is formed by interfering a reference beam with the focussed aerial image of an object rather than with the Fresnel or Fraunhofer field of the object.
10. See Appendix B. This formula follows immediately from application, in one dimension, of the Rayleigh resolution criterion. Implicit assumptions are equal-amplitude, monochromatic light beams in phase quadrature and diffraction- limited optics.
11. In this case, the Wray Micro Lens is operating at  $f/5.865$ . Its resolving power is  $\Delta X = 1.22 \lambda f/\text{no.} = 3.68 \mu\text{m}$ . Hence, even smaller reductions are possible, e.g., up to 20.65X.
12. This formula is simply a statement of the sampling theorem. Since the hologram is in the Fourier plane, its clear aperture defines a low pass filter. Recall that  $1/\lambda f_T$  scales "length" into "spatial frequency", and thus  $\nu_m = (1/\lambda f_T)(\bar{d}/2)$ .

13. Lee, W. H., J. Opt. Soc. Am. 62, 797, 1972.
14. Exposure for laser recording is the product of time-averaged irradiance multiplied by exposure time. The time-averaged irradiance, which has spatial dependence, is the magnitude square of the complex amplitudes of the reference and signal beams. We can measure only space averaged irradiance; hence, the use of average signal irradiance  $\bar{I}_s$  in Equation 2.11.
15. Luxenberg, H. R., R. L. Kuehn, Eds., Display System Engineering, McGraw-Hill, New York 1968, p.180.
16. Reference 2, p. 37.
17. Large K-values ensure linearity, and hence, good signal-to-noise ratio. However, as K becomes large, the phase modulation  $\beta L$ , which is a function of K (through  $M_0$ ) must remain essentially constant for a prescribed DE level. This requires that  $\Delta n$  must increase as the  $\sqrt{K}$  to maintain  $\beta L$  constant. The implication is that to achieve high values of DE and SNR simultaneously the dynamic range of the recording material must be quite large. Moreover, the exposure process must not itself generate scatter noise. No existing recording media satisfy this requirement.
18. Reference 2, pp. 194-217.
19. Reference 2, pp. 13-16.
20. Lee, W. H. and M. O. Greer, J. Opt. Soc. Am. 61, 402, 1971.
21. Reference 15, Chapter 3
22. Reference 2, pp.229-239.
23. This analysis ignores the possible negative effects of absorption by the hologram. The use of very low loss recording materials such as dichromated gelatin or photopolymers would minimize this risk.
24. At the beginning of the MEGIS Program, Fresnel holography was not considered an attractive approach for the storage of graphic information. However, related R&D activities revealed that excellent displays of continuous tone objects could be obtained. We found that a careful choice of illumination techniques and recording parameters yielded hologram reconstructions characterized by more than adequate brightness, resolution and brightness uniformity. Speckle noise was studied as a function of hologram size and was found to be a problem for hardcopy reproduction only as the Nyquist limit was approached, i.e., for hologram sizes that just resolved the finest spatial detail in the object. A strong threshold effect was observed. By reconstructing holograms at least three-times larger than required by the Rayleigh criterion, the impact of speckle noise was greatly minimized.

25. This is an original concept first proposed by R. G. Zech in April 1976.
26. Leith, E. N. and B. J. Chang, Applied Optics 12, 1957 1973.
27. To prevent "chromatic" dispersion effects, it may be necessary to use holographic Fourier-transform lenses.
28. Reference 6.
29. Reference 6, pp. 132-133.
30. For spatially coherent light, the MTF is a square-top function having the value of unity for all spatial frequencies  $\nu < \nu_m$ . The MTF cutoff frequency for incoherent light is  $2\nu_m$ . For a complete discussion of this subject, which has a certain subtleness, see: J.W. Goodman, Introduction to Fourier Optics, McGraw-Hill, New York 1968, pp.101-126.
31. Reference 15, Chapter 6.



SECTION III  
RECORDING MATERIALS

### SECTION III

#### RECORDING MATERIALS

Recording materials play a central role in the development, operation, and performance of both conventional and holographic map storage systems. Areas of primary impact include information storage density, display luminance, color reproduction and image fidelity. These parameters are related in the holographic case to variables such as diffraction efficiency, signal-to-noise ratio, surface quality and so forth. The ultimate performance of any type of analog optical map storage system, however, will depend upon the availability and proper utilization of high-quality recording materials.

To assure the identification of the most promising storage media, a broad class of recording materials was surveyed. We recognized, however, that other factors, especially those related to the development and utilization of a map storage system, also required consideration. Therefore, we focused on recording materials that not only provided a high level of storage performance, but also satisfied at least some of the following criteria:

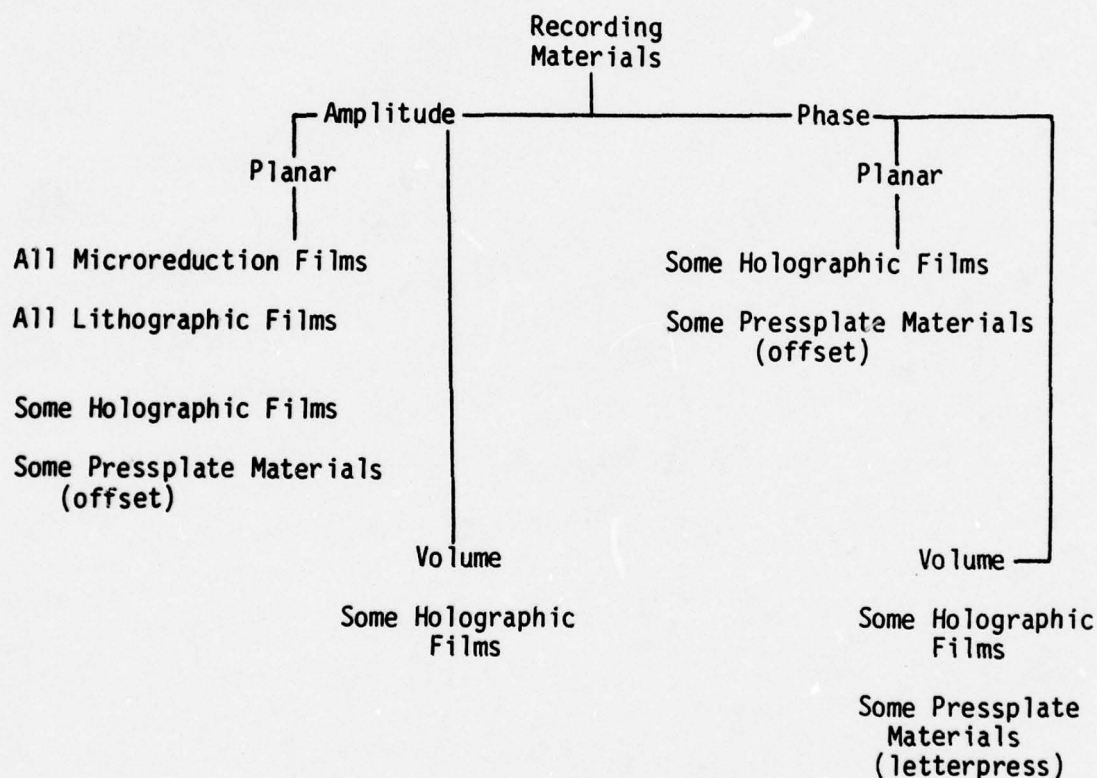
1) relatively conventional; 2) easily used and processed; 3) readily available and modestly priced; 4) stable; 5) manufactured with high levels of quality control; 6) produced by a reliable U.S. manufacturer; and 7) dimensionally stable.

A recording material is broadly defined in this report as any light-sensitive system used for the storage and retrieval of graphic information. As the MEGIS Program evolved, we identified several categories of recording materials that merited attention: microreduction and holographic films for data storage and lithographic films and pressplate materials for data retrieval (hardcopy reproduction; see Section V). In the remainder of

this section we discuss the various film types and outline their specifications relative to the storage and retrieval of map separations. Whenever possible, specific examples are cited, and baseline characteristics are summarized. We begin with a general introduction to some important and basic considerations relevant to all types of recording materials.

### 3.1 BASIC CONCEPTS<sup>1</sup>

A recording material is a light-sensitive medium used to store or process data in optical form. The generic types of recording materials can be illustrated in the following way:





An amplitude recording material is a light-sensitive medium that stores information in the form of absorption variations; a phase recording material is a light-sensitive medium that stores information in the form of refractive index or optical thickness variations. The term planar implies that the light-sensitive layer of the recording material is coated in thin layers, typically less than 5  $\mu\text{m}$ ; the term volume means that the light-sensitive layer of the recording material is coated in relatively thick layers. For holographic recording, the distinction is more subtle. That is, the term planar implies that the finest spatial detail or variation of the stored data is large when compared to the physical thickness of the recording material. In this context, the term volume is used to mean that the finest spatial detail or variation of the stored data is on the order of, or smaller than, the physical thickness of the recording material. Specifically, the following definitions are applicable:

Planar (Thin) Hologram - This is a hologram for which the average spatial periodicity is large compared to the thickness of the recording material. It is analogous in certain respects to classical gratings and zone plates. Important general characteristics are negligible orientation sensitivity and high spectral dispersion.

Volume (Thick) Hologram - This is a hologram for which the average spatial periodicity is less than the thickness of the recording material. Classical analogies are interference filters, the Fabry-Perot interferometer, and Bragg diffraction in crystals. Important general characteristics are angular orientation sensitivity and wavelength selectivity.

A quantitative distinction between planar and volume holograms is provided by the Kogelnik Q-factor:

$$Q = 2\pi\lambda_0 L/nd^2 \quad (3.1)$$

where  $\lambda_0$  is the recording wavelength,  $L$  is the hologram thickness,  $n$  is the refractive index, and  $d$  is the spatial period (fringe spacing). When  $Q < 10$ , the properties of planar holograms are dominant. For  $Q > 10$ , there is strong coupling between incident and diffracted fields and the characteristics of volume holograms are evident.

### 3.1.1 Storage Mechanisms

Information is stored in recording materials by means of effects caused by exposure to light. The exposure process produces chemical or physical changes that are collectively called the storage or recording mechanism. The nature of the storage mechanism has a profound impact upon the properties and characteristics of recording materials. There are many types of storage mechanisms, some of which are generally well-known, whereas others are relatively new. Some specific examples of recording materials that have potential for map storage applications are the following:

<u>Material</u>	<u>Mechanism</u>	<u>Type</u>
cis/trans isomers*	photoexcited changes in the spatial conformation of organic molecules	volume phase
diazo <sup>†</sup>	photolytic cleavage of diazonium bonds to create dye-formers, initiate polymerization, or cause preferential insolubilization	planar amplitude
dichromated gelatin*	photoinitiated cross-linking followed by stress-relieving layer splitting caused by chemical processing	planar and volume phase
electrophotographic* <sup>†</sup>	the attraction of opaque dielectric particles to the surface of a photoconductor bearing an electrostatic latent image	planar amplitude
free radical (dye) films**	the change of a dye from its leuco (colorless) form to a highly colored form	planar amplitude

<u>Material</u>	<u>Mechanism</u>	<u>Type</u>
photodegradable thermoplastics*	photoinitiated cross-linking or random chain scission	volume phase
photographic emulsions*†	the formation of latent image sites that permit the chemical reduction of entire silver halide grains	planar phase or amplitude
photoplastics*	surface relief generated by electrostatic forces and heat	planar phase
photopolymers ††	the photoinitiated polymerization of a light-sensitive monomer	planar or volume phase
photoresists ††	the photoinitiated cross-linking or polymerization of one or more chemical species	planar phase

\*Suitable only for holographic recording

† Suitable in appropriate formulations for microreduction and holographic films and pressplate materials

†† Suitable in appropriate formulations for microreduction, holographic, and hardcopy films and pressplate materials

\*\*Suitable for microreduction and holographic films

†† Suitable in appropriate formulations for holographic films and pressplate materials

### 3.1.2 Definitions and Special Terms<sup>1,2</sup>

A discussion, comparison, or specification of recording materials requires the use of terminology that may be unfamiliar, and often obscure. Recording materials are an important part of this Report because of their impact on breadboard experiments (Section IV) and hardcopy reproduction (Section V). Hence, baseline terminology is briefly discussed.

#### 3.1.2.1 Performance Parameters

##### Exposure Sensitivity

Exposure sensitivity is the reciprocal of the exposure (typical units are  $\text{ergs/cm}^2$ ,  $\mu\text{J/cm}^2$  or  $\text{mJ/cm}^2$ ) required to produce a fixed level of absorption or phase change for a prescribed set of exposure conditions.



### Spectral Sensitivity

Spectral sensitivity is a measure of the exposure, as a function of wavelength, required to produce a given absorption or phase change. It is usually specified by means of a graph of sensitivity versus wavelength.

Orthochromatic spectral sensitivity is defined as exposure sensitivity in the blue-green region (420-580 nm) of the visible spectrum; panchromatic spectral sensitivity means a recording material has red light sensitivity (580-700 nm) as well as blue-green sensitivity. Ultraviolet (UV) sensitivity means that a recording material has a photoresponse in the 300-420 nm range, and generally no visible light sensitivity.

### Resolution (Resolving Power)

Resolution is a measure of the capability of a recording material to record small spatial detail. The smallest spatial detail that can be unambiguously recorded as an absorption or refractive index variation defines resolving power. These variables are generally specified by MTF or spatial frequency response curves.

### Diffraction Efficiency (DE)

Diffraction efficiency is the ratio of the power diffracted into the first order image to the incident power minus reflection and other losses. By other losses we mean irrelevant absorption losses caused by base scatter, spectral sensitizers, etc., that do not play a role in recording information. Since in practical applications the amount of light is carefully budgeted, an insertion loss must be specified together with diffraction efficiency.

### Signal-to-Noise Ratio (SNR)

Signal-to-noise ratio is defined as the ratio of average signal to rms background noise. In photographic work both signal and noise are measured

in terms of optical density. For holography it is generally more convenient to measure and use an average signal-to-average noise ratio, as obtained from the reconstruction of an image of a diffuse target having an opaque center.

#### Storage Capacity

Storage capacity is the maximum density in bits/unit area or bits/unit volume at which information can be stored in a recording material, and subsequently retrieved with a bounded error rate. The intrinsic capacity of a storage material is determined by its resolution capability (the effects of noise are ignored). In general, it is more meaningful to specify capacity in terms of a recording technique, relative to a prescribed information recovery error rate. For example, a photographic emulsion that can resolve 1,000 cycles/mm in two dimensions has an intrinsic capacity of  $10^6$  bits/mm<sup>2</sup>. When holography is used as the recording method and a 20 dB per bit signal-to-noise ratio is specified (corresponding to an error rate of about  $10^{-6}$ ), the capacity is experimentally found to be about  $10^4$  bits/mm<sup>2</sup>. Any attempt to record at a higher information packing density will reduce signal-to-noise ratio, thus increasing the error rate. Similar conclusions hold true for any analog or digital storage technique.

#### Point Spread Function

The point spread, or spatial impulse response function defines a recording material's ultimate capability for the reproduction of point and line images. It forms a Fourier transform pair with the optical transfer function, whose magnitude versus spatial frequency plot is the familiar MTF curve.

#### Acutance

Acutance is a measure of the variation of density across a boundary. Specifically, it is the rms slope of the density versus

displacement curve, as measured for the image of a sharp edge. Recording materials with high edge acutance are required for the optimum generation of microreductions and reprints.

### 3.1.2.2 Experimental Characterization

#### Sensitometry

Sensitometry defines the experimental determination of absorption or refractive index changes as a function of exposure, with processing and wavelength as parameters. Consider first amplitude materials. The only measurable quantity is the ratio of transmitted to incident power, or the intensity transmittance  $T_i$ . Defined quantities are  $D$  and  $T_A$ , i.e.,

$$D = -\log T_i \text{ (optical density)} \quad (3.2)$$

$$T_A = \sqrt{T_i} \text{ (amplitude transmittance)}. \quad (3.3)$$

By measuring  $T_i$  over a range of exposures, data are obtained for generating the following curves:

- D-log E curve - useful for photography and analog data storage. The slope of the straight line portion of this curve  $\gamma$  is generally used as a measure of contrast.
- D-E curve - useful for volume phase and amplitude holograms because of the explicit relationship between density and refractive index and absorption coefficient changes, respectively.



$T_i$ -E curve - useful for digital data storage and incoherent optical data processing.

$T_A$ -E curve - useful for planar amplitude holography and coherent optical data processing.

The exposure sensitivity is obtained from these curves in terms of the exposure required to produce a given value of  $D$ ,  $T_i$ , or  $T_A$ . Varying processing changes the slope (contrast) and/or shape of these curves. A family of these curves, with wavelength as a parameter, is used to generate spectral response curves, i.e., sensitivity versus wavelength.

The sensitometry of phase materials is more difficult, but fortunately it is only required for holographic recording materials. Refractive index changes can be measured, for example, with an Abbe refractometer or surface relief with an interference microscope. These measurements are tedious and time consuming, however, and thus we usually measure diffraction efficiency as a function of exposure instead. By either method, curves giving refractive index change or surface relief as a function of exposure can generally be obtained. Processing and wavelength are again important variables.

#### Spatial Frequency Response

The spatial frequency response of a recording material can be determined in a number of ways. The conventional method is to image sine-wave transparencies with a well-corrected, low  $f$ /number lens whose frequency response is known from independent measurements. Each transparency image is scanned in a microdensitometer, and the output modulation, corrected for the effects of the lens, is computed. The ratio of output to input modulation is

plotted as a function of spatial frequency  $\nu$ ; this curve is called a modulation transfer (MT) curve. The ratio of output to input modulation is called the modulation transfer function (MTF).

The method just described is well-suited for low spatial frequencies and amplitude recording media. For high spatial frequencies or phase media, an interferometric technique is required. The easiest to implement is the recording of holographic gratings with two uniform plane waves of laser light. The contrast of the fringes is determined by the beam ratio  $K$  and the spatial frequency  $\nu$  is a function of beam offset angle  $\theta$  and recording wavelength  $\lambda_0$ , i.e.,

$$\nu = 2 \sin \theta / \lambda_0.$$

A Mach-Zehnder interferometer is a convenient way to generate spatial frequencies in the 0-800 cycles/mm range. For a set of fixed recording parameters, a series of gratings is constructed, and the ratio of diffraction efficiency at frequency  $\nu$  to the diffraction efficiency at some prescribed minimum spatial frequency, e.g., 50 cycles/mm is called the (relative) frequency response  $R(\nu)$  of the recording material. It is not exactly the MTF, but is closely related. For high resolution recording materials there is negligible difference.

#### Scatter Noise

Most recording materials have one or more sources of scatter noise that are independent of the technique used for data storage. The most important sources of scatter noise are usually discrete structures in the light-sensitive layer. However, other parts of the recording material, such as the base or substrate, also contribute to scatter noise.

Photographic emulsions are a good example. Scatter noise is due to small particles or grains of silver, and is often called grain noise. For

Lippmann emulsions, such as Kodak 649F or Agfa 8E75, the silver grains are very small (before development the silver halide microcrystals are sphere-shaped with diameters of about  $0.05 \mu\text{m}$ ; after development the silver grains resemble twisted filaments about  $0.25 \mu\text{m}$  long and  $0.05 \mu\text{m}$  wide.)

The Wiener spectrum  $\Phi_n(\nu)$ , which is the normalized scatter noise power spectral density, is often used to specify the random noise generated by recording materials such as photographic emulsions<sup>4</sup>. The Wiener spectrum is determined by measuring the ratio of scattered power to incident power for uniformly-illuminated exposed film sample. That is,

$$\Phi_n(\nu) = \frac{\text{SCATTERED POWER}}{\text{INCIDENT POWER}} (\nu) \quad (3.4)$$

where  $\langle \rangle$  means the average over many samples, and where  $\nu$  is related to the scatter angle  $\theta_s$  by

$$\nu = \sin \theta_s / \lambda. \quad (3.5)$$

The accurate experimental measurement of  $\Phi_n(\nu)$  is usually very difficult because of the low light levels involved.

Although we have discussed a specific example, a Wiener spectrum can be determined for any recording material. For data storage using direct digital or holographic techniques, scatter noise usually places an upper bound on storage capacity.

#### Holographic Data

Holography has generated the need for characteristic curves that can be used to compare the relative quality of recording materials. The most important characteristic curves are diffraction efficiency (DE) and



signal-to-noise ratio (SNR) as a function of average exposure  $E$ ,  $K$ -ratio, and so forth. The usual procedure is to record plane wave gratings and Fresnel holograms of a ground glass diffuser with an opaque center.

For grating experiments we usually measure  $DE$  as a function of  $E$  with beam ratio  $K$  and spatial frequency  $\nu$  as parameters. The curves plotted include  $DE$  versus  $E$  with  $K$  as a parameter,  $(DE/DE_{\max})^{1/2}$  versus  $E$  (amplitude response),  $(DE/DE_{\max})^{1/2}$  versus  $\nu$  (frequency response), and  $DE$  versus  $K$ .

The Fresnel hologram experiments are used to measure data storage parameters. The ground glass diffuser simulates a wideband stochastic signal; the opaque center serves as an absolute noise reference. A set of holograms is recorded as a function of exposure with  $K$ ,  $\nu$ , and packing density  $\rho$  as parameters. The real image is reconstructed, and the average signal and noise powers are measured. Signal-to-noise ratio is defined as the ratio of the average signal power to average noise power. The curves plotted are SNR and  $DE$  versus  $E$ ,  $\nu$ , and  $\rho$ , and maximum SNR (and corresponding  $DE$ ) versus  $K$ . These curves provide data that are useful for estimating storage capacity.

#### 3.1.2.3 Physical and Chemical Properties

There are a number of physical and chemical properties of recording materials, independent of the storage mechanism, that can affect the performance of map storage and retrieval systems. Important examples are nondestructive readout (image permanence), dimensional stability, shelf life, and archival lifetime (especially environmental integrity). A convenient way to measure these variables is to use holography.

Nondestructive Readout (image permanence) - Holographically stored maps are expected to be retrieved for visual display and/or hardcopy a large number of times. A number of recording materials do not permit unlimited data readout. For example, dry silver films, certain dye films, and most diazo films are well-known to suffer image degradation under conditions of extended playback or high-intensity illumination. Nondestructive readout implies the inherent capability of recording materials to undergo extended data recovery at some prescribed level of readout irradiance without serious loss of information content or detectability.

The nondestructive readout capability of a recording material is tested by recording a series of information-bearing holograms. Initial values of diffraction efficiency and signal-to-noise ratio are measured. Then, for a fixed set of environmental conditions, e.g., 20<sup>0</sup> C temperature and 50 percent relative humidity, the hologram is subjected to extended readout at a fixed reconstruction beam irradiance level. At periodic intervals, DE and SNR are remeasured. A relative measure of nondestructive readout is then obtained by noting the readout duration required for a 3 dB loss in SNR and/or a 50 percent change in DE. This procedure is repeated a number of times at higher and lower irradiance levels to determine if threshold effects are present.

Dimensional Stability - For map storage applications, holographic recording materials will most probably be coated on thermoplastic substrates. While materials have a number of attractive properties, thermoplastics often have some serious disadvantages. A principal disadvantage is lack of dimensional stability. Thermoplastic substrates shrink or swell with changes in ambient temperature and relative humidity by relatively large amounts. In addition, these materials show hysteresis effects when environmental

variables are cycled. Processing (wet or dry) is also known to produce irreversible dimensional changes.

A relative measure of dimensional stability is obtained by recording and subsequent playback of holograms under controlled conditions. For example, the positional shift of digital data reconstructed from microholograms as a function of temperature and relative humidity provides a meaningful and practical test of dimensional variations. A spatial filter used for correlation detection also provides a sensitive measure of dimensional changes because of output irradiance changes.

Shelf Life - Shelf life is a measure of the preexposure stability of a recording material for a prescribed set of environmental conditions. Normally, materials are stored at either room temperature and humidity or under refrigeration. Preliminary data suggests that most recording materials have a shelf life of many months at  $-20^{\circ}\text{C}$ , and some will remain stable for years at this temperature. However, at room temperature ( $20^{\circ}\text{C}$ ) the dark reaction rates that govern recording material degradation can increase by orders of magnitude. As a consequence, room temperature shelf life is a concern for some recording materials.

Shelf life is determined by recording holograms over periodic time intervals after receipt of a fresh supply of a given recording material. In every case an identical set of holograms is recorded, and exposure sensitivity, DE and SNR are measured. By plotting the degradation of the reconstruction parameters, as a function of shelf storage time, a good indication of shelf life is obtained. In practice, variations of key parameters greater than 20 percent over one month at room temperature is unacceptable for most applications.



Archival Lifetime - Many recording materials are degraded by conditions of extreme temperature and relative humidity. Some materials are unstable even in protected, room-temperature storage. Almost all recording materials are affected by nuclear radiation, and many are severely degraded by ultraviolet light, fungus, and so forth.

To test archival properties two conditions are specified, namely length of storage required and environment of storage. Because testing periods are of limited duration, the following procedure is often followed. Holograms are recorded and initial measurements of parameters such as DE and SNR are made. The recording material is then placed in dark storage under specified set of conditions. After a number of months holographic parameters are remeasured. Changes in the values of these parameters will give an indication of archival properties. Experience indicates that if a material remains stable for a number of months, then long-term stability can be expected. In addition, holograms are constructed on fresh recording media samples that are then subjected to a high level of temperature and relative humidity in an environmental chamber. Hologram reconstruction parameters are measured before and after cycling. This procedure provides an indication of environmental integrity under extreme conditions such as those produced by air conditioner failure in hot humid climates.

#### 3.1.2.4 Anomalous Effects <sup>5,6,7</sup>

##### Processing Effects

There are a number of processing effects that affect the density distribution of a photographic image. Some may be critical relative to the recording of micromimages.

- a. Edge Effect - adjacent but different exposure levels can have a nonuniform density boundary between them. This is due to developer diffusion from the region of lower exposure to that of higher exposure. The severity of this effect varies with emulsion type and processing conditions. It should be minimal for machine processing. However, for multilevel recording the edge effect may be a consideration.
- b. Eberhard Effect - images of different sizes recorded with equal exposures can have different net densities. As image size becomes significantly less than 1 mm, net density increases until some maximum value is reached for an image size that is a function of the film impulse response, exposure and processing. If the image size is further reduced, the net density decreases in some cases to a very low level. The image size at maximum density generally relates to the size of the film/processing spread function. An important point is that microsensitometry and macrosensitometry are different. The characteristic curves of microimages often have a higher  $D_m$  and  $\gamma$ .
- c. Kostinsky Effect - two small images recorded close to each other may have a density minimum between them that arises because of developer inhibition caused by an accumulation of reaction products. The result is an asymmetrical density distribution near the common border of the two images, which exaggerates their separation.

### Gelatin Effects

Gelatin, which is the matrix material of a silver halide emulsion, can be the cause of a number of apparently anomalous effects. Processing and drying that is not carefully controlled causes reticulation and water spotting. Shrinkage caused by tanning and fixation can cause both lateral and normal emulsion shift. Because both tanning and fixation shrinkage are functions of image density, gelatin effects are signal dependent. For micro-image storage at high reduction this could be a serious problem. A specific gelatin anomaly is called the Ross effect. This effect describes the changes in size and position of very small adjacent images. Shifts on the order of 1 to 2  $\mu\text{m}$  are reported for 100  $\mu\text{m}$  spots. Point image deviations of 2 to 5  $\mu\text{m}$  are reported for emulsions on glass plates. To minimize these effects, a hard emulsion, a nontanning developer, a hardening fixer, and short processing time are required; elimination of all gelatin effects is probably not possible. As a final note, films are coated and dried on line which tends to create along-track stresses. These stresses are relieved in processing, but because of hysteresis effects the emulsion does not reacquire its original dimensionality.

### Temperature and Relative Humidity

Modern photographic emulsions are formulated to give good performance over reasonable ranges of temperature and relative humidity. Larger variations can be expected to affect shelf life and to cause significant differences in photographic response. As a rule, increasing temperatures increase both speed and fogging; decreasing temperatures decrease speed, but also increase shelf life. It is more difficult to gauge the impact of relative humidity changes. High relative humidity causes the hygroscopic



gelatin of the emulsion to become tacky. A tightly rolled film having both a gelatin emulsion and a dyed-gel backing can be badly damaged. Fogging is also aided by high relative humidity because of the role of water as halogen acceptor. Low relative humidity makes the emulsion brittle and causes well known problems with static electricity. Handling and storage properties, however, are generally improved. An especially critical situation is one of low temperature and high relative humidity, which leads to condensation on the emulsion surface. Perhaps of greater consequence for map storage applications are the dimensional changes caused by temperature and relative humidity changes. For full scale graphics this may not be of major concern, but for film chips and holograms these effects may lead to distortion.

#### Turbidity

Turbidity is a measure of the rate of spread (growth, blooming, flare) of a photographic image with increasing exposure. The result of this effect is that the geometry or format of the recorded data is not true. Line images spread and spots broaden with increasing density. The cause of turbidity is intergrain scattering. It increases with increasing silver/gelatin ratio and emulsion thickness, but can be minimized by the use of internal absorption dyes. Turbidity always causes a decrease in resolving power.

#### Latent Image Decay

Latent image decay (LID) is a loss of density and contrast caused by delayed processing. This effect is most noticable for fine-grain and Lippmann emulsions. Generally, initial rates of density and contrast loss are quite high, but often level off after several hours.

### Miscellaneous Latent Image Effects

Several classical latent image anomalies such as the intermittancy, Clayden, Villard, Herschel, Sabattier, and solarization effects caused speed loss and image reversal. They are not, however, relevant to the present study.

#### 3.2 MICROREDUCTION FILMS

The microreduction of high-resolution, large format graphic data requires both a lens and recording material of exceptional quality. The lens problem is discussed elsewhere; here we discuss microreduction films and outline their specifications.

The function of the microreduction film is to allow the production of film chips which reproduce upon projection a full-scale facsimile of a binary map separation with high metric fidelity. As some map separations have spatial detail as small as 3-mils, a nominal 10X reduction requires a microreduction film to record at least  $8\text{ }\mu\text{m}$  lines, or equivalently, to resolve more than 64 cycles/mm. To record an  $8\text{ }\mu\text{m}$  line with high edge definition requires an overall lens/film combination with considerably high resolving power.

In practice a high resolution, flat-field lens is used at a diffraction limited f-number to microreduce map separations; the properties of some of these lenses were discussed in Section II. The map separations, are back-illuminated by fluorescent mercury lamps with a narrowband green light output centered on 546 nm. The lens, which is corrected for the 546 nm Hg line, forms a microreduced image of the map separation on a high-resolution, high-contrast microreduction film. The map separation image is characterized by high resolution over its entire field, high contrast, and negligible metric

distortion. The microreduction film used to produce the film chips must be capable of recording this image without degradation.

The key specifications for a microreduction film can be inferred from performance and operational considerations. They are summarized in Table 3-1. These specifications are applicable for film chips used ultimately conventional or holographic storage.

Some candidate microreduction films are listed in Table 3-2. Only a few films meet the criteria of Table 3-1, but practical considerations require trade-offs in any event. The films used to produce Government-supplied transparencies were Kodak AHU microfilm, Type 5460 and Holographic Recording Film, SO-141. As these films are negative-working, it was necessary to reverse process to obtain a positive image of the graphic input for holographic storage experiments. The AHU Microfilm did not yield satisfactory film chips; the SO-141 film chips were of better quality, but not entirely satisfactory. Both films are adequate when used in their normal negative-working mode. Table 3-2 contains several other negative-working films that merit experimental evaluation for film chip production. Kodak SO-253 and Agfa 10E56 films are especially recommended. By way of direct positive-working films, Table 3-2 lists Kodak SS4 Duplicating film and Kodak Direct Duplication Print film, together with two electrophotographic films: Scott Graphics TEP film (binary mode) and Coulter Information Systems KC101 film. Each film is capable of producing positive film chips. The electrophotographic films offer the advantages of on-line, dry-processing and very long archival life.



Table 3-1. Specifications for Microreduction Films

I. PHOTOGRAPHIC

Densitometric Properties -  $\gamma$  (contrast)  $>2$   
 $D_{\max}$   $>2$   
 $D_{\min}$   $<0.1$

Image Polarity - positive or negative working.

Latent Image Decay - negligible for time delays between exposure and processing of up to 4 hours.

Reciprocity Failure - negligible for exposure times in the 1 to 100 second range.

Sensitometric Properties - exposure requirement;  $<100$  ergs/cm<sup>2</sup>: spectral sensitivity; orthochromatic.

Substrate - best photographic grade polyester; similar or equivalent to Kodak Estar <sup>®</sup>.

II. DATA STORAGE

Acutance - very high.

Dimensional Stability - less than  $100 \times 10^{-6}$  inch dimensional variations for  $\pm 10\%$  changes in relative humidity and for  $\pm 10^\circ\text{C}$  changes in temperature.

Distortion - less than  $\pm 150 \times 10^{-6}$  inch deviations from metric fidelity due to dimensional changes and processing, as measured with reference to the spatial coordinates of UTM reference grid vertices at 10X reduction.

Granularity - less than 0.01 when measured with a  $48 \mu\text{m}$  aperture at 12X magnification at a net density  $D=1$ .

Noise - less than 1% of the transmitted light should be scattered because of scratches, particulate matter, and pelloid backing, if present.

Point Spread Function - compatible in shape and half width with the recording and reproduction of line widths as small as  $4 \mu\text{m}$ .

Processing Effects - negligible relative to line widths as small as  $4 \mu\text{m}$ .

Resolution - at least 50% response at 300 cycles/mm for a high contrast (1000:1) tribar target.

Signal/Noise Ratio (SNR) - a minimum average maximum density to rms background density ratio of 20 (13 dB) for binary graphic input data.

Table 3-1. Specifications for Microreduction Films (Continued)

Turbidity - less than 10% line broadening up to a net density of three for line widths as small as 4  $\mu\text{m}$ .

III. SYSTEMS

Archival Life - a minimum of 5 years at 20°C and 50% RH.

Availability - 30 days ARO.

Cost - less than \$2.00/square foot.

Environmental Sensitivity - no measurable changes in sensitometric, densitometric, and data storage parameters for temperatures in the 10-30°C range and relative humidity in the 35-65% range.

Format - available in 70 mm rolls on 4-mil polyester base and 105 mm x 148 mm fiche on 7-mil polyester base.

Handling Durability - low susceptibility to surface damage and contamination by ordinary handling and processing; high resistance to scratching and a low affinity for particulate matter.

Image Permanence - no measurable changes in densitometric or data storage parameters for repeated or extended illumination at high irradiance levels with either UV or visible light.

OSHA/EPA Impacts - none.

Performance Consistency - less than 10% rms variation of sensitometric, densitometric, and data storage parameters within and between production units.

Processing - fully compatible with automatic equipment.

Shelf Life - greater than 6 months at 20°C and 50% RH; at least 2 years if refrigerated.

Table 3-2. Microreduction Films

FILM PARAMETER	Exposure <sup>a</sup> at 546 nm (ergs/cm <sup>2</sup> )	Spectral Sensitivity	Resolution at 50% Response (cycles/mm)	Granularity ( $\times 10^3$ )	Imaging Mode	$\gamma$ , $D_{\max}$ , $D_{\min}$	Film Base
RECORDING MATERIAL							
Kodak AHU Microfilm, Type 5460	10	Ortho	>200	8	Neg.	>2 >2 <0.15	5.25 mil Triacetate
Kodak Photomicrog- raphy Monochrome Film, S0-410	10	Pan	>100	7	Neg.	>2 >2 <0.15	4 mil Polyester
Agfa Scientia 10E56	20	Ortho	>1000	5	Neg.	>4 >3 <0.15	4 mil Polyester
Kodak High Speed Holographic Film, S0-253	30	Pan	>1000	5	Neg.	>4 >4 <0.15	4 mil Polyester
Kodak Direct Dupli- cating Print Film, Type 7468	100	Ortho	>300	4	Post.	<-1 >2 <0.15	5.2 mil Triacetate
Kodak Minicard Film, Type 6451	100	Ortho	>800	<5	Neg.	>4 >3 <0.15	5.4 mil Triacetate
Agfa Scientia 8E56	200	Ortho	>1000	<5	Neg.	>4 >4 <0.15	4 mil Polyester
Kodak Holographic Recording Film, S0-141	500	Ortho	>800	<5	Neg.	>3 >2.5 <0.15	4 mil Polyester
Kodak Minicard Film, Type II, S0-424	500	Ortho	>800	<5	Neg.	>3 >2.5 <0.15	5.2 mil Triacetate



Table 3-2. Microreduction Films (Continued)

FILM PARAMETER	Exposure <sup>a</sup> at 546 nm (ergs/cm <sup>2</sup> )	Spectral Sensitivity	Resolution at 50% Response (cycles/mm)	Granularity (x 10 <sup>3</sup> )	Imaging Mode	$\gamma$ , D <sub>max</sub> , D <sub>min</sub>	Film Base
RECORDING MATERIAL							
Kodak SS4 Dupli- cating Film	100	Ortho	200	10	Post.	-4 >4 <0.15	4 mil Polyester
Kodak High Resolu- tion Film, SO-343	1000	Ortho	1000	<5	Neg.	>4 >4 <0.15	7 mil Polyester
Kodak Holographic Film, SO-173	2000	Pan	1000	<5	Neg.	>3 >3 <0.15	4 mil Polyester
Coulter Information Systems KC101 Film <sup>b</sup>	100	Ortho	600	~10	Post.	<-1 > 2 < 0.15	4 mil Polyester
Scott Graphics TEP Film <sup>b</sup>	N/A	550- 650 nm	400	~10	Post.	<-1 > 2 < 0.15	5 mil Polyester

<sup>a</sup>For a net density of two

<sup>b</sup>Electrophotographic Film. Scott Graphics TEP  
Film requires special sensitization for this application

### 3.3 HOLOGRAPHIC FILMS

The storage of graphic information in holographic form requires very high quality recording materials. General requirements are very high resolving power ( $>1,000$  cycles/mm), very low noise, and high contrast. These properties are major determinants of diffraction efficiency, signal-to-noise ratio, and storage capacity which in turn are the key factors affecting luminance, resolution, and contrast of full-scale graphic images. An important point about holographic recording materials is that the optical quality of the entire film (light-sensitive layer and substrate or base) must be very high. This is because in many applications the hologram is positioned in a nonoptimum location relative to the rest of the optical system. As a consequence, phase errors and scattering, together with the finite thickness of the film, often cause a decrease in image resolution, contrast, and metric fidelity.

We now review the properties of several photographic and conventional holographic recording materials. A large number of recording materials are available for the holographic storage of maps and other graphics. Not all recording materials, however, are well-suited for the present application. Some have attractive baseline characteristics, but also have several inherent disadvantages. Of all existing recording materials, it appears the Lippmann photographic emulsions are presently the best qualified storage media.

An initial consideration in the selection of a candidate recording material is the choice between amplitude and phase recording materials. In general, phase media are preferred because of their higher diffraction efficiency potential and low insertion loss. From a practical viewpoint, the

most attractive phase media are bleached photographic emulsions even though they often have a nonnegligible insertion loss, and unless carefully processed, can be unstable. Amplitude materials are, of course, inherently lossy, but may nevertheless be useful for hardcopy reproduction. For example, a planar amplitude hologram is optimally recorded with a density level of 0.6, which implies that 75 percent of the incident light is absorbed. However, more light flux is still obtained in a full-scale map separation image than is possible by direct projection, assuming equal input laser power. Obviously a bright display in this case ( $\sim 35$  fL) would require a high level of laser power, and would probably result in heat distortion or destruction of the hologram. When display luminance is not critical or a video pickup can be used, stable amplitude recording materials can be competitive with phase media.

The trade-offs between planar and volume materials are also an important consideration. For practical reasons, a planar medium is preferred. Planar media generally have better surface quality, are more easily processed, and are representative of most commercially available light-sensitive systems. Moreover, because Bragg effects are absent in planar holograms, alignment to the first order is not critical. However, we mention that geometrical alignment of the hologram and readout beam is already critical relative to a distortion limit of  $\pm 2$  mils rms. Volume media usually provide the best diffraction efficiency performance and have the highest storage capacity. The Bragg angular orientation sensitivity of volume holograms is often considered a disadvantage. But for the present application, this is immaterial, since alignment requirements are already



relatively severe if holographically-generated aberrations are to be avoided. A volume phase recording material permits bias buildup compensation, which is a natural consequence of multiwavelength or incoherent holographic storage, and hence, the realization of maximum diffraction efficiency potential. Finally, an important point that merits emphasis is the following: the choice of amplitude or phase or of planar or volume recording materials does not influence the quality of the holographic image. The parameter affected most significantly is diffraction efficiency (image brightness).

Candidate recording materials for the holographic storage of graphic information are the following:

Lippmann Photographic Emulsions - High quality photographic emulsions such as Kodak SO-343 film have relatively high exposure sensitivity, orthchromatic spectral response, and excellent holographic properties. They are readily available at low cost. A major disadvantage of these materials is the requirement for carefully controlled and complicated wet chemical processing. However, all anticipated processing is well within state of the art equipment in the photographic industry. Photographic emulsions were used in the amplitude and phase modes for all baseline experiments.

Dichromated Gelatin - Gelatin films sensitized with ammonium dichromate are lossless phase media with a high diffraction efficiency capability. They are often used for holographic optical elements and high-brightness displays. Disadvantages of dichromated gelatin are short-shelf life, sensitivity to environmental conditions, low exposure sensitivity, and critical processing requirements.

Photopolymers - Several light-sensitive systems are known that provide high quality volume phase holograms through photopolymerization of a

highly reactive monomer, e.g., acrylate and vinyl carbazole monomers. These materials are characterized by high diffraction efficiency and storage capacity and dry (in situ) self-development. Major disadvantages are short shelf life and low exposure sensitivity.

Photodegradable Thermoplastics - Thermoplastics of optical quality, such as poly (methyl methacrylate) and cellulose acetate butyrate sensitized with p-benzoquinone, have the greatest storage capacity of any known recording material, together with a high diffraction efficiency capability. They are self-developing and can be produced as films or chips. The main disadvantage of these materials is extremely low exposure sensitivity.

Photoresists - Several photoresists have a demonstrated capability for high-density, high-efficiency holographic map storage. These materials are lossless after processing, and have excellent archival properties. Major disadvantages are short coated shelf life and low exposure sensitivity.

Specifications for holographic recording materials relevant to the MEGIS Program are summarized in Table 3-3. Clearly, very few recording materials meet these criteria. This is particularly true of the nonconventional light-sensitive media. However, several photographic emulsions closely approximate the specification; they are listed in Table 3-4. Overall, the most suitable films for holographic recording are Kodak High Resolution Film, S0-343, and Agfa Scientia Film, 8E56. The properties and characteristics of several nonconventional recording materials are summarized and compared with Kodak S0-343 film in Table 3-5. Although in most cases the nonconventional recording material provides better storage performance than S0-343 film, practical considerations preclude their utilization.

Table 3-3. Specifications for Holographic Films

I. PHOTOGRAPHIC

Densitometric Properties -  $\gamma(\text{contrast}) > 3$

$$\begin{matrix} D_{\text{max}} > 3 \\ D_{\text{min}} < 0.1 \end{matrix}$$

Image Polarity - positive or negative working

Latent Image Decay - negligible for time delays between exposure and processing of up to 4 hours

Reciprocity Failure - negligible for exposure times in the 10 ms to 10 second range

Sensitometric Properties - exposure requirement;  $< 1,000 \text{ ergs/cm}^2$ ; spectral sensitivity; orthochromatic

Substrate - best photographic grade polyester; similar or equivalent to ESTAR®

II. DATA STORAGE

Acutance - very high

Diffraction Efficiency (DE) - at least two percent in the amplitude mode and 10 percent in the phase mode for gratings recorded with 50 percent fringe contrast

Dimensional Stability - less than 10 percent variation in hologram thickness through processing and in storage; hologram imaging properties are not sensitive to small changes in the transverse dimensions due to processing or temperature and relative humidity changes

Distortion - not generally caused by dimensional variations or processing effects associated with the recording material; mainly due to spatial misalignment or spectral shift of readout beam, which is assumed to be avoidable or correctable

Noise - less than five percent of the light diffracted into the holographic image; inclusive of nonlinear, Wiener, base, and surface scatter noise

Processing Effects - negligible relative to spatial dimensions as small as  $1 \mu\text{m}$

Resolution - at least 50 percent response at 1500 cycles/mm, as measured for a holographic grating with 50 percent fringe contrast



Table 3-3. Specifications for Holographic Films (Continued)

Signal/Noise Ratio (SNR) - a minimum average signal to average noise ratio, as measured in the image plane, of 30 (15 dB) for binary graphic input data

Storage Capacity - at least  $5 \times 10^4$  pixels/mm<sup>2</sup> with a SNR of 15 dB and a DE of two percent

Turbidity - less than 10 percent degradation of fringe contrast for spatial frequencies in the 500 to 1500 cycle/mm range and for net densities in the 0.5 to 2.5 range

### III.

#### SYSTEMS

Archival Life - a minimum of 5 years at 20<sup>0</sup> C and 50 percent RH

Availability - 30 days ARO

Cost - less than \$2.00/square foot

Environmental Sensitivity - no measurable changes in sensitometric and holographic parameters for temperatures in the 10-30<sup>0</sup> C range and relative humidity in the 35-65 percent range

Format - available in 70 mm rolls on 4 mil polyester base and 105 mm x 148 mm fiche on 7 mil polyester base

Handling Durability - low susceptibility to surface damage and contamination by ordinary handling and processing; high resistance to scratching and a low affinity for particulate matter

Image Permanance - no measurable changes in holographic parameters for repeated or extended illumination with laser light at high irradiance levels

OSHA/EPA Impacts - none

Performance Consistency - less than 10 percent rms variation of sensitometric and holographic parameters within and between production units

Processing - fully compatible with automatic equipment

Shelf Life - greater than 6 months at 20<sup>0</sup> C and 50 percent RH; at least 2 years if refrigerated

Table 3-4. Photographic Films for Holographic Recording

FILM PARAMETER RECORDING MATERIAL	Exposure <sup>a</sup> at 514.5nm (ergs/cm <sup>2</sup> )	Spectral Sensitivity	Resolution at 50% Response (cycles/mm)	Diffraction <sup>b</sup> Efficiency (%)	Signal-to- Noise Ratio <sup>c</sup> (dB)	Emulsion Thickness (μm)	Film Base
Agfa Scientia, 10E56	15	Ortho	>1000	0.8	20	6	4 mil Polyester
Kodak High Speed Holographic Film, S0-253	20	Pan	>1000	0.8	21	6	4 mil Polyester
Kodak Holographic Recording Film, S0-141	20	Ortho	>1000	0.6	20	6	4 mil Polyester
Kodak Minicard Film, Type 6451	20	Ortho	> 800	0.5	18	6	5.4 mil Triacetate
Agfa Scientia 8E56	100	Ortho	>1000	1	22	6	4 mil Polyester
Kodak High Resolu- tion Film, S0-343	500	Ortho	>1000	1	22	6	7 mil Polyester
Kodak Spectroscopic Film, 649F	500	Pan	>1000	1	22	6	7 mil Polyester
Kodak Holographic Film, S0-173	1000	Pan	>1000	1	23	6	4 mil Polyester

<sup>a</sup>To obtain a net density of 0.6

<sup>b</sup>Typical maximum level for a diffuse input signal, the amplitude recording mode, and maximum SNR

<sup>c</sup>Optimum recording conditions and an information packing density of  $5 \times 10^6$  pixels/cm<sup>2</sup>

Table 3-5. Comparison of S0-343 Photographic Film With Nonconventional Recording Materials

TYPE PARAMETER	Kodak S0-343	Dichromated Gelatin	Acrylic Photopolymer	CAB 55 <sup>f</sup>	PVK Photo- resist <sup>g</sup>
Type	Volume Phase	Volume Phase	Volume Phase	Volume Phase	Planar Phase
Typical Thickness	6 $\mu\text{m}$	15 $\mu\text{m}$	25- 100 $\mu\text{m}$	100- 750 $\mu\text{m}$	1 $\mu\text{m}$
Exposure Sensitivity <sup>a</sup>	0.05 mJ/ $\text{cm}^2$	100 mJ/ $\text{cm}^2$	10 mJ/ $\text{cm}^2$	500 mJ/ $\text{cm}^2$	5 mJ/ $\text{cm}^2$
Spectral Response	350- 650 nm	350- 550 nm	350- 550 nm	400- 500 nm	350- 650 nm
Resolving Power	>3000 $\ell/\text{mm}$	>3000 $\ell/\text{mm}$	>1000 $\ell/\text{mm}$	>3000 $\ell/\text{mm}$	>500 $\ell/\text{mm}$
Diffraction Efficiency a. Grating b. Diffuse Target	>50% >20%	>95% >25%	>80% >25%	>95% >35%	>30% >20%
Max. SNR (diffuse target) <sup>b</sup>	22 dB	27 dB	28 dB	34 dB	22 dB
DE at Max. SNR	~2%	~3%	~2%	~7%	~2%
Typical Angular Sensitivity <sup>c</sup>	>2 <sup>o</sup>	>2 <sup>o</sup>	>0.5 <sup>o</sup>	>0.2 <sup>o</sup>	>40 <sup>o</sup>
Typical Insertion Loss <sup>d</sup>	25%	10%	15%	25%	10%
Shelf Life a. Room Temperature b. Refrigerated <sup>e</sup>	>1 year >5 years	~1 day >30 days	~1 week >90 days	~1 year >2 years	<1 day <14 days
Image Permanence <sup>e</sup>	~30 days	>1 year	>1 year	>30 days	>1 year
Archival Lifetime <sup>e</sup>	>10 years	>1 year	>1 year	>1 year	>3 years

<sup>a</sup>Exposure at 514.5 nm to achieve maximum SNR

<sup>b</sup>For an equivalent information packing density of  $5 \times 10^6$  pixels/ $\text{cm}^2$  and optimized recording parameters at  $\lambda = 514.5$  nm

<sup>c</sup>Half-power response

<sup>d</sup>Includes reflection losses

<sup>e</sup>Estimated from available experimental data

<sup>f</sup>Cellulose Acetate (55%) Butyrate sensitized with p-benzoquinone

<sup>g</sup>Horizons Research Incorporated Type L photoresist



### 3.4 HARDCOPY FILMS

The retrieval of graphic information from storage in microreduced form, either conventional or holographic, is generally complimented by hardcopy reproduction of some kind. For map production, this could be done on a graphic arts film to form a repromat or directly onto a pressplate; the latter case is treated separately in the next section. Here, we focus our attention on dimensionally stable, very high contrast lith films.

The basic function of the hardcopy film is to form high-contrast repromats. As conventional diazo pressplates used for map production are negative-working, the graphic information on the repromats should appear as clear areas on an opaque background. Since the film chip (or holographic image) of the reduced graphic can be either negative or positive, polarity is not critical. However, the present program utilized positive film chips, and hence, a positive-working (duplication) film or negative film with reversal processing was required. The most important factors are edge acuity, contrast and a dimensionally stable substrate.

As hardcopy reproduction of full-scale map separations is a key aspect of the MEGIS Program, considerable care was used in the specification and selection of the recording materials. After a preliminary survey, Eastman Kodak was chosen as the vendor. Based on both experimental and future operational consideration, the film specification outlined in Table 3-6 were generated. The desired hardcopy film can be characterized by high contrast, high  $D_{\max}$ , relatively high speed at argon laser wavelengths, good resolution, clean working properties, dimensional stability, a 7-mil polyester base, and compatibility with machine processing. We identified very few lith films that satisfied these criteria.

Table 3-6. Specifications for Hardcopy Films

I. PHOTOGRAPHIC

Densitometric Properties -  $\gamma$  (contrast)  $> 4$

$$\begin{matrix} D_{\max} & > 4 \\ D_{\min} & < 0.1 \end{matrix}$$

Image Polarity - positive or negative working

Latent Image Decay - negligible for time delays between exposure and processing of up to 4 hours

Reciprocity Failure - negligible for exposures in the 0.1 to 100 second range

Sensitometric Properties - exposure requirement;  $< 100 \text{ ergs/cm}^2$ ; spectral sensitivity; orthochromatic

Substrate - 7 mil photographic grade polyester

II. DATA STORAGE

Acutance - very high

Dimensional Stability - less than  $\pm 1$  mil dimensional variations for  $\pm 10\%$  changes in relative humidity and for  $\pm 10^\circ \text{C}$  changes in Temperature

Distortion - less than  $\pm 1.5$  mil deviations from metric fidelity due to dimensional changes and processing as measured with reference to the spatial coordinates of UTM reference grid vertices at full scale

Granularity - less than 0.025 when measured with a  $48 \mu\text{m}$  aperture at 12X magnification for a net density  $D = 1$

Processing Effects - negligible relative to line widths as small as 3 mils

Resolution - at least 50 percent response at 100 cycles/mm for a high contrast (1000:1) tribar target

Signal/Noise Ratio (SNR) - a minimum average maximum density to average background density ratio of 15 (12 dB) for binary graphic input data

Turbidity - less than 10 percent line broadening up to a net density of four for line widths of 3 mils or greater

Table 3-6. Specifications for Hardcopy Films (Continued)

III. SYSTEMS

Availability - 30 days ARO

Cost - less than \$2.00/square foot

Environmental Sensitivity - no measurable changes in sensitometric and densitometric parameters for temperatures in the 10-30° C range and relative humidity in the 35-65 percent range

Format - available in sizes from 24 x 30 inches to 48 x 72 inches sheets on 7 mil polyester base

Handling Durability - low susceptibility to surface damage and contamination by ordinary handling and processing; high resistance to scratching and a low affinity for particulate matter

Image Permanence - no measurable changes in densitometric parameters for repeated or extended illumination at high irradiance levels with either UV or visible light

OSHA/EPA Impacts - none

Performance Consistency - less than 10 percent rms variation of sensitometric and densitometric parameters within and between production units

Processing - fully compatible with automatic equipment

Shelf Life - greater than 6 months at 20° C and 50 percent RH; at least 2 years if refrigerated

After careful analysis, we selected and evaluated Kodak Super Speed Duplication Film, SS7. This is a very high contrast, positive-working film with high contrast (1000:1) tribar resolution greater than 228 cycles/mm. The SS7 film was used exclusively for hardcopy reproduction, and consistently provided high-quality reprostats. We add that Kodak High Speed Duplicating Film, Type 4575, and Kodak Kodalith Ortho Film, Type 4556, were also successfully used for hardcopy reproduction. These and other hardcopy films are listed in Table 3-7.



Table 3-7. Hardcopy Films

FILM PARAMETER RECORDING MATERIAL	Exposure at <sup>a</sup> 488-514.5 <sub>2</sub> nm (ergs/cm <sup>2</sup> )	Spectral Sensitivity	Resolution at <sup>b</sup> 50% Response (cycles/mm)	Granularity <sup>b</sup> (x 10 <sup>3</sup> )	Imaging Mode	$\gamma$ , D <sub>max</sub> and D <sub>min</sub>	Film Base
Kodakline Reproduction Film, Type 4566	20	Ortho	>100	<25	Neg.	>4 >3 <0.15	7 mil Polyester
Kodak High Speed Duplicating Film, Type 4575	<100	Ortho	>50	<25	Post.	<-3 >3 <0.15	7 mil Polyester
Kodalith MP High Speed Duplicating Film, Type 4565	<100	Ortho	>50	<25	Post.	<-4 >4 <0.15	7 mil Polyester
Kodalith MP Ortho Film, Type 4557	100	Ortho	>50	<25	Post.	>4 >4 <0.15	7 mil Polyester
Kodalith Ortho Film, Type 4556	100	Ortho	>100	<25	Neg.	>4 >3 <0.15	7 mil Polyester
Kodak Super Speed Duplication Film, Type SS7	100	Ortho	>100	<25	Post.	<-4 >4 <0.15	7 mil Polyester
Kodak High Resolution Film, SO-343	<1000	Ortho	>1000	<5	Neg.	>4 >4 <0.15	7 mil Polyester

<sup>a</sup>For a net density of two<sup>b</sup>In some cases the data are estimated

### 3.5 PRESSPLATE MATERIALS

A key element in the total development of either a conventional or holographic graphic information storage and retrieval system is the pressplate material. For map production there may be favorable performance and operational impacts. Although not a consideration of the present study, it may be possible to eliminate the use of film separations and still maintain a color proofing capability by selecting an electrophotographic pressplate material. Thus, in this section we present a brief review of current pressplate technology at DMA production centers, an outline of pressplate considerations and specifications, and a summary of pressplate materials which are attractive for direct laser projection from either a conventional or holographic store.

#### 3.5.1 Current Pressplate Technology

Wipe-on surface plates, which are light-sensitive diazo compounds coated on treated aluminum plates, together with presensitized pressplates of similar composition, form the lithographic basis for map and chart generation within DMA production centers. Wipe-on plates are prepared by first mixing a diazo powder and solvent to form a coating resin. The light-sensitive resin is then coated onto an anodized or silicated aluminum substrate, usually with a roller coater, and dried. In use, the plate is exposed under a negative, processed, and dried. Processing is quite simple, and requires only 1 to 2 minutes. Development, desensitization, and lacquering are often done in a single step. Both preparation and use can be partially automated. Advantages of these materials include low cost (about \$0.40 per square foot), high quality, good press life (100,000 impressions have been obtained), long uncoated shelf life, and relatively easy handling characteristics. As is characteristic of all diazo compounds, exposure sensitivity is very low and powerful light sources rich in UV light (Xenon, high-pressure mercury, and

carbon arc lamps) are required to keep exposure times reasonably short (typically about 4 minutes). Resolution is excellent; 133 line screens are well resolved.

Overall, current materials and techniques appear to be both compatible and cost-effective relative to current map and chart production technologies. They do not, however, match well with many aspects of direct analog (or digital) laser platemaking. Of particular concern are exposure sensitivity and spectral response. Exposure sensitivity dictates writing speed and type of laser; spectral sensitivity mainly influences the choice of laser. It is highly desirable to choose a reliable, proven laser. With respect to the MEGIS Program, this means an argon laser operating in the visible region, i.e., at 488 nm or 514.5 nm. Diazo materials appear to be inherently UV sensitive, with only trace sensitivity for wavelengths greater than 420 nm; no commercial dye-sensitized diazo pressplate materials are known, although the Western Litho Plate and Supply Company is attempting to develop an argon laser-sensitive pressplate.

### 3.5.2 Candidate Direct Pressplate Materials

We now focus our attention on direct pressplate materials. The direct generation of a press-ready plate with a laser recording system creates a need for the evolution of new or modified pressplate material characteristics. Among the most important of these are high exposure sensitivity, spectral response closely matched to reliable commercial lasers, relatively high resolution (at least 2000 cycles/inch), and full compatibility with automated, on-line preparation and processing. In addition, the pressplate materials must provide cartographic printing quality and have attractive systems properties, such as consistency of performance, a stable shelf life, long term commercial availability, a reasonable unit cost, environmental sensitivity,



good handling durability, a run length of up to 25,000 or more impressions, and negligible OSHA and EPA impacts. These considerations are summarized in Table 3-8. Complete specifications for the desired offset pressplate material are given in Table 3-9.

A survey of commercial vendors identified several direct pressplate materials that closely match the requirements of the MEGIS Program and that are either commercially available or in an advanced development stage, i.e., approaching commercial status. The properties and characteristics of the most promising pressplate materials are summarized in Table 3-10. As a basis for comparison, the Western Litho Plate and Supply Company's Laser Plate is included, even though it is primarily intended for UV laser exposure.

Finally, in Table 3-11, we outline the key features of preferred pressplate materials, which are diazo and electrophotographic. Clearly, the currently used diazo pressplate materials are attractive in terms of performance, operational, and economic considerations. However, the electrophotographic pressplate materials are far more compatible with respect to the implementation of either a conventional or holographic projection system. If the continued use of repromats is desirable, then diazo pressplates will remain usable. But if repromat generation is to be avoided by direct pressplate generation, then we believe that an electrophotographic material will be needed.

### 3.6 SUMMARY AND COMMENTS

To gain an overall perspective of necessary recording materials considerations, important parameters and variables are summarized in Tables 3-12, 3-13, and 3-14. These tables list photographic, data storage, and

Table 3-8. Major Pressplate Considerations

- Speed
- Spectral Response
- Cost
- Run Length
- Compatibility with On-line, Automatic Processing
- Supplier Reliability
- Record Laser
- Resolution
- Copy Quality
- Performance Consistency
- Shelf Life
- OSHA-EPA Impacts

Table 3-9. Specifications for Direct Offset Pressplate Materials

I. PHOTOGRAPHIC

Densitometric Properties -  $\gamma(\text{contrast}) \sim 1$   
reflective  $D_{\text{max}} \sim 1$   
reflective  $D_{\text{min}} < 0.1$

Image Polarity - positive or negative working

Latent Image Decay - negligible for time delays between exposure and processing of up to 4 hours

Reciprocity Failure - negligible for exposure times in the 0.1 to 100 second range

Sensitometric Properties - exposure requirement;  $< 100 \mu\text{J}/\text{cm}^2$ :  
spectral sensitivity; orthochromatic

Substrate - brushed aluminum or equivalent

II. DATA STORAGE

Acutance - high

Dimensional Stability - less than +10 mil dimensional variations for +10% changes in relative humidity and for  $\pm 10^\circ\text{C}$  changes in temperature

Distortion - less than +20 mil deviation from metric fidelity due to dimensional changes and processing, as measured with reference to the spatial coordinates of UTM reference grid vertices printed at full scale

Processing Effects - negligible relative to the printing of line widths as small as 3 mils

Resolution - at least 75% response for 133 line tint screens with 10 to 90% occupancy

Signal/Noise Ratio - a minimum line density to rms background density on printed copy of 100 (20 dB) for graphic input data

III. SYSTEMS

Availability - 30 days ARO

Cost - less than \$1.00/square foot



Table 3-9. Specifications for Direct Offset Pressplate Materials (Continued)

Environmental Sensitivity - no measurable changes in sensitometric, densitometric, and data storage parameters for temperatures in the 10-30°C range and relative humidity in the 35-65% range

Format - available on 9 mil brushed aluminum substrates in sizes from 24 x 30 inches to 48 x 72 inches

Handling Durability - low susceptibility to surface damage and contamination by ordinary handling and processing; high resistance to scratching and a low affinity for particulate matter

Image Performance - a minimum of 25,000 impressions without degradation of printed copy

OSHA/EPA Impacts - none

Performance Consistency - less than 10% rms variation of sensitometric, densitometric, and data storage parameters within and between production units

Processing - fully compatible with automatic equipment

Shelf Life - greater than 6 months at 20°C and 50% RH; at least 2 years if refrigerated

Table 3-10. Pressplate Recording Materials

PARAMETER	VENDOR					
	Agfa- Gevaert	Azoplate	Coulter Information Systems	Horizons Research	S. D. Warren <sup>†</sup>	Western Litho Supply and Plate Company
Type	Silver Halide	Electro- photo- graphic	Electro- photo- graphic	Photo- resist	Electro- photo- graphic	Diazo
Mode of Use	Offset	Offset	Offset	Offset	Offset	Offset
Spectral Response	UV, visible (panchro- matic)	UV, Blue/ Green	UV, Blue/ Green	UV, Blue/ Green	Orange/ Red	UV, Blue/ Green
Speed ( $\mu\text{J}/\text{cm}^2$ )	<5 at 515 nm	75 at 515nm	<5 at 515 nm	$5 \times 10^3$ at 515 nm	100 at 633 nm	$100 \times 10^3$ at 515 nm
Record Laser Power*	25 mW Argon	375 mW Argon	50 mW Argon	25 W Argon	25 mW He-Ne	500 W Argon
Cost**	\$1 - \$1.50	\$2 - \$3	\$1.50 - \$2		\$2 - \$3	<\$1
Run Length	~25 K	50-100K	50-100K	75-100K	75-125K	50-100K
Automa- tion Capability	Full	Full	Full	Partial	Full	Full

\*For direct projection assuming uniform exposure over  $5000 \text{ cm}^2$  (24" x 30"), overall light efficiency of 0.85%, and 120 second exposure time; these data are upper bounds. A comparable holographic system would require 5 to 10X less output laser power.

\*\*Estimates based on latest data available; assumes a 24" x 36" x 9 mil brushed aluminum substrate.

<sup>†</sup> The same sensitivity level is achievable for argon laser light if different spectral sensitizers are used.

Table 3-11. Features of Preferred Pressplate Media

- A. DIAZO - Best overall in terms of performance, cost, and operational convenience.

Advantages

- \* Low cost (less than \$1.00 per plate)
- \* Ease of use (presensitized or wipe-on)
- \* Multiple commercial sources (generally)
- \* Long run lengths (about 100,000)
- \* Excellent copy quality
- \* Established technology

Disadvantages

- \* Low speed
- \* UV sensitive
- \* Low probability of higher speeds or extended spectral response

- B. ELECTROPHOTOGRAPHIC - Best for laser projection systems, either conventional or holographic.

Advantages

- \* High speed in the visible spectrum
- \* Spectral response at key commercial laser wavelengths
- \* Long run lengths (more than 25,000)
- \* Evolving technology and active R/D

Disadvantages

- \* Relatively high cost (between \$2.00 and \$3.00 per plate)
- \* Few reliable commercial sources
- \* Limited map production experience



Table 3-12. Photographic Considerations

Variable	Film			
	Microreduction Films	Holographic Films	Hardcopy Films	Pressplate Materials
Densitometry	✓	✓	✓	-
• $\gamma$ (contrast)	✓	✓	✓	-
• $D_{max}$	✓	✓	✓	-
• $D_{min}$	✓	✓	✓	-
Image Polarity	✓	-	✓	✓
Latent Image Decay	✓	✓	✓	-
Light Source	✓	✓	✓	✓
Processing	✓	✓	✓	✓
Reciprocity Failure	✓	✓	✓	-
Sensitometry	✓	✓	✓	✓
• Exposure requirement	✓	✓	✓	✓
• Spectral sensitivity	✓	✓	✓	✓

Table 3-13. Data Storage Considerations

Variable \ Film				
	Microreduction Films	Holographic Films	Hardcopy Films	Pressplate Materials
Acutance	✓	✓	✓	✓
Diffraction Efficiency	-	✓	-	-
Dimensional Stability	✓	✓	✓	✓
Distortion	✓	✓	✓	✓
Emulsion Thickness	-	✓	-	-
Granularity	✓	-	✓	-
Noise	✓	✓	✓	-
• Base	✓	✓	-	-
• Scatter	✓	✓	✓	-
• Wiener	-	✓	-	-
Point Spread Function	✓	✓	-	-
Processing Effects	✓	✓	✓	-
Resolution	✓	✓	✓	✓
SNR	✓	✓	✓	✓
Storage Capacity	✓	✓	-	-
Turbidity	✓	✓	✓	-

Table 3-14. Systems Considerations

Film Variable				
	Microreduction Films	Holographic Films	Hardcopy Films	Pressplate Materials
Archival Life	✓	✓	-	-
Availability	✓	✓	✓	✓
Cost	✓	✓	✓	✓
Environmental Sensitivity	✓	✓	✓	✓
Format	✓	✓	✓	✓
Handling Durability	✓	✓	✓	✓
Image Permanence	✓	✓	✓	✓
Method of Preparation	✓	✓	✓	✓
Method of Use	✓	✓	✓	✓
OSHA/EPA Impacts	✓	✓	✓	✓
Performance Consistency	✓	✓	✓	✓
Processing Equipment	✓	✓	✓	✓
Quality Control	✓	✓	✓	✓
Secure Storage	✓	✓	-	-
Shelf Life	✓	✓	✓	✓



systems considerations for microreduction, holographic, hardcopy, and pressplate materials. If a particular parameter or variable is a relevant consideration for one of these materials, this is indicated with a check. A study of these tables suggests that both the complexity of recording materials specification and selection and the relatively common nature of rather diverse light-sensitive systems.

The general conclusion of this part of the study is that suitable recording media are available for all aspects of graphic information storage and retrieval.<sup>8</sup> Well-qualified films of excellent quality are available for film chip generation, holographic recording, and hardcopy reproduction. Furthermore, it appears that high-quality pressplate materials with projection speed will soon be commercial products. Several of the pressplate materials we studied have sufficient exposure sensitivity for use with either a conventional or holographic projection system. Thus, all recording materials required for a cartographic microreduction and enlargement system are currently available or will be in the near future.

3.7 NOTES AND REFERENCES

1. Zech, R. G., "Data Storage in Volume Holograms," Ph.D. Thesis, U. of Michigan, May 1974, Section 3.
2. Zech, R. G., L.M. Ralston and M.W. Shareck, "Real-time Recording Materials Study," Final Technical Report, RADC Contract No. F30602-74-C-0030, July 1974.
3. For certain amplitude recording materials, especially photographic emulsions, both an amplitude and a surface relief (phase) grating are present. Diffraction efficiency data must be corrected to reflect only the contribution of the amplitude grating to obtain the correct frequency response function. Generally, the test holograms are index matched to eliminate the undesired phase gratings.
4. Brandt, G. B., Applied Optics 9, 1424 (1970).  
Stark, H., Applied Optics 10, 333 (1971).  
Smith, H. M., Applied Optics 11, 26 (1972).
5. "Kodak Plates and Film for Scientific Photography," Kodak Data Book, 1973, p. 315.
6. Thomas, W., Jr., Ed., SPSE Handbook of Photographic Science and Engineering, John Wiley and Sons, New York, 1973, pp. 953-955.
7. Mees, C. K. and T.H. James, Eds., Theory of the Photographic Process, MacMillan Company, New York, 1966, pp. 521-523.
8. An exception to this general conclusion relates to the phase errors generated by current polyester film bases, as discussed in Section II.

SECTION IV  
BREADBOARD EXPERIMENTS



## SECTION IV

### BREADBOARD EXPERIMENTS

In this section the results of an in-depth experimental evaluation of holographic and direct projection recorder/reproducer performance are presented. We begin with a description of the construction and evaluation of important components such as the film chips, the Fourier-transform HOE lens the diffuse phase randomizer, the Wray Micro Lens, and so forth. Then we discuss in detail the actual performance of several Fourier-transform holographic recorder/reproducer concepts. Important parameter measurements included diffraction efficiency, resolution and signal-to-noise ratio. Various recording and readout techniques are characterized as is hardcopy reproduction. Speckle-noise minimization experiments are outlined and, finally, the performance of a simple space invariant interferometer is described.

#### 4.1 FILM CHIP EVALUATION

The reduction of the full-scale map separation to a 70 mm film format was performed by ETL; the resultant film chips represented both 10X and 20X reductions. These film chips were used for both direct projection (micrographic) and holographic storage and retrieval studies. The overall quality of an image obtained either by direct or holographic projection is greatly affected by the quality of the film chip. The cosmetic and photographic characteristics were examined to determine if these properties of the film chips imposed any limitations on system performance.

The film chips, made from Kodak SO-141 film, were reversal processed to yield positive images. The film chips generally had a minimum amount of clear area (low average transmittance). For holographic storage

this condition is optimum since the information packing density requirement is reduced, the signal-to noise ratio is improved and a brighter image for the same laser readout power is obtained.

The overall cosmetic appearance of the film chips was good. However, dust and scratches were noted on the film chips under microscopic examination. These film chip defects do not affect image quality for diffuse (coherent or incoherent) illumination but are a source of noise for specular coherent illumination.

The irradiance uniformity<sup>1</sup> attainable in the focal plane of a projected image of an enlarging system is an important system consideration. This uniformity is related directly to the variation in transmittance of the film chips as a function of spatial position.<sup>2</sup> To estimate the acceptable variation in initial transmittance, we contact copied a sandwich of a film chip and density stepwedge onto Kodak SS7 film (the Kodak SS7 film has extremely high contrast and is well-suited for recording the projected images). Acceptable copies were produced over a 40 percent range of transmittance variation.

Images projected directly from the 10X reductions had a 10 to 15 percent variation in intensity, but images projected from 20X reductions had more than a 40 percent variation. To ensure that these variations were not inherent in the optical system, we exposed a sample of Kodak SS7 film to the projected image of a silk screen at a magnification of 20X. Figure 4-1 is a section of the recorded image near the edge of the field and shows excellent contrast. A similar exposure was made for the projected image of a film chip which had been made at a reduction of 20X. Figure 4-2 shows the same area near the edge of the image, and the loss in line weight caused by the variation in film chip transmittance. The Kodak SS7 film did not faithfully

AD-A051 532

HARRIS CORP MELBOURNE FL ELECTRO-OPTICS DEPT  
MICRO-REDUCTION AND ENLARGEMENT OF GRAPHIC INFORMATION STUDY (M--ETC(U)  
DEC 77 R G ZECH, L M RALSTON, B R REDDERSEN DAA653-75-C-0155  
HESD/EOD-1624-F ETL-0063 NL

UNCLASSIFIED

3 OF 5

AD  
A051 532





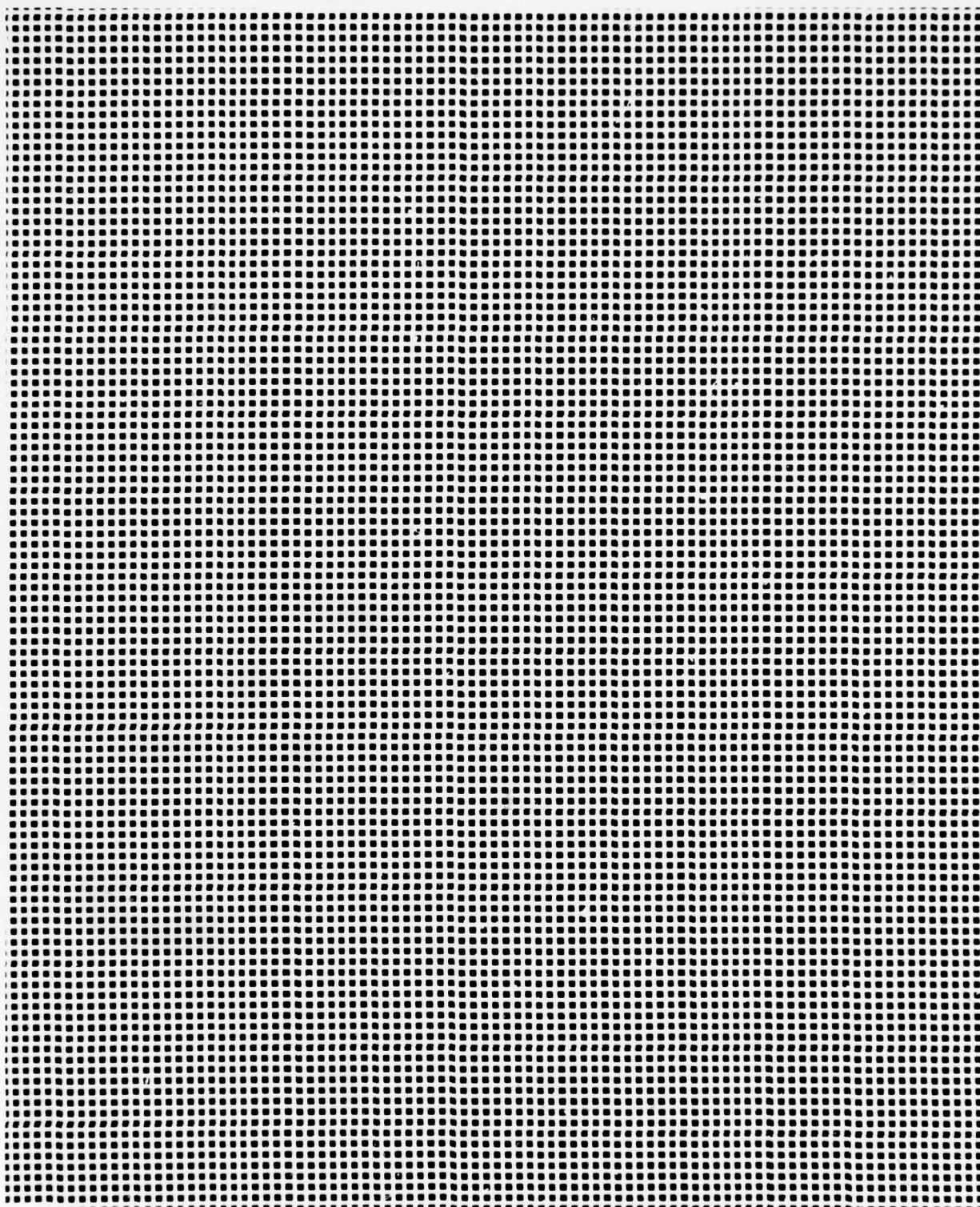


Figure 4-1. Enlargement With Incoherent Light of a Silk Screen Test Target  
at 20X Magnification Using Kohler Projection System



Figure 4-2. Enlargement With Incoherent Light of a 20X Reduced Film Chip Using a Kohler Projection System

reproduce images projected from film chips with variations in transmittance levels typical of the 20X reductions.<sup>3</sup>

There was no direct method by which we could measure the resolution of the film chips made from the various types of map separation. Special film chips made from an array of nine Air Force resolution targets, each with maximum possible resolution of 228 cycles/mm, were furnished at our request by ETL at reductions of 10X and 20X. We assumed that film chips for a given reduction ratio have a resolution equivalent to the corresponding film chips produced from the resolution target array.<sup>4</sup>

The resolution of the resolution target film chips was determined visually by microscopic examination. Figure 4-3 shows the resolution of the 10X and 20X reductions in several selected areas of the film chips. The resolution values reported here are referenced to the reduced resolution target film target. As such, the resolution achieved is greater than the resolution for a standard resolution target by either 10 or 20 depending on the reduction ratio. The resolution of the 10X reductions varied in a random manner over the film chip, ranging from 80 to 280 cycles/mm. For spatial frequencies below 150 cycles/mm, astigmatism appeared to be the limiting factor. For the chips made at a 20X reduction, resolution varied from 65 to 290 cycles/mm in a definite pattern. Resolution was greatest in the center of the array and decreased in radial directions. The bottom half of the film chip had lower resolution than the top half. The cause of this is probably related to the increase in density along one edge of the 20X reductions. Again, astigmatism appeared to be the factor limiting resolution.

Two film chips of special interest were a monochrome map and an array of moiré targets.<sup>5</sup> Both were made at 10X reductions and had good density uniformity. The monochrome map showed a slight decrease in resolution



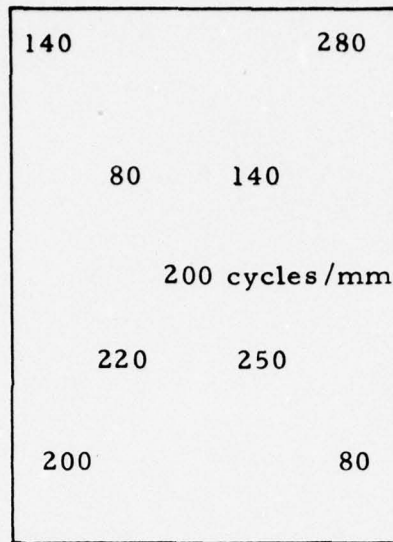


Figure 4-3 a  
RESOLUTION OF THE 10X REDUCED TARGET ARRAY

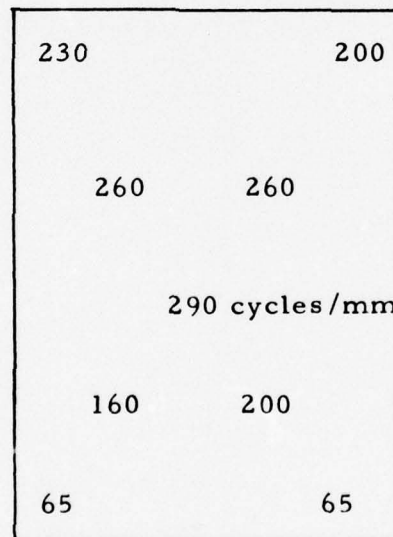


Figure 4-3 b  
RESOLUTION OF THE 20X REDUCED TARGET ARRAY

Figure 4-3. Resolution of Film Chip Target Arrays After Imaging to Full-Scale Using a Kohler Projection System

along the top edge, but the resolution of the center and bottom sections was good. Some of the half-tone screens were resolved in these areas. Four of the five moiré patterns were excellent; one corner was blurred. However, the center plus three corners provided adequate information for the alignment procedure discussed in Section V.

Several conclusions can be drawn from our examination of the film chips. They are as follows:

- High quality direct projections and holographic reconstructions should be possible using diffusely<sup>6</sup> illuminated 10X reduced film chips.
- The film chips made at a 20X reduction are not acceptable for high quality work. The intensity variation in the projected image is too great for acceptable film hardcopy to be made. The quality of these film chips can be improved.
- None of the film chips are usable when illuminated with specular<sup>7</sup> coherent light because of the coherent noise generated by dust, scratches, and other surface imperfections.
- The effects of astigmatism observed in certain film chips will degrade the quality of the projected image for either direct projections or holographic reconstructions.

#### 4.2 HOE FABRICATION

Holographic techniques can be used to generate optical elements to replace conventional lenses in an optical system. The advantages of holographic optical elements (HOE's) over conventional optics are that they are relatively easy to fabricate to required specifications, have a diffraction limited imaging capability under certain conditions of use, and are more lightweight and compact, especially for large elements.

The efficiency of a holographic optical element depends on the material on which it is recorded. Table 4-1 lists recording materials and their properties. Photoresists and photoplastics were eliminated because of low exposure sensitivity. Photodegradable plastics were not considered because of their low exposure sensitivity. Table 4-2 lists some of the characteristics of the most promising candidate materials. From a systems viewpoint, dichromated gelatin is best. However, long exposure and preparation times make it undesirable for situations in which the design specifications may require frequent alteration. The silver halide recording materials (bleached,<sup>8</sup> high resolution photographic emulsions) are the most versatile. Two members of this group are bleached Kodak HR plates and bleached Kodak 649F plates. Bleached Kodak HR plates are the favored material because it has better surface quality.

The holographic properties of high resolution silver emulsions are dependent on processing conditions and merit consideration. The use of Kodak developer D-19, a clean high-contrast developer, results in high efficiency. However, D-19 produces such a high contrast that the intensity distribution used to expose the HOE must be extremely uniform (better than 10 percent from center to edge). This imposes stringent requirements on the uniformity of the beams<sup>9</sup> used to record the HOE. To alleviate these requirements we tested low and medium contrast Kodak developers, D-165 and D-76, respectively. The resulting HOE's had lower diffraction efficiency with no appreciable reduction in uniformity requirements. Therefore, D-19 was chosen as the primary developer.

The bleaching process is necessary to increase the diffraction efficiency of the HOE. Two bleaching processes were considered and tested for use in our experimental effort. Table 4-3 compares the relative advantages



Table 4-1.

## Candidate HOE Recording Media

## Recording Material

	Type <sup>a</sup>	Speed <sup>b</sup> (mj/cm <sup>2</sup> ) at 488 nm	R.P. <sup>c</sup> (cycles/ mm)	Spectral Response	D.E. <sup>d</sup> (%)	SNR <sup>e</sup> (dB)	Processing Req'ts.
• Dichromated Gelatin	VP	100	>3000	Blue- green	>90	>25	Chem.
• Acrylate Photopolymer- (DuPont)	VP	10	>2000	UV blue- green	>50	>25	None
• Bleached Photographic Emulsions	PP VP	10 <sup>-2</sup>	>3000	UV visible	>50	>20	Chem.
• Photoresist a) Shipley AZ1350 b) Horizons LHS7	PP	10 <sup>4</sup> 5	>1500 >1000	UV blue UV blue- green	>25 >25	>15 >20	Chem. Heat
• Photodegradable Thermoplastics	VP	10 <sup>3</sup>	>3000	Blue- green	>60	>30	None
• Photoplastics	PP	10 <sup>-2</sup>	>1000	UV visible IR	>20	>15	Heat

a VP = Volume phase  
PP = Planar phase

d D.E. = Diffraction efficiency  
(ratio of diffracted light  
to incident light for a  
plane wave grating).

b Speed = Exposure for maximum  
diffraction efficiency.

e SNR = Signal/noise ratio. All  
data for a fixed packing  
density and beam ratio.

c R.P. = Resolving power

Table 4-2. Advantages and Disadvantages of HOE Recording Materials

	<u>Advantages</u>	<u>Disadvantages</u>
Kodak 649-F (Bromine Vapor Bleached)	<ul style="list-style-type: none"> <li>● High efficiency (75%)</li> <li>● Readily available</li> </ul>	<ul style="list-style-type: none"> <li>● Noisy because of poor surface quality</li> <li>● Insertion loss ~25%</li> <li>● Not archival</li> </ul>
Kodak HR Plate (Bromine Vapor Bleached)	<ul style="list-style-type: none"> <li>● High efficiency (75%)</li> <li>● Low noise (max SNR &gt;20 dB)</li> <li>● Readily available</li> </ul>	<ul style="list-style-type: none"> <li>● Insertion loss ~25%</li> <li>● Not archival</li> </ul>
Dichromated Gelatin	<ul style="list-style-type: none"> <li>● High efficiency (95%)</li> <li>● Low noise (max SNR &gt;27 dB)</li> <li>● Low insertion loss (10%)</li> <li>● Good archival properties when protected by a cover plate</li> </ul>	<ul style="list-style-type: none"> <li>● Not readily available</li> <li>● Long exposure times (&gt;1 hour)</li> </ul>
Photopolymer	<ul style="list-style-type: none"> <li>● High efficiency</li> <li>● Low noise (max SNR &gt;25 dB)</li> </ul>	<ul style="list-style-type: none"> <li>● Not readily available</li> <li>● Short shelf life</li> <li>● Requires index matching</li> </ul>

TABLE 4-3. Advantages and Disadvantages of Candidate Bleaches

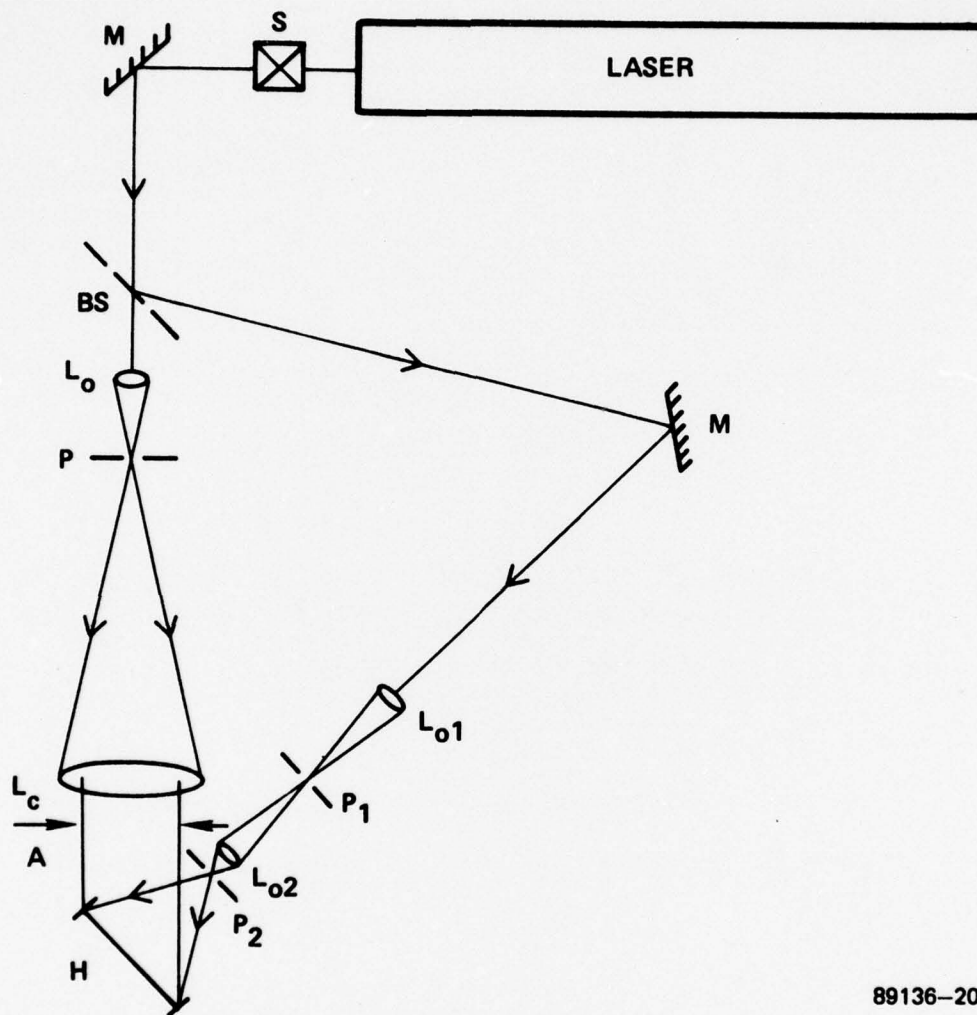
	<u>Advantages</u>	<u>Disadvantages</u>
● ZB Bleach (Ferric Chloride and Cupric Bromide)	<ul style="list-style-type: none"> <li>● High efficiency (50%)</li> <li>● Does not cause emulsion breakdown</li> </ul>	<ul style="list-style-type: none"> <li>● Darkens overnight under readout</li> <li>● Shrinkage effects</li> <li>● Poor surface quality</li> </ul>
● Bromine Vapor	<ul style="list-style-type: none"> <li>● High efficiency (75%)</li> <li>● Low noise</li> <li>● Low distortion</li> </ul>	<ul style="list-style-type: none"> <li>● Not archival (lifetime is about 6 months)</li> </ul>

and disadvantages of these bleaches: ZB (Ferric Chloride and Cupric Bromide) bleach and bromine vapor bleach.<sup>10</sup> Neither bleaching process produces a permanent recording. The HOE's prepared with the ZB bleaching process darken overnight under intense laser readout. However, the HOE's prepared with bromine vapor bleach lasted about 6 months. Therefore, we chose the bromine vapor bleaching process for the production of HOE and other holograms.

The design specifications of the HOE are dependent on the system geometry in which the HOE is used. The holographic optical element for the Fourier-transform lens in the holographic system must be compatible with the Wray Micro Lens. Because of the juxtapositioned principal planes of the Wray Micro Lens, the film chip plane and the front surface of the lens are separated by only 125 mm. The distance between the transparency and hologram is even less. In the Fourier-transform holographic system, the HOE must focus the beam in front of the Wray Micro Lens, while illuminating the film chip uniformly. On the other hand, for the Kohler illumination used in direct projection, the focal plane of the HOE must be at the aperture stop of the Wray Micro Lens. The aperture stop is located inside the lens, approximately 125 mm from the outside lens surface. Hence, differing requirements for the several system configurations investigated necessitated the fabrication of three HOE's; that is, a 184 mm, f/1.8 HOE for 10X reductions, a 145 mm, f/1.4, HOE for 20X reductions, and a 270 mm, f/2.5 HOE for direct projection (Kohler illumination).

Figure 4-4 illustrates the optical system used to construct HOE's. The beam from an argon ion laser ( $\lambda = 514.5$  nm) is split to form two paths. The reference beam is spatially filtered, expanded, and collimated. The collimated reference beam was incident on the recording plane at an angle of  $45^\circ$  from the normal. The signal beam is first expanded with a 3.5-power





89136-20

Figure 4-4. Experimental Geometry Used to Record Holographic Optical Elements

microscope objective  $L_{01}$ . The expanded beam is subsequently apertured and reexpanded with a 20-power microscope objective  $L_{02}$ , then spatially filtered with a  $5\text{ }\mu\text{m}$  pinhole  $P_2$ . The 20-power microscope objective produces an  $f/1.2$  cone of light with approximately 10 percent center-to-edge intensity falloff at the recording plane. The lower falloff limit of 10 percent is a limit imposed by the Gaussian nature of the laser beam. The final objective-pinhole combination is critical; a  $5\text{ }\mu\text{m}$  pinhole did not provide a complete uniform beam, while a  $2.5\text{ }\mu\text{m}$  pinhole did not yield illumination over the entire area of the HOE. The optimum pinhole diameter is somewhere between these two values.

Although all HOE's were astigmatic, no degradation of the projected image quality was traceable to the HOE aberration<sup>11</sup>. The HOE's had overall efficiencies of up to 76 percent. Uniformity was measured in the range of 2 to 20 percent center-to-edge, depending on exposure and processing condition. Holograms recorded with Fourier transform HOE's generally reconstructed full-scale images with 5 percent falloff from center-to-edge. We mention that 6 months after the HOE's had been recorded, their efficiency had dropped to 10 percent. It was found that the gelatin had dehydrated to the point of causing observable disintegration. As an expoxied glass cover was used to protect the HOE's, there is no obvious reason for this behavior.

The results of our investigations of the use of holographic optical elements as Fourier-transform lens can be summarized as follows:

- HOE's are excellent Fourier-transform lenses. They are efficient and can be made to match the recording format of the system.

- To ensure maximum reliability and highest efficiency dichromated gelatin, rather than silver halide, HOE's should be used.
- HOE's can be designed to provide a high level of image illuminance uniformity.

#### 4.3 PHASE RANDOMIZER FABRICATION

Recording in the exact Fourier-transform plane is difficult because of the large dynamic range of the signal spectrum intensity distribution. Phase randomization has the effect of spreading the energy of the signal transform over the entire hologram recording plane. No information is lost, and generally a high degree of redundancy is obtained. The phase randomizers used for the MEGIS Program were often diffusive; that is, objects which completely randomized the phase of the illuminating laser beam.<sup>12</sup> The characteristics of the phase randomizer affect the projected or reconstructed image quality. If the phase randomizer is too diffusive, a significant amount of laser power falls outside the hologram aperture<sup>13</sup>; if it is not sufficiently diffusive, the dynamic range problem is not reduced. One disadvantage of a phase randomizer is speckle noise, which causes the image to have a granular appearance and which breaks up the fine line structure of the image. For optimum image resolution, it is obviously desirable to minimize the size of the speckle; that is, to maximize speckle density, the number speckles per resolution element.<sup>14</sup>

Both photographic and nonphotographic phase randomizers of a diffusive nature were tested. The photographic types were made by contact copying a ground glass diffuser or a random amplitude pattern onto photographic emulsions which were subsequently developed and bleached using R-10 bleach and the Altman process,<sup>15</sup> which is the following:



a. Procedure

<u>Process Step</u>	<u>Process Time</u>
Develop	5 minutes
Wash	10 minutes
Bleach (R-10)	2 minutes
Wash	4 minutes
Fix	8 minutes
Wash	15 minutes
Dry	Still room temperature air

b. Chemical Composition of the R-10 Bleach

<u>Chemical</u>	<u>Amount</u>
Solution A:	
Distilled water	500 milligrams
Ammonium dichromate	20 grams
Sulfuric acid (concentrated)	14 milligrams
Distilled water	To make 1 liter
Solution B:	
NaCl	45 grams
Distilled water	To make 1 liter.

Working solution is prepared by mixing one part of Solution A and one part of Solution B with ten parts of distilled water.

Critical parameters of the process include the type of emulsion used for the contact printing, the type of developer used for processing, the characteristics of the target used for contact copying, and the level of exposure used to form the phase randomizer. The types of emulsions tested were Kodak HR, Agfa 8E75, and Kodak 649F. The Kodak HR plates did not produce acceptable results. This was due in part to the prehardening to the emulsion,

which prevents high levels of surface relief from occurring. Both the Agfa 8E75 and Kodak 649F plates did produce acceptable results. However, the thicker emulsion of the Kodak 649F plates provided greater surface relief. The spatial bandwidth is a function of surface relief; more diffusive phase randomizers are produced with high values of surface relief. The development and exposure tests were performed using Kodak 649F as the recording material.

The Kodak developers D-19, D-76, and D-165 were tested for performance levels. The lower contrast developers, D-76 and D-165, allowed a larger exposure latitude, but did not produce enough surface relief. Only the high contrast developer D-19 produced acceptable phase randomizers. All subsequent testing used D-19 for development.

The step most critical in producing an acceptable phase randomizer is the exposure level used for the particular target being contact copied. A range of exposures was made for each type of target contact copied. The series of phase randomizers produced were tested for their ability to provide a uniform intensity in the Fourier transform plane of appropriate bandwidth.

Photographic diffusers were made by contact copying satin ground glass, commercial nonglare glass, opal glass, a polacoat screen, and a random amplitude mask. Nonphotographic randomizers tested included satin ground glass, commercial nonglare glass, and glass ground in house using No.9 (9  $\mu$ m) grit. The performance of each phase randomizer type is discussed later in Paragraph 4.8.

#### 4.4 DIRECT PROJECTION STUDY

The throughput image of a holographic system is the direct projection of the signal beam. Because holography cannot improve image quality, and in fact generally degrades it, it is desirable to optimize the

throughput image and to determine the effects of system components on image quality.

Three kinds of illumination were compared: specular coherent illumination produced by expanding and collimating the laser beam; diffuse coherent illumination produced by passing the beam through a stationary phase randomizer; and, diffuse incoherent illumination produced by passing the laser beam through a moving phase randomizer. To compare the resolution obtained for each illumination condition, we inserted a standard 1951 Air Force resolution target in the film chip plane. An image of the resolution target was projected with a magnification of 10X, and the resolution of the image on-axis was measured whenever systems components were changed.

In the first system tested, a HOE was used as the Fourier-transform lens. The phase randomizer, when present, was placed in arbitrary position in front of the HOE. An adjustable aperture located in the hologram recording plane allowed us to determine the effect of hologram size. The effect of the recording film was observed by inserting an unexposed, but processed, Kodak SO-343 fiche, which has an Estar<sup>®</sup> polyester base, in the hologram plane.

Figure 4-5 summarizes the results obtained. Resolution in the projected image increased with aperture size up to about 25 mm diameter, beyond that resolution is limited by other factors. Incoherent illumination yielded the highest resolution in the projected image; specular coherent illumination, the next best; and diffuse coherent, the least. Inserting the film base into the optical system caused a 30 to 60 cycle/mm decrease in maximum resolution. Although incoherent light provided the best resolution transfer, it cannot be used to record holograms except under special conditions (e.g. with a space-invariant interferometer). We did not use incoherent illumination when



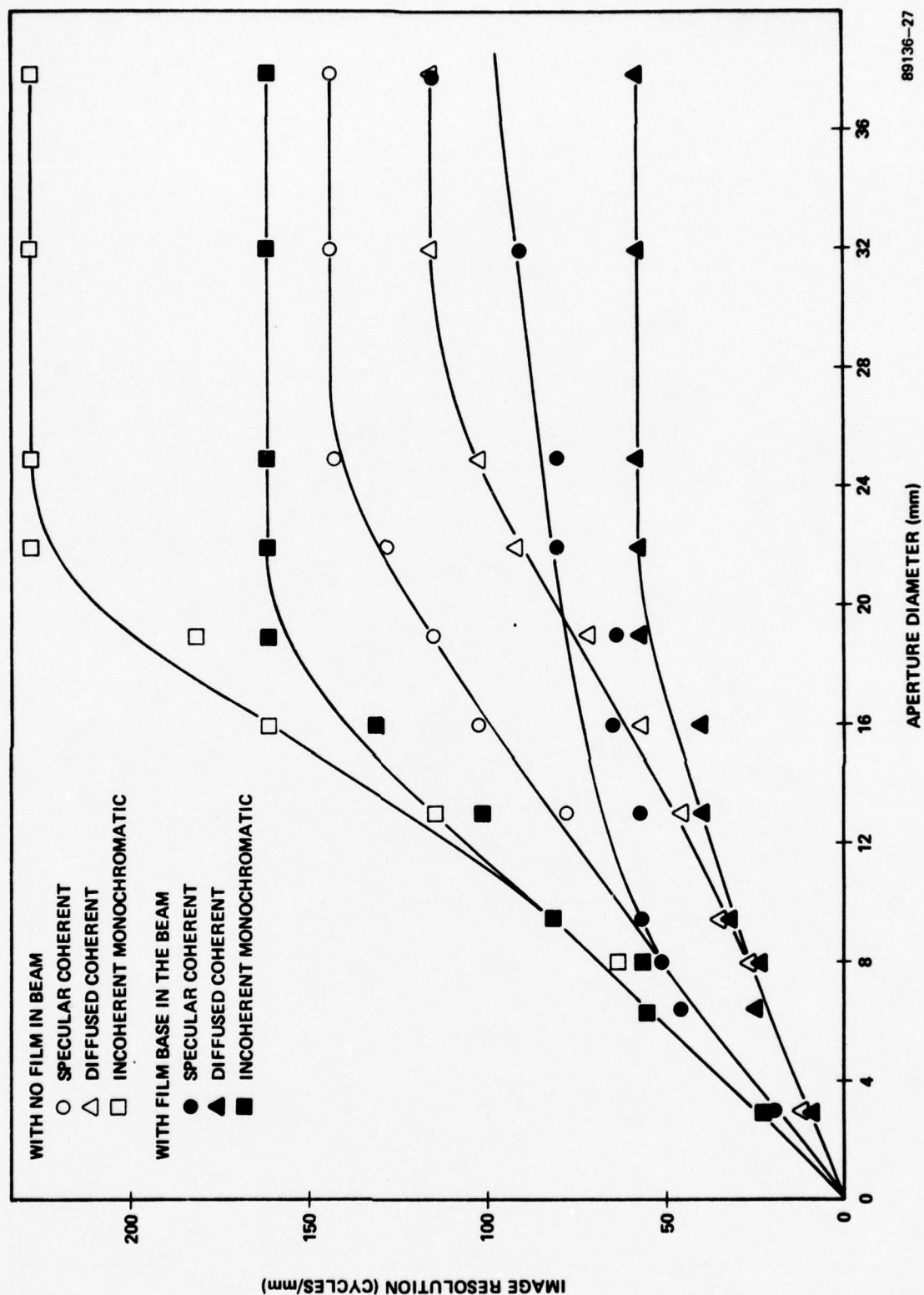


Figure 4-5. Image Resolution as a Function of Aperture Diameter With the Type of Object Illumination as a Parameter

measuring the effect of holographic system components on resolution transfer. Numerical data are summarized in Table 4-4.

Specular illumination provided better image resolution than diffuse illumination for each test condition. Of particular significance, a film base inserted into the optical system caused a 30-cycle/mm drop in resolution with specular illumination and a 60 cycle/mm drop with diffuse illumination. For diffuse illumination, a glass plate inserted into the optical path caused the resolution in the projected image to decrease. This effect is apparently dependent upon the glass thickness for plates less than 0.25 inch thick. Index-matching the film using a liquid gate did not improve image resolution.

All the evidence so far indicates that specular illumination provided a better resolution transfer than diffuse illumination. However, coherent noise has not yet been considered. Figure 4-6 shows a photograph of a resolution target projected using specular illumination. The hardcopy was purposely underexposed to the type of noise generated by flaws in a specular coherent optical system. Figures 4-7 and 4-8 are direct projections obtained using specular illumination for two map separation film chips. In this case, the exposure was optimized to obtain the best resolution transfer. The fine line details in Figure 4-7 are broken by coherent noise. A large percentage of the clear area of Figure 4-8 contains significant coherent noise. A section of a direct projection from the resolution target array is shown in Figure 4-9. This projected image was obtained using diffuse illumination. Although the speckle noise is clearly evident, coherent noise is not discernible.

Near the end of the contract, the Kohler illumination method described in detail in Paragraph 2.4, was implemented. Briefly, it involves positioning the diffuser or point source in such a position that the condenser

Table 4-4. Resolution Transfer Obtained for  
Different Film Support Techniques

Film Support Technique	Resolution (cycle/mm)	
	Specular Coherent Illumination	Diffuse Coherent Illumination
None	144	114
Unprocessed 649F glass plate - 0.060 inch thick	114	91.2
Unprocessed S0343 film on 7 mil Estar base	114	57
Polished glass flat - 0.25 inch thick	114	57
Processed S0343 film on 7 mil Estar base	114	57
Liquid gate - empty 1.5 inches thick	114	57
Liquid gate containing processed film	114	57



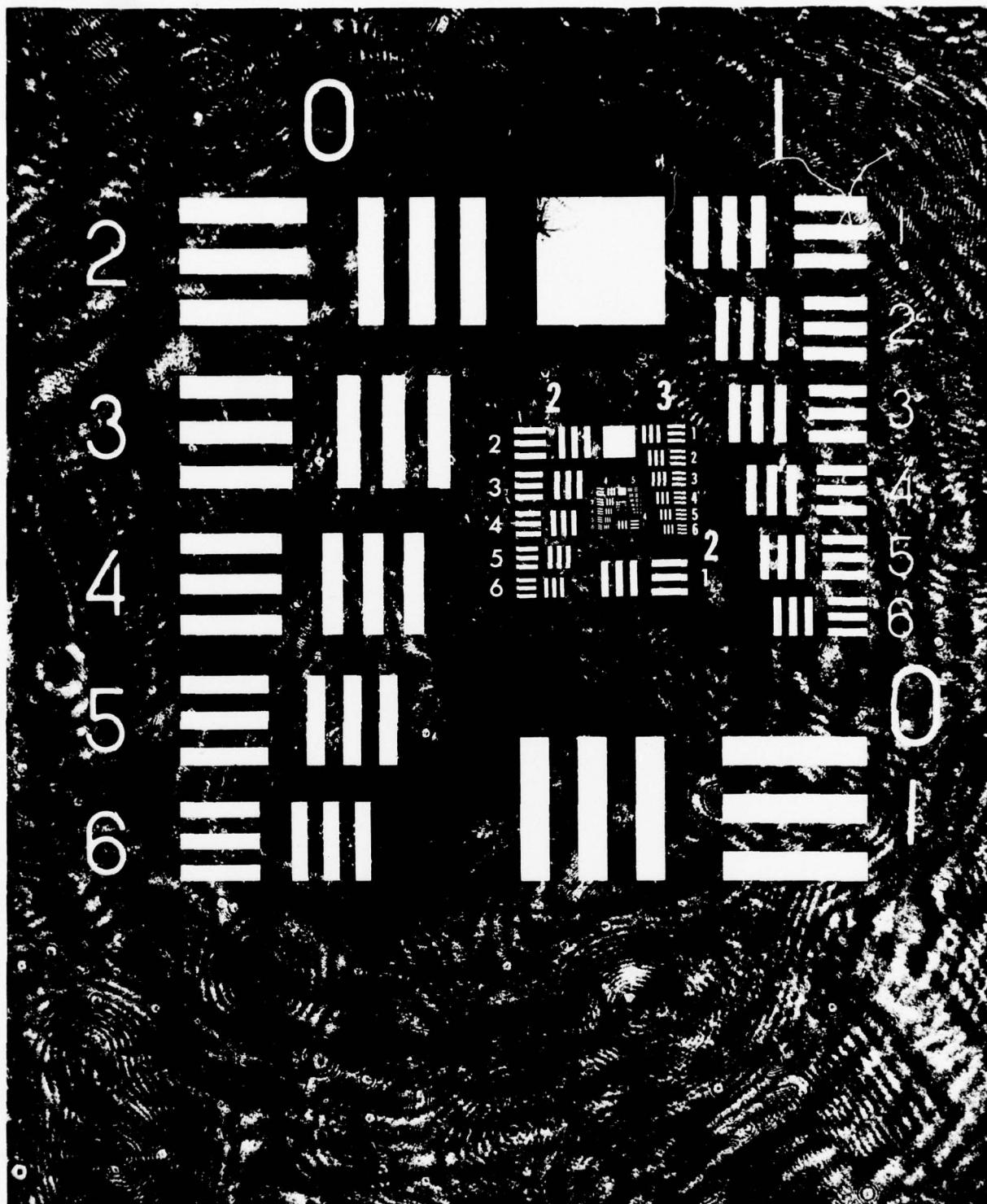


Figure 4-6. Direct Projection Image of a Resolution Target, Illuminated With Specular Coherent Light, Showing Noise Effects

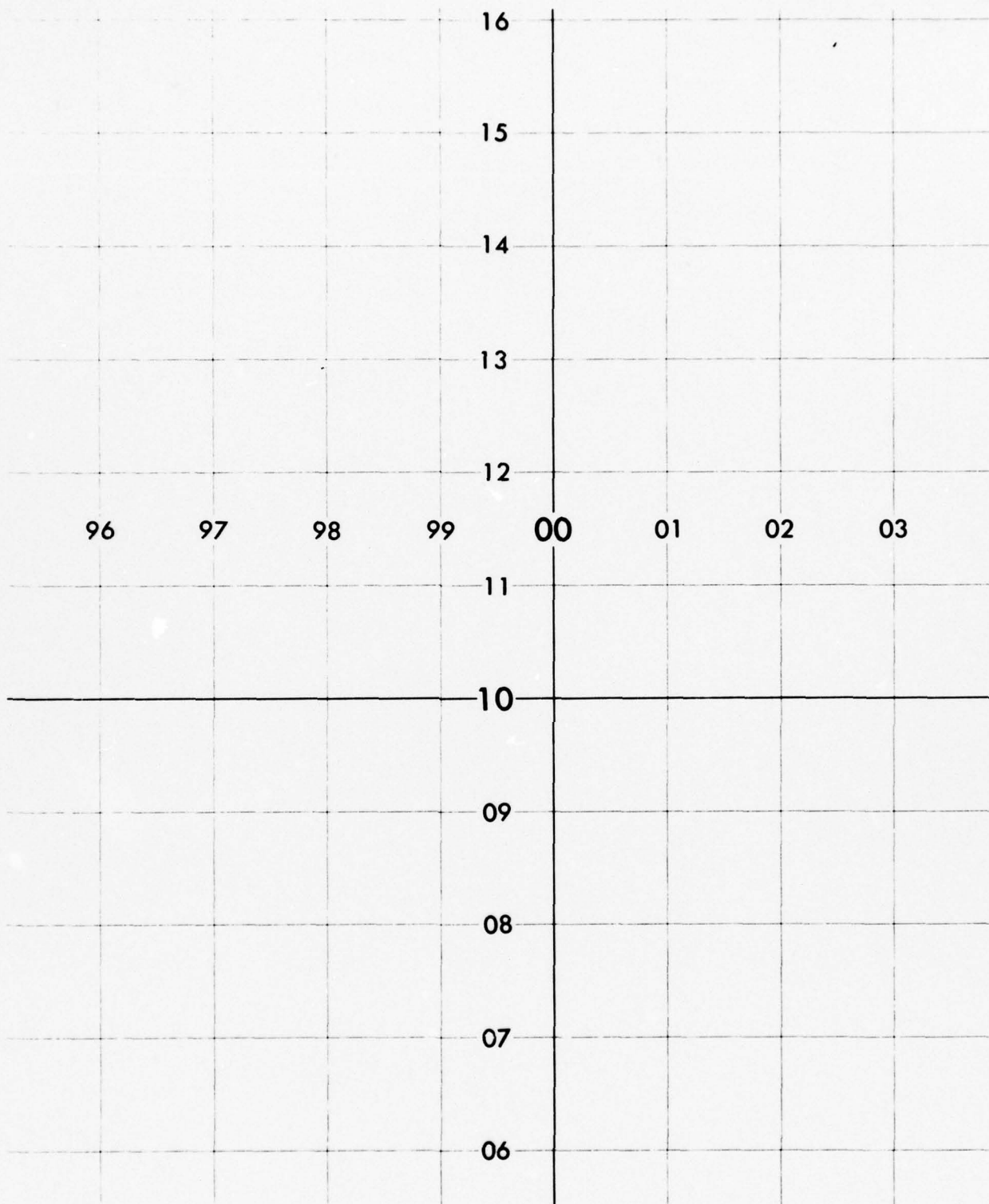


Figure 4-7. Direct Projection Image of a UTM Grid Film Chip, Illuminated With Specular Coherent Light, Which Was Reproduced With Optimum Hardcopy Exposure



Figure 4-8. Direct Projection Image of a Vegetation Film Chip, Illuminated With Specular Coherent Light, Which Was Reproduced With Optimum Hardcopy Exposure



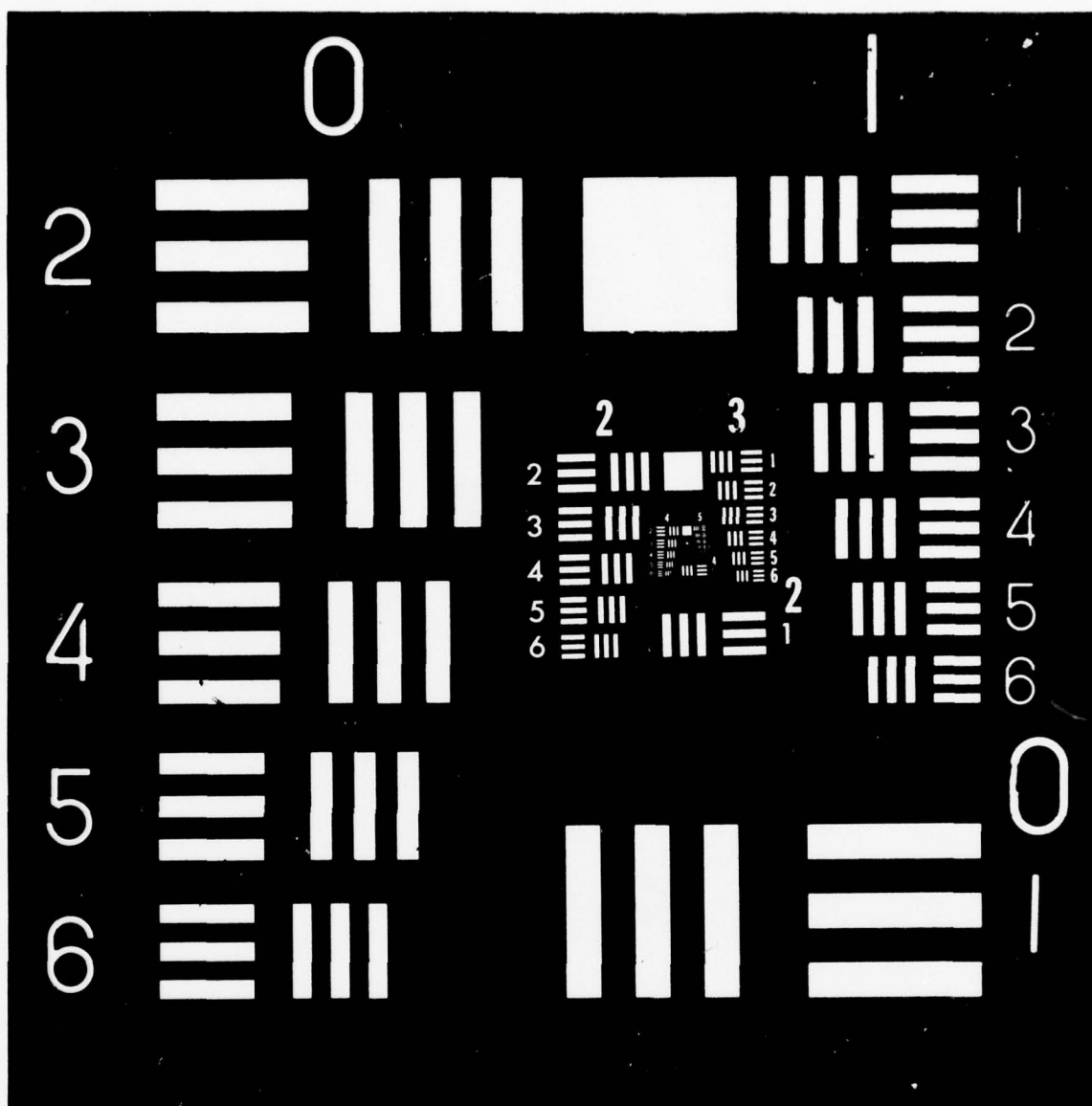


Figure 4-9. Direct Projection Image of a Resolution Target  
Illuminated With Diffuse Multiwavelength Coherent Light

lens images it in the limiting aperture of the system. For direct projections, the limiting aperture is the aperture stop of the Wray Micro Lens; for holography, it is the hologram aperture. With coherent light, use of the Kohler illumination method provided a higher resolution transfer than any other illumination technique.

Table 4-5 compares the systems effects of the three types of illumination, and specifies the resolution for both holographic Kohler and projection Kohler.<sup>16</sup> For a direct projection system, diffuse incoherent light was best. It provided maximum resolution transfer with no problems caused by speckle or coherent noise. Both diffuse coherent light and specular coherent light exceeded the resolution transfer requirements when the Kohler projection condition was satisfied. However, diffuse light generated speckle noise, while specular light generated coherent noise and produced a nonuniform Fourier transform. We believe that diffuse light, despite speckle, is best suited for a holographic system.

The results of this study indicated the following:

- With Kohler projection, the 125 cycle/mm resolution requirement is met regardless of the kind of illumination used.
- Specular coherent light degrades image quality because of coherent noise.
- In a direct projection system, incoherent illumination provided the highest quality image. In a holographic system, diffuse coherent illumination yielded best image quality.
- Polyester film base significantly degrades image quality and resolution.

Table 4-5. Resolution and Image Quality Performance for  
Holographic and Direct Kohler Projection

	Specular Coherent Light (cycles/mm)	Diffuse Coherent Light (cycles/mm)	Diffuse Incoherent Light (cycles/mm)
Maximum resolution - Holographic Kohler			
• Open aperture	144	114	>228
• 20 mm aperture	114	72	182
( $\lambda = 514.5$ nm)			
Maximum resolution- Projection Kohler			
20 mm aperture	163	128	>228
( $\lambda = 488$ and 514.5 nm)			
Speckle	Some	Present	None
Coherent noise	Present	None	None
Transform uniformity	Extremely nonuniform	Uniform	Uniform



#### 4.5 WRAY MICRO LENS EVALUATION

The 250 mm, f/4, 10:1 reduction Wray Micro Lens supplied by USA-ETL as the projection lens for the MEGIS Program performed high-resolution, low-distortion imaging with few problems. Before summarizing its performance characteristics, a few comments on its physical condition must be made. The surface quality of the Wray Micro Lens appeared acceptable when examined using the normal incoherent light for reduction camera work. When using coherent light for examination, however, flaws were observed. Straight-line streaks associated with inadequate lens cleaning were evident on lens surfaces. Circular scratches were also visible on the surfaces. Dust was noted on all surfaces. Periodic cleaning of any lens is required to maintain good lens performance, and the cleaning technique was adequate for uses of the lens with incoherent light. However, for coherent light an extremely careful cleaning process must be used to protect the optical surfaces. Any limitations on image quality mentioned in this report should be interpreted with regard to the flaws described above.

Overall resolution of the lens was quite good. Projections of the special resolution target array film chip showed the resolution on axis for incoherent light exceeded 228 cycles/mm, but decreased to 204 cycles/mm at the edges of the field. Further, when the lens was stopped down to f/5.6 to reduce the effects of lens flare on the projected image, there was no measurable decrease in lens resolution, either on axis or at the edges of the image field.

Measurements of the focal point positions of the lens were made in the following manner: a collimated beam of light was incident on one side of the lens, and the position of the resulting focal point on the opposite side measured. This procedure was then repeated for the opposite side of the lens to obtain the position of the other focal point. The front and back focal

points were symmetrically positioned approximately 5.1 inches from the external lens surfaces. Since the effective focal length is known, the locations of the principal planes, important lens parameters for system design, can be determined. Figure 4-10 is a schematic of the Wray Lens based on their measurements. The Rank Optics Group of England, the present source of the Wray Special Copy Lens technology, provided us with additional data. Figure 4-11 is the lens diagram used by Rank Optics to describe the construction of the Wray Micro Lens.

#### 4.6 SYSTEM COMPONENTS

Overall system performance is determined by the properties and characteristics of individual components. In this paragraph, we discuss the characteristics of film supports and readout assembly, specially constructed for system use. These devices, although not altogether unusual in nature, were required for satisfactory system performance.

##### 4.6.1 Liquid Gates

A liquid gate, consisting of two pieces of glass with a gap wide enough for a piece of photographic film and a much thinner layer of liquid on each side of the film, is a logical choice for both the film chip and the hologram holder. A liquid gate provides a means of holding film flat without stressing it and eliminates the coherent noise associated with emulsion surface roughness. In the present application, a liquid gate also acts as an optical delay line because of the presence of the additional glass thickness. The effective focal point of the condenser lens is shifted farther into the projection lens than this point would be without the gate. This requires the f-number of the Fourier-transfer lens to be decreased.

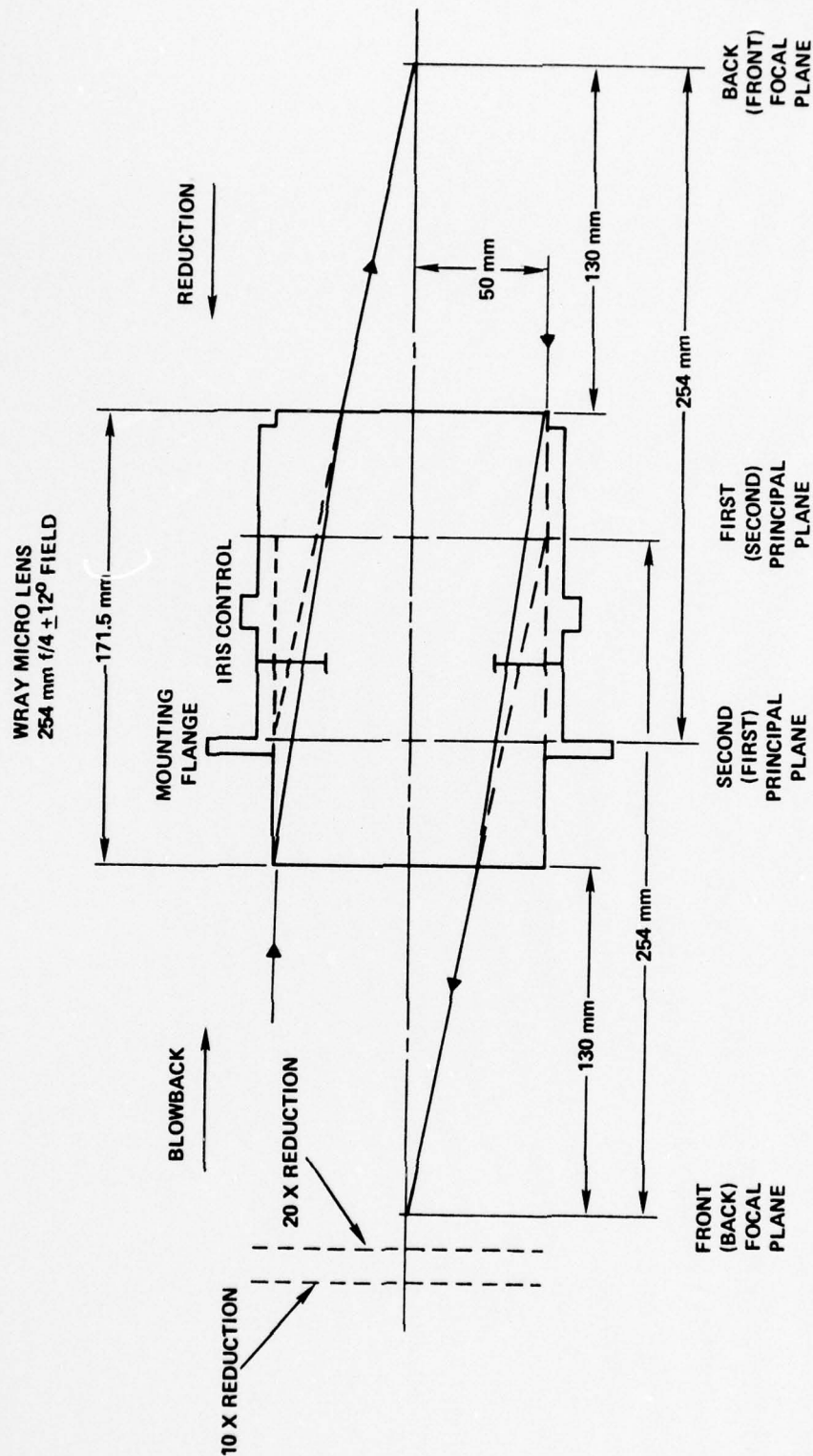


Figure 4-10. Schematic of the Geometrical Optics Equivalent of the Wray Micro Lens



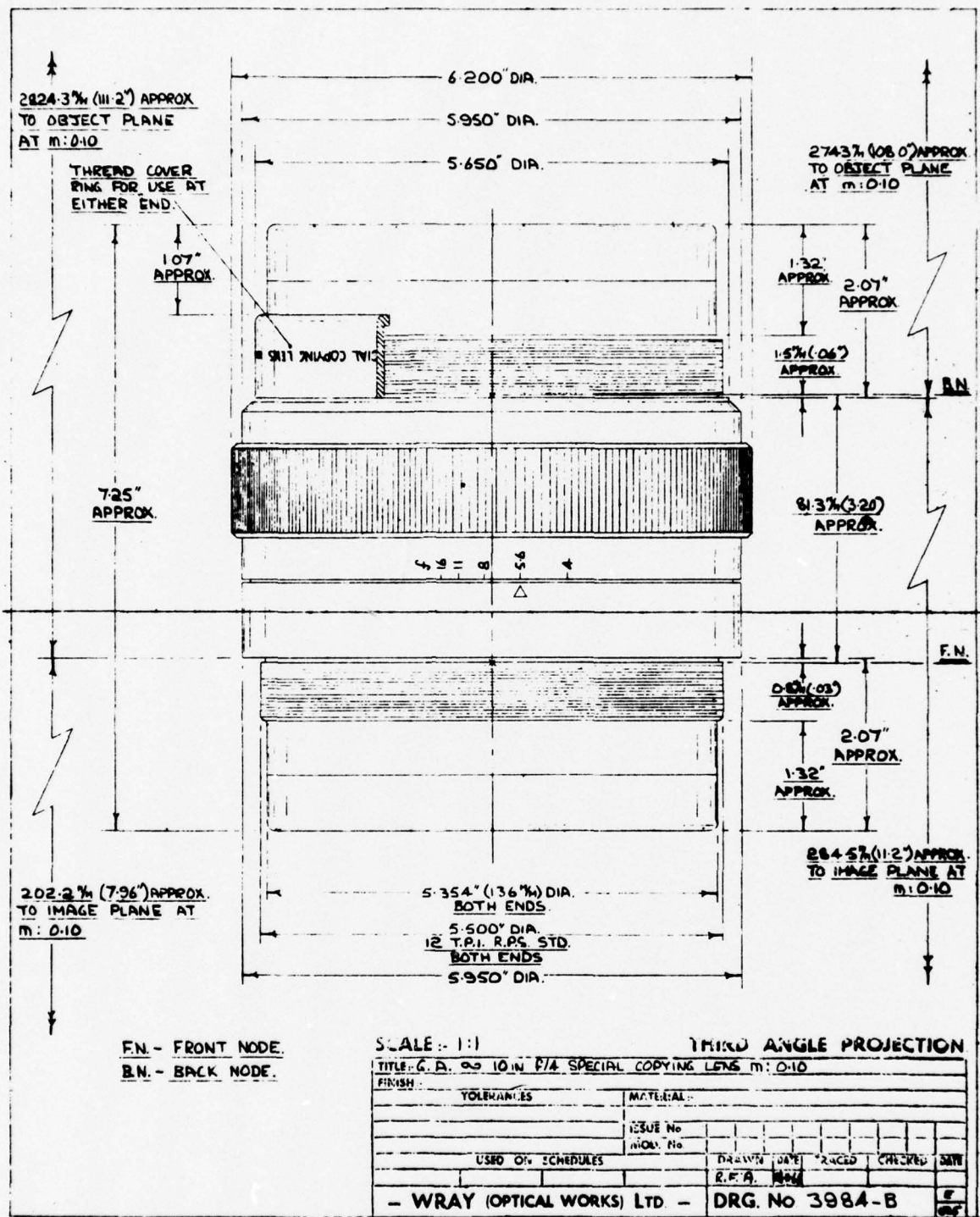


Figure 4-11. Wray Micro Lens Layout Supplied by Rank Optics

To exploit these advantages, a liquid gate consisting of two 4 x 5 x 0.25 inch polished glass plates ground flat to  $\pm 2.6 \times 10^{-4}$  inches and spaced to allow 7-mil thick photographic film between them was fabricated to hold holograms. A smaller, but similar device, was fabricated to hold film chips. The index-matching fluids used were Terpolene<sup>®</sup> and xylene.

Liquid gates have disadvantages which are important in any system with stringent distortion requirements. As described in Paragraph 5.4, the use of glass plates causes astigmatism and spherical aberration in the projected images. We inserted a glass resolution target in the transparency plane to check for aberrations. The resolution of the projected image was different for vertical bars than for horizontal bars. This is indicative of astigmatism.

Liquid gates are not convenient to use. They are bulky and difficult to precisely reposition. Film placed in them must be washed before processing. The gates required repeated cleaning to ensure that none of the index matching fluid dried on the outer surfaces. While sometimes necessary, liquid gates should be avoided in a production-environment system.

#### 4.6.2 Film Holders

Vacuum film holders were developed as a means of supporting flexible film. The film chip holder must have a large clear area and must hold the film flat. The film chip holder was fabricated from a 0.25 inch glass plate of the same kind used for the liquid gates. It was cut to 66 x 96 mm and mounted in a metal frame with vacuum grooves between the metal and the glass to pull the edges taut. Adjustments in both lateral position and angular orientation were provided for the device to ensure alignment of the film chip, lens, and easel. Because the glass was behind the transparency, no imaging aberrations were introduced by the film chip holder. This device worked well, except for

occasional fringing in the image caused by an air interface introduced between the transparency and the glass.

For the hologram vacuum holder, there were severe problems. The holograms had to be held flat without using glass for support to avoid introducing aberrations. We constructed several devices with either circular or square 20 mm apertures which were arranged to provide at least six holograms per 4 x 5 inch sheets of photographic film. Vacuum grooves were placed only around the edges of the apertures. One design had a pair of grooves of equal depth around the edges of each aperture. Another used a sequence of three grooves whose depth increased as the distance from the aperture. This technique placed the vacuum stress as far from the hologram as possible. Beveled input faces on the film holder allowed the reference beam to be incident at  $45^\circ$  from the normal with no vignetting. Repositioning was achieved with a magnetic bar on the holder and metal clips on each piece of film. The main difficulty with hologram vacuum platens was the distortion of the hologram surface by the vacuum, which caused the image to focus on a curved surface rather than in a plane. Further study of vacuum holding techniques is recommended to solve this problem.

The film holder used for supporting the hologram was for 0.25 inch thick photographic plates. The film holder consisted of a metal lens cap mounted on the Wray Micro Lens and a track for the plates to move along. Of all the devices tested, it had the least positioning problems. In addition, the device made repositioning of the signal beam optics possible regardless of how any component is moved. The device is simply remounted flush with the lens and the desired hologram is aligned with the reference beam. The hologram will then reconstruct with minimum alignment requirements. The lens



plus hologram assembly is moved as a unit to focus the projected image. This type of device could be adapted for use with photographic film.

#### 4.6.3 Special Components

The special lens mount and transport assembled for the MEGIS Program is shown in Figure 4-12. The mount for the lens is fastened to a dovetail steel slide; a stepping motor moves the lens in increments as small as  $2 \times 10^{-5}$  inches. The precise positioning is required to minimize distortion of the projected image.

Another device used for incoherent and coherent projections in the Kohler illumination systems is a spinning diffuser. This consisted of a circular piece of ground glass mounted on a motor. The spinning diffuser destroys the temporal coherence of the laser light in order to simulate incoherent illumination. When the diffuser was not in motion, it acted as a light-spreading device to uniformly illuminate the second diffuser.

The final special component designed for the system is a "beamjitter" mirror assembly. This, in its most basic form, is a solenoid mounted on the back of a spring mounted mirror. When an electrical waveform is applied to the solenoid, the mirror vibrated about a point on the mirror. A beam of laser light can be bounced off the mirror to form a moving read-out beam. For holographic projections, this device has been used successfully to reduce the effect of speckle noise.

#### 4.7 RECORDER/REPRODUCER PERFORMANCE

Two types of film chip storage and retrieval were experimentally investigated: holographic and micrographic (direct project readout). These approaches are complementary in that the micrographic technique provides a baseline against which the holographic technique can be compared, and vice versa. Each method has its advantages and limitations, as will become clear

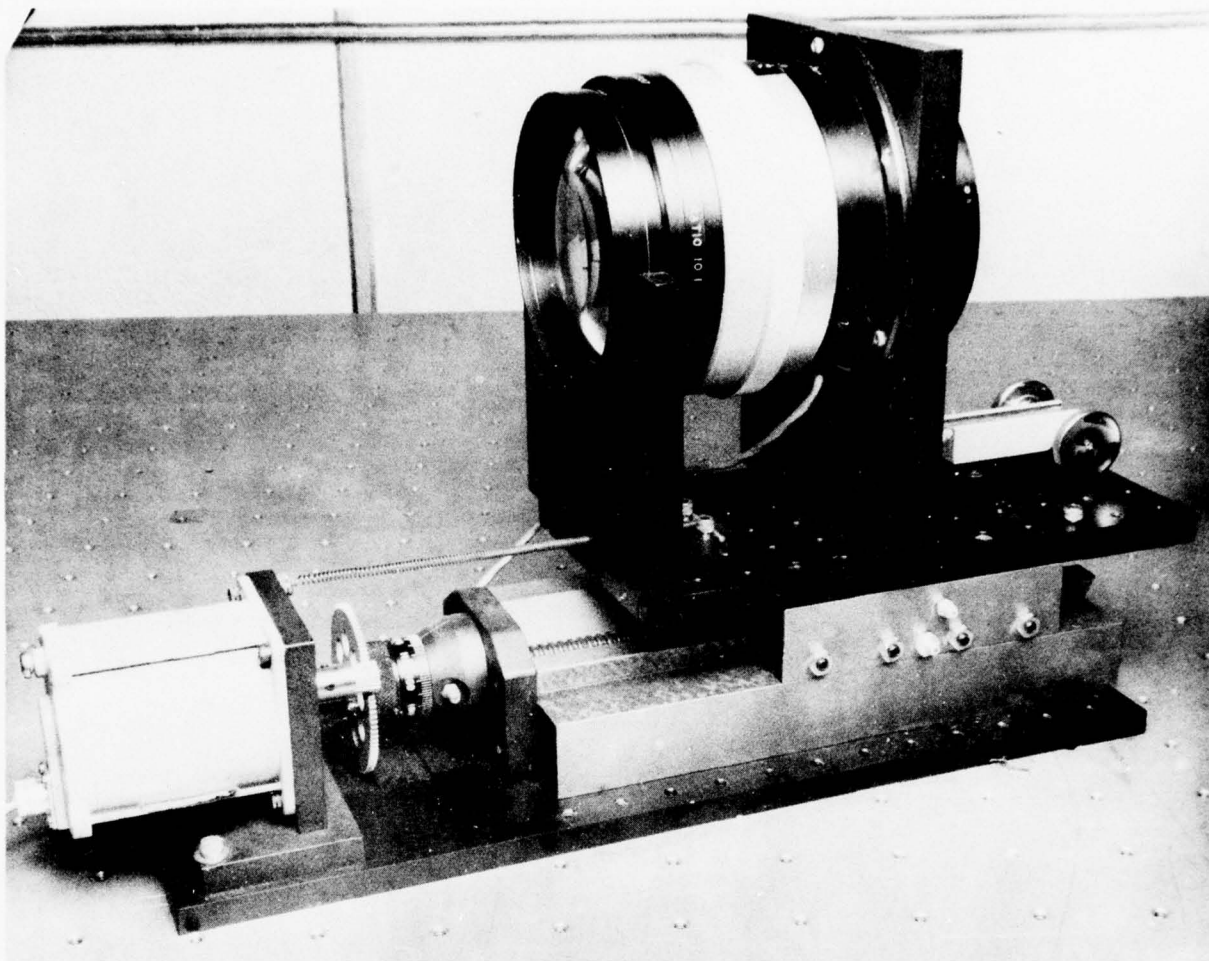


Figure 4-12. Wray Micro Lens Mount and Transport System

subsequently. The frame of reference in each case is a recorder/reproducer breadboard and its associated performance.

#### 4.7.1 Direct Projection (Micrographic) System

The direct projection system discussed in Paragraph 2.3.2 was implemented and tested. As shown in Figure 2-7, the unexpanded laser beam passes through the spinning diffuser providing incoherent and uniform illumination for the second diffuser. The position of the second diffuser was chosen so that the condenser lens would image it in the aperture of the Wray Micro Lens and would completely fill that aperture. This combination utilized the maximum resolution transfer and illuminance uniformity potential of the Wray Lens. The condenser lens must not only image the second diffuser into the aperture of the Wray Micro Lens, but must also uniformly illuminate the film chip. A 10-inch focal length,  $f/1.5$  lens was used as the condenser lens.

The image contrast of the direct projection system was determined for various types of film chips. A pair of film chips of opposite polarity were used to measure average signal-to-average noise ratio (SNR). The positive film chip had a clear center with a black border, while the negative film chip had a black center with a clear border. The area of the border was three times the area of the center for each of the chips. Three Eilerslie map film chips with different light distributions were also measured. The culture chip consisting of narrow lines such as road and lettering had 1.4 percent transmittance. The open water sheet had 1.5 percent transmission. The vegetation sheet with large dark areas in a clear background was 40 percent transmissive. Table 4-6 lists the type of film chip, its characteristics, and the measured signal-to-noise ratio.



Table 4-6. Contrast Performance of a Direct Laser Projection System

Film Chip	Transmittance	Type of Illumination	Film Chip Characteristics	SNR
SNR Positive	25%	Incoherent	Large clear area in center	20 dB
SNR Negative	75%	Incoherent	Large dark area in center	15 dB
SNR Positive	25%	Diffuse Coherent	Large clear area in center	19 dB
SNR Negative	75%	Diffuse Coherent	Large dark area in center	15 dB
Vegetation	40%	Diffuse Coherent	Large dark areas randomly scattered in clear background	12 dB
Culture	1.4%	Diffuse	Clear lines in dark background	17 dB
Open Water	1.5%	Diffuse Coherent	Small clear areas in dark background	20 dB

The signal-to-noise ratio, although dependent on the film chip characteristics, was greater than 10 dB in every case. A lithographic film such as Kodak SS7 film, exposed to an image with a SNR of 10 dB results in good, high-contrast hardcopy. Figure 4-13 is a section of a print made from the direct projection of a contour sheet film chip using Kohler illumination. Note the good contrast of the image and the absence of speckle.

Image uniformity is also an important consideration. Measurements of the image uniformity obtained with three different types of illumination were made. Two of the types of illumination were spatially incoherent. These were provided by a spinning diffuser of commercial nonglare glass and a spinning diffuser of satin ground glass. The third illumination type was specular. The commercial nonglare glass was not sufficiently diffuse. The image intensity obtained with this spinning diffuser decreased by 61 percent from the central to outer regions. The specular illumination suffered vignetting by passage through the optical system. The image intensity for



Figure 4-13. Hardcopy Image of a Contour Map Separation Film Chip, Illuminated With Incoherent Multiwavelength Laser Light in the Kohler Projection Mode

specular illumination decreased by 47 percent from the central to outer regions. Only the illumination obtained with the spinning diffuser of satin glass provided acceptable uniformity. The intensity of the image projected with this diffuser varied only 13 percent from center to edge.

The resolution of the breadboard using incoherent illumination has been discussed in Paragraph 4-4. Resolution was 228 cycles/mm at the center and decreased to 204 cycles/mm at the edges of the field. This exceeded the resolution requirement of the MEGIS Program.

One problem with the direct projection system is the low light level present at the image plane. With 600 mW of power incident on the spinning diffuser, the image intensity is about  $1 \mu\text{W}/\text{cm}^2$ . This corresponds to a brightness of 1.3 fL. An image projected with this intensity would require a hardcopy exposure time of 12 seconds for Kodak SS7 film. Although this is not a long exposure time, it may be a significant system constraint if a large number of exposures per unit time are required.

#### 4.7.2 Holographic Recorder/Reproducer

In a holographic system the 70 mm film chip is placed in the recording system and illuminated by a converging beam of coherent light. In the back focal plane of the Fourier-transform lens, the interference pattern formed between this signal beam and an off-axis reference beam is recorded on a photographic emulsion. A matrix of step-and-repeat exposures are made on one 4 x 6 inch fiche. After exposure, the fiche is removed, developed, and replaced in the breadboard for readout.

The basic retrieval system is extremely simple, requiring only a holder for the fiche containing the holograms and the Wray Micro Lens. An individual hologram can be selected from the array on the 4 x 6 inch fiche by an x-y translation stage and illuminated by the readout beam (a replica of the



reference beam). The signal beam wavefront will then be reconstructed. The reconstructed signal beam can be used to obtain a full-scale enlargement from the holographic format, which can be more compact than the 70 mm film chip format.

Two breadboard holographic recorder/reproducers were evaluated. The major difference between them was the illumination technique used to generate the signal beam. The first system, shown in Figure 4-14, was a phase-randomized Fourier transform recording scheme. A holographic optical element (HOE) was the Fourier-transform lens. A phase randomizer was placed directly in front of the HOE. The hologram was recorded near the focal plane of the HOE. Liquid gates were used to hold both the film chip and the film used to record the holograms.

We recorded holograms of a vegetation sheet with 40 percent transmission to determine the holographic parameters to optimize the image quality. Figure 4-15 shows the effect of the variation of exposure and K-ratio on both diffraction efficiency and signal-to-noise ratio. The best results for this test series were obtained for a K-ratio of 5 for which DE = 11 % and SNR = 13 dB. A second exposure series was made for K = 10. The results are shown in Figure 4-16. Diffraction efficiency increased to 12 % for an exposure of  $140 \mu\text{J}/\text{cm}^2$ , whereas maximum SNR of 15 dB was obtained for an exposure of  $110 \mu\text{J}/\text{cm}^2$ . For an exposure of  $110 \mu\text{J}/\text{cm}^2$ , diffraction efficiency was about 11 %. Since image contrast is more critical than diffraction efficiency in a holographic projection system, the remaining tests were made with holograms recorded at about  $110 \mu\text{J}/\text{cm}^2$  to maximize SNR.

Once these parameters were maximized, holograms were recorded for the Talbotton map chips. Table 4-7 shows the results. Diffraction efficiency tended to be higher for chips with higher transmission, but since the light



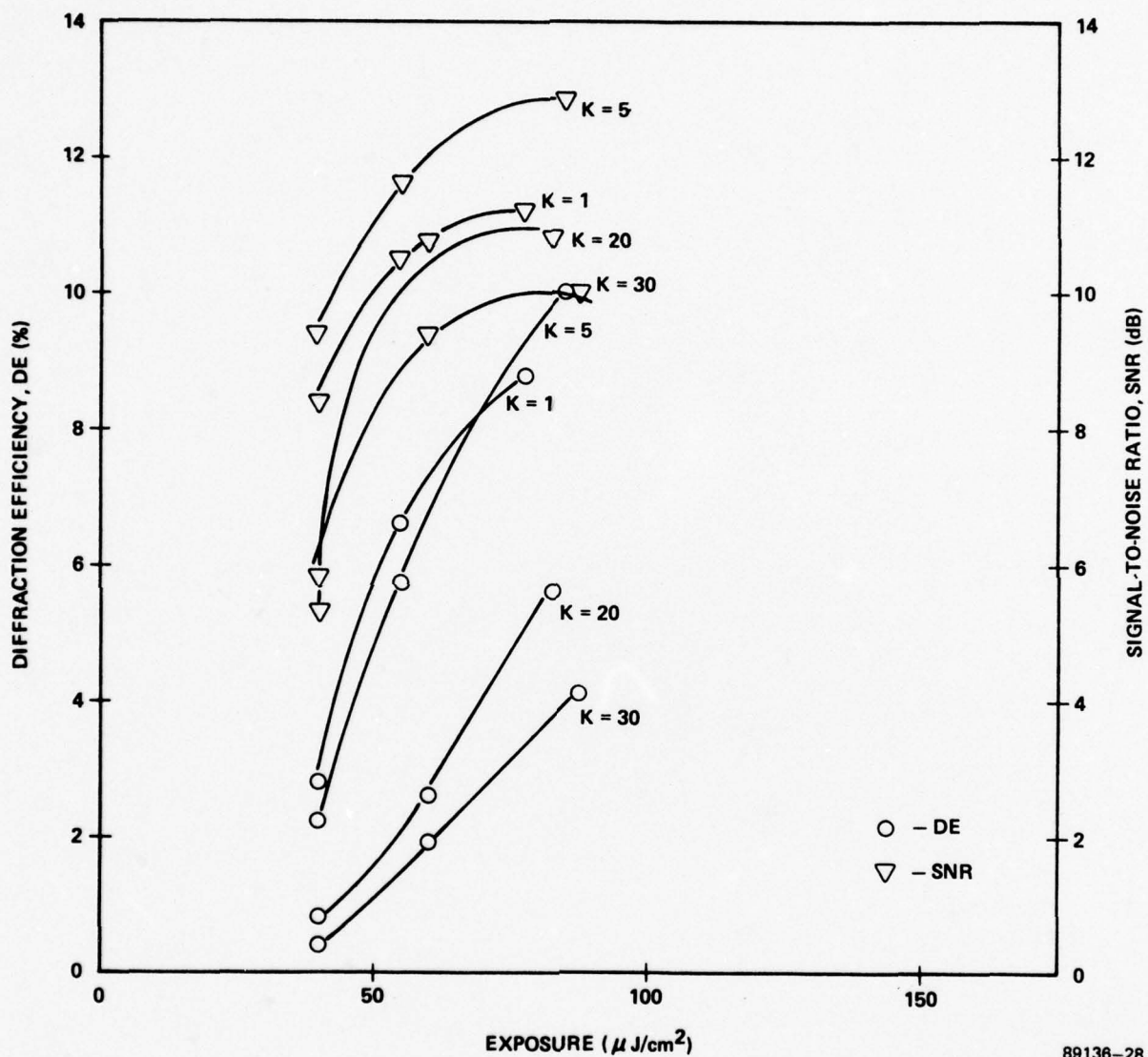


Figure 4-15. Diffraction Efficiency and Signal-to-Noise Ratio as a Function of Exposure with K-Ratio as a Parameter



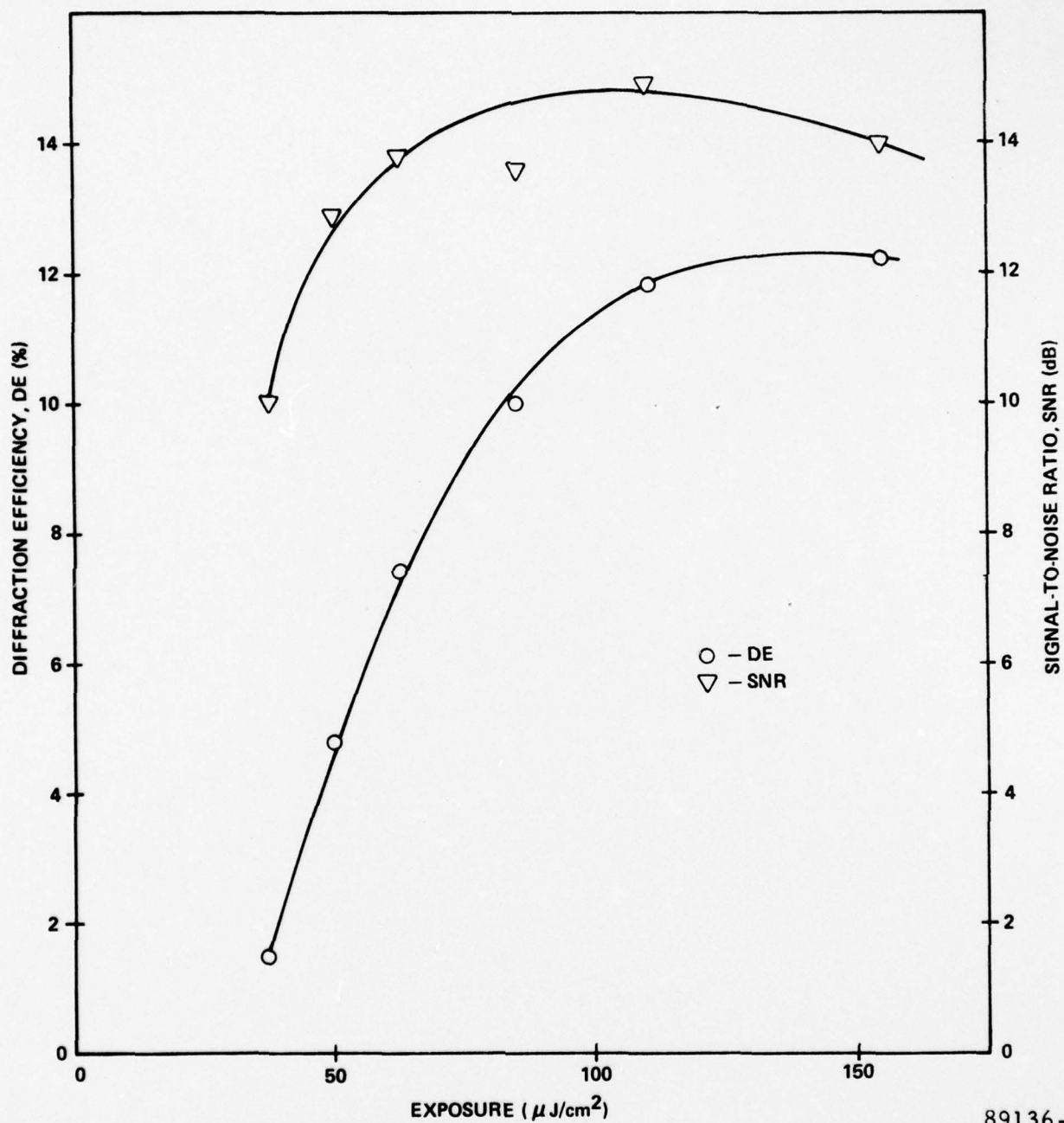


Figure 4-16. Diffraction Efficiency and Signal-to-Noise Ratio as a Function of Exposure for  $K = 10$

Table 4-7. Holographic Storage and Retrieval at 38X  
Reduction for 22 x 30 Inch Repromats

Transparency	Transmittance (%)	Diffraction Efficiency (%)	<Luminance (fL)>		SNR
			a) Bright Area	b) Dark Area	
1) Grid	1.5	2.9	>40	<2.5	>12
2) Contours	9.4	7.6	>25	<2.5	>10
3) Culture	1.9	3.1	>60	<2.5	>14
4) Drainage	1.6	2.3	>40	<2.5	>12
5) Vegetation Positive	39.0	8.7	>40	<2.5	>12
6) Vegetation Negative	69.0	10.1	>25	<2.5	>10

must be distributed over a larger area, the image illuminance is no greater. SNR exceeded 10 dB in all cases, and image luminance was greater than 35 fL except for vegetation film chip (negative mode).

Film hardcopy was made by exposing to the reconstructed image; Polaroid<sup>®</sup> film was used. Directly projected images were also recorded, and the relative quality compared. Figure 4-17 shows a directly projected image of a section of a culture film chip and its corresponding reconstructed holographic image. The only defect in the holographic reconstruction is speckle noise. Figure 4-18 compares the quality of a directly projected image with its corresponding holographic reconstruction for a section of a contour sheet film chip. The contour map had the highest resolution requirement of all the film chip samples furnished by USA/ETL. Again, the major defect in the hardcopy obtained from the holographic reconstruction is speckle noise. The speckle noise tended to cause sharp line edges to appear uneven.

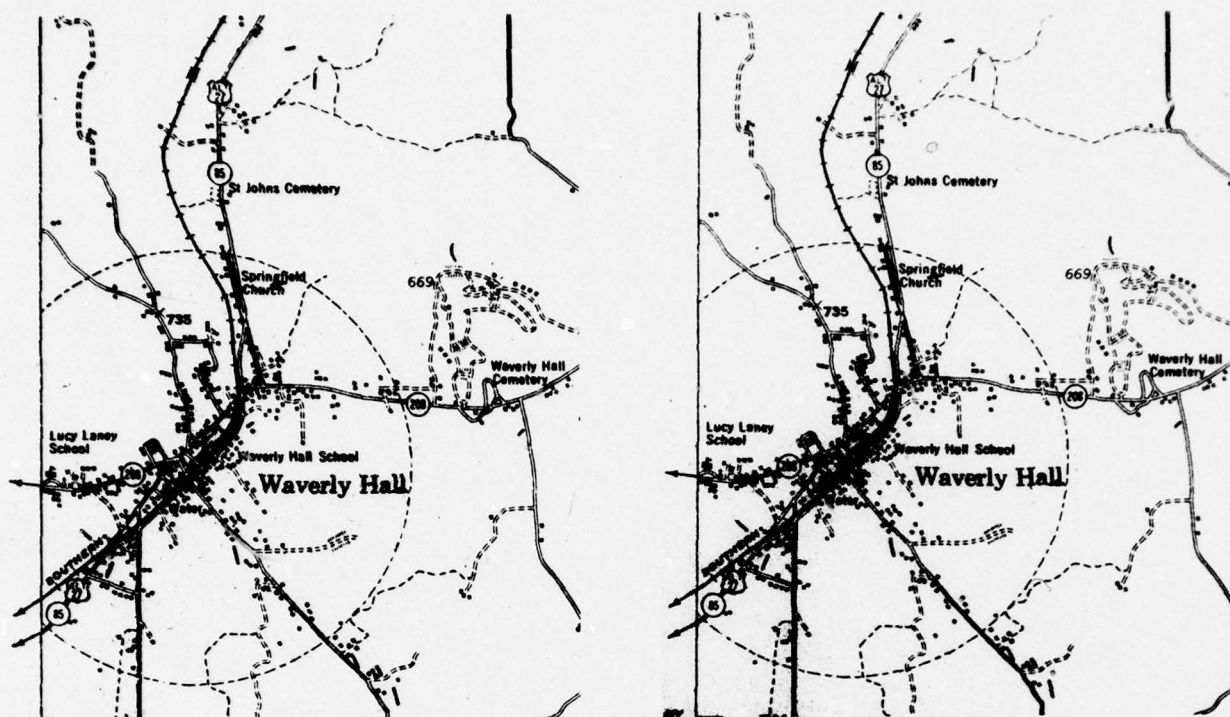


Figure 4-17. Comparison of Throughput Image and Holographic Reconstruction for a Culture Sheet Film Chip





Figure 4-18. Comparison of Throughput Image and Holographic Reconstruction of a Contour Sheet Film Chip

This set of holograms had an extremely short storage time. The index matching fluid apparently interacted with the residual bromine bleach in the hologram. The interaction caused the holograms to deteriorate after only a 48 hour period. The information obtained from the display and hardcopy reproduction of these holograms indicated that our future work should be directed toward speckle noise reduction. We had found that image brightness and contrast would meet or exceed contract requirements. The details of the effort to minimize speckle noise are described in Paragraph 4.8.

Figure 4-19 shows the geometry of a two wavelength holographic Kohler system developed with the aim of minimizing speckle. Two argon lasers operated at wavelengths of 514.5 nm and 488 nm produce beams which are split into reference and signal beams. The reference beams are expanded, collimated, and incident on the hologram plane at an angle of 45 degrees on either side of the hologram plane normal. The signal beams, which are made to be coincident, illuminate the first diffuser, are scattered and uniformly illuminate a second diffuser. The second diffuser is placed in the holographic Kohler position, i.e., the diffuser is imaged in or very near the hologram recording plane. The two wavelength system was chosen because of the results of the investigation into speckle reduction techniques, discussed later in Paragraph 4-8.

Since different wavelengths do not interfere, an incoherent addition of two simultaneously recorded holograms is obtained. Data for diffuse Fourier-transform holograms is not immediately applicable to holograms recorded with two or more wavelengths. Hence an exposure series was made to determine the optimum holographic recording parameters. With two incoherent additions, an effective<sup>18</sup> K-ratio of 14 is obtained by recording each hologram with  $K = 1$ . An exposure series for both amplitude and bleached

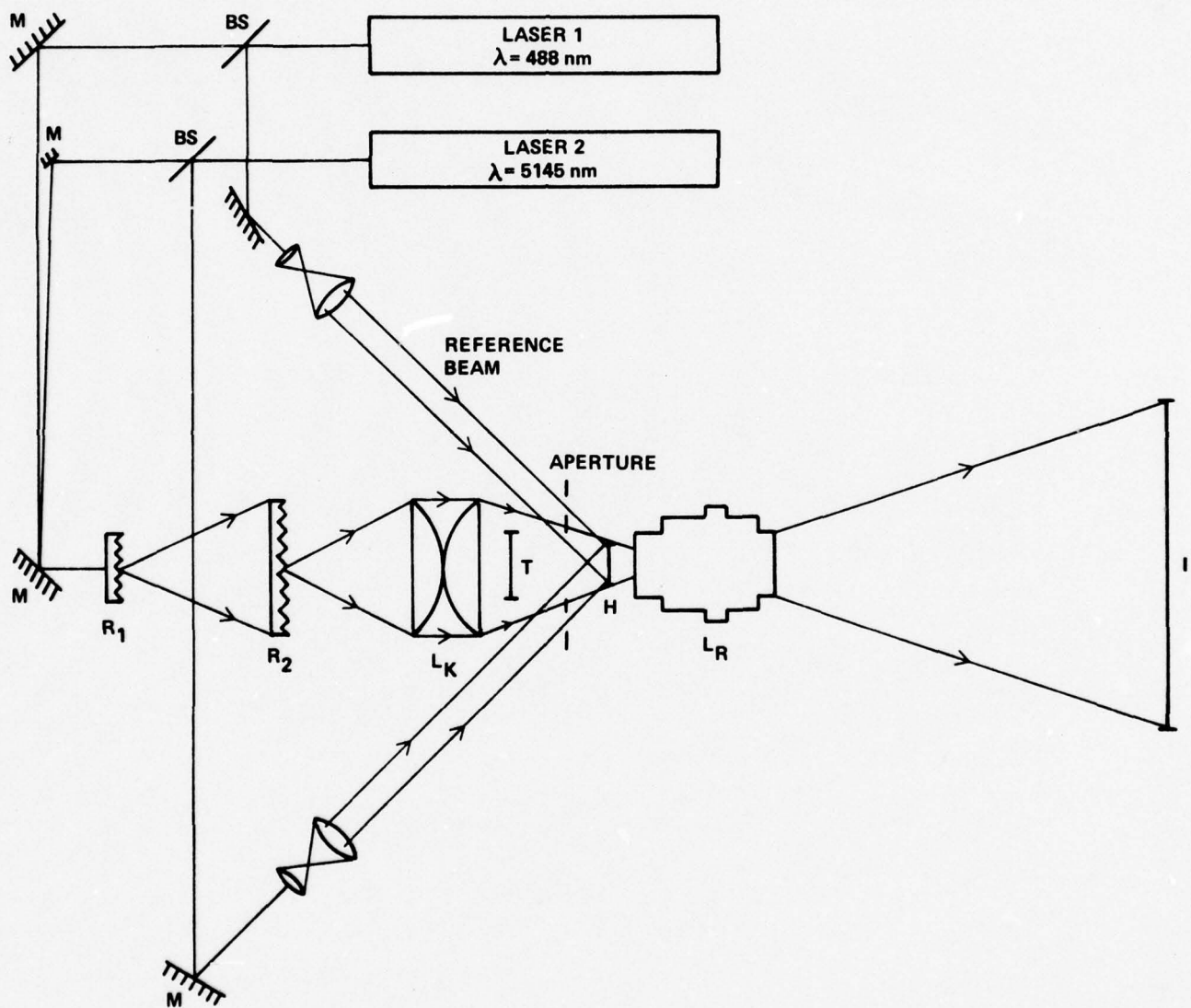


Figure 4-19. Two Wavelength Kohler Holographic Recorder/Reproducers



holograms was generated for this case. Figure 4-20 shows the diffraction efficiency and signal-to-noise ratio of the amplitude holograms as a function of the exposure for each wavelength. Both DE and SNR were maximum for a total exposure of  $30 \mu\text{J}/\text{cm}^2$ . Maximum DE was 0.43 percent and maximum SNR was 14.7 dB. Although this is an acceptable signal-to-noise ratio, diffraction efficiency is too low. Figure 4-21 shows similar data obtained for bleached holograms. Diffraction efficiency monotonically increases with exposure, but signal-to-noise ratio reaches a maximum of 9 dB for an exposure of  $80 \mu\text{J}/\text{cm}^2$ . For an  $80 \mu\text{J}/\text{cm}^2$  exposure, the diffraction efficiency is 1.4 percent.

To determine the effects of film chip characteristics on holographic performance, measurements of the DE and SNR obtained for reconstructed images were made. The holograms were recorded from the Ellerslie map series. The effective K-ratio for recording was 14. The exposure at each wavelength was  $100 \mu\text{J}/\text{cm}^2$ . Table 4-8 summarizes the results obtained for the bleached holograms. In general, a higher reconstructed signal-to-noise ratio is obtained for those chips with low transmittance values. Image brightness is also highest for these chips since all the diffracted light to form the image is concentrated into a smaller fraction of the available image area. The results obtained for holograms of the vegetation film chip make this clear. Although this film chip has three to four times the diffraction efficiency of either the grid or drainage film chips, the image brightness obtained is lower. The bleached holograms of the Ellerslie map series recorded in the holographic Kohler system were used for all measurements of the equipment test plan (ETP) described in Appendix A. The holographic recording parameters used for the ETP were an effective K-ratio of 14 and individual exposures at both 488 nm and 514.5 nm of  $100 \mu\text{J}/\text{cm}^2$ .

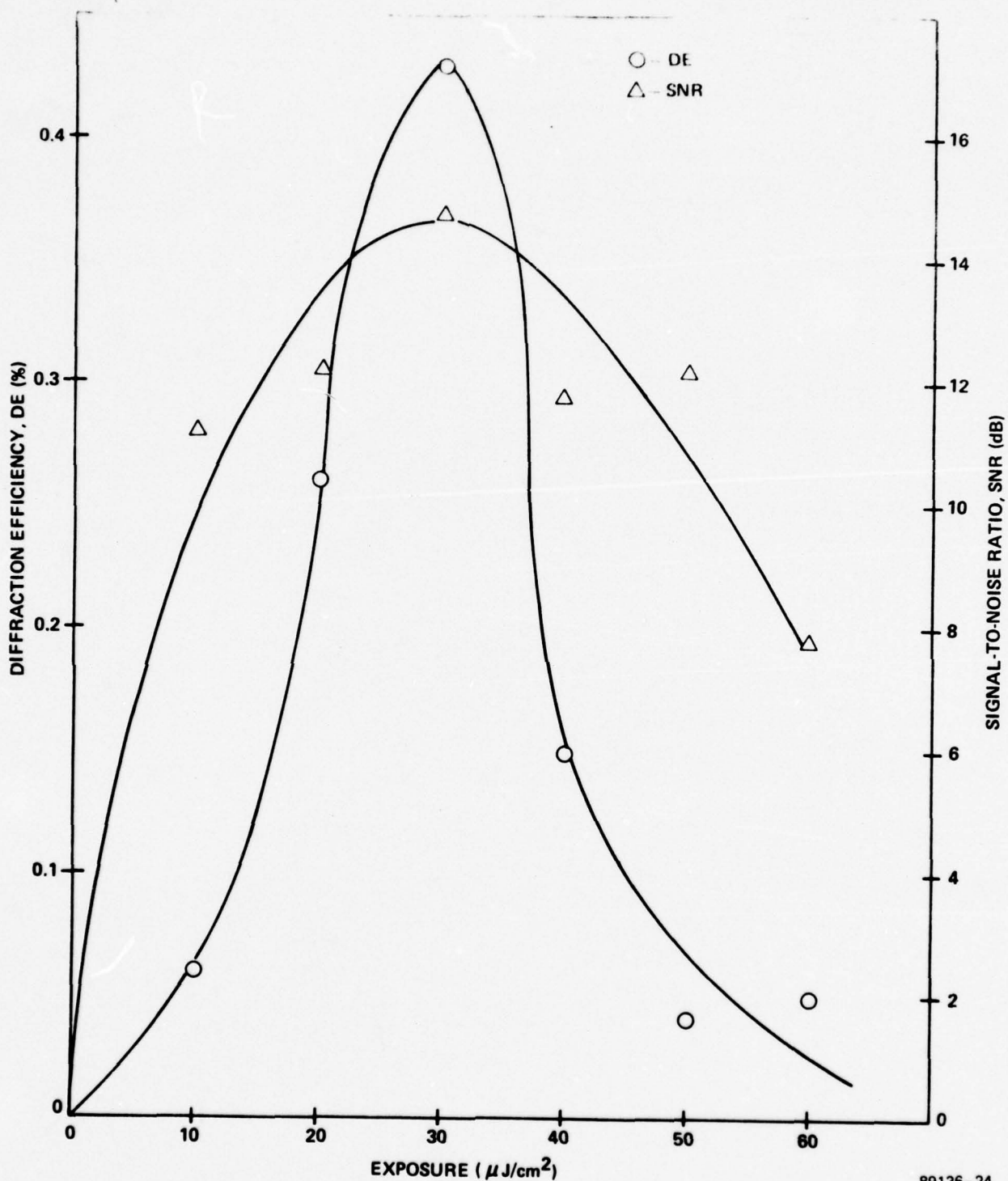
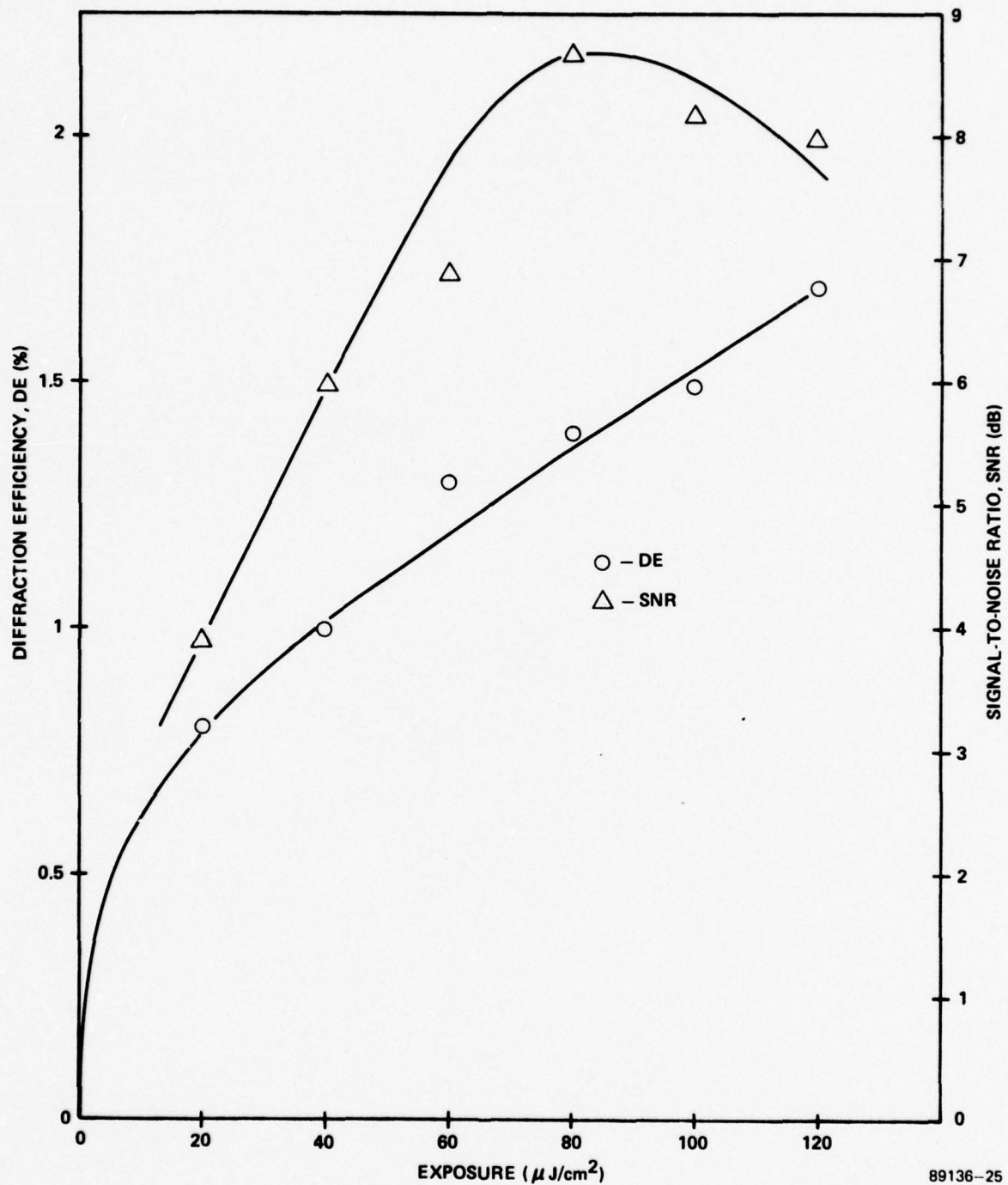


Figure 4.20. DE and SNR as Functions of Exposure for Two Wavelength Amplitude Holograms Recorded With the Holographic Kohler Breadboard



89136-25

Figure 4.21. DE and SNR as Functions of Exposure for Two Wavelength Bleached Holograms Recorded With the Holographic Kohler Breadboard



Table 4-8. Performance of a Holographic Kohler Recorder/Reproducer\*

Ellerslie Chip	Transmittance (%)	Diffraction Efficiency (%)	Luminance (fL)		SNR (dB)
			Maximum	Minimum	
Grid	0.6	4.6	126	5.1	14
Drainage	0.9	2.3	42	2.3	13
Culture	1.4	18.0	211	3.0	18.5
Contour	2.0	1.5	1.6	0.34	7
Vegetation	40.0	13.0	16	5.4	5

\*K = 14 (effective)

E = 100  $\mu\text{J}/\text{cm}^2$  at 514.5 nm and 100  $\mu\text{J}/\text{cm}^2$  at 488 nm

Bromine vapor bleached

Readout power = 260 mW at 514.5 nm

The preceding data are the result of reconstructing the two wavelength holograms at 514.5 nm only. We did this because of alignment problems. The plate holder we used did not permit adequate repositioning accuracy. This caused the images of two wavelengths to reconstruct in slightly different positions. This was not an inherent problem, since both reconstructions could be aligned for several of the holograms. The angle of incidence of the 488 nm reference beam was adjusted slightly to optimize the overlap. We believe the slight misalignment is due to emulsion shrinkage caused by processing. Emulsion shrinkage causes the hologram fringes to rotate, changing the effective reference beam angles.<sup>19</sup> As a result, the angular positions of both images shift. We corrected for this in certain cases by adjusting the angle of incidence of the 488 nm reference beam. Ideally, both beams should be simultaneously adjusted. Future systems can include adjustments for both reference beam angles. The image misalignment was due to the plate holder which was not designed for multiwavelength hologram recording. This is not a fundamental

problem, and can be solved by redesigning the plate holder for better alignment accuracy.

Holographic images were reconstructed and film hardcopy recorded. Figure 4-22 shows a section of printed hardcopy from an amplitude hologram readout at 514.5 nm. Although contrast and resolution are good, the granular appearance caused by speckle noise makes the hardcopy unacceptable for map production.

Figures 4-23 through 4-25 show the effects of the holographic process on resolution transfer. Figure 4-23 was obtained from the single-wavelength, direct projection of a resolution target in the holographic Kohler system. The resolution on-axis was 128 cycles/mm in the film hardcopy. Figure 4-24 was obtained from a single wavelength holographic reconstruction of the same resolution target as in Figure 4-23. The resolution on-axis is still 128 cycles/mm in the film hardcopy. The holographic process did not cause a loss of resolution. Figure 4-25 shows a direct projection obtained with incoherent illumination. Resolution on-axis is about 220 cycles/mm. The use of coherent illumination decreased the resolution transfer by a factor of two.

Figure 4-26 through 4-31 are photographs of a section of the monochrome map projected using the various systems discussed in this report. Figures 4-26 and 4-27 show reconstructions from holograms recorded with two wavelengths. Figure 4-26 shows a reconstruction with the 514.5 nm wavelength only, while Figure 4-27 shows a reconstruction at the 514.5 nm and 488 nm wavelengths simultaneously. The single-wavelength reconstruction contains more speckle, particularly in the lines. In both cases, line edges are uneven. The existence of the half-tone screens is suggested by ordering in the speckle, but the screens are not resolved. Figures 4-28 and 4-29 are reconstructed from holograms recorded using diffuse coherent illumination in



Figure 4-22. Single-Wavelength Reconstruction of a Two-Wavelength Amplitude Hologram



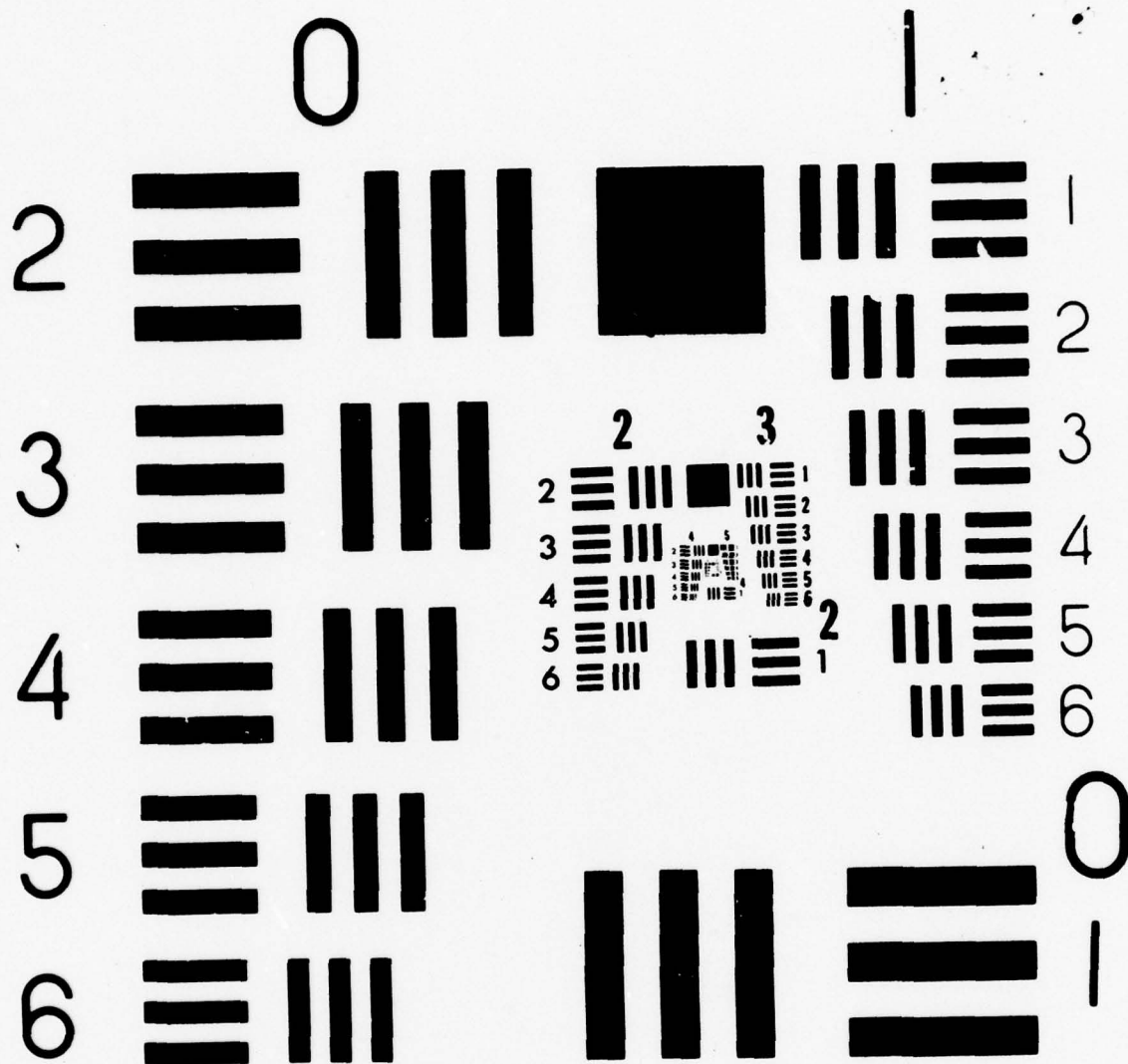


Figure 4-23. Direct Projection of a Resolution Target Illuminated With Diffuse Coherent Light in the Holographic Kohler Mode

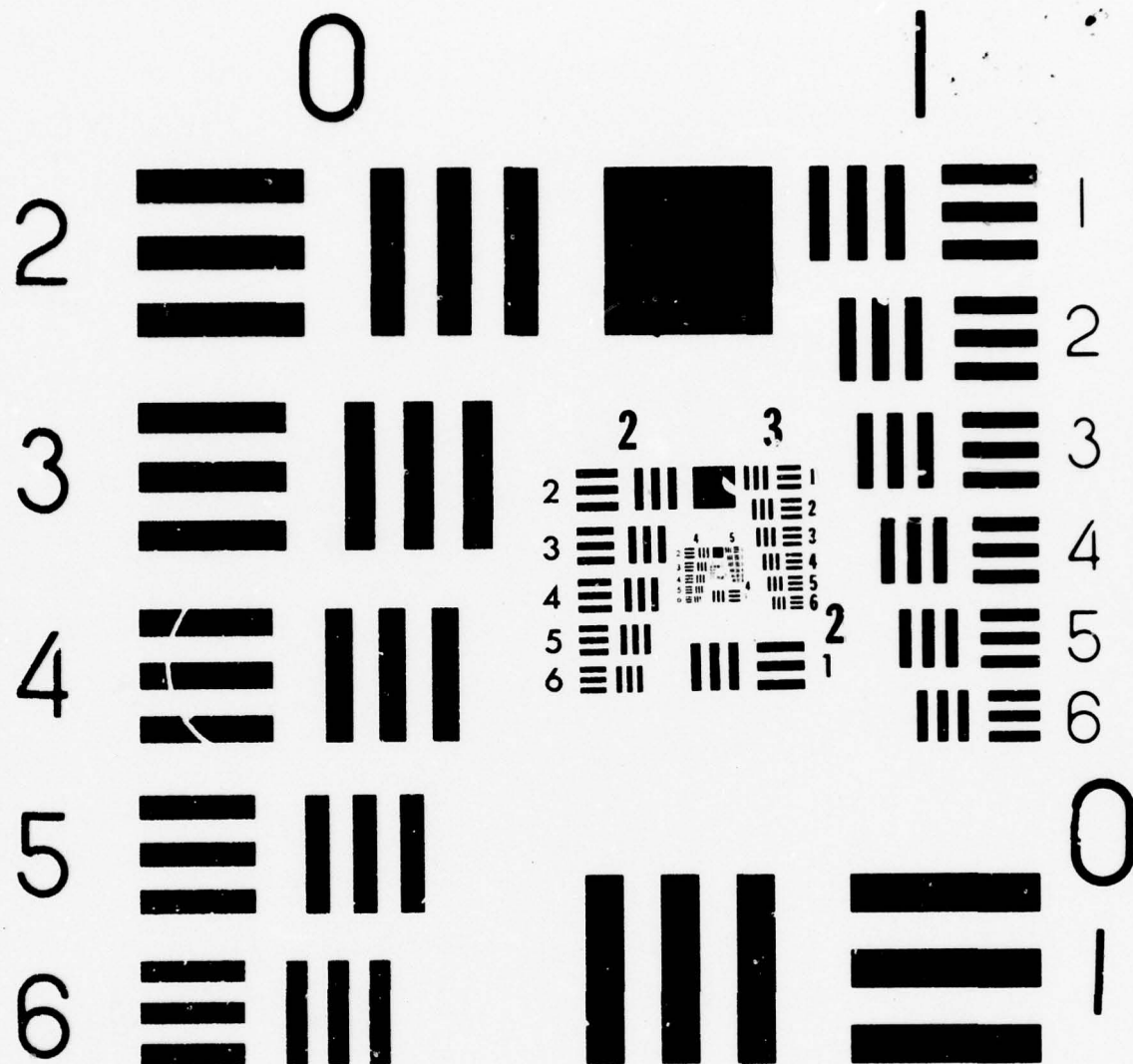


Figure 4-24. Single Wavelength Holographic Reconstruction of a Resolution Target Using the Holographic Kohler Breadboard

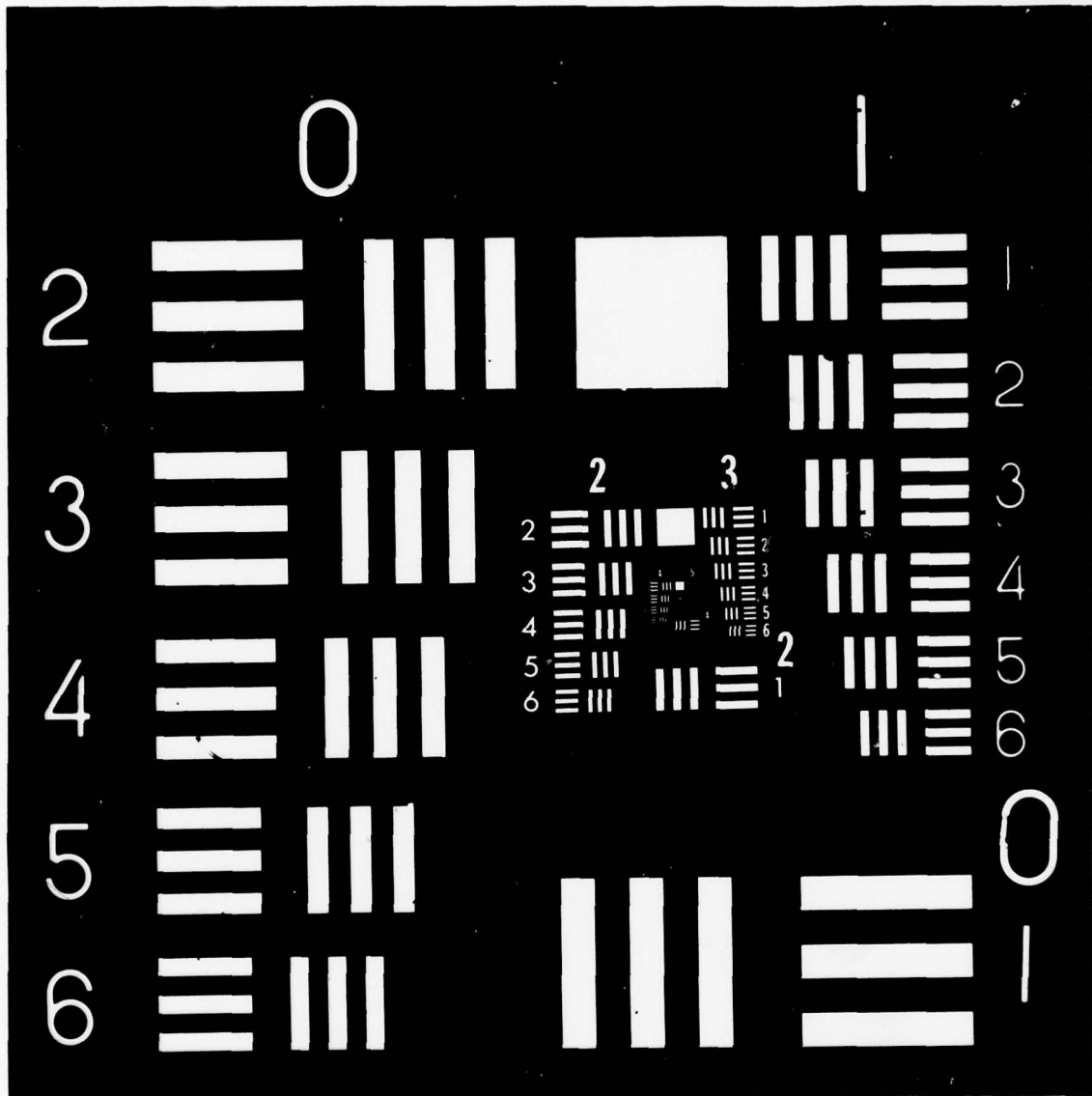


Figure 4-25. Direct Projection of a Resolution Target, Illuminated With Incoherent Laser Light, Using the Holographic Kohler Breadboard



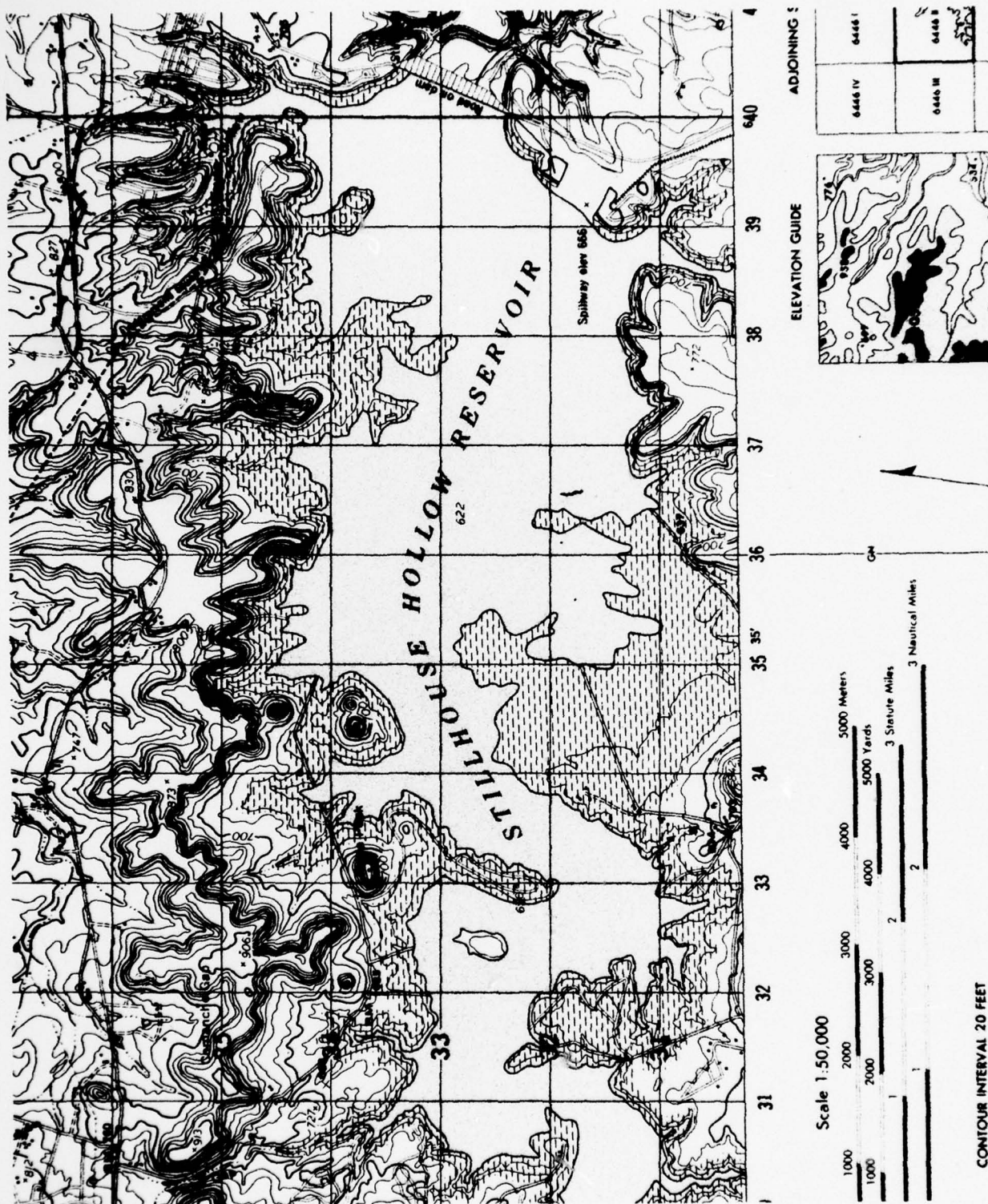


Figure 4-26. Single-Wavelength Reconstruction of a Two-Wavelength Hologram Recorded in the Holographic Kohler Breadboard

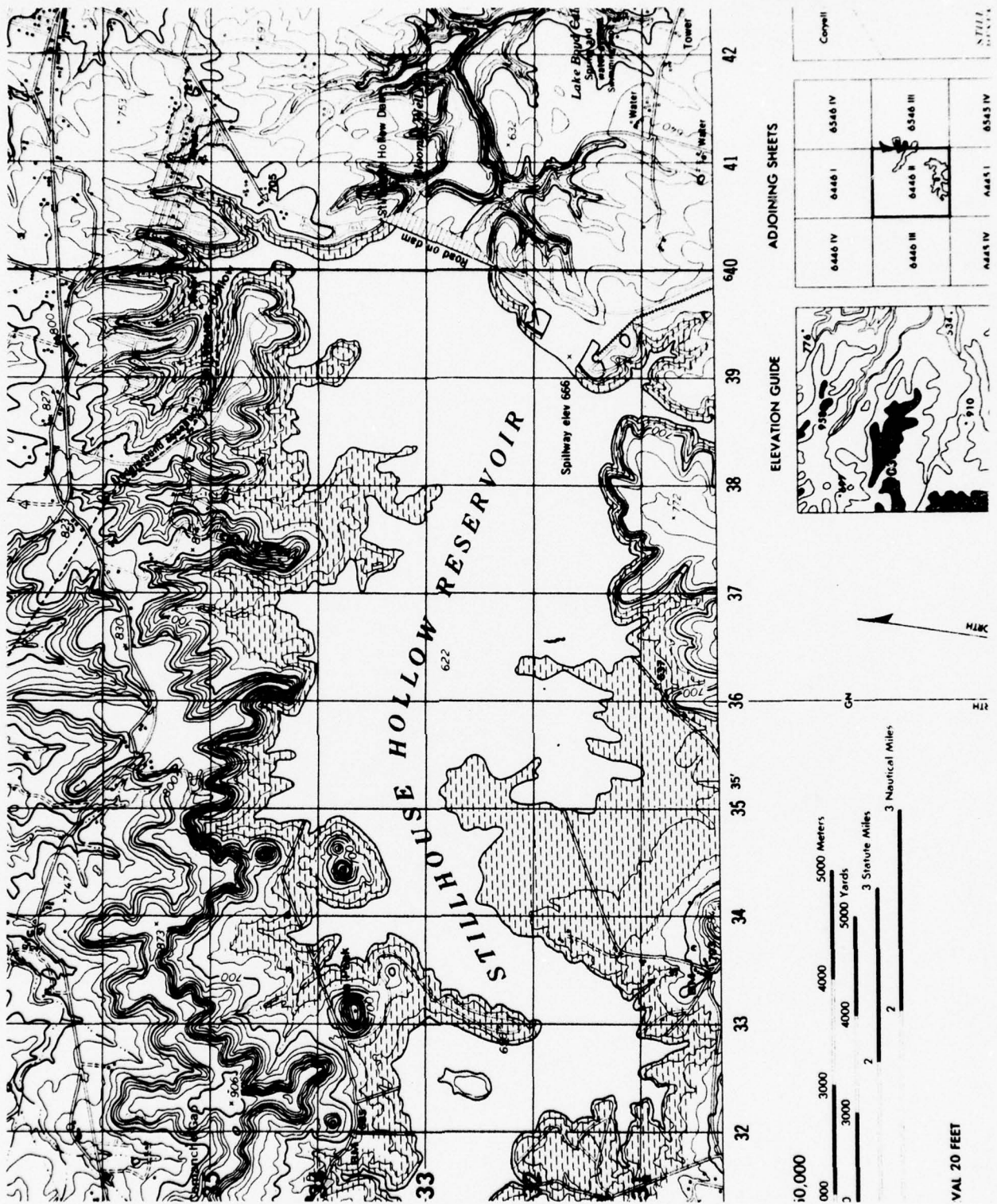
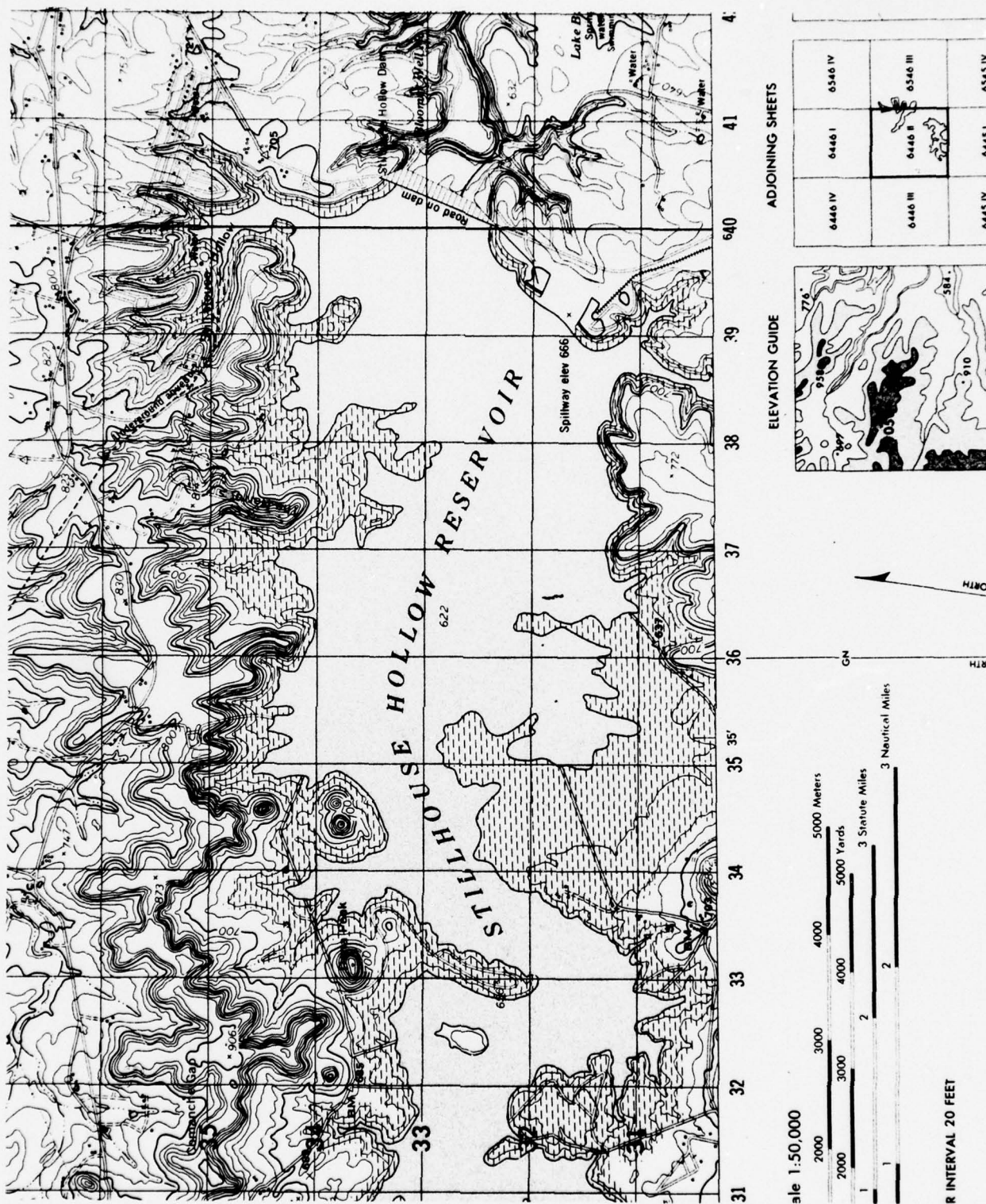


Figure 4-27. Two-Wavelength Reconstruction of a Two-Wavelength Hologram Recorded in the Holographic Kohler Breadboard













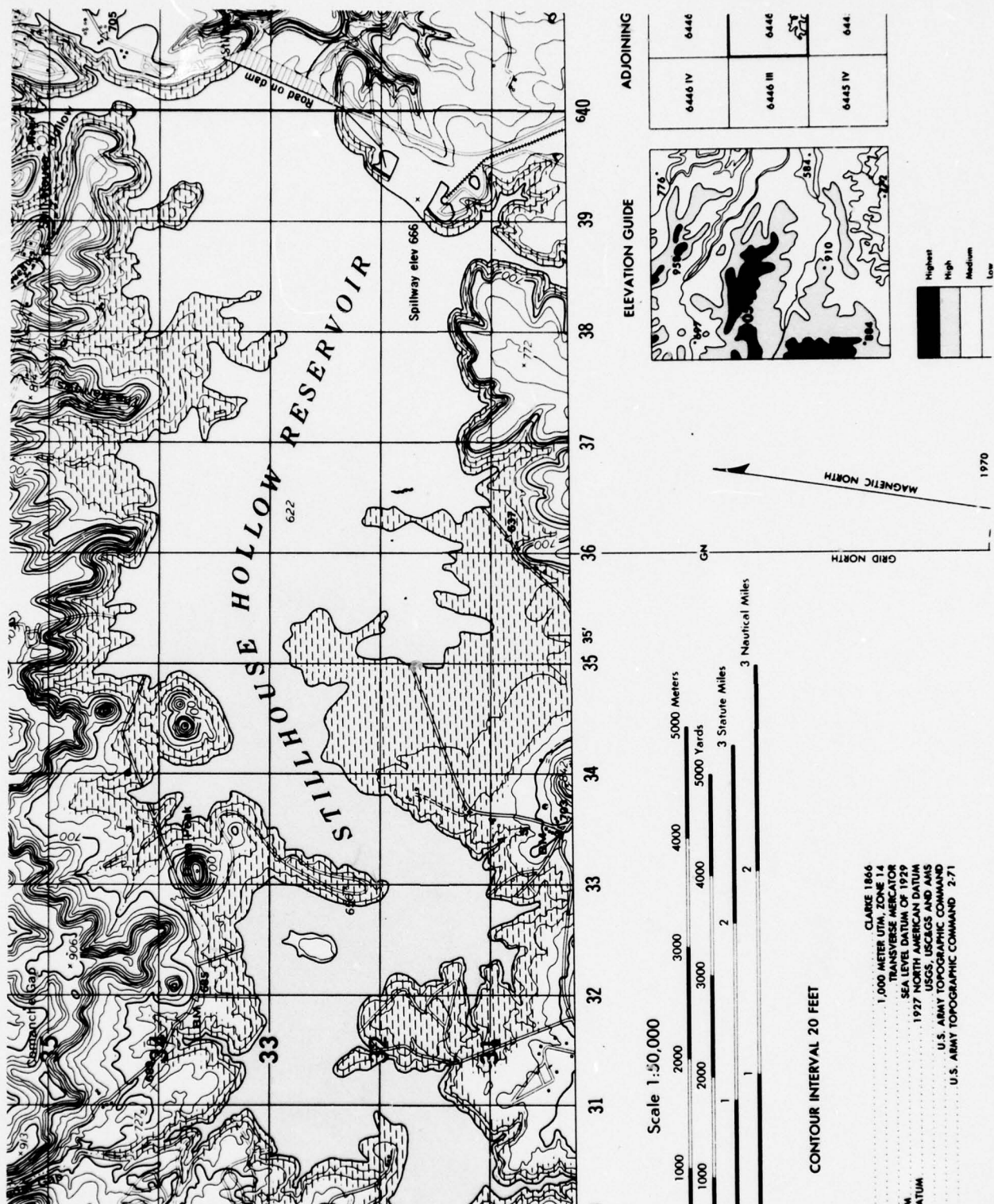


Figure 4-31. Direct Projection, With Incoherent Light, Using the Holographic Kohler Breadboard





(low duty cycle), it is a problem for those, such as the vegetation sheets, that have large clear areas. Coherent noise was evident in these areas. Direct projections obtained using incoherent illumination had excellent contrast and resolution. The quality of the images was very high. However, they were of low image luminance. Direct viewing was possible in a darkened room, but not in a lighted room. The hardcopy exposure times necessary to reproduce directly projected images was 15 times longer than those required for the holographic reconstructions.

Using the two wavelength holographic system, high quality images were obtained, even though the breadboard was not optimized. Further development work is recommended to improve system performance.

#### 4.8 SPECKLE REDUCTION

Phase randomization of coherent light and subsequent band limiting creates speckle noise. Images formed with phase randomized light have a granular appearance which is objectionable and limits resolution transfer. For optimum image quality, the size of the speckle must be minimized: that is, speckle density must be maximized. In Paragraph 4.3, techniques for generating phase randomizers were discussed. Here we describe experimental results obtained with various phase randomizers, and describe other techniques for speckle minimization.

##### 4.8.1 Phase Randomizers

The speckle size is determined by the smallest effective aperture in the optical system, the distance from the aperture to the image plane, and the position and characteristics of the phase randomizer being used. Table 4-10 shows the effect on image quality of the type of target used to record photographic phase randomizers. The only photographic phase randomizers that produced acceptable results were generated by contact copying satin ground

Table 4-9. Hardcopy Reproduction Characteristics for Direct and Holographic Laser Recorder/Reproducers

	Incoherent Throughput	Specular Throughput	Coherent Throughput At 514.5 nm and 488 nm	Holographic Projection At 514.5 nm and 488 nm
Image irradiance for 500 mW total laser power	1 $\mu\text{W}/\text{cm}^2$	2 $\mu\text{W}/\text{cm}^2$	1 $\mu\text{W}/\text{cm}^2$	>15 $\mu\text{W}/\text{cm}^2$
Typical exposure for SS7 hardcopy film	12 seconds	6 seconds	12 seconds	< 1 second
Contrast	12 to 20 dB	12 to 20 dB	12 to 20 dB	5 to 20 dB
Image resolution • Center (cycles/mm) • Edge	>228 200	>228 ~200	128 100	128 80
Image Quality	Excellent	Coherent Noise	Speckle Noise Uneven Line Edges	Speckle Noise Uneven Line Edges



Table 4-10. Performance of Photographic Phase Randomizers

<u>Random Source</u> <u>Contact Copied</u>	<u>Diffuser</u> <u>Appearance</u>	<u>Effect on</u> <u>Transform</u>	<u>Effect on</u> <u>Image and Speckle</u>
Satin ground glass	Fine random pattern	Varied depending on exposure	Varied depending on exposure and position in system
Commercial nonglare glass	Gross random pattern	Large dc spike	Speckle became very large
Opal glass	Uniform Intensity	No effect	Coherent noise was observed
Polacoat screen	Very fine uniform pattern	Large dc spike	Coherent noise was observed
Random amplitude mask	Random phase pattern	Large dc spike	The phase pattern was observable in the image plane

glass. The exposure level used in the contact copying was critical in obtaining optimum performance.

Table 4-11 lists the effects of the best photographic and nonphotographic diffusers on speckle size and image appearance. Three illumination schemes were compared. In the diffuse illumination Fourier transform system, the hologram plane was the transform plane of the HOE. The phase randomizer, in contact with the HOE, was about 0.5 inch from the transparency. For the Abbe illumination system, the diffuser was placed in contact with the transparency. In the holographic Kohler illumination system, the diffuser, positioned in front of the condensing lens, was demagnified and imaged near the hologram recording plane. The effects investigated were the average size of the speckle, the brightness uniformity of the image, and the spread of light in the hologram plane setting the minimum hologram size.

All diffusers when placed in the diffuse Fourier position caused an intensity falloff at the edges of the field of at least 50 percent. Abbe illumination provided better results. The average speckle size was reduced to about 25  $\mu\text{m}$ , but an intensity falloff of 30 percent was typically observed. Kohler illumination provided the best results. The throughput image was uniform to better than 15 percent, and the average speckle diameter was about 8  $\mu\text{m}$ . The hologram size was larger than 20 mm because in this case the hologram plane did not coincide with the transform plane of the Fourier-transform lens. As the hologram plane was shifted toward the transform plane, the speckle size and appearance approach that of the diffuse illumination Fourier transform system.

Figure 4-32 shows sections of the direct projection images made before implementing the Kohler-illumination system. Figure 4-32a was recorded in the diffuse illumination Fourier transform configuration, while Figures

Table 4-11. Phase Randomizer Characteristics

<u>Phase Randomizer</u>	<u>Illumination System</u>	<u>Hologram Diameter (mm)</u>	<u>Speckle Diameter (<math>\mu\text{m}</math>)</u>	<u>Image Appearance</u>
Photographic:				
60 $\mu\text{J}/\text{cm}^2$	Diffuse Fourier	13	40.1	Intensity and resolution falloff
80 $\mu\text{J}/\text{cm}^2$	Diffuse Fourier	19	35	Intensity and resolution falloff
100 $\mu\text{J}/\text{cm}^2$	Diffuse Fourier	20	33	Slight resolution loss at bottom of image
120 $\mu\text{J}/\text{cm}^2$	Diffuse Fourier	22	38	Slight intensity and resolution falloff
140 $\mu\text{J}/\text{cm}^2$	Diffuse Fourier	25	39	Intensity and resolution falloff
160 $\mu\text{J}/\text{cm}^2$	Diffuse Fourier	27	34	Intensity and resolution falloff
220 $\mu\text{J}/\text{cm}^2$	Diffuse Fourier	28	35	Intensity and resolution falloff
360 $\mu\text{J}/\text{cm}^2$	Diffuse Fourier	28	34	Intensity and resolution falloff
Satin Ground Glass	Diffuse Fourier	30	27	Vignetted
Opal Glass	Diffuse Fourier	40	25	Very dim, vignetted
Polacoat Screen	Diffuse Fourier	40	23	Dim with intensity falloff
Nonglare Glass	Diffuse Fourier	14	39	Large, nondense speckle
Hand Ground Glass 9 $\mu\text{m}$ Grit	Diffuse Fourier	19	26	Slight vignetting
Satin Ground Glass Abbe		20	24	Some intensity falloff



Table 4-11. Phase Randomizer Characteristics (Continued)

<u>Phase Randomizer</u>	<u>Illumination System</u>	<u>Hologram Diameter (mm)</u>	<u>Speckle Diameter (<math>\mu\text{m}</math>)</u>	<u>Image Appearance</u>
Photographic 100 $\mu\text{J}/\text{cm}^2$	Abbe	15	25	Some intensity falloff
Nonglare Glass	Holographic Kohler	15	35	Severe intensity falloff
Satin Ground Glass	Holographic Kohler	23	8	Good; uniform luminance
Hand Ground Glass	Holographic Kohler	23	5.5	Good; uniform luminance

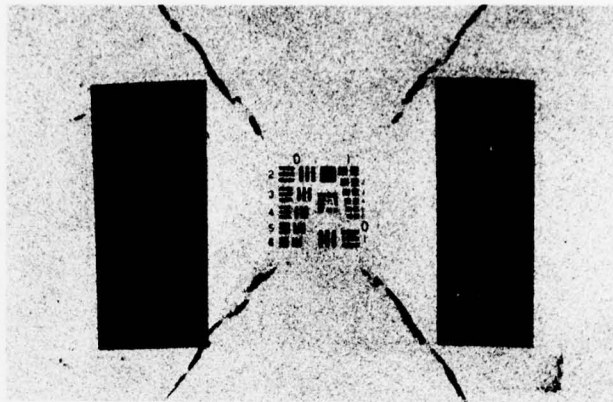
4-32b and 4-32c were recorded using the Abbe illumination condition. Speckle is obvious in all three cases.

#### 4.8.2 Multiple Signal Beams

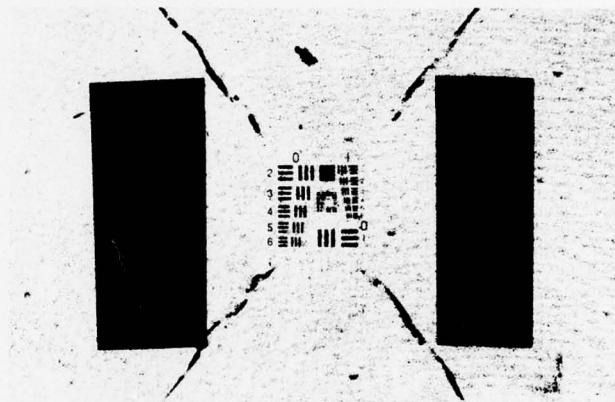
One way to reduce the dynamic range in the Fourier plane is to generate multiple transforms. Each of these transforms has a fraction of the energy that would be present with only a single transform. The holograms are recorded using a single reference beam. Upon reconstruction, the images from the holograms are aligned in the image plane. This technique provides redundancy in the hologram, and reduces the coherent noise problem. Only the image defects in the film chip contribute to cosmetic noise in the projected image.

To implement this type of breadboard, we generated a series of 300 cycle/inch phase gratings. Gratings having both a square-wave phase profile and a sine-wave phase profile were made. Square wave gratings were made by contact printing a Ronchi ruling. Sine-wave gratings were prepared in two ways: a Ronchi ruling was contact printed with spacers between the ruling and the film to soften the edges and holographic plane wave gratings with  $K = 20$  were recorded.

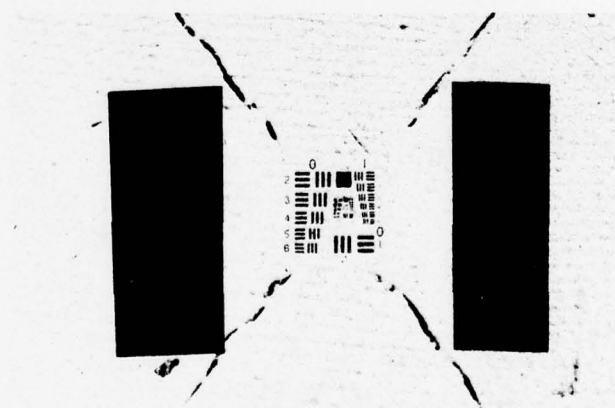
We mounted the square-wave grating on a positioning rail and inserted it into the collimated signal beam. The grating was positioned to self-image in the transparency plane. The multiple beams generated by the grating recombine at the image plane, and the transparency is illuminated by a single beam. In theory, the phase grating will generate no image. In practice, the edges of the grating were sharply focussed when the projected image of the map separation film chip was optimized.



A) DIFFUSER ON HOE



B) DIFFUSER IN CONTACT WITH FILM CHIP BASE.



C) DIFFUSER IN CONTACT WITH FILM CHIP EMULSION.

Figure 4-32. The Effect of Diffuser Position on Speckle

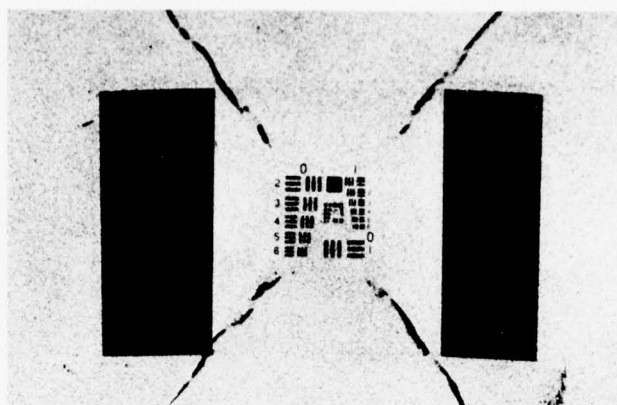


We replaced the square-wave grating with a sine-wave grating, and performed a similar test. When properly positioned, the grating could be eliminated from the image in only small localized regions. The grating pattern was never entirely eliminated. If the resolution of the grating were finer than the maximum resolution of the film chip, the grating would not degrade the image quality. However, in this case, the multiple transforms would be spread outside the hologram area and would not contribute to the hologram. Figure 4-33 shows the effects that use of the sine-wave gratings had on projected image quality. The Figure 4-33a was made with only the diffuser in the system. Figure 4-33b is the direct projected image obtained with a single sine grating. Figure 4-33c is the image obtained with crossed sine gratings. An effort was made to eliminate the presence of the grating pattern in the projected image of the film chip. One approach was to include an additional light diffuser in the signal beam optics. Figure 4-34 is the image obtained with the additional diffuser. Image quality did not noticeably improve.

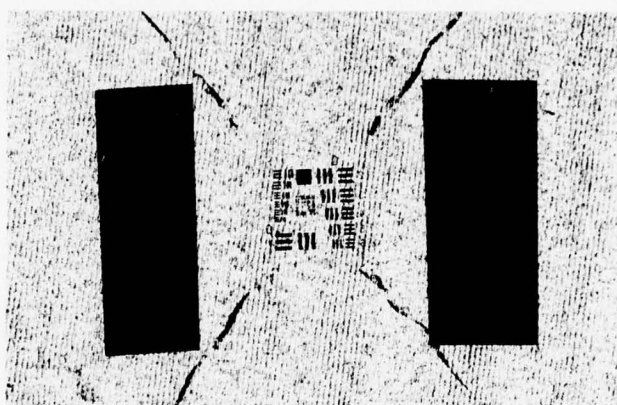
#### 4.8.3 Holographic Recording Techniques

Several holographic recording techniques were explored in an effort to reduce speckle noise to an acceptable level. These techniques included recording conventional specular Fourier transform holograms, recording conventional diffuse Fourier transform holograms, recording matched Fourier transform holograms, and recording diffuse reference and signal beam holograms. Only one of these techniques produced acceptable image quality.

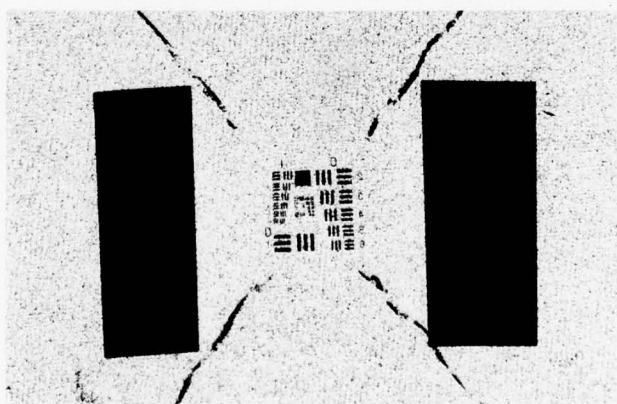
Exact Fourier transform holograms of map chips were recorded using specular illumination and a conventional plane wave reference beam. Because of the large dynamic range present in a specular Fourier transform, not all the spatial frequency components of the film chip could be recorded without



A) DIFFUSER ON HOE.

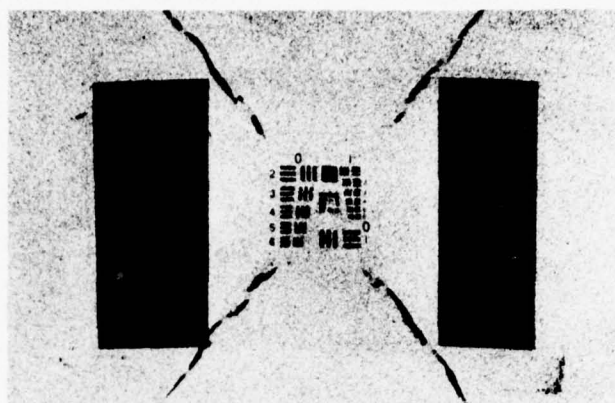


B) SINGLE GRATING.

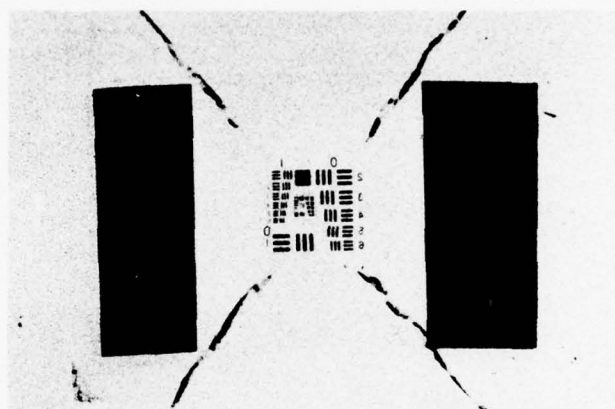


C) CROSSED GRATINGS.

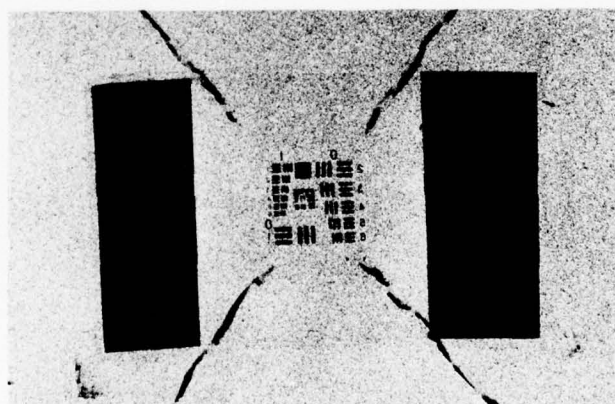
Figure 4-33. The Effect of Self-Imaging Gratings on Speckle



A) DIFFUSER ON HOE.



B) SINGLE GRATING PLUS DIFFUSER.



C) CROSSED GRATING PLUS DIFFUSER.

Figure 4-34. The Effect of a Combination of Diffuser and Grating on Speckle



distortion. Both low and high spatial frequency components were degraded in the recording process. Upon reconstruction, the hologram produced only a band-limited version of the original image, corresponding to the band of spatial frequencies that were faithfully recorded. In addition to this disadvantage, a ghost image, displaced slightly from the true image, was present in the image plane. The ghost image was caused by the nonlinear recording process.

A technique was devised in an attempt to record faithfully the entire range of spatial frequencies in the Fourier transform. This involved recording holographically the Fourier transform of the film chip with a point source reference beam. For this arrangement, the dynamic range of the Fourier transform of the film chip corresponded to the intensity levels of the point source when both complex amplitude distributions were precisely aligned in the hologram recording plane. It was hoped that this would eliminate the band-limited reconstruction. Holograms were recorded and reconstructed with this technique. However, the projected images were of low contrast.

Another technique to reduce the dynamic range problem in the Fourier-transform plane involved recording holograms in which both beams were diffuse illumination. The intensity in the Fourier transform plane was uniform for holograms recorded in this fashion. However, the images reconstructed from the holograms had very poor contrast. Rotating the diffuser in the reference beam during the reconstruction process eliminated speckle. However, image contrast decreased to an unacceptable level.

Fourier transform holograms were also recorded using a plane-wave reference beam with the film chip illuminated by diffuse light. The quality of the reconstructed image obtained was dependent on the distance between the diffuser in the signal illumination beam and the film chip. If the diffuser was positioned far from the film chip during recording, the reconstructed

image had large speckles. The best results were obtained with the diffuser as close to the film chip as possible, i.e., Abbe illumination.

#### 4.8.4 Hologram Readout Techniques

Various readout techniques were investigated with the objective of minimizing speckle noise. These techniques were attempts to temporally integrate (time average) the speckle noise, and thus to minimize its effects. All of the techniques utilized the temporal movement of one of the beams used to record the hologram.

One readout technique investigated involved spinning an object which randomizes the phase of the laser beam illuminating the hologram. Several objects were tested. For example, a glass wedge was used. When rotated in the reference beam a time varying linear change of the wavefront phase was produced. No change in the speckle distribution of the reconstructed image was observed. A diffusing piece of glass was also used. The phase of the reference beam after passage through the spinning diffuser was made spatially incoherent. However, the contrast in the reconstructed image was severely reduced. A random binary phase mask was also used. No noticeable decrease in speckle noise occurred.

Dithering the reference beam, i.e., moving it through very small angular and/or positional changes, was extensively tested. For this technique to work effectively, the speckles must be small. This minimizes the distance the speckle distribution must be sifted to obtain a uniform image. If the phase of the speckle pattern can be rapidly varied, while maintaining the reconstructed image stationary, high image quality (cosmetic) is possible. Obviously, the trade-off is lower image resolution.

Two methods of beam dithering were tested. The first method utilized an acousto-optic beam deflector (AOBD). An AOBD was incorporated in

the reference beam optics. The acoustic wave in the AOB<sub>D</sub> was frequency modulated from 60 to 80 MHz. The frequency of the acoustic wave in the AOB<sub>D</sub> determines the angle through which an optical beam passing through the device is deflected. For an input frequency ranging between 60 and 80 MHz, the angle of the deflected beam changed approximately 1 degree. The dithered beam was subsequently expanded and collimated to form reference beam.

The results achieved with this technique were promising. The speckle could be blurred in the direction of dithering with only a small decrease in the resolution of the reconstructed image. However, since the speckle distribution was not integrated in the direction normal to the dithering direction, qualitative judgement was difficult. To dither the beam in two dimensions requires the use of two AOB<sub>D</sub>'s. The use of two-dimensional AOB<sub>D</sub> beam dithering requires a telecentric scanner configuration. Although this subsystem is not difficult to design and fabricate, the resources of the current effort did not permit its implementation.

We did design and fabricate a pair of mirrors mounted on solenoids, as described in Paragraph 4.6.3. The unexpanded laser beam was incident on the first mirror and scanned through a small vertical angle at a scanning frequency  $f_1$ . The first mirror was imaged on the second solenoid mirror so that the scanned beam pivoted about a point on  $M_2$ .  $M_2$  scanned the reference beam in the horizontal direction at a scanning frequency  $f_2$ . The beam reflected by  $M_2$  was imaged onto the pinhole of a microscope assembly used to expand the beam. Thus, the mirrors and optics formed a telecentric scanner. The pinhole was magnified by suitable optics and imaged onto the hologram plane. This arrangement allowed the beam to pivot about the center of the hologram plane with no lateral movement. Mirrors  $M_1$  and  $M_2$  oscillated at different frequencies, both of which were greater than 50 Hz.



Thus, there was no visible movement (flicker) of the image reconstructed with this technique. However, the shifting of the speckles in the reconstructed image was not great enough to allow complete smoothing.

The optical system was altered to put the hologram plane in the exit pupil of the final collimating lens. This resulted in the reference beam moving only laterally, while the angular orientation was held constant. However, using this optical configuration, the speckle moved synchronously the reconstructed image. This was clearly unacceptable.

The two systems were combined by arranging the first configuration to image the pinhole a small distance from the hologram plane. This allowed a combination of both angular and lateral movement. Figure 4-35 shows hardcopy reconstructed with both dithered and undithered reference beams using this system. Note that dithering has smoothed the speckle noise. However, a decrease in the line weight of the road has also occurred. If the speckle could be made small enough, this degradation would be undetectable. The images reconstructed from the holograms of this study had an average speckle diameter of 25  $\mu\text{m}$ . The use of the dithered readout technique for holograms recorded with the Kohler illumination remains a possibility with which to obtain projected images of satisfactory quality.

#### 4.8.5 Hardcopy Exposure and Processing

The presence of a speckle noise in a projected image is objectionable to a viewer. A series of exposures of the projected image were made onto Kodak SS7 film to determine the amount of speckle that would be transferred to the hardcopy. The granular nature of the hardcopy image was evident. A section from two of the hardcopy reproductions is shown in Figure 4-36a and b. The sample in Figure 4-36a was purposely underexposed, whereas that in Figure 4-36b was overexposed. The effect of speckle noise on the hardcopy image was

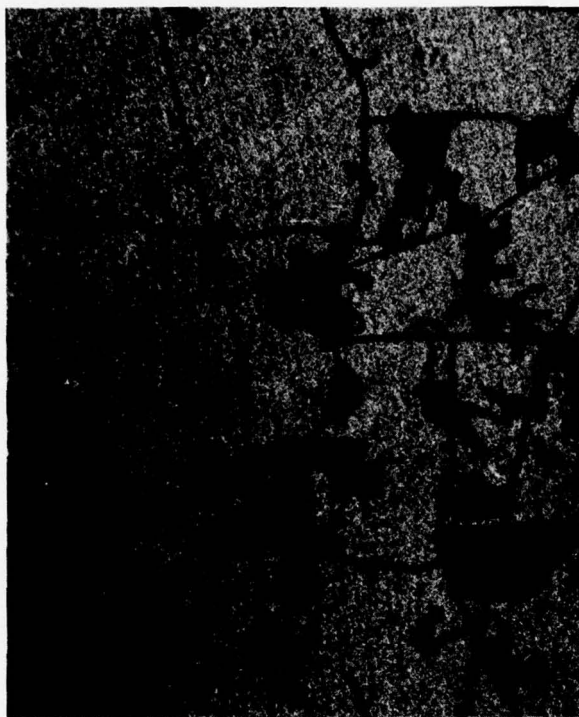


Figure 4-35. The Effect of Dithering the Reconstruction Beam on Speckle

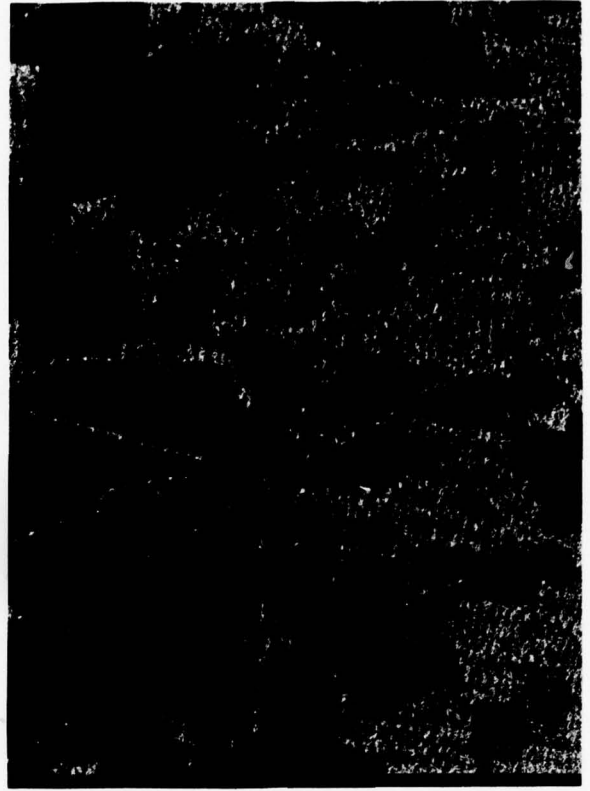


Figure 4-36. The Effect of Hardcopy Exposure on Speckle

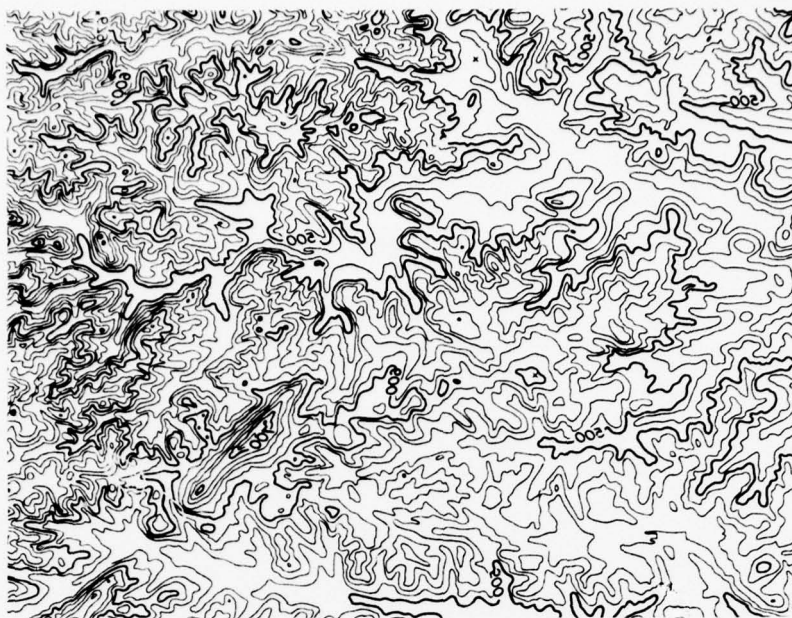


was minimized with increased exposure. This is because the optical density (fill in) of the speckle distribution is increased. However, an exposure level that was high enough to reduce the effect of speckle also resulted in a decrease of resolution. For a projected image obtained from a single wavelength holographic reconstruction, no satisfactory hardcopy images were produced by direct exposure onto Kodak SS7.

A series of exposures was made onto Kodak SS7 film to determine if reversal processing would minimize the degradation caused by speckle. Two sheets of the Kodak SS7 film were exposed to the same level by the projected image obtained with diffuse illumination. One of the exposed sheets was processed in the conventional manner. The other sheet was reversal processed using the method summarized in Table 4-12. A sample from each of these films is shown in Figure 4-37. The speckle noise was reduced for the film that was reversal processed. This effect is clear from the uniformity of the interior lines shown in Figure 4-37b. However, the edges of the sharp boundaries shown in the figure remained poorly defined. In summary, while improvements were noted no entirely satisfactory results were obtained with the reversal processing technique.

#### 4.8.6 Incoherent Addition of Holograms

The incoherent addition of holograms was investigated as a means for the reduction of speckle in projected images. The possibility that an overlapping series of holograms of the same image, when reconstructed simultaneously, could yield a low speckle noise projected image motivated the effort. Initially, the incoherent addition process was simulated. A series of exposures were made of a direct projection obtained with diffuse illumination. The film being exposed remained stationary, while the diffuser providing the illumination was slightly shifted between exposures. The



A) NORMAL PROCESSING



B) REVERSAL PROCESSING

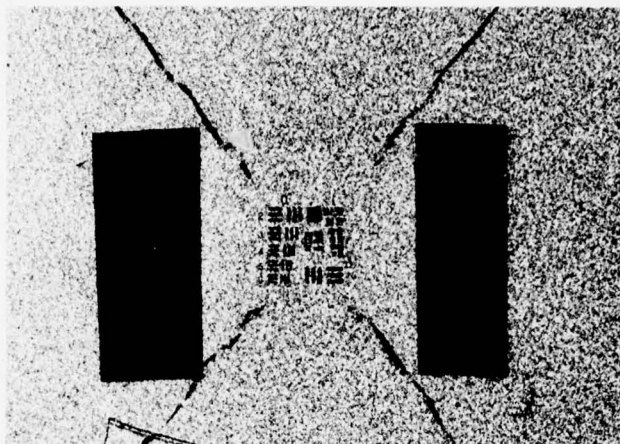
Figure 4-37. The Effect of Reversal Processing on Speckle

resulting hardcopy thus consisted of one image with shifted speckle distributions. The hardcopy obtained with 1, 4, and 100 separate exposures is shown in Figures 4-38 and 4-39. Reduction of the speckle effect is discerned only in the hardcopy that received 100 exposures.

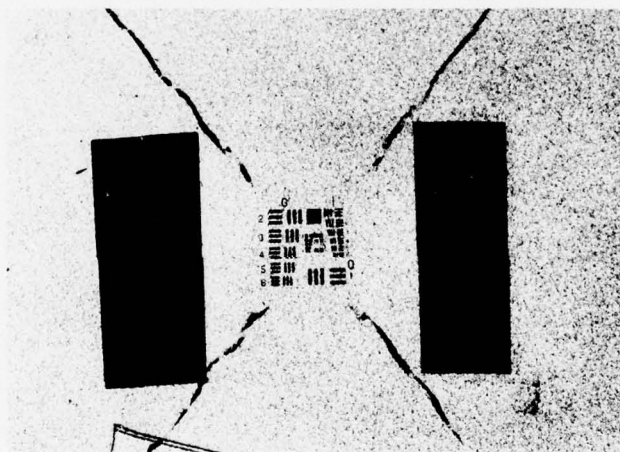
Holograms were recorded using the incoherent addition technique for diffusely illuminated film chips. Holograms were recorded with up to 12 separate exposures. The projected images obtained from these holograms were visually examined. No noticeable decrease in speckle was observed. In addition, a substantial decrease in the diffraction efficiency of the holograms and signal-to-noise ratio for the projected image had occurred.

The use of holographic incoherent additions, although decreasing the magnitude of the speckle pattern, did not eliminate it. The reason that the speckle effect remained was the mutual interference of the incoherently superimposed reconstructions with each other. This mutual interference created its own characteristic speckle distribution. The two wavelength holographic Kohler breadboard, discussed previously and shown in Figure 4-19, was designed to avoid this effect. The use of two wavelengths to record and reconstruct the hologram eliminated the mutual interference since light of two different wavelengths cannot interfere. Examples of prints made with two wavelength diffuse illumination are shown in Figures 4-40 and 4-41. The projected images obtained from the holographic reconstruction do not contain an obvious contribution from speckle. This is evident from the uniformity seen in the clear regions of the image. However, the effect of speckle is evidenced by the uneven and broken edges in these regions. For comparison, a sample obtained by direct projection from the film chip using incoherent illumination is given in Figure 4-42. There is no evidence of speckle in the clear areas, and the boundaries have well-defined edges. The two wavelength





A) SINGLE EXPOSURE



B) FOUR EXPOSURES

Figure 4-38. The Effect of Simulated Incoherent Addition on Speckle



Figure 4-39. The Effect of Simulating 100 Incoherent Additions on Speckle



Figure 4-40. Holographic Projection of a Contour Separation Film  
Chip Illuminated With Two Wavelength Diffuse Coherent Light







Figure 4-42. Direct Projection of a Culture Separation Film Chip  
Illuminated With Two Wavelength Diffuse Coherent Light

recording and reconstruction technique, although not completely eliminating the effects of speckle, did produce the best results obtained.

#### 4.8.7 Summary and Conclusions

We investigated phase randomizers, multiple transforms, beam dithering, hardcopy processing, and speckle overlap from multiple holograms as possible ways to minimize the impact of speckle. We found multiwavelength recording to be the only speckle reduction technique that did not cause a decrease in resolution. The other approaches did yield a satisfactory reduction of speckle noise. Therefore, a two wavelength system is recommended to obtain the highest quality holographic images.

#### 4.9 SPACE-INVARIANT INTERFEROMETER

Holography is an interferometric process. The use of laser light which is both spatially and temporally coherent removes the constraint on white light interferometers that path lengths within the interferometer be equal. The coherent nature of the light, however, does introduce additional features that are significant for image storage applications. If the laser illumination used is specular in nature, phase defects not normally visible on the object or its image are seen. If the laser illumination is diffuse in nature, the image defect problems are eliminated. However, diffuse illumination introduces speckle noise in the image.

Incoherent light can be used to record holographic images under special conditions. One configuration that allows the use of incoherent illumination is the space-invariant interferometer<sup>20</sup> (SII). The SII is basically an equal path length interferometer. In the SII the incident illumination is divided into a signal and reference beam by a dispersive optical component (generally, a grating). These beams traverse optical paths that depend only on the initial orientation of the light rays, and are



recombined on a point-by-point basis by suitable optical components. Since the recombination occurs on a point-by-point basis and the path lengths in the interferometer are precisely equal, interference can occur.

Two characteristics of the space-invariant interferometer are notable. First, a disadvantage of the SII is the requirement for equal path lengths. The equal path lengths require precise positioning controls for optical components used in the interferometer. The degree of precision required is determined by the coherence length of the light source, which may be an arc lamp or spatially incoherent laser light. For some sources, significant control may be required. The second characteristic of interest is the incoherent nature of the illumination. Since incoherent illumination is used, no speckle problems are introduced during hologram recording or readout. This is of considerable significance in the present application, and prompted the experimental investigation of the space-invariant interferometer.

#### 4.9.1 Experimental System

The configuration of optical elements used to configure the space invariant interferometer is shown schematically in Figure 4-43. The incident laser beam is expanded and passed through a spinning diffuser. The spinning diffuser is used to make the laser beam spatially incoherent. The spatially incoherent laser source is approximately collimated prior to illuminating the first, or beam splitting, grating. The incident beam is divided to form two symmetrical paths by the grating  $G_1$ . The beams are incident on the gratings  $G_2$  and  $G_3$  which diffract and recombine the beams in the plane containing grating  $G_4$ . Grating  $G_4$  is used for alignment. A transmissive object may be placed in one of the beam paths to amplitude and/or phase modulate the beam. A hologram of the object is recorded in the plane where the two beams exactly coincide.

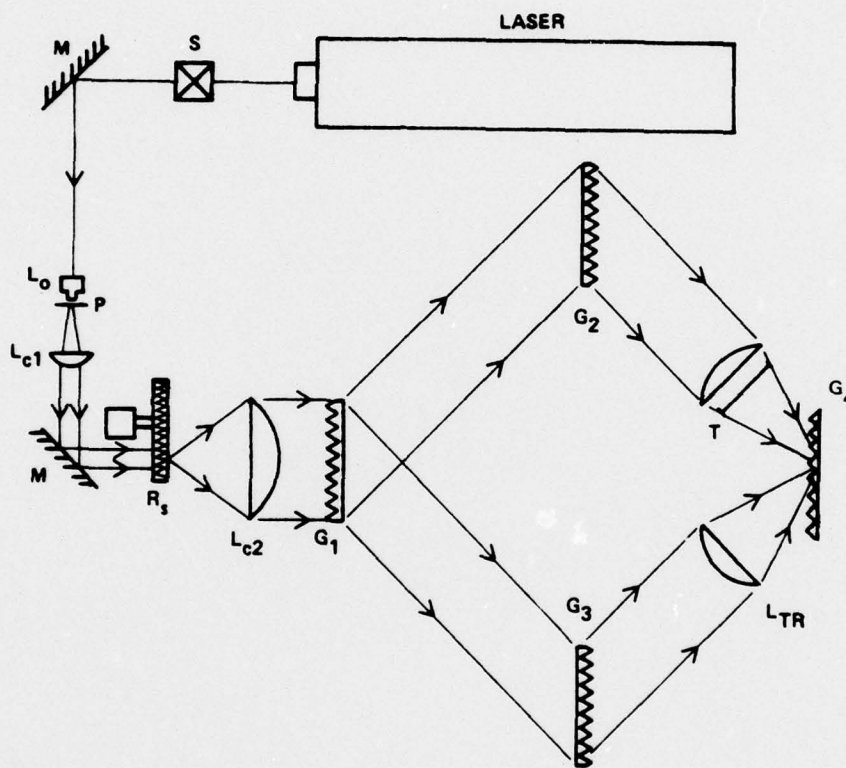


Figure 4-43. Experiment Breadboard Version of a Space-Invariant Interferometer

The gratings used in the experimental testing were made using well known holographic techniques. The K-ratio was 1 (100 percent modulation) and the offset angle was 45 degrees. After exposure and processing, the grating holograms were bleached. The bleaching step was used to convert the holograms to high efficiency phase gratings. The diffraction efficiency for each of the gratings was 60 percent.

The degree of positioning precision required for the gratings is determined by the spatial coherence of the light source. The coherence in this system is determined by the distance between the point source and the spinning diffuser. As the distance between these two points is increased, the coherence is decreased. This relationship was used in the alignment of the SII.

For initial alignment the spinning diffuser is located in plane of the point source. This configuration provides the maximum spatial coherence. A lens is then used to minimize the beam divergence angle. The beam is incident on grating  $G_1$  and is split into two paths. Gratings  $G_2$  and  $G_3$  are approximately positioned to recombine the beams in the plane of the grating  $G_4$ . These gratings are supported on optical rails to provide positioning control. The moiré fringes between the recombined beams and grating  $G_4$  are observed. The positions of gratings  $G_2$  and  $G_3$  are chosen to minimize the number of moiré fringes. After this minimization, the diffuser is moved a small distance from the plane containing the point source. The alignment process is repeated until the diffuser is approximately 1 inch from the point source. The final location of grating  $G_4$  is coincident with the hologram recording plane.



#### 4.9.2 Experimental Results

Holograms were recorded using the space invariant interferometer. However, because of the coarse adjustments provided for positioning gratings  $G_2$  and  $G_3$ , only a small section (approximately 1 inch in diameter) of the total field could be recorded holographically. All parts of the total field interfered. However, the surface containing the interference pattern was not planar.

The small section of the field that was recorded by the hologram provided a reconstructed image. The quality of the reconstructed image was poor. The contrast of the projected image was extremely low. However, no speckle was evident in the image.

#### 4.9.3 Summary and Conclusions

The absence of speckle in the reconstructed image of SII holograms is important for the present application. Further development is necessary to obtain good performance over the entire image field. Future implementation of the SII concept should utilize precision micropositioning devices for all optical components. These devices are necessary to satisfy the equal path length condition. When this condition is obtained, holograms whose reconstructed images are speckle-free can be recorded.

#### 4.10 NOTES AND REFERENCES

1. Irradiance (physical) or illuminance (visual, photometric) uniformity is measured relative to the center of the projected image, which is generally an array of squares, e.g., one in the center and in each of the four corners. The MEGIS Program goal was 10 percent center-to-edge uniformity.

2. The film chips are ideally formed of clear lines on an opaque background. Hence, the transmittance at any point  $(x, y)$  should have been either 0 or 1. This was not generally the case.
3. Film chips produced at 10X reduction were made in a single step under well-controlled conditions. The opposite is true for the 20X reduced film chips. There is no fundamental reason why 20X reduced film chips cannot be produced with density uniformity similar to that obtained for the 10X reduced film chips.
4. Resolution here is analogous to bandwidth in this case. High resolution is required not for the sake of identifying small spatial detail, but for the reproduction of well-defined narrow lines. In simple terms, high resolution is needed to avoid the "spatial ringing" caused by diffraction, which has a negative impact on the quality of fine line structure.
5. The monochrome map film chip was made by 10X reduction of a full-color, screened map onto a black-and-white (S0-141) film. The moiré array consisted of similar moiré patterns placed at the center and four corners of a clear 22- x 30-inch topographic sheet. It was used as an alignment aid for hardcopy production. Other special maps will be referred to throughout the report.
6. Diffuse illumination always implies an illumination source of relatively large spatial extent. Diffuse illumination in this study is usually monochromatic (although in some cases more than one wavelength of laser light is used) and either spatially coherent or incoherent.

7. Specular illumination means light from a point source. By definition, specular illumination is spatially coherent since it is obtained from a point light source. A collimated laser beam directly illuminating an object is an example of what is meant by specular illumination. Specular illumination can be either mono- or poly-chromatic.
8. Bleaching is a chemical process that converts silver into a silver halide. This process follows normal development and fixing. Bleached photographic emulsions are generally lossy volume phase recording media.
9. The laser beams used to record the HOE have a Gaussian intensity profile. To achieve uniformity to within 10 percent requires that the laser beam be greatly overexpanded and then apertured to intercept only the center of the beam. Over 90 percent of the original laser power is lost. This greatly increases exposure time and the difficulty of recording high efficiency holograms.
10. Graube, A., Applied Optics 13, 2942 (1974).
11. The HOE itself is diffraction limited. However, the thick (0.25 inch) glass substrate is not optically flat. This gives rise to the observed astigmatism. If a reflective HOE, rather than a transmissive HOE, had been used, no substrate aberrations would occur.
12. A helpful analogy is to consider the phase randomizer as a "white noise" source which is "modulated" by the signal. In the Fourier plane, the complex amplitude distribution is the convolution of the "white noise" spectrum and the signal spectrum.



13. It should be understood that the hologram size (or aperture, in function) determines the spatial bandpass of the system. Since the hologram is located in the Fourier plane of the Fourier-transform HOE, it functions as an ideal low-noise filter.
14. Speckle size (and hence, density) will be determined by the overall resolution of the optical system. Hence, the ideal phase randomizer produces speckles that just match the size of a resolution element. There is no advantage to a courser or finer phase randomizer structure. The effect of speckle can only be minimized by increasing system resolution (making the speckle smaller) or by time averaging during the hardcopy exposure.
15. Altman, J. H., Applied Optics 5, 1689 (1966).
16. Holographic Kohler means that the illumination source of the film chip is imaged by the Fourier-transform lens into the hologram aperture. Projection Kohler means that the illumination source of the film chip is imaged into the aperture stop of the projection lens. The latter method is ideal. A major problem of the MEGIS Program was to find a solution to the "aperture stop" mismatch problem. We did not succeed. However, by recording holograms large enough to pass the marginal rays of the illuminating cone, both holography and optimum Kohler projections are possible. The holograms are now near-Fourier, rather than exact Fourier, transform holograms.
17. This is a direct consequence of the f/number mismatch between the holographic and optical subsystems. The Fourier-transform HOE is f/1.4, whereas the projection lens operates at f/5.6. Not

surprisingly, marginal rays are vignetted by the Wray Micro Lens aperture stop.

18. Zech, R. G., "Data Storage in Volume Holograms," Ph.D. Thesis, University of Michigan, May (1974), p. 238.
19. Reference 18, pp. 99-104.
20. Leith, E. N. and B. J. Chang, Applied Optics 12, 1957 (1973).

SECTION V  
HARDCOPY REPRODUCTION



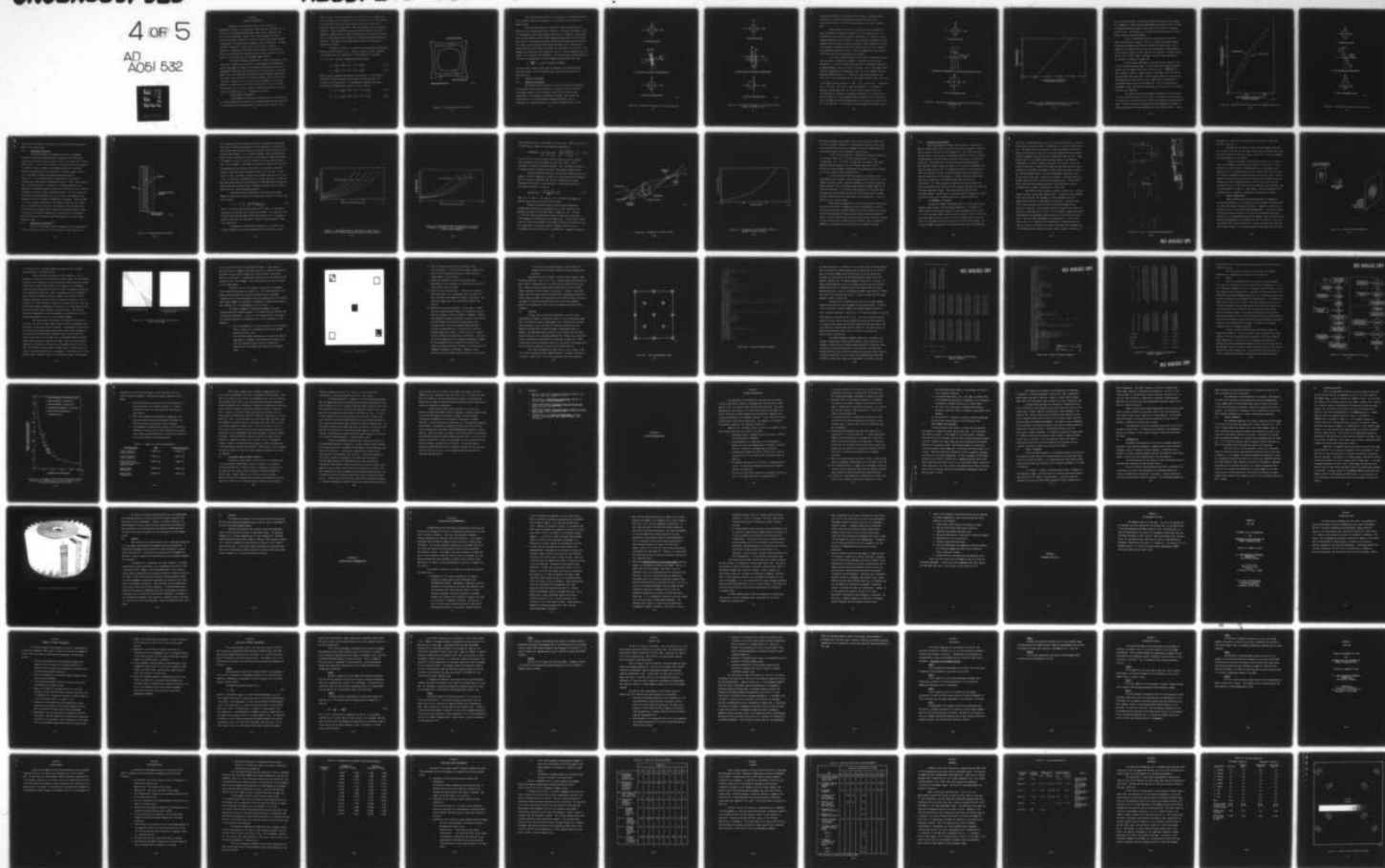
AD-A051 532

HARRIS CORP MELBOURNE FL ELECTRO-OPTICS DEPT  
MICRO-REDUCTION AND ENLARGEMENT OF GRAPHIC INFORMATION STUDY (M--ETC(U).  
DEC 77 R G ZECH, L M RALSTON, B R REDDERSEN DAA653-75-C-0155  
HESD/EOD-1624-F ETL-0063 NL

UNCLASSIFIED

4 OF 5

AD  
A051 532



## SECTION V

### HARDCOPY REPRODUCTION

Hardcopy, as the term will be used in this section, is a photographic recording of a cartographic image blown back (projected) to its full size in a microreduction/enlargement camera system. Because of the flexibility of the present concept, this includes blowbacks from one or multiple wavelengths, incoherent or coherent light sources, and microreduced transparencies or holograms onto photographic film and pressplates. An image recorded as hardcopy will always have some distortion, and limited resolution. The purpose of the analysis which follows is to minimize the distortion and maximize the resolution through careful attention to all the details of a microreduction and enlargement camera system.

The problem of hardcopy reproduction is really two problems, as was noted above: distortion and resolution. The holographic and conventional optical requirements to produce fine resolution with minimum distortion in a cartographic system have been discussed earlier to some extent, but here the emphasis will be on those special problems related to hardcopy reproduction that result in a distortion of the finished reprostat as well as some loss of resolution. Because of the strict distortion requirement in this system, however, it turns out that the resolution requirements of 12.5 cycles/mm in the blowback plane is far less stringent, and need be considered only when a cause of distortion results in a resolution loss as well.

#### 5.1 A DEFINITION OF DISTORTION<sup>1,2</sup>

In the language of conventional geometrical optics, the distortion of a given image point is defined as the distance between the actual position of an image point and that predicted by a paraxial optics analysis of the

imaging system. The normal appearance of distortion in such a system either causes a bending of the imaging rays closer to the optical axis than predicted or further away from the axis than predicted, the cases of barrel and pincushion distortion, respectively. These two possibilities are pictured in Figure 5-1. Gross errors such as these are clearly evident in the case of inexpensive imaging lenses at large field angles, but for high precision work, such as in the present system, distortion is ordinarily much more complicated than this. Accordingly, a more sophisticated definition of distortion is required at this point.

To begin, first note it is possible to represent any two-dimensional map by an array of points  $(x_i, y_i)$ . Whenever the map is copied, regardless of the method used, each object point is transformed into a new point  $(x'_i, y'_i)$ , and a "perfect" transformation requires that:

$$x'_i = m_x [x_0 + [(\cos \theta)x_i - (\sin \theta)y_i]] \quad (5.1)$$

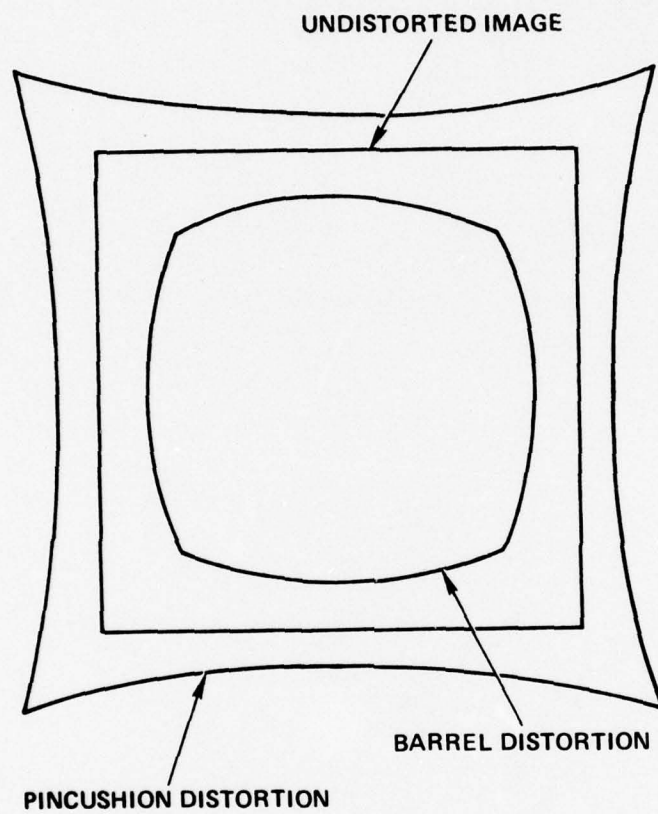
$$y'_i = m_y [y_0 + [(\sin \theta)x_i + (\cos \theta)y_i]] \quad (5.2)$$

where  $x_0$  and  $y_0$  represent coordinate axis translations,  $\theta$  = the angle of rotation of the map reproduction with respect to the original map, and  $m_x$  and  $m_y$  are scaling factors. If the mapping is imperfect and we have distortion, the equations must include a residual factor  $V$ :

$$x'_i + V_{x,i} = m_x [x_0 + [(\cos \theta)x_i - (\sin \theta)y_i]] \quad (5.3)$$

$$y'_i + V_{y,i} = m_y [y_0 + [(\sin \theta)x_i + (\cos \theta)y_i]] \quad (5.4)$$





89136-11

Figure 5-1. Pincushion and Barrel Distortion

This residual factor, which will later appear as the standard deviation in a statistical analysis of distortion, is a true measure of distortion in a mapping system.

Before moving to sources of distortion, a brief discussion of the  $\pm 0.002$  inch distortion specification is necessary. The actual requirement is that if a measurement of the distance between any two points is made on a map blowback copy, and then compared to the distance between the same two points on the original copy, there will be no more than  $\pm 0.002$  inch difference between the two distances. This clearly fits the residual factor definition above, but for some analysis a second definition, derived from this  $\pm 0.002$  inch requirements, will be used. This assumes that we take the 5 foot dimension of the 4 x 5 foot 20X blowback size, and compare it to the  $\pm 0.001$  inch requirement. In that case, the distortion specification can also be considered to be that distances be distorted by less than

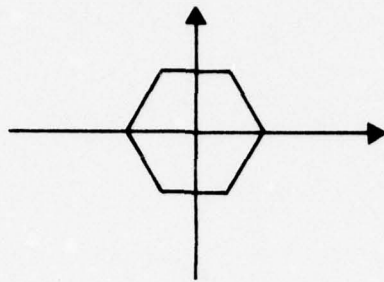
$$\pm \frac{0.002"}{60"} = \pm 1 \text{ part in } 30,000 \text{ or } \pm 0.0033\%.$$

The final results, however, must always be compared to the required  $\pm 0.002$  inch specification, since the 0.0033 percent figure was derived only as an analytical tool.

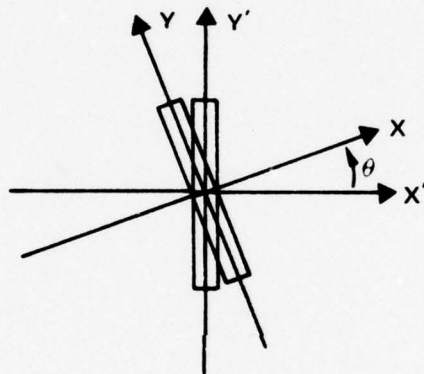
## 5.2 SOURCES OF DISTORTION

### 5.2.1 Mechanical Distortions

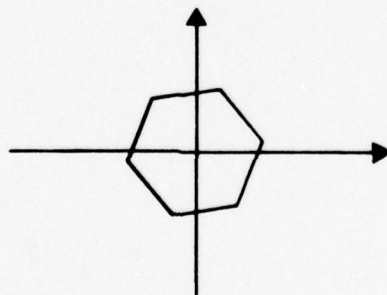
Pure translation and rotation of either the hologram or transparency do not produce any real image distortions; as Figures 5-2 and 5-3 indicate, the blowback image will only translate or rotate as the original signal transparency or the hologram is translated or rotated. What rotation and translation will do in the holographic reconstruction that is not a consequence for transparency motion is to reduce the effective size of the



a. ORIGINAL MAP IMAGE



b. ROTATION OF HOLOGRAM OR TRANSPARENCY

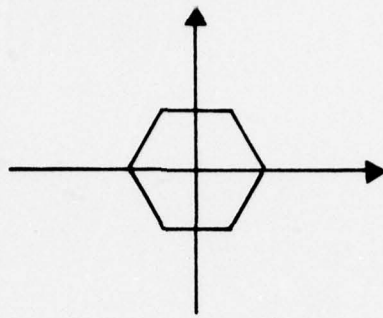


c. EFFECT AT BLOWBACK PLANE

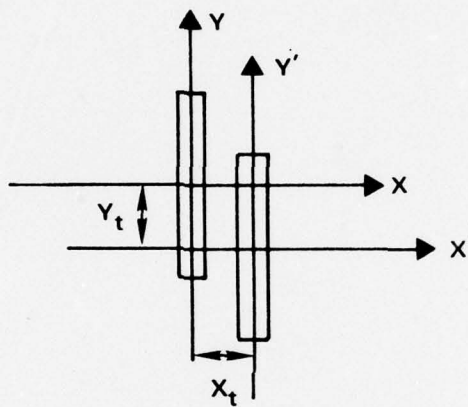
89136-1

Figure 5-2. The Effect of Hologram or Film Chip Rotations

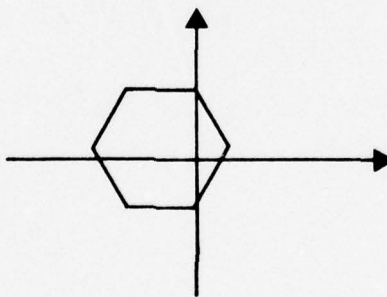




a. ORIGINAL MAP IMAGE



b. TRANSLATION OF HOLOGRAM OR TRANSPARENCY



c. EFFECT AT BLOWBACK PLANE

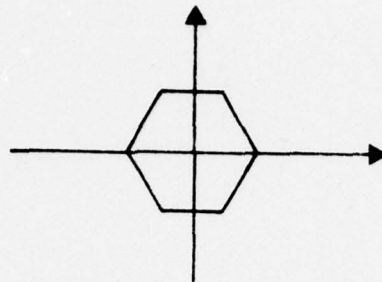
89136-6

Figure 5-3. The Effect of Hologram or Film Chip Translations Normal to the Optical Axis

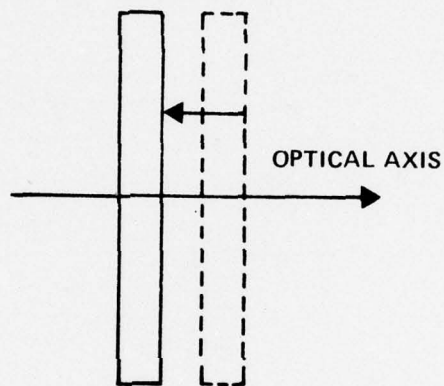
hologram and, therefore, the resolution of the image; in addition, severe rotations will eventually add aberrations because the angle of the reconstruction beam will shift from the position of the original reference beam.

Severe effects will occur as a result of axial misalignments of optical components as depicted in Figure 5-4. If the hardcopy easel, the microreduction lens, and the hologram or transparency are aligned for a given blowback/reduction ratio at one point in time, and one or any number of these components allowed to move along the optical axis before attempting to produce a new blowback or reduction, then clearly both a focus error and a change in the system magnification will occur. Axial misalignments will then severely affect both resolution and distortion in the system.

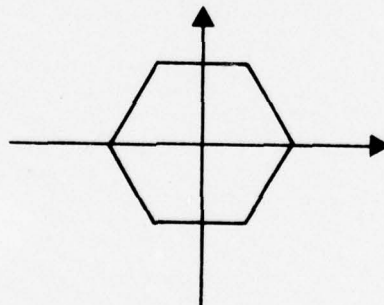
For a total allowed distortion of only  $\pm 0.002$  inch between any two map coordinates, a theoretical treatment is required to predict system performance. To do this, the Wray Micro Lens used for the MEGIS Program will be approximated by a thin lens with a 10 inch EFL. Then, if the magnification from the transparency to the map plan is  $|m| = 10X$  (as an example), from the Newtonian imaging formula  $zz' = f^2$  where  $z$  is the distance from the first focal point to the transparency and  $z'$  the distance from the second focal point to the image, and the relation  $m = -\frac{z'}{f} = -\frac{f}{z}$ , we have that  $z' = 100$  inches and  $z = 11$  inches. With these as baseline parameters, it is possible to calculate the map focus error  $\Delta z'$  and the change in magnification  $\Delta m$  corresponding to a hologram or transparency translation  $\Delta z$ , which has been done for Figure 5-5. Here, because of the 10X reduction ratio selected, the curves for magnification error and map focus error coincide; for other ratios, this is not the case. At this point it could be argued that the Wray lens is



a. ORIGINAL MAP IMAGE



b. HOLOGRAM OR TRANSPARENCY TRANSLATION ALONG OPTICAL AXIS



c. EFFECT IN BLOWBACK PLANE

89136 /

Figure 5-4. The Effect of Hologram or Film Chip Translations Along the Optical Axis



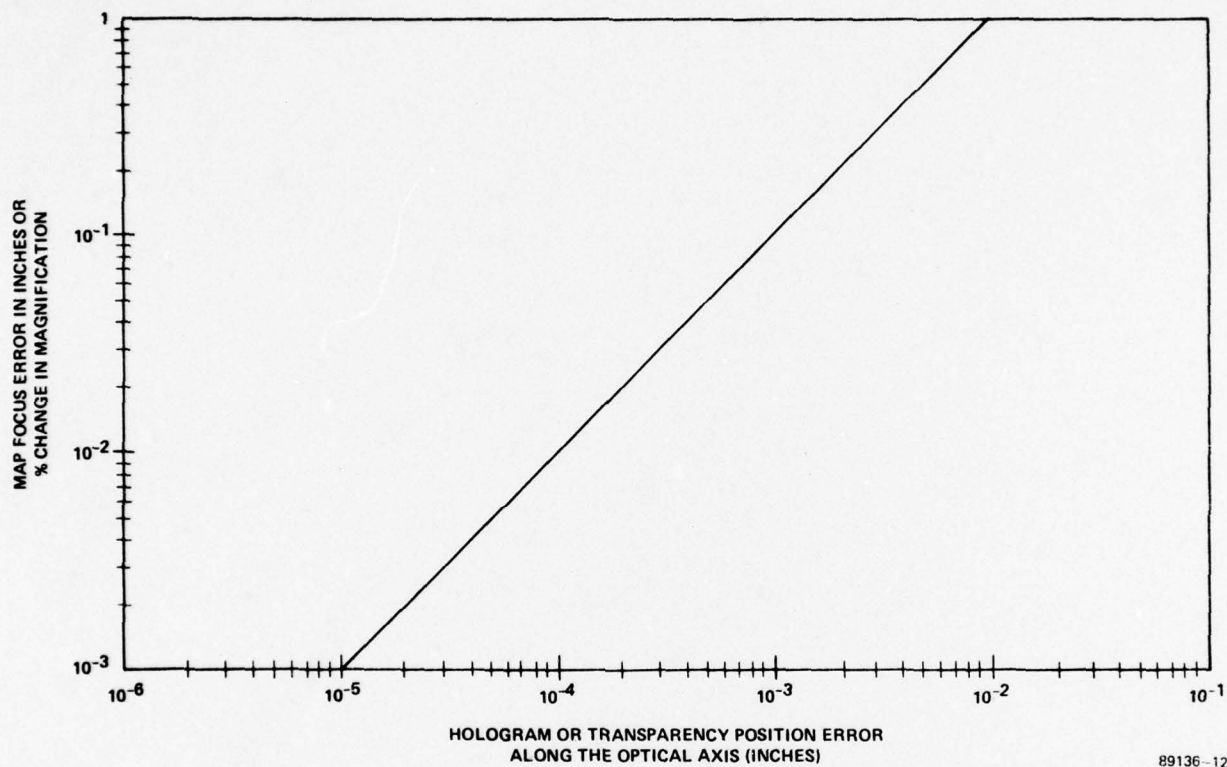


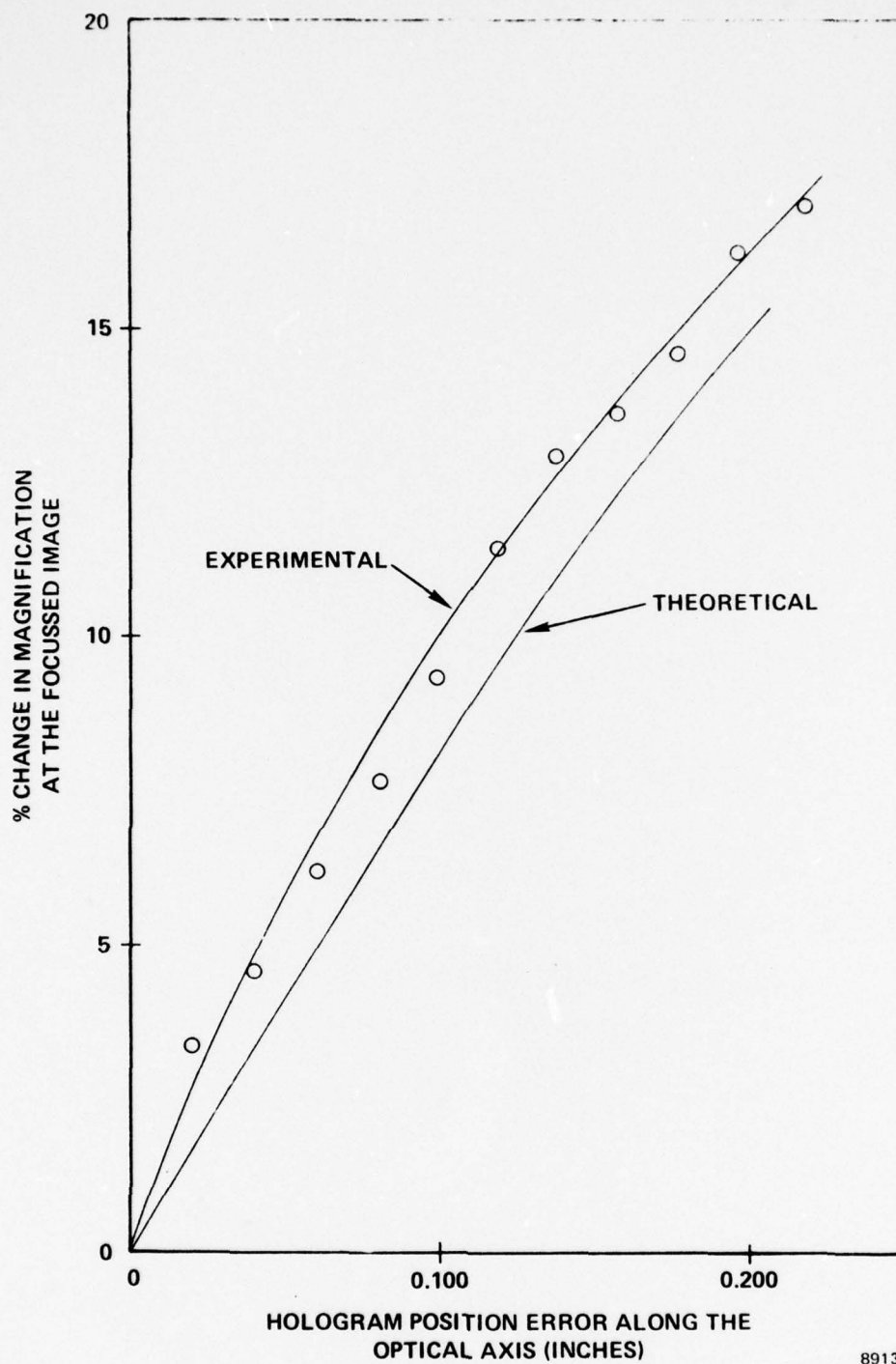
Figure 5-5. Focus and Magnification Errors as a Function of Hologram or Film Chip Axial Misalignments

not a thin lens and that its performance cannot be modeled this way; however, this assumption is supported by the experimental and analytical data in Figure 5-6 showing the percent change in magnification as a function of hologram position error. The theoretical curve agrees with the experimental curve well enough to predict system performance.

To aid in interpreting the data in these figures, the design specifications must be consulted. The first of these, the  $\pm 0.0033$  percent distortion requirement derived from the  $\pm 0.002$  inch specification, can be thought of as a magnification error at the focussed image. Reading directly off the graph in Figure 5-4, this means that the hologram or transparency must be held to  $\pm 3.3 \times 10^{-5}$  inches of movement, and that the map plane must be restrained to a movement of  $\pm 0.0033$  inch.

A second system requirement is the resolution of 0.003 inch lines in the full scale projected image. A relation derived by diffraction theory requires that the depth of focus must fall within  $\pm \Delta z' = m^2 \left[ \frac{8\lambda}{\pi} (f\#)^2 \right]$  to avoid substantial spatial frequency rolloff in the image, and can be used to assure maximum system resolution. For the present system, this requires that the blowback easel cannot move more than  $\pm 0.080$  inch, corresponding to a hologram positioning accuracy of  $\pm 0.0008$  inch. Clearly if the distortion requirement is met, the resolution requirement will be met as far as alignment tolerances are concerned.

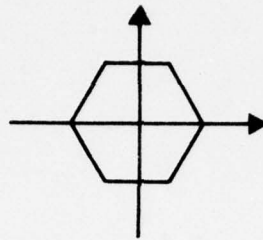
The impact of this analysis appears throughout the present system. Tilts such as that in Figure 5-7 will result in a difference in scaling across the image field, and must be held to the axial positioning tolerance specified above. Further, any method of holding either the transparency, hologram, or hardcopy easel must have axial repeatability to that same tolerance. Finally,



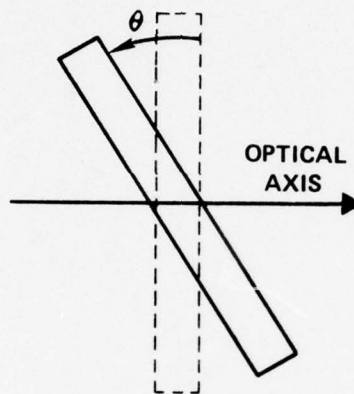
89136-4

Figure 5-6. Experimental Verification of Curve of Magnification Error

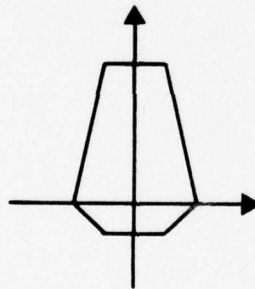




a. ORIGINAL MAP IMAGE



b. TILT OF HOLOGRAM OR TRANSPARENCY



c. EFFECT AT BLOWBACK PLANE

89136-8

Figure 5-7. The Effect of Hologram or Film Chip Tilts

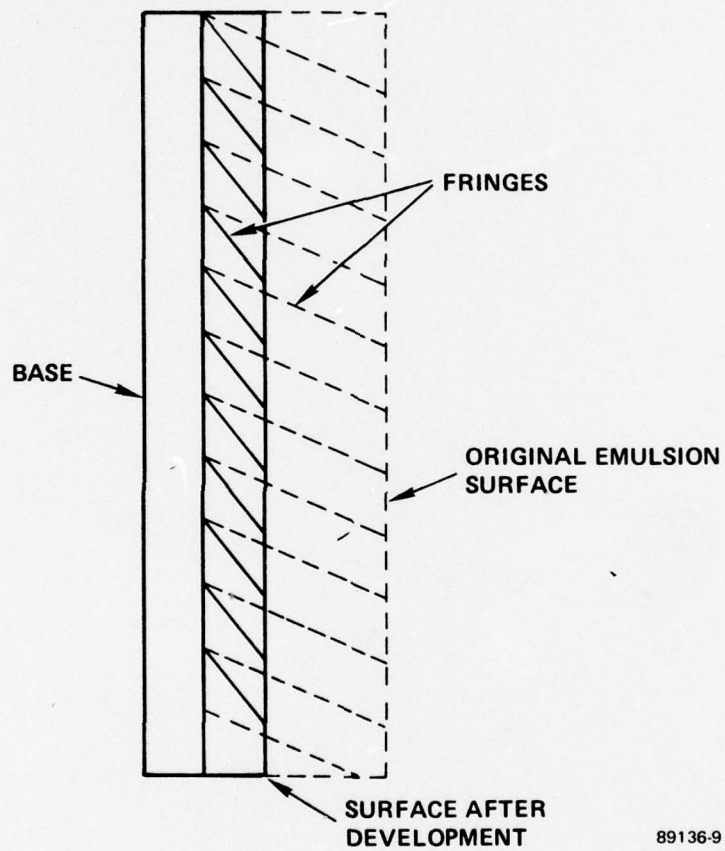
because the fine focusing is necessary, the lens and easel must have precise means of axial positioning.

#### 5.2.2 Holographic Distortions

As mentioned above, misalignments can distort a holographic reconstruction when the hologram cannot be repeatably repositioned after processing; this applies to the bulging of film in liquid gates and on vacuum plates as well - if the film is distorted in its holder either during exposure or readout, or both, the image at the blowback plane will be distorted. Assuming a repeatable positioning mechanism is developed, however, there is still the problem of hologram shrinkage during processing as in Figure 5-8. In any volume holographic recording, the interaction of a reference and a signal beam on a photographic material forms a latent image of their interference pattern in the emulsion. During processing of the hologram, the interference pattern develops and the emulsion shrinks, changing the shape of the latent image's interference fringes. This will distort the reconstruction from the hologram as well as causing a misalignment of the hologram as far as its original reference beam is concerned. The effect here is to cause astigmatic aberrations as the primary distortion, plus a marked loss in diffraction efficiency due to the mismatch of the reference vector with the effective reference vector forming the developed hologram's fringes. In addition, the resulting blowback may be translated due to the change in angle of the processed hologram fringes when compared to the latent image's hologram fringes.

#### 5.2.3 Other Optical Distortions<sup>2,5</sup>

Clearly an ideal means of holding holograms or input transparencies is with a liquid gate consisting of two glass plates, typically 0.25 inch



89136-9

Figure 5-8. Hologram Emulsion Shrinkage



thick, spaced by a gap wide enough to hold the film comfortably between the glass while allowing easy replacement of either holograms or transparencies. Even assuming that the plate surfaces are optically flat and parallel with few internal flaws, however, it will introduce problems. When a plane parallel plate of any kind, whether the glass of a liquid gate or simply the polyester film support, is placed in an optical system, at the very least an optical delay line is produced, so that where an optical path length  $d$  existed earlier (corresponding to the thickness of the plate,  $d$ ) a new path of length  $\frac{d}{n}$  replaces it when the plate of refractive index  $n$  is put in place. If the plate is tilted in the beam, the path of any incident light rays will also be tilted. In addition, if anything other than a plane wavefront is incident on the plate, aberrations will result because of the different optical paths the various rays take through the plate. Geometrical analysis gives a series of formulas to use in analyzing these distortions.

Longitudinal spherical aberration is defined as the distance between the focus of an off-axis ray's focus point and that of a paraxial ray, and is given by

$$\text{L. S. A.} = \frac{t}{n} \left[ 1 - \frac{n \cdot \cos \theta}{(n^2 - \sin^2 \theta)^{\frac{1}{2}}} \right], \quad (5.5)$$

where  $\theta$  is the half-angle of the incident cone of light,  $n$  is the index of refraction for the plate, and  $t$  is the plate thickness. This turns out to be the most significant aberration for most applications, and it is plotted in Figures 5-9 and 5-10 for glass plates of index 1.52 and film base of index 1.50, respectively.

Astigmatism as a quantitative characteristic is defined as the distance between the sagittal and tangential foci of the optical system

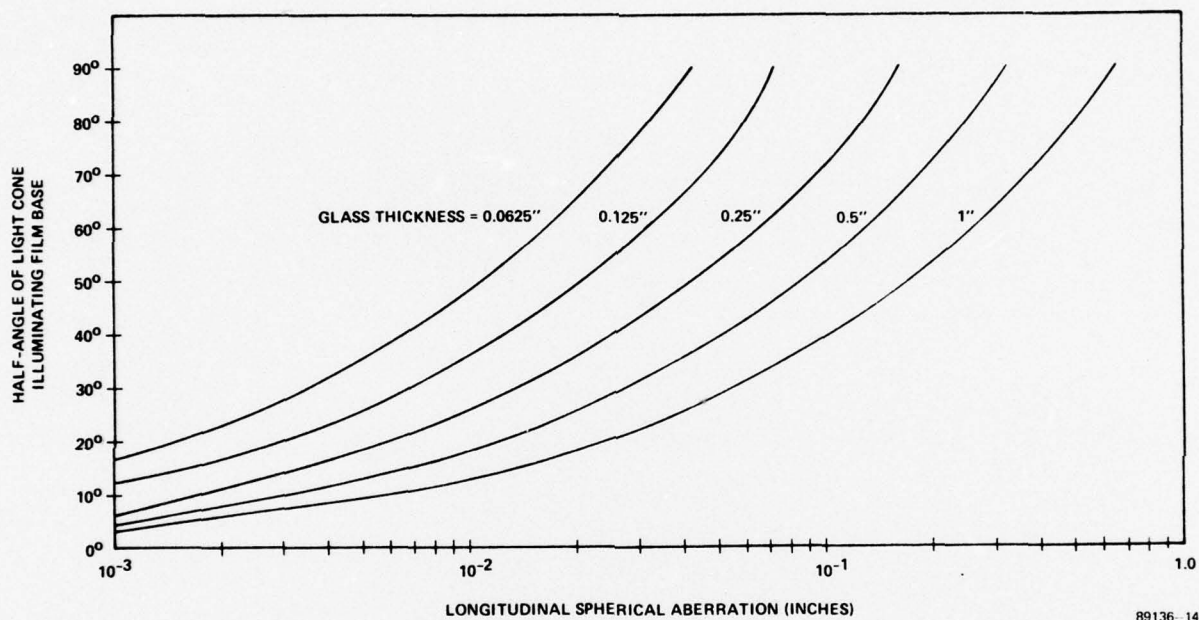


Figure 5-9. Longitudinal Spherical Aberration of Glass Plates as Functions of the Illuminating Cone Half-Angle and Plate Thickness

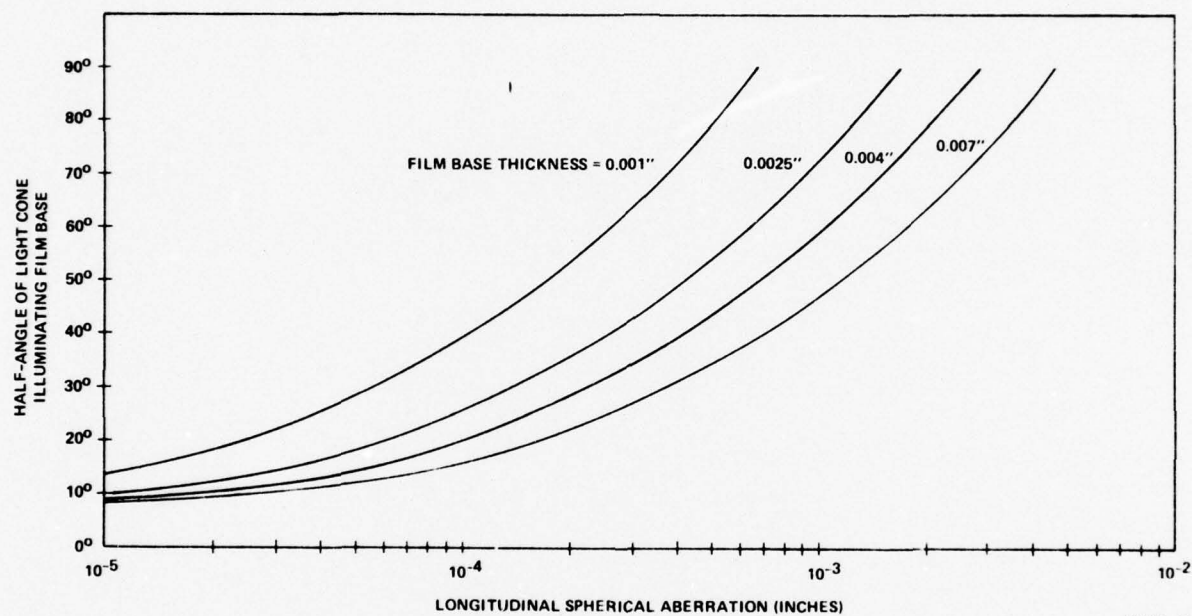


Figure 5-10. Longitudinal Spherical Aberrations of Polyester Film Base as Functions of the Illuminating Cone Half-Angle and Film Base Thickness



(see Figure 5-11), and is due to plate tilt in this case. When the plate tilt is given by  $\theta_p$ , a formula for the astigmatism introduced is:

$$\text{Astigmatism} = \frac{t}{(n^2 - \sin^2 \theta_p)^{\frac{1}{2}}} \left[ \frac{n^2 \cdot \cos^2 \theta_p}{(n^2 - \sin^2 \theta_p)} - 1 \right] \quad (5.6)$$

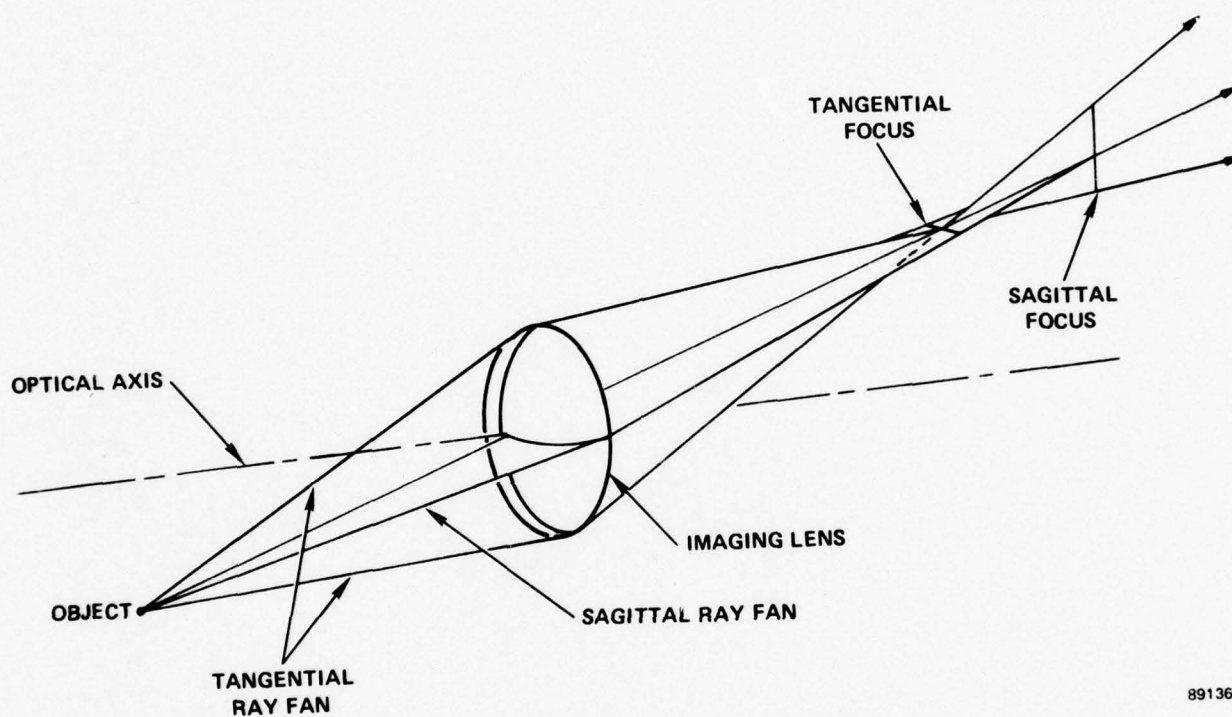
For a tilt of  $1^\circ$ , a 0.25 inch glass plate of Index 1.52, and an incident cone half-angle of  $15^\circ$ , this amounts to  $2.83 \times 10^{-5}$  inches. (A  $15^\circ$  half-angle is typical of the present system.) This is plotted in Figure 5-12 to show the effect of changing tilt angle on the degree of magnification.

Sagittal coma can be defined as the variation of magnification with aperture. What this amounts to in practice is the altitude of the triangular blur of an off-axis "focussed" spot, and this triangle contains about 55 percent of the energy in the "coma patch." The sagittal coma (SC), a third-order aberration, is given by:

$$\text{Sagittal Coma} = \frac{t \theta^2 \theta_p (n^2 - 1)}{2n^3} \quad (5.7)$$

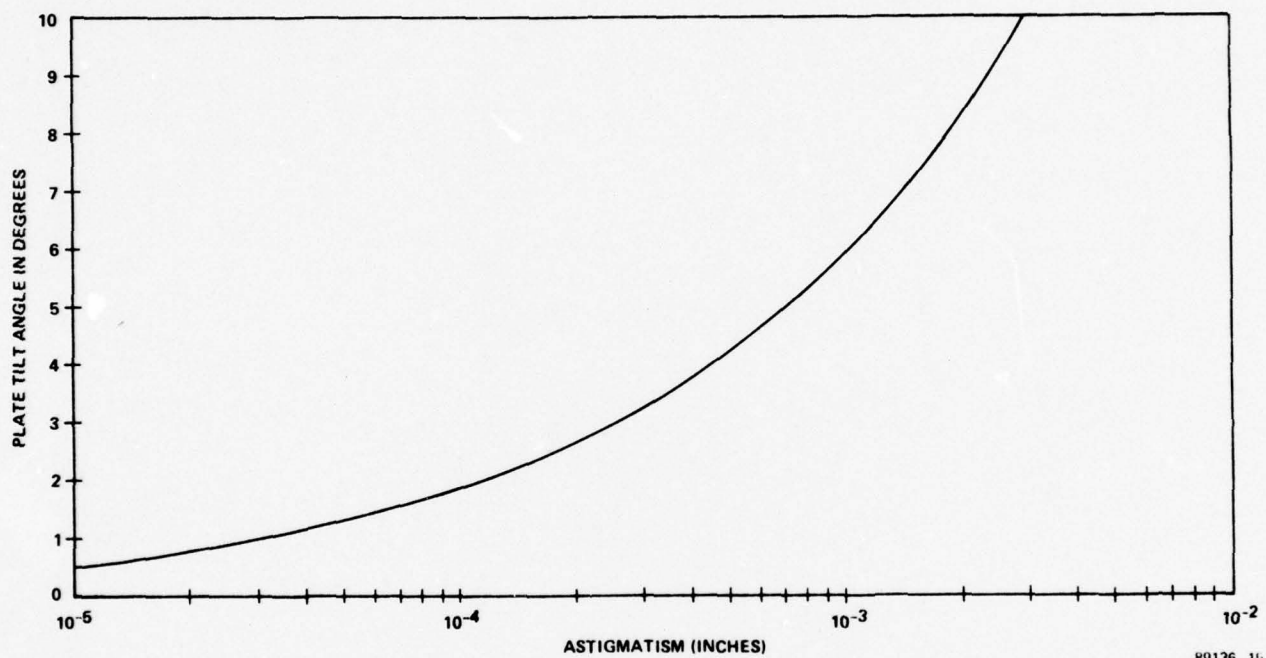
Again, for  $\theta = 15^\circ$ ,  $n = 1.52$ , and  $\theta_p = 1^\circ$ , a calculation was made, and sagittal coma turned out to be  $5.57 \times 10^{-5}$  inches.

Because the distortion specification requires hologram and transparency positioning to an accuracy of  $\pm 3.3 \times 10^{-5}$  inches of axial movement, the spherical aberration alone ( $= 0.0032$  inch for  $\theta = 15^\circ$  and  $t = 0.25$  inch) would eliminate glass plates from any part of the optical system between the transparency and the imaging lens. A thick piece of glass could also reduce the resolution at the edges of the map field unless the lens was stopped down, as substantial spatial frequency rolloff occurs for transparency axial positioning errors of  $\pm 0.0008$  inch. Compared to spherical



89136-10

Figure 5-11. Astigmatism in Optical Systems



89136 15

Figure 5-12. Astigmatism of 0.25 Inch Glass Plates as a Function of Plate Tilt Angle



aberration, astigmatism and sagittal coma resulting from small angle plate tilt are quite small (though still sizeable when considered relative to the distortion specification); they do, however, distort the image further and give another reason for the elimination of glass plates.

A final result to consider is that while the spherical aberration of film base is small relative to that of glass plates, it is not insignificant. For  $\theta = 15^\circ$  and  $t = 0.004$  inch, for example, longitudinal spherical aberration equals  $5.16 \times 10^{-5}$  inches; once again, this is a distortion of the same order of magnitude as the system distortion tolerance. It will not, however, affect the system focus.

If glass plates are absolutely necessary, a principle from photogrammetry may be helpful. The Porro-Koppe principle states that if the imaging rays used to form a reduction transparency in an optical system are simply reversed to form the blowback image, then the blowback image will be free from distortion. In this case it may be possible to record the input transparencies with the glass required for film handling already in place; then the distortions would be prerecorded in the transparencies. This is a possibility for a future system.

Other optical problems which will affect the system distortion and resolution include that of coherent noise due to imperfections in optical surfaces and film bases, chromatic aberrations of the hologram and all lenses for multiple-wavelength recording, and the limiting resolution problem of speckle. Careful attention must be paid to these and the traditional problems of lens centering, auto collimation, and filtering in order to construct a repeatable, high-resolution, and distortion-free reproduction system.

#### 5.2.4 Hardcopy Film Distortions

Processing dimensional changes caused by chemical reactions and physical changes such as rapid drying and roller stretch account for the most obvious source of distortion in the hardcopy film. For a 0.007 inch thick polyester base of the kind used in the present system's SS7 film, this amounts to approximately -0.01% to +0.02%, with most of the change in the thickness dimension.<sup>3</sup> Since distortion is minimized based on the developed copy, a more important problem, though less obvious, is the effect of temperature and humidity changes on the film. The thermal coefficient of linear expansion of 0.007 inch polyester film base is 0.002 percent/ $^{\circ}\text{C}$ , and the corresponding humidity coefficient of linear expansion is 0.0015 percent/ $^{\circ}\text{C}$ , both of the same order of magnitude as the  $\pm 0.0033$  percent derived distortion requirement.<sup>4</sup> This indicates precise temperature and humidity conditions must be maintained before, during, and after hardcopy exposure to minimize any film base dimensional changes. These same conditions should also be maintained whenever a printed copy is to be made from the separations in order to duplicate the original recording conditions as closely as possible.

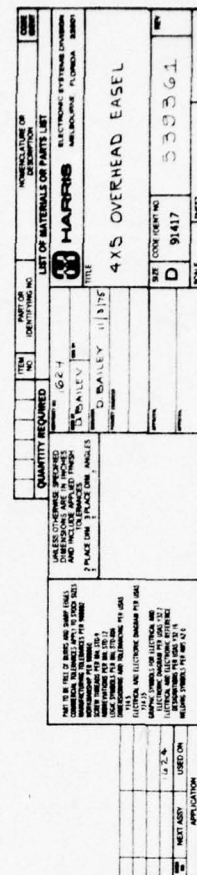
#### 5.3 THE BORROWDALE FILM HOLDER

The precise alignment requirements over a 4 x 5 foot scale at the blowback plane provided a difficult design problem for a film holder. In order to meet the traditional purpose of a reduction camera easel, first of all it must be large enough to hold any size of film up to the 4 x 5 foot size at the 20X magnification position, while still allowing translation of the easel to a 10X magnification position with no shift in the easel center line. To meet alignment requirements, this translation must have a fine adjustment

along with a locking mechanism, as well as be coupled to precise tilt controls to ensure that the easel surface is perpendicular to the camera system optical axis. The necessity for using the easel in both the blowback and reduction phases, plus the desire to be able to focus the system while viewing through the easel suggested using glass for the surface which holds the film. Vacuum grooves would not be allowed because they would appear in any reduction transparency, so instead a method of dc pinning was selected, in which the surface of the glass is coated with a conductive, grounded coating to allow trapping of the hardcopy film between a static charge laid down by a corona bar and the grounded surface. As a final requirement, regardless of the surface used for the easel, flatness of the surface is extremely important to prevent distortion of the film during the holding process. These criteria, then, along with human engineering factors, formed the basis of design discussions with a number of manufacturers in this field.

The solution to this problem is pictured in Figure 5-13. The basic concept includes a prestressed framework which is designed to hold a hanging easel level to  $\pm 0.125$  inch throughout its entire movement from a 10X magnification position to a 20X magnification position. The easel itself rolls on four bearings and can be locked at any desired magnification position; in addition, it has framing curtains to eliminate stray light from the easel, a charging bar, a 52 x 64 x 1/2 inch conductive coated glass plate, and motorized tilt adjustments about the two axis in the plane of the glass plate. The glass plate, manufactured by Liberty Mirror, is select float glass, flat to 7.5 fringes per inch, coated with a transparent conductive layer of indium-tin oxide with a resistance of 500 ohms/inch<sup>2</sup>, bordered with silk-screened markings spaced 0.5 cm apart along two edges of the glass, and





**BEST AVAILABLE COPY**

grounded by a 1 inch silver ink strip around the perimeter of the coated surface of the glass.

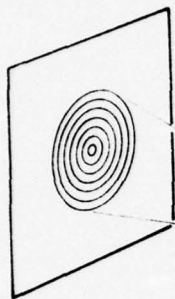
The motorized tilt controls rotate the easel 0.00643 radians per turn of the tilt arm for the axis normal to the floor, and 0.00745 radians per turn of the tilt arm for the axis parallel to the floor. The easel framework was constructed by R. W. Borrowdale.

In practice, the easel is generally very easy to use: a piece of Estar film is taped up on the easel, the corona bar lifted across it with a potential of 7-10 KV, and the film rubbed down to roll out bubbles of air under the film. Tilt controls work very well, and for short-term stability of up to 8 hours, repeatability from one exposure to the next is good. The main problem in using the easel turns out to be decay of the grounding strip with continued use; after considerable erosion of this strip, corona from the charging bar can arc to the side of the easel with sufficient intensity to fog the SS7 hardcopy film in the 4 x 5 feet format. Periodic repainting of the grounding strip is, therefore, recommended to eliminate this problem.

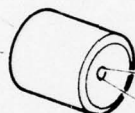
#### 5.4 MOIRÉ ALIGNMENT METHOD

Before proceeding with the actual production of hardcopy and distortion minimization, it is necessary to align the easel and camera system as close to the proper orientation as possible. Otherwise, a great deal of time will be lost in the making of distorted repromats. Initially, of course, scaling can be set by blowing up a two-axis grid transparency on the easel, setting a ruler or comparator up against the blowback image, and adjusting the translation adjustments on the reduction lens and the easel until the scale is set properly while retaining good focus. To meet the  $\pm 0.002$  inch distortion specification, however, would require hundreds of measurements over the entire

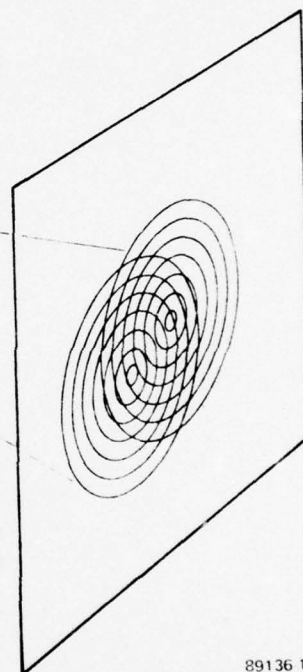
FILM CHIP OR HOLOGRAM  
OF MOIRE' TRANSPARENCY



MICROREDUCTION/  
ENLARGEMENT  
LENS



MOIRE'  
REPROMAT  
(ORIGINAL)  
ILLUMINATED  
BY MOIRE' TARGET  
ENLARGEMENT



89136 16

Figure 5-14. The Moiré Alignment Technique



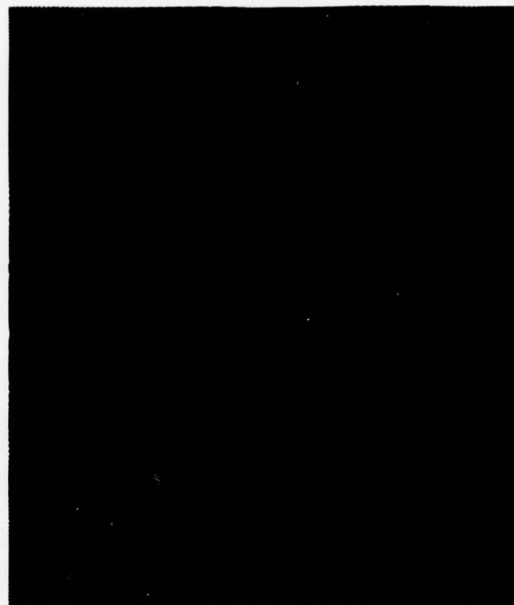
4 x 5 feet surface. The moiré alignment technique cuts this alignment technique down to a few visual checks.

Figure 5-14 shows the essentials of the technique. First, a repro of the particular moiré target to be used is made. For this system a concentric circle target was selected as the basic target because the fringes formed by the overlap of two concentric circle patterns, unlike those of linear gratings, remain within the field of view of an observer no matter how close together the targets are. Next, a microreduction of this repro is made at the exact alignment for future blowbacks (or reductions, as this alignment technique can be used to set the system for reductions as well as blowbacks). To reset the optical system to its original position, either the reduced moiré target transparency or a hologram of it is blown back up to the easel against the original repro of the moiré target. The resulting parabolas and hyperbolas of the fringe patterns will then point to tilt and translation adjustments to set an initial system alignment.

The fringe patterns which appear in a system of this kind are of two kinds. The first of these, shown in Figure 5-15(a), corresponds to pure translation of one target relative to another. An experimental calibration of this effect on the targets made for the present system, with a frequency of 100 cycles/inch with 0.005 inch linewidths of the circles on 0.010 inch centers, shows that for every 0.004 inch of misalignment between the target centers there is one dark fringe and one light fringe in the moiré pattern. Compared to the  $\pm 0.002$  inch distortion error allowable over the full field, then, this indicates that the target can detect errors of down to twice the level of allowable distortion with an unaided eye. The second kind of fringe pattern, shown in Figure 5-15(b), is a scaling error pattern, which appears



a) PURE TRANSLATION



b) SCALING ERROR WITH SOME  
TRANSLATION

Figure 5-15. The Effect of Translation and Scaling on  
Moiré Target Fringes

as a curving of the lines of the translation pattern. In the case of a translation error, alignment is achieved by moving one target with respect to the other along the center-to-center axis clearly evident in the fringe pattern; a scaling error is compensated by moving the lens and easel until the curvature of the lines disappear. Focus errors show up as a lack of contrast in the fringe patterns.

To put this into use in a system, a target with five concentric circle figures was designed as in Figure 5-16. The fringe frequency of the target, 100 cycles/inch, was selected to provide an easily resolvable linewidth as far as the microreduction lens was concerned while still allowing good system alignment, and the general arrangement of targets was designed to give information for tilt adjustments as well as scaling.

The target arrangement is deliberately asymmetric to avoid replacing the moiré alignment repromat in a different position from that used to record the transparency. To use it as an alignment tool for the system, the following procedure is followed every time a set of repromats is to be produced:

1. Place a microreduction of a grid transparency in the system and align its image with the approximate moiré target repromat magnification with a ruler.
2. Place the moiré target transparency in the system and form its image against a repromat of the original moiré target array. Align the repromat by hand to minimize rotations and translations of the repromat with respect to the projected image.



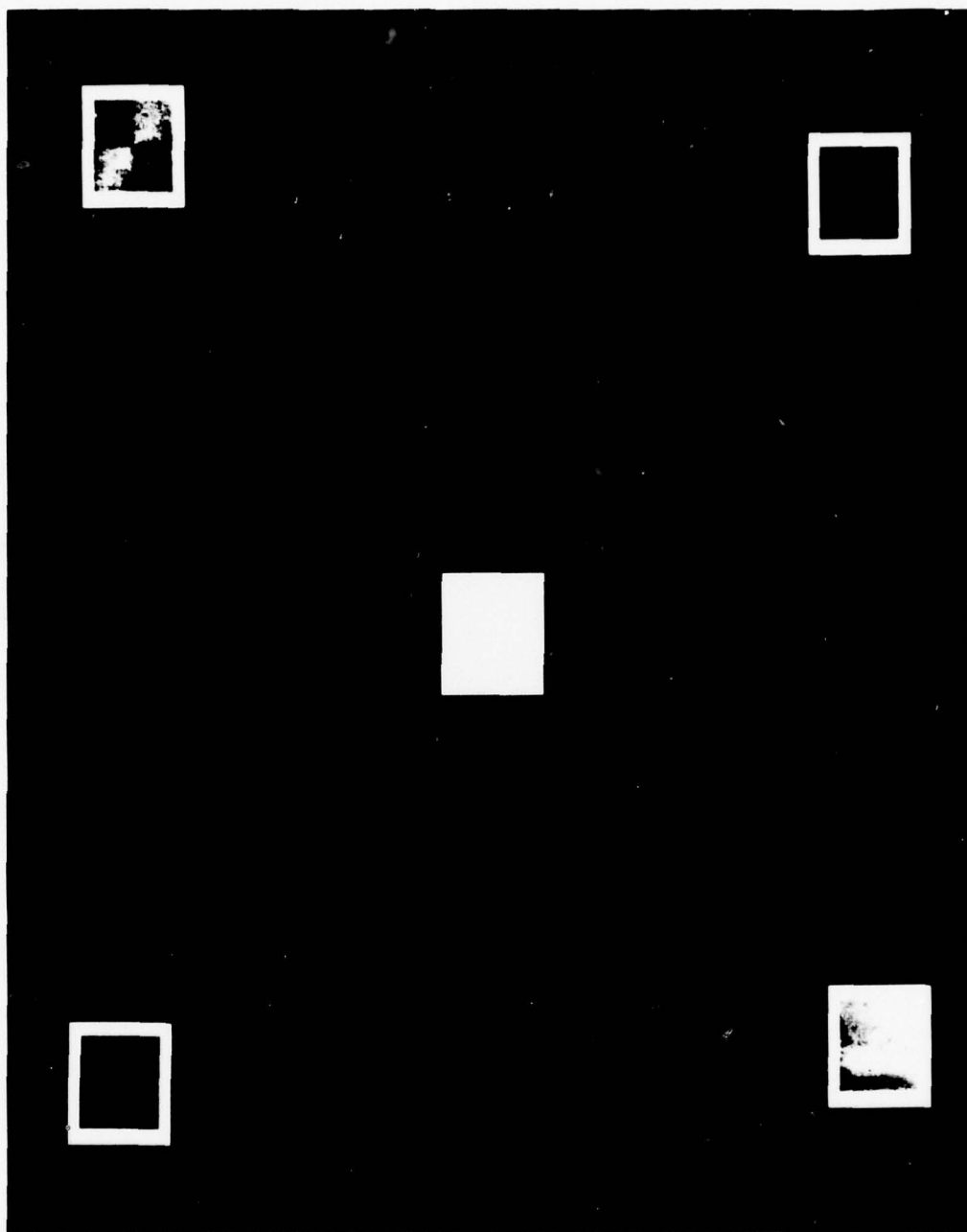


Figure 5-16. The Moiré Target

3. Focus the center target with the microreduction lens translation motor. If a scaling error appears, readjust the easel and lens translation devices until pure translation fringes appear in sharp contrast.
4. Realign the repromat as in Step 2, using translation adjustments on the transparency for fine positioning until the center pattern shows no fringes.
5. Observe the four corner patterns. Adjust the tilt controls with large motions first to guarantee focus, and then fine adjust to equalize the number of fringes in each corner. This leaves the image at most only rotated with respect to the original.
6. Recheck the focus of all patterns. If the center is zeroed, the four corners have equal numbers of fringes and no scaling errors are evident, the moire alignment is complete. Clearly, for holographic blowbacks, holograms of the grid film chip and the moiré target film chip would be substituted in the directions above. With this alignment method, the mean distortion (corresponding to a scaling error) of the first repromat ranged from -0.0192 to -0.0222 inch with a standard deviation ranging from 0.0100 inch to 0.0114 inch. The scaling error may be produced solely by processing dimensional changes, but the standard deviation indicates the combination of processing effects and system limitations in setting an initial alignment, regardless of the method. Compared to mean distortions of up to 0.1254 inch with the use of a ruler alone

to set scale, and processing effects of up to 0.007 inch standard deviation, however, the moiré target alignment works very well.

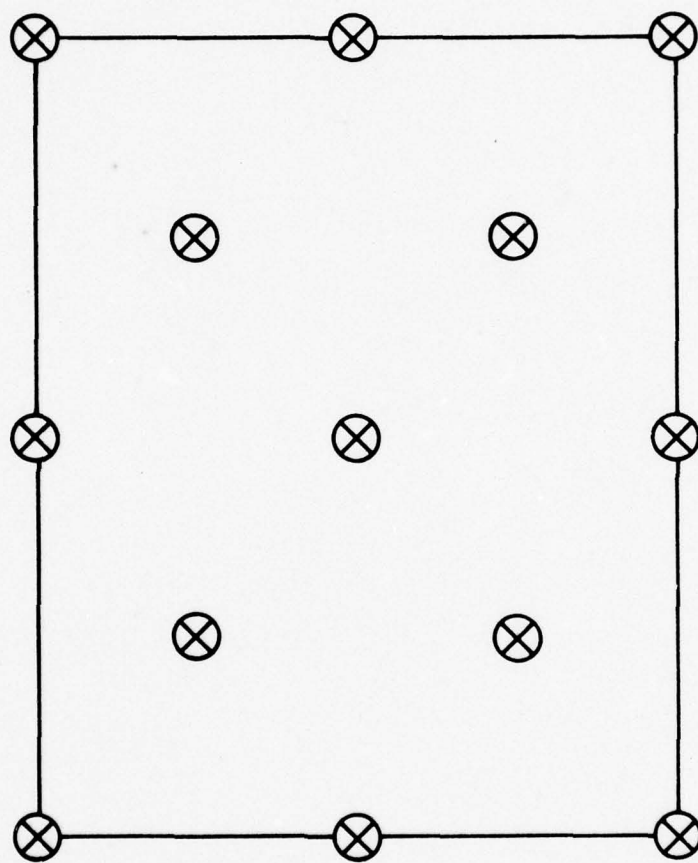
Some possibilities for changes in a future moiré alignment target should be noted here. First of all, a 3 x 3 array of targets would provide an easier means of compensating for tilts than the five-target array now being used. Second, the center target should be made larger and with a higher spatial frequency to better predict scaling errors. Finally, if two moiré targets with dark borders were being aligned with a photodetector behind the second target, the amount of light gathered by the detector would increase as the number of fringes decreased and the targets moved closer together. Coupled to a microprocessor, then, the moiré alignment technique could be automated.

#### 5.5 ITERATION

The next step to distortion minimization is to place a grid transparency or hologram in the system, project it back to the moiré-aligned easel, and record the image on photographic film. Following this, the grid must be measured in such a way that the distortion characteristics are adequately analyzed while holding the number of measurements down to a minimum. The measurement device selected for this analysis was the Bendix Datagrid Digitizer, with a measured repeatability of 0.0013 inch, and the set of point coordinates to be measured by it pictured in Figure 5-17. These thirteen points provide coverage of the field, and, except for extremely small local distortions, completely characterize the system distortion.

Once these measurements are made, they are used as inputs to the first of two distortion analysis computer programs. A computer printout of it is listed in Figure 5-18. This initial processing of the data takes the





89136 17

Figure 5-17. The Grid Measurement Layout

```

1 COM D(13,13),L(13,13)
10 DIM X(13),Y(13)
12 PRINT "ORIGINAL COORDINATE VALUES"
13 PRINT
14 PRINT
15 Q=0
20 FOR I=1 TO 13
30 READ X(I),Y(I)
40 NEXT I
50 FOR I=1 TO 13
60 WRITE (15,170)I,X(I),Y(I)
70 J=1
80 D(I,J)=SQR((X(I)-X(J))2+(Y(I)-Y(J))2)
90 J=J+1
100 IF J=14 THEN 120
110 GOTO 80
120 NEXT I
130 PRINT
140 PRINT
150 PRINT "      1      2      3      4      5      6      7"
170 FORMAT F3.0,2X,F7.3,2X,F7.3,2X,F7.3,2X,F7.3,2X,F7.3,2X,F7.3,2X
180 FOR I=1 TO 13
190 WRITE (15,170)I,D(I,1),D(I,2),D(I,3),D(I,4),D(I,5),D(I,6),D(I,7)
200 NEXT I
210 PRINT
220 PRINT
230 PRINT "      8      9     10     11     12     13"
240 FOR I=1 TO 13
250 WRITE (15,170)I,D(I,8),D(I,9),D(I,10),D(I,11),D(I,12),D(I,13)
260 NEXT I
270 Q=Q+1
280 IF Q=2 THEN 350
290 FOR I=1 TO 13
300 FOR J=1 TO 13
310 L(I,J)=D(I,J)
320 NEXT J
330 NEXT I
340 PRINT
342 PRINT
343 PRINT "COPY COORDINATE VALUES"
344 PRINT
345 PRINT
346 GOTO 20
350 PRINT
360 PRINT
362 STORE DATA 8
365 STOP

```

Figure 5-18. Distortion Analysis Program A

thirteen coordinates of a theoretical 2 cm grid and those of the copy measured here, calculates the distance between each of these points, prints out the array of distance between each of these points, prints out the array of distances for each (Figure 5-19) and stores the two distance arrays on a magnetic cassette file. The second program of Figure 5-20 is now used. It takes the data generated by the first program and calculates the difference between the two sets of distances and the ratio between them to give the magnification error, as well as the maximum, minimum, range, mean and standard deviation of the differences and ratios. A typical printout from the second program is shown in Figure 5-21.

The addition of a few extra calculations to the second computer program turns these data into adjustments for the hardcopy easel. A scaling error in the ratio is readily changed into a percent magnification error, which, using the relations  $m = \frac{z'}{f}$  and  $zz' = f^2$ , yields the amount of lens and easel motion to bring the scaling in line. Tilts are calculated using the length of the two sides of the grid pattern to evaluate rotations about the axis normal to the ground, and using the length of the top and bottom of the grid pattern for rotations about the axis parallel to the ground; these can then be translated into turns of the tilt controls using the easel specifications listed earlier.

The system of making a repromat, measuring it, analyzing it by computer, adjusting the scaling and tilt controls, and then making a new repromat is continued until minimum standard deviations are achieved. Mean distortions are really scaling errors, not distortions, and affect the standard deviation only in that the distance calculations are made relative to a properly scaled grid. For this reason, the standard deviation for mean distortions of more than 0.020 inch in magnitude will be higher than the



# ORIGINAL COORDINATE VALUES

1	0.000	0.000
2	26.000	0.000
3	52.000	0.000
4	40.000	16.000
5	12.000	16.000
6	0.000	34.000
7	26.000	34.000
8	52.000	34.000
9	40.000	52.000
10	12.000	52.000
11	0.000	68.000
12	26.000	68.000
13	52.000	68.000

## BEST AVAILABLE COPY

	1	2	3	4	5	6	7
1	0.000	26.000	52.000	43.081	20.000	34.000	42.802
2	26.000	0.000	26.000	21.260	21.260	42.802	34.000
3	52.000	26.000	0.000	20.000	43.081	62.129	42.802
4	43.081	21.260	20.000	0.000	28.000	43.863	22.804
5	20.000	21.260	43.081	28.000	0.000	21.633	22.804
6	34.000	42.802	62.129	43.863	21.633	0.000	26.000
7	42.802	34.000	42.802	22.804	22.804	26.000	0.000
8	62.129	42.802	34.000	21.633	43.863	52.000	26.000
9	65.605	53.852	53.367	36.000	45.607	43.863	22.804
10	53.367	53.852	65.605	45.607	36.000	21.633	22.804
11	68.000	72.801	85.604	65.605	53.367	34.000	42.802
12	72.801	68.000	72.801	53.852	53.852	42.802	34.000
13	85.604	72.801	68.000	53.367	65.605	62.129	42.802

	8	9	10	11	12	13
1	62.129	65.605	53.367	68.000	72.801	85.604
2	42.802	53.852	53.852	72.801	68.000	72.801
3	34.000	53.367	65.605	85.604	72.801	68.000
4	21.633	36.000	45.607	65.605	53.852	53.367
5	43.863	45.607	36.000	53.367	53.852	65.605
6	52.000	43.863	21.633	34.000	42.802	62.129
7	26.000	22.804	22.804	42.802	34.000	42.802
8	0.000	21.633	43.863	62.129	42.802	34.000
9	21.633	0.000	28.000	43.081	21.260	20.000
10	43.863	28.000	0.000	20.000	21.260	43.081
11	62.129	43.081	20.000	0.000	26.000	52.000
12	42.802	21.260	21.260	26.000	0.000	26.000
13	34.000	20.000	43.081	52.000	26.000	0.000

# COPY COORDINATE VALUES

1	-0.001	0.002
---	--------	-------

Figure 5-19. A Typical Printout From Distortion Analysis Program A

BEST AVAILABLE COPY

```
1 COM DC13,131,LC13,131
10 LOAD DATA 8
20 DIM FC13,131,RC13,131
370 A1=0
380 B1=0
390 A2=0
400 B2=0
410 F2=DC1,13-LC1,11
420 F3=F2
430 R2=1
440 R3=R2
450 FOR I=1 TO 13
460 FOR J=I+1 TO 13
470 FC1,J)=DC1,J)-LC1,J)
480 IF FC1,J)>F3 THEN 510
490 IF FC1,J)<F2 THEN 530
500 GOTO 540
510 F3=FC1,J)
520 GOTO 540
530 F2=FC1,J)
540 RC1,J)=DC1,J)/LC1,J)
550 IF RC1,J)>R3 THEN 580
560 IF RC1,J)<R2 THEN 600
570 GOTO 610
580 R3=RC1,J)
590 GOTO 610
600 R2=RC1,J)
610 A1=A1+FC1,J)
620 A2=A2+FC1,J)*2
630 B1=B1+RC1,J)
640 B2=B2+RC1,J)*2
650 NEXT J
660 NEXT I
670 C1=A1/78
680 C2=B1/78
690 S1=SQR(ABS((A2-(78*C1*2))/77))
700 S2=SQR(ABS((B2-(78*C2*2))/77))
710 G1=F3-F2
720 G2=R3-R2
740 PRINT "FROM TO COPY ORIG DIFF RATIO";
745 PRINT
750 FOR I=1 TO 13
760 FOR J=I+1 TO 13
770 FORMAT F4.0,2X,F4.0,2X,F7.3,2X,F7.3,2X,F7.3,2X,F8.4
780 WRITE (15,770)I,J,DC1,J),LC1,J),FC1,J),RC1,J)
790 NEXT J
800 NEXT I
802 PRINT
810 FORMAT "MAXIMUM",23X,F7.3,2X,F8.4
820 FORMAT "MINIMUM",23X,F7.3,2X,F8.4
830 FORMAT "RANGE",25X,F7.3,2X,F8.4
840 FORMAT "STANDARD DEVIATION",11X,F8.4,2X,F8.4
845 FORMAT "MEAN",25X,F8.4,2X,F8.4
850 WRITE (15,810)F3,R3
860 PRINT
870 WRITE (15,820)F2,R2
880 PRINT
890 WRITE (15,830)G1,G2
900 PRINT
910 WRITE (15,845)C1,C2
920 PRINT
930 WRITE (15,840)S1,S2
940 STOP
```

*DISTORTION ANALYSIS*

*PROGRAM B*

Figure 5-20. Distortion Analysis Program B

FROM	TO	COPY	ORIG	DIFF	RATIO
1	2	26.000	26.000	0.000	1.0000
1	3	51.990	52.000	-0.010	0.9998
1	4	43.062	43.081	-0.019	0.9995
1	5	19.992	20.000	-0.008	0.9996
1	6	33.991	34.000	-0.009	0.9997
1	7	42.795	42.802	-0.007	0.9998
1	8	62.116	62.129	-0.013	0.9998
1	9	65.589	65.605	-0.016	0.9998
1	10	53.349	53.367	-0.018	0.9997
1	11	67.992	68.000	-0.008	0.9999
1	12	72.797	72.801	-0.004	0.9999
1	13	85.595	85.604	-0.008	0.9999
2	3	25.990	26.000	-0.010	0.9996
2	4	21.240	21.260	-0.020	0.9990
2	5	21.249	21.260	-0.011	0.9995
2	6	42.793	42.802	-0.009	0.9998
2	7	33.989	34.000	-0.011	0.9997
2	8	42.788	42.802	-0.014	0.9997
2	9	3.832	53.852	-0.019	0.9996
2	10	831	52	-0.921	0.9996
2	1	790	1	-	0.9998

8	10	27.994	28.000	-0.006	0.9998
9	11	43.076	43.081	-0.005	0.9999
9	12	21.263	21.260	0.002	1.0001
9	13	20.008	20.000	0.008	1.0004
10	11	20.007	20.000	0.007	1.0004
10	12	21.272	21.260	0.012	1.0006
10	13	43.076	43.081	-0.005	0.9999
11	12	26.000	26.000	0.000	1.0000
11	13	51.985	52.000	-0.015	0.9997
12	13	25.985	26.000	-0.015	0.9994
MAXIMUM				0.012	1.0006
MINIMUM				-0.021	0.9990
RANGE				0.033	0.0015
MEAN				-0.0072	0.9998
STANDARD DEVIATION				0.0077	0.0002

Figure 5-21. A Typical Printout From Distortion Analysis Program B



standard deviation for the same data scaled down so that a mean distortion of 0.000 inch results.

The entire process of distortion minimization and hardcopy reproduction is summarized in flow chart form in Figure 5-22.

## 5.6 RESULTS

Though the standard deviation of the mean distance measurement error does fit the definition of the residual factor of Paragraph 5.1, it is still necessary to somehow tie this to a meaningful physical concept as far as the system distortion specification is concerned. As mentioned earlier, this states that the distance between any two points on a reproduced map separation be within  $\pm 0.002$  inch of the theoretical grid measurements. To interpret this specification, Figure 5-23 is useful. Using the standard deviation of the distance measurements falling within  $\pm 0.002$  inch of the mean distortion has been constructed from a selection of the data generated by the second distortion analysis program. The selection of 0.002 inch as the standard deviation corresponding to this distortion specification then implies that 60 out of the 78 different distances available on the thirteen-point measurement scheme are within  $\pm 0.002$  inch of the mean. This then gives a physical interpretation of the standard deviation.

The basic results of the distortion minimization process are summarized in Table 5-1. The Ellerslie Sets 1 and 2 represent direct laser imaging of the Ellerslie repromat series produced in February and March of 1976, respectively. Ellerslie Set 3 is a holographic reproduction set produced from multiple-wavelength holograms on 0.25 inch glass plates during the Equipment Test Plan on March 30, 1976, and shows distortion less than the second of the direct blowback sets. The two contract copy data points are based on coordinate measurements provided by the Engineering Topographic

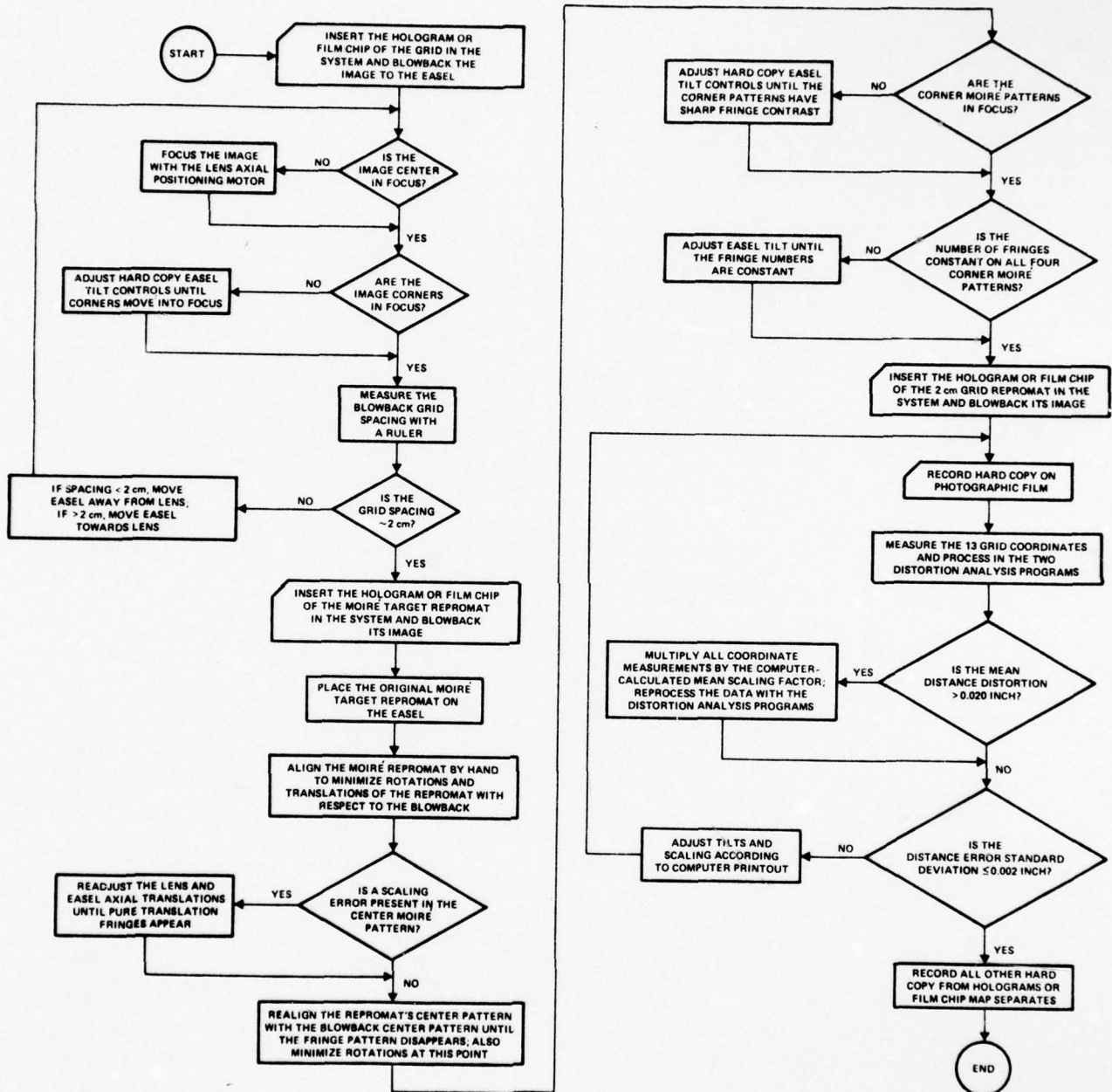
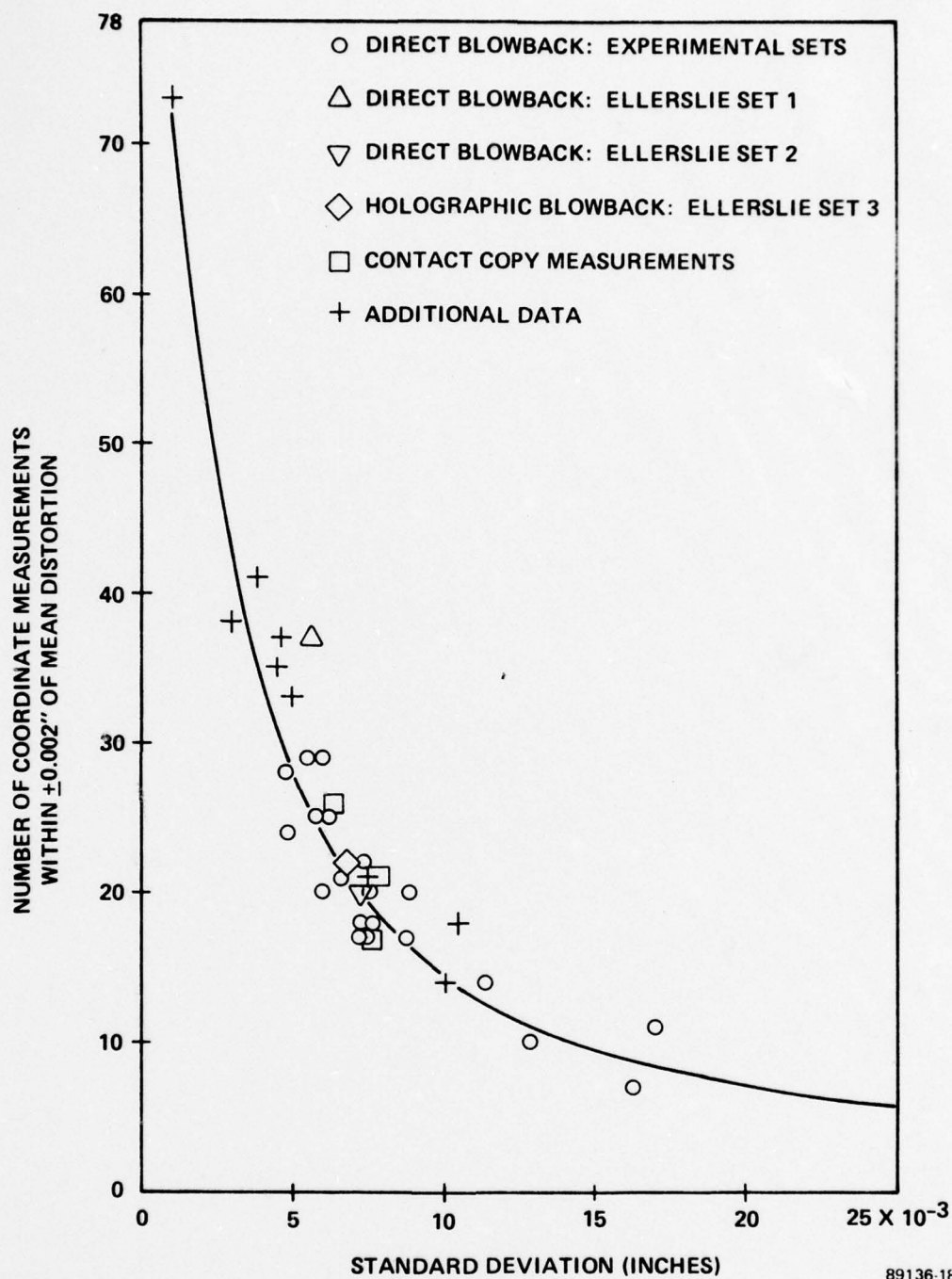


Figure 5-22. Hardcopy Reproduction Flow Chart



89136-18

Figure 5-23. The Number of Grid Coordinate Measurements Within  $\pm 0.002$  Inch of the Mean Distance Error as a Function of the Calculated Standard Deviation From Mean



Laboratory of a full-scale grid contact copy and processed in the two distortion analysis programs. From these data several important results emerge:

- Distortion caused by processing, the only cause possible for the contact copy to be distorted, results in a standard deviation of almost four times the  $\pm 0.002$  inch distortion specification.
- Both direct blowbacks and holographic reproductions, with proper distortion minimization techniques implemented, can partially correct for processing distortion changes.
- The holographic recording process, despite the fact that the holograms of Ellerslie Series 3 were recorded on glass plates (which added to system aberrations), can produce distortion as low as that achieved with direct projection.

Table 5-1. Summary of Distortion Measurements

<u>Map Separations</u>	<u>Mean</u>	<u>Standard Deviation</u>
Ellerslie Series 1, direct projection	0.0045 inch	0.0056 inch
Ellerslie Series 2, direct projection	-0.0036 inch	0.0073 inch
Ellerslie Series 3, holographic projection (after scaling)	-0.0001 inch	0.0068 inch
Contact Copy Measurements 1	-0.0030 inch	0.0076 inch
Contact Copy Measurements 2	-0.0022 inch	0.0078 inch

These results suggest several important recommendations for a future stage of development of an optical cartographic storage system. First, there is no reason to avoid the use of holography; as the results of Table 5-1 show, holograms do not distort the image beyond the distortion photographic processing produces, and as explained in Section IV, holograms do not decrease system resolution beyond the limitations imposed by coherent illumination alone. Second, as the data of Figure 5-22 show, the distortion limit of direct projection reproductions made with incoherent illumination is at least 0.005 inch. This is true even with distortion minimization techniques, which have lowered the standard deviation from greater than 0.007 inch as a result of processing dimensional changes alone. This then indicates a practical lower limit to the distortion of optical map storage techniques relative to the present state of photographic processing development and optical imaging techniques. A decision should be made at this point as to what level of distortion is genuinely tolerable for the various levels of cartographic storage: displays, pressplate-quality hardcopy, and rapid copy production. If the requirement of  $\pm 0.002$  inch distortion is maintained, it does not appear that optical storage will meet this value, whether by repromats, film chips, or holograms.

#### 5.7 EXPERIMENTAL WORK ON HARDCOPY MATERIALS

The Kodak SS7 (Super Speed) film was used for all hardcopy work. It was experimentally determined to require an exposure of  $10 \mu\text{J}/\text{cm}^2$  at 515 nm and processing at 3 feet per minute in a Supermatic 55 processor to reproduce the high contrast graphic information recorded throughout the present study. Contact copies of U.S. Air Force resolution targets demonstrated resolution exceeding 228 cycles/mm, and the emulsion tolerated intensity rolloffs of up to 40 percent before suffering loss of contrast.

Halftones reproduced very well also. Overall, it more than met the requirements for a high-speed duplicating film for the system.

Pressplate generation in support of a direct pressplate generation goal was demonstrated using the hardcopy easel to expose occupied most of the work not done on SS7 film. A Western Litho Foto Plate 8 provided a test of UV plate generation from an 8 x 10 foot direct projection negative, and it shows good resolution despite halftone dropout in the reservoir area. All the 8 x 10 foot hardcopy of Section IV is printed using this plate. Another early test involved the use of the EOCOM Corporation's laser platemaking system to scan a copy of a photographic paper reproduction from the hardcopy easel. Its reproduction method, which allows some digital processing of the optical input data read in by reflection off the original copy, appears to have more latitude in picking up gray scales than direct contact copying on a UV plate, but it suffers halftone dropout to a certain extent as well.

The major experimental pressplate work involved the testing of a Horizons Research Aquarist-L photoresist. Brushed aluminum plates, produced by stripping the emulsion from some available Western Litho pressplates, were used for the substrates. The Aquarist-L photoresist was coated on the substrates with a 64-thread per inch roller bar. Using a 100 W mercury arc light source, contact copy exposures of  $25 \text{ mJ/cm}^2$  were sufficient to initiate image formation, with optimum exposures requiring  $80 \text{ mJ/cm}^2$ . Experiments on the problem of heat-fixing, which this material requires after exposure to ensure proper volatilization of the photoresist activator, show that acceptable prints were produced from two identically-exposed plates, one of which was fixed for 5 minutes at  $160^\circ \text{ F}$  with forced air and one of which was not. It may be possible to drop this step from the processing procedure. In a separate experiment, pressplate resolution was demonstrated by resolution



target contact copies to be about 14 cycles/mm, which appears more than adequate for most cartographic work (see Figure 5-24). In conclusion, then, other than because of coating nonuniformities caused by the hand-coating process and low speed, the Horizons Research pressplate material appears well suited for cartographic reproduction.

Another problem studied was the possibility of using diazo materials to make rapid contact copies of repromats. Ordinary blueprint paper did not have the necessary resolution or exposure latitude to handle cartographic information, but this appears to be because of the paper substrate. A similar emulsion on frosted Mylar, No. 1708 Accufilm produced by Bishop Graphics, Incorporated, produced excellent results with only minor halftone dropout when the Kileen, Texas Monochrome map was used as a contact negative. There was, however, a problem: the finished 0.003 inch thick copy was distorted by about 0.5 percent compared to the original, so this will not produce distortion-free copies; the large amount of heat introduced into the mylar base appears responsible for the stretch. At the speed used for processing (a GAF 240 Diazo Printer at Speed 3) 120 copies of any given map could be turned out per hour, so this approach does merit attention for high-speed map duplication.

## REFERENCES

1. Born, M., and E. Wolf, Principles of Optics, Pergamon Press, New York, 1970, pp. 211-218.
2. Smith, Warren J., Modern Optical Engineering, McGraw-Hill, New York, 1966, pp. 56-57 and 82-84.
3. Eastman Kodak Company, Dimensional Stability of Estar Base Films, Rochester, New York, 1970.
4. Eastman Kodak Company, Physical and Chemical Behavior of Kodak Aerial Films, Rochester, New York, 1974.
5. Thompson, M. M., Ed., Manual of Photogrammetry, American Society of Photogrammetry, Falls Church, Virginia, 1966, pp. 113-114.

SECTION VI  
SYSTEMS CONSIDERATIONS



## SECTION VI

### SYSTEMS CONSIDERATIONS

The techniques and configurations investigated on this program relate to high density storage of cartographic data and high quality reproduction of full size maps and charts from the stored data base. The useful application of these concepts will require that certain other aspects of an overall system be considered together with the constraints imposed by the selected microreduction and enlargement approach. In this section we briefly consider some of these other system aspects. Our purpose is to provide a representative sampling of the important alternatives.

Below we list a functional chain of events for an automated system which might be the basis for a system of the future:

1. Cartographic data is accepted from various sources, including the existing base of repromats.
2. Each transparency (or opaque copy) to be microreduced is mounted to an easel and appropriately illuminated. Both back and front illumination subsystems might be required.
3. A conventional reduction to 70 mm or 105 mm film is made for each series of full size inputs, with closed-loop control of exposure.
4. The exposed film (possibly in roll form) is automatically processed. The processing equipment must provide consistently high quality reductions.
5. The quality of the initial reductions is assessed, either automatically (no human decisions) or semiautomatically

(screening by machines, final decision by a human operator). Unacceptable reductions are reduced from the originals again with appropriate parameter adjustments to improve the results.

6. Acceptable initial reductions are inputted to an automated microreduction unit where a further reduced version of each image is exposed onto a high quality film product in microfiche form (105 mm x 148 mm). Each microfiche will likely accept from 6 to 98 microreductions.
7. The exposed microfiche is automatically processed and then inserted into a projection system where the quality of each enlarged image is assessed, most likely with some human operator involvement.
8. Unacceptable microreductions are noted and logged into an indexing file in a central controller. If some predetermined number of bad microreductions is exceeded for a given microfiche, the entire microfiche will be made again. Otherwise, the bad ones are catalogued for that microfiche to prevent subsequent use, and instructions are provided through the central controller to include the unaccepted ones on subsequent microfiche.
9. Each verified and accepted microfiche is given a unique code by affixing a permanent indexed metal clip to one edge of the film.
10. Each clipped microfiche is logged into an automated storage and retrieval system consisting of many carousel modules, with each module capable of containing about 750 clipped microfiche.
11. A request for a map separation is entered into the central controller which instructs the retrieval mechanisms to locate

the desired microfiche, remove it from storage, and insert it into a projection subsystem.

12. In the projection system, a full size image is produced from the microreduction and either a lithographic film is exposed or a pressplate is exposed directly by this output image.
13. The litho film or pressplate is automatically processed, assessed for quality, re-shot if necessary, and provided to the requestor.
14. The microfiche is returned to storage by retrieval mechanisms.

We now consider certain details of this functional chain.

#### 6.1 INPUT PRODUCTS AND PROCEDURES

A primary purpose of the system is to reduce the storage space requirements for present and future map and chart data. The existing data base consists of about  $3 \times 10^6$  repromats (or the equivalent). Therefore, this data base will be the major source of input to the microreduction system initially. However, the longer range uses of the system must be considered carefully in any specific design. Cost-effective means for infiling the existing data base are only needed for a relatively brief period (such as 1 to 2 years). Once this essentially continuous infiling is complete, subsequent infiling will be at a much reduced pace. In fact, subsequent infiling might be done only on a weekly or monthly basis, depending upon the rate at which inputs accumulate and on how critical it is to have these inputs in the micro-reduced data base. Of course, retrieval and reproduction of data in the base must be able to continue essentially uninterrupted, independent of how and when new data is infiled.



Most inputs to the system will be transparencies so that back illumination is a preferred approach. Provision for front illumination to handle opaque copy might be required. However, a contact copy of opaque inputs onto litho film could be made to permit use of back illumination only.

The positioning precision and uniformity of illumination during initial reduction are very important factors which affect the quality of the final product. Another important consideration is the performance of the reduction lens. We have learned (and verified by direct observation) that initial reductions onto 70 mm film (10X to 20X for typical input sizes) provide only marginally adequate enlargements. The reasons are not fundamental, but are related to such practical issues as lens flare or forward scattering (which tends to reduce contrast), illumination uniformity, and film processing in automatic equipment. An in-depth investigation of these issues is in order with one possible trade-off being a change in reduction format (either larger or smaller). This size change will modify the aperture requirements of both the initial microreduction and holographic Fourier-transform lenses, but it could have a net positive benefit.

## 6.2 QUALITY ASSESSMENT

In the two-step procedure to a microreduced product, the quality of the reduction at each step must be assessed carefully to preserve the integrity of the map and chart data. It is conceivable that certain optical data processing procedures can be applied to aid in quality assessment, or at least in screening.

For example, all edges in repromats must be sharp. A measure of the sharpness of edges in the reductions can be made by examining the spatial power spectrum of the imagery in the reductions. A reduction could be inserted in an optical processor which projected a Fourier transform onto a

special photosensor. The modulus squared of the Fourier transform (the spatial power spectrum) is detected by the photosensor. The ratio of the light collected in selected annular regions centered on the optical axis to the total light collected is a quantitative assessment of edge sharpness. Departures of this factor from some predetermined acceptance range could be used as a rejection criterion.

However, since certain cosmetic degradations could also occur which might not cause a rejection on this basis, other criteria must be applied, which might include a visual inspection by a human operator. This operator would be relieved of the need for detailed inspection and would only be required to examine for relatively gross defects.

These approaches to quality assessment and data verification could be applied at both levels. As experience and confidence in the equipment is gained, the assessment criteria might be adjusted to make the process more efficient.

### 6.3 MICROREDUCTION

Holographic microreduction, possibly using incoherent addition of holograms at two distinct wavelengths or somewhat larger Fresnel (lensless) holograms, remains an important candidate approach. Conventional microreduction is another candidate approach which must be traded off against holography. We have previously indicated many of the key trade-offs.

The microreduction unit may require a closed-loop exposure and processing control technique to ensure optimum results.

The use of 105 mm x 148 mm standard microfiche is selected here as a convenient unit record size and because a well-developed storage and retrieval concept based on microfiche is available. A vacuum platen would likely hold a microfiche in place for exposure. A straightforward mechanical

means to advance the platen and microfiche to successive positions for successive exposures would be incorporated.

The importance of the performance of the automatic film processor for both initial reductions and microreductions cannot be overemphasized. It is our judgment that the required performance can be achieved, but careful initial design and continuing upkeep is required to produce uniform quality products. The selection of a developer is often constrained by certain automatic processor characteristics; a special design might be beneficial.

#### 6.4 CENTRAL CONTROLLER

Any automated system which will handle literally millions of graphics can best be controlled and indexed with a central controller (CC). This CC will include conventional memory (core, disk, and/or magnetic tape) to store instructions and execution procedures and to maintain an index of the location of each graphic inputted to the system. Through this CC new data would be entered and requests for retrievals and enlargements would be executed. It is likely that multiple satellite terminals would be interfaced to the CC to allow users rapid and convenient access to the data base.

With any realistic infiling procedure, there will be recordings made on a microfiche which do not meet quality specifications for one reason or another. If, for example, a microfiche contained 24 recordings, it would be unreasonable to destroy the entire unit if one or two recordings were bad; this would waste the effort required in infiling all 24 graphics. Some maximum number of bad recordings (say four to six) could be allowed per microfiche; the CC can keep track of these and can issue commands to re-record these bad ones on future microfiche. The flexibility offered by the small computer and peripherals which comprise the CC is a very worthwhile feature of such a system.



## 6.5 STORAGE AND RETRIEVAL

Harris has performed an extensive survey of alternative mass storage and retrieval devices and components for the U.S. Air Force, Rome Air Development Center, as part of Contract No. F30602-73-C-0112. Our Final Technical Report on this contract was delivered to RADC in January 1974. Based on this extensive survey, we concluded that the CARD device produced by Image Systems, Inc., of Culver City, California, was the most promising. (This machine is also sold by Remington-Rand as the REMKARD apparatus.) A photograph of the basic storage and retrieval carousel in the CARD and REMKARD units is presented in Figure 6-1. This automatic storage and retrieval device will retrieve and display any one of 750 105 mm x 148 mm microfiche upon operator command. It is manufactured in large volume by Image Systems. It is only available from Image Systems as an operator controlled microfilm display station. Fiche retrieval is accomplished by mechanical selection of fiche identified by unique code bars attached to one edge. As of this writing, the CARD unit is the largest capacity 105 mm x 148 mm microfiche storage and retrieval system that works reliably.

Because of its adequate capacity and proven reliability, the Image Systems CARD unit is considered to be presently the best candidate for incorporation as a basic building block in a multiple carousel mass storage and retrieval subsystem. The CARD unit is a simple keyboard controlled microfiche storage and retrieval unit with an integral optical image viewer. It has been thoroughly engineered, utilizes a very reliable theory of operation and is ideally suited for modification and modularization for handling many thousands of microfiche. A specific design for the HRMR Mass Memory System under development by Harris for RADC employs the CARD carousel in a nine-carousel vertical configuration and stores 6750 microfiche with automatic retrieval and reading.

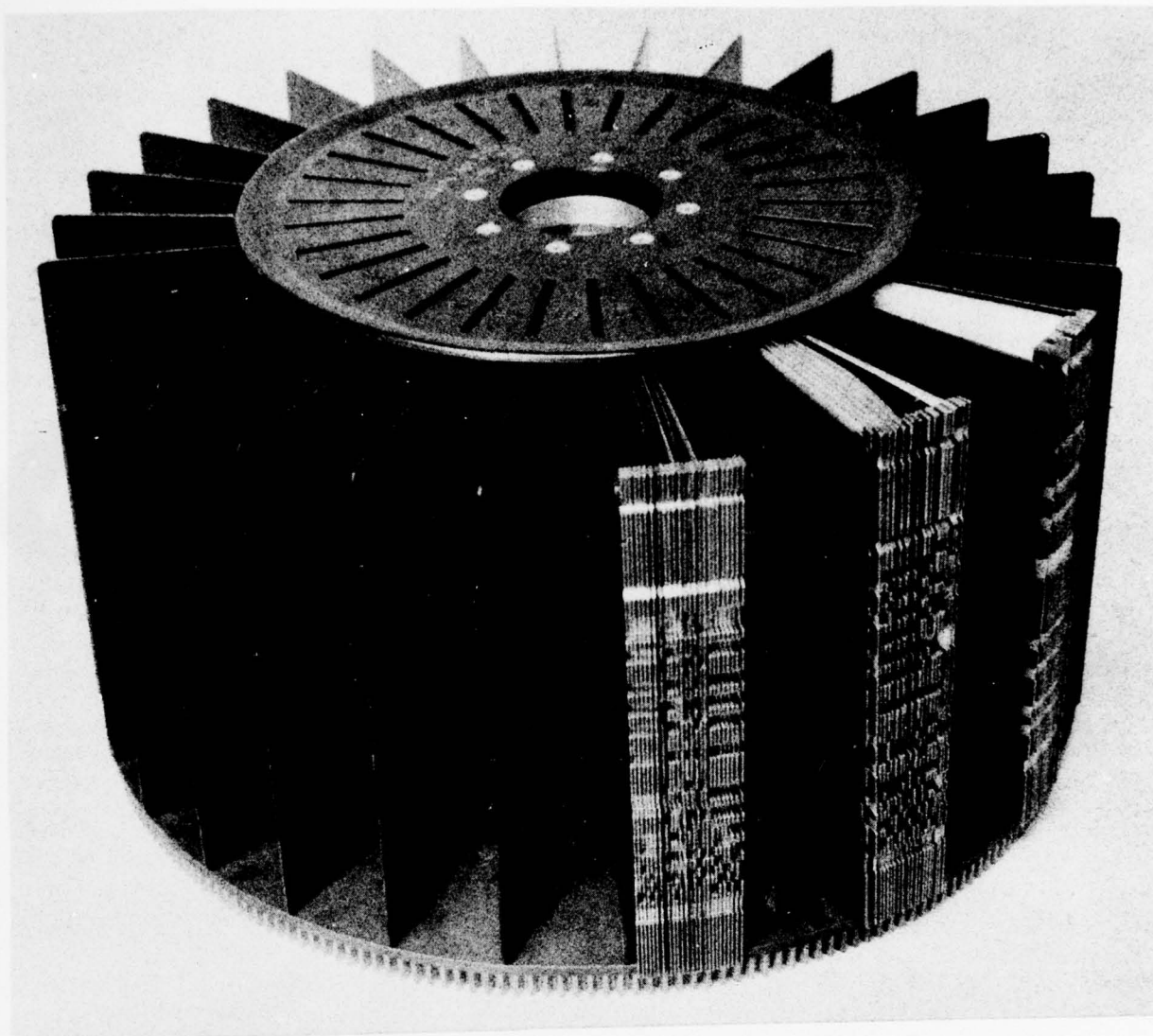


Figure 6-1. Storage and Retrieval Carousel Unit

The results of the tests conducted by Harris on the Image Systems unit confirmed the basic reliability of the unit's design, especially the microfiche extraction subassembly. However, to minimize scratching, the present method of carousel control has been improved; the solid platen has been replaced by an air bearing type for the specialized HRMR application. This modification might be required for the microreduction and enlargement system.

#### 6.6 BLOWBACK

Much has been said in other sections of this report about producing full size output copy by means of enlargement from the microreductions. A single-step enlargement can be achieved from either holographic or conventional microreductions. Clearly the lens system used for enlargement must perform to rigorous standards; the same design used for the reductions appears to be essential.

The exposure of a lithographic film sheet (reprostat) is straightforward and relatively fast because of the high exposure sensitivity of the silver-halide films. However, as has been demonstrated on this contract, certain types of pressplates can be generated directly by exposure to the output image. As the visible sensitive pressplate technology emerges further from the developmental laboratories and becomes truly practical, this alternative also becomes very practical. Maps and charts can be generated more quickly and at less cost with such an approach. It should be noted that a system of the type we are suggesting here could take advantage of these new pressplates even if it were initially based on lithographic film outputs, if the illumination wavelength in the system was a reasonable match to the spectral sensitivities of the new pressplates. Design foresight can ensure such a match.



## 6.7 OVERVIEW

The system view presented is one of several possible alternatives. The one we have portrayed encompasses many of the key issues of importance to ETL and to the Defense Mapping Agency.

When the technology for such a system is more fully developed, a specific design effort must account for many other factors. Two important examples are: 1) human engineering and 2) user acceptability. The human engineering area includes safety, comfort, location, traffic patterns, and the like. The user acceptability issue involves, at the first level, identification of the users. This group must then be permitted to review and contribute to the system design as much as possible to ensure that any future operational hardware will, in fact, be effectively utilized.

SECTION VII  
CONCLUSIONS AND RECOMMENDATIONS

## SECTION VII

### CONCLUSIONS AND RECOMMENDATIONS

The MEGIS Program has contributed new technology to help solve the problem of microstorage and retrieval of topographic map separations and other forms of graphic information. Both direct and holographic breadboard recorder/reproducers were designed, fabricated and tested. A large number of experiments were performed to generate the data required to define system performance. The recorder/reproducer operation was investigated from end to end; each step required for microstorage and retrieval was analyzed and experimentally studied. The outcome of the overall program is evident from the full-scale repromats reproduced from film chips and holograms, the color proofs generated from these repromats and shown at the in-process review meeting by W. R. Graves, and the data presented in Sections II through VI of this report.

We conclude on the basis of our research and experience gained on this effort that:

1. Holography still has significant potential for graphic information storage despite certain experimental and implementation problems. Advantages of holography relative to conventional microstorage are very high image luminance, high storage density, and scratch and dust immunity. Fourier-transform holography, the baseline approach of the MEGIS Program, while optimum from a theoretical viewpoint, was found to be difficult to implement in practice. This was due, in part, to factors which limited the trade-offs required for performance optimization. With greater freedom to specify



critical dimensions and components in a consistent way, we believe that Fourier-transform holography may also be optimum from a systems viewpoint if the film base problem can be solved. However, as indicated in Section II, we maintain that other forms of holography are competitive and may be in certain cases better suited for the needs of the Government mapping community. In particular, Fresnel and Kohler-TIR holography appear to exploit the key advantages of holography in an optimum way; this must, however, be experimentally verified.

2. A direct laser microstorage and retrieval system can be implemented now. Advantages of this approach are simplicity, excellent cosmetic quality, high resolution, high luminance uniformity, and a usable level of image luminance. There are no problems with this approach that cannot be solved with state of the art technology. Although now highly sophisticated technically, a direct laser microstorage system is, in our opinion, a key first step towards new and more cost-effective map production. It should be adaptable and usable in DMA production centers without extensive facility modifications, staff retraining, or capital investment. These considerations aside, the performance of the breadboard direct laser projection system was exceptional and meets all relevant contract requirements except for storage format size. As we believe that a single step format smaller than 70 mm is feasible (35 mm for 22 inch x 30 inch repromats), this limitation is not a major negative factor. Image luminance is adequate for hardcopy reproduction on litho films and electrophotographic pressplates.

3. Most required recording materials are commercially available, practical and useable. As is apparent from a careful study of Section III, this is not an unimportant consideration. In fact, there are several well-qualified recording materials, both silver halide and unconventional, that match requirements for film chip generation, hologram recording, hardcopy reproduction, and pressplates (mainly, electrophotographic). This is in contrast to most optical memory applications in which recording materials are often a limiting factor. However, there is still much to be learned about the handling and processing of these materials. Moreover, in certain cases the relatively poor optical quality of polyester film base will be an important factor.
4. Distortion, measured relative to the hardcopy medium, does not appear to be the problem originally anticipated. That is, it appears that full-scale images, from either a direct or holographic store, can be projected with less than  $\pm 2$  mil rms distortion. The real distortion problem was shown by our experimental work to be caused by dimensional changes of the hardcopy recording material's polyester film base. This is, of course, an unavoidable phenomenon, which we assume has been tolerated of necessity in production centers since the widespread introduction of polyester film base more than a decade ago. It is a fundamental limitation, and can be avoided only by going directly to metal-based pressplates. The important point, however, is that the microreduction and enlargement of graphic information, using either a direct or

holographic approach, does not introduce significant metric distortion. In fact, as the data in Section V show, we can actually minimize overall distortion by careful iterative focusing.

5. All primary contract goals relating to system performance, such as resolution, image luminance, image luminance uniformity, and so forth, probably can be satisfied with the exception of storage format. Fully aware of the quality standards applied to map production and of the limitations of both direct and holographic recorder/reproducers, we conclude that for the near term a 20 mm x 20 mm or smaller storage format is not achievable. A more realistic size goal, which we believe to be fully implementable, is in the 35 mm to 70 mm format range.

We believe our conclusions, which follow from a careful reading of the entire report, are supported by relevant experimental data. They should be evaluated in terms of the scope of the overall contract effort, which is considerably broader than originally intended. In most instances, our conclusions are positive. We hope that techniques or component limitations which in some instances resulted in less than hoped for outcomes will not cause discouragement. It is our opinion that this study, although uncovering several unexpected problem areas, is in its overall context a confirmation of the merit and desirability of the optical microstorage and retrieval of cartographic data.

To obtain maximum benefit from this program and to achieve near term advances in analog cartographic data storage state of the art we recommend the following plan:



1. Make a commitment for the design, fabrication and installation over a 2 to 3 year time frame of a direct laser microreduction enlargement system for test and evaluation in a topographic production center. A complete system could be operational within 1 year, but since there are several sophisticated components which require careful design and fabrication (especially the microreduction enlargement lens) there is some risk associated with a short term implementation. A potential near and long term application of this equipment is for the projection of EBR-generated film chips directly onto pressplates.
2. Continue advanced research and development in promising areas of holography, in particular, Fresnel, Kohler-TIR, incoherent, and Fourier-transform holography, with special emphasis on the optimization of diffraction efficiency, signal-to-noise ratio, image resolution and the minimization of speckle noise, and with the goal of fabricating and evaluating an operational holographic recorder/reproducer. We believe that a holographic approach, because of redundancy, high reduction ratio, defect immunity and high image luminance capability, is ultimately the best technology for high-density cartographic information storage. We concede that there are problem areas. However, it is not possible to conclude on the basis of a single experimental investigation that holography is intractable. We feel that, if properly supported, an operational holographic recorder/reproducer can be developed in about 5 years.

3. Support these programs with baseline study activities important to systems implementation, which should include, but not be limited to, the following:
  - a. Specification and/or design of microreduction lenses
  - b. Copy easel/film holder specification and design
  - c. Symbolology and alignment techniques study
  - d. Design and optimization of laser Kohler illumination systems
  - e. Optimization of film chip generation
  - f. Projection speed pressplate study
  - g. Distortion measurement and compensation study with emphasis on sizing and alignment and effects due to recording material dimensional change
  - h. Systems definition and operational considerations study

Study activities of this type are needed for both the direct and holographic approaches. In most cases, the recommended study areas identify key technology areas that, in our opinion, are not state of the art.

APPENDIX A  
EQUIPMENT TEST PLAN



APPENDIX A  
THE EQUIPMENT TEST PLAN

This Appendix consists of two parts. The first, the proposal for the equipment test plan required for the present study, is an edited version of the form accepted by the COTR on March 31, 1976. The second part is a detailed presentation of the results of and comments on the actual test plan performed from March 31, 1976 to April 2, 1976 and witnessed by Mr. William R. Graver, Mr. John Odell and Mr. Henry Weiner of the U.S. Army Engineering Topographic Laboratories, and by Mr. J. E. Holmes, Ms. L. M. Ralston, Mr. B. R. Reddersen and Dr. R. G. Zech of the Electro-Optics Department of HARRIS Electronic Systems Division (Harris ESD).

APPENDIX A

PART ONE

EQUIPMENT TEST PLAN (NONSYSYEM)

FOR

MICROREDUCTION AND ENLARGEMENT OF  
GRAPHIC INFORMATION STUDY

Contract No. DAAG53-75-C-0155

U.S. ARMY ENGINEERING TOPOGRAPHIC  
LABORATORIES  
FORT BELVOIR, VIRGINIA

W. R. Graver, COR  
Research Institute  
USA-ETL  
Fort Belvoir, Virginia 22060

R. G. Zech, Program Manager  
Electro-Optics Operation  
Harris Corporation  
Melbourne, Florida 32901

## SECTION 1

### PURPOSE AND SCOPE

The purpose of our equipment test plan (ETP) is an evaluation of technical performance relative to program goals and contract requirements. The ETP is designed to demonstrate new technologies, measure technical progress, illustrate problem areas, and provide direction for future efforts as it relates to the storage and retrieval of cartographic information. The scope of the ETP encompasses holographic recording and playback in the display mode, the measurement of image brightness, uniformity, and resolution, hardcopy reproduction, and distortion measurement. In following sections the principal components of the ETP, such as background data, a summary of contract requirements, the testing plan and so forth are discussed in detail.



## SECTION 2

### SUMMARY OF CONTRACT REQUIREMENTS

This section summarizes and abstracts the specific requirements of the contract Statement of Work, which is Section F of Contract No. DAAG53-75-C-0155. These line items are discussed and interpreted in the following section.

1. Design and fabricate one or more breadboard systems with a capability for both display and hardcopy reproduction to demonstrate the microreduction and blowback of different sizes of black and white graphic materials.
2. Derive the mathematical relationships between parameters that affect system performance.
3. Study and define problems involved in designing a full-color microreduction and blowback system.
4. Reduce to a format not to exceed 20.0 mm on a side transparencies of black and white graphic materials such that a set of transparencies is reduced and recorded in a matrix format on a film chip not more than 4 x 6 inches in size.
5. Project full-scale images from the transparencies or their equivalent of the original black and white graphic materials that are available for both visual display and hardcopy.
6. Demonstrate, to be consistent with the reproduction of 3-mil line widths, a minimum capability of displaying and copying the equivalent of 125 cycles/mm for each transparency of a furnished array using Government-supplied USAF resolution target arrays.

7. Produce full-scale hardcopy that deviates in metric fidelity by no more than  $\pm 2$  mils from the full-scale original graphic material.
8. Demonstrate visual displays of graphic inputs with a) a luminance level of 35 footlamberts and b) a luminance variation of less than 25 percent over the display format when a constant nonzero transmittance input is projected.
9. Analyze parameters affecting operation and performance of the breadboard to provide data on the effects of changes to input format, line focal length, recording film, input reduction ratio, and recording film sensitivity.
10. Provide all equipment necessary to demonstrate the full size display of graphic data using stored input produced from Government-supplied transparencies at USA-ETL, Fort Belvoir, VA prior to the completion date of the contract; equipment available at the above facility may be substituted for demonstration purposes.

### SECTION 3

#### ANALYSIS OF CONTRACT REQUIREMENTS

This section defines contract line items that are part of the ETP and discusses the interpretation and exceptions to these contract line items. Specifically excluded from the ETP are Line Items 1, 2, 3, and 9 of Section 5; they will form part of the final technical report. Line Items 4, 5, 6, 7, 8, and 10 define the scope of the ETP; they are discussed below and referenced to Section 5.

##### Item 4

The format specification not to exceed 20.0 mm on a side appears to be an artificial constraint; no fundamental reason for this choice has been identified. Nonetheless, we intended to restrict hologram size to the 20 mm square or smaller format.

The equation governing hologram size is

$$\bar{d} = \frac{\lambda f_T}{d} \quad (A.1)$$

where  $d$  is the hologram length,  $\lambda$  is the recording wavelength,  $f_T$  is the focal length of the Fourier-transform lens, and  $d$  is the finest spatial detail (line width) in the transparency. For 22 x 29 inch and 48 x 60 inch graphics a 3-mil line width yields  $d = 7.62 \mu\text{m}$  (10X reduction) and  $d = 4.12 \mu\text{m}$  (18.5X reduction). With  $\lambda = 0.5145 \mu\text{m}$  and  $f_T = 160 \text{ mm}$ ,  $\bar{d} = 10.8 \text{ mm}$  and  $\bar{d} = 20.0 \text{ mm}$ , respectively. The maximum spatial frequency recorded is proportional to the length of the hologram, which is a low-pass spatial filter. The dimension of 20 mm on a side is chosen to ensure by the sampling theory criterion the reproduction of 3-mil line widths for the greatest reduction ratio. This is true, however, only for a diffraction-limited optical system, and ignores



effects such as aberrations, flare, scatter noise, vignetting, and so forth. Phase errors due to film base nonuniformities are also an important factor, as will be discussed later.

A full set of cartographic transparencies plus test and alignment transparencies can be stored in matrix form on a film chip 4 x 6 inches in size or smaller provided that the total number of holograms is 24 or less and the maximum hologram dimension is 20 mm or smaller. This is a geometric constraint that is independent of recording format. The COR and program manager have agreed that a demonstration of this capability need not be incorporated into the ETP.

#### Item 5

We plan to project full-scale images from selected transparency sets that will be available for both visual display and hardcopy production. There are no problem areas related to this requirement. The precision film holder that forms part of the overall breadboard serves as a display module with the addition of a frosted mylar sheet to the copy platen.

#### Item 6

A minimum resolution requirement of 125 cycles/mm follows from Equation (A.1) if we recognize that the maximum spatial frequency  $\nu_M$  is given by

$$\nu_M = \frac{1}{2d} = \frac{\bar{d}}{2\lambda f_T} \quad (A.2)$$

That is, for a fixed  $\lambda$  and  $f_T$ ,  $\nu_M$  depends only upon  $\bar{d}$ . If the maximum reduction ratio is 18.5X, then  $d = 4.12 \mu\text{m}$  and  $\nu_M = 125 \text{ cycles/mm}$ . (We note that for the 48 x 60 inch repromats the reduction was in consecutive steps of 2X and 10X to give an overall reduction of 20X. This makes  $d = 3.81 \mu\text{m}$  and  $\nu_M \approx 131 \text{ cycles/mm}$ .)

Our analysis assumes that the hologram acts like an ideal low-pass filter. However, a hologram recorded on photographic quality polyester film base does not fit this model. Experimental data show that the maximum resolution for a 20 mm square hologram is 64 cycles/mm for specular laser light and 57 cycles/mm for diffuse laser light. (When the diffuser is rapidly rotated to produce spatially incoherent laser light, the resolution is 162.5 cycles/mm.) Without film base, i.e., using only a 20 mm square aperture, the resolution is 114 cycles/mm and 71.8 cycles/mm, respectively (182.4 cycles/mm for the spinning diffuser). The probable causes of the observed resolution loss are film base phase errors and aberrations generated when the film base intersects the converging laser beam (see Section 2.3 of MPR No. 9); the latter may be the more important cause.

In summary, the resolution requirement can be satisfied by direct blowback with spatially incoherent laser light for microreductions of at least 20X. For holographic recording and blowback the maximum resolution is about 64 cycles/mm, which is satisfactory for microreductions of 10X or less.

#### Item 7

The primary objective of the present effort is to satisfy the distortion specification. As hardcopy reproduction experiments have just begun, we are not in a position to judge the feasibility of reaching this goal. Major concerns are film base phase errors and aberrations. To date an average deviation from metric fidelity of 1.5 mils with a standard deviation of 10 mils has been achieved for direct blowback of a 22 x 29 inch repromat of a grid; this compares favorably with a contact copy of a similar grid made at ETL and measured at E00.

Item 8

Visual displays from holograms that equalled or exceeded contract performance requirements were demonstrated to the COR during his first program review at EOO for 10X repromat blowbacks (see Paragraph 2.4 of MPR No. 2). We expect to repeat this demonstration as part of the ETP for select 10X and 20X blowbacks.

Item 10

We plan to fully comply with this requirement. Equipment required by the COR for both display and hardcopy reproduction will be provided on a temporary basis as needed.



SECTION 4  
OVERALL PLAN

The ETP will consist of two phases. The first phase will be at the Electro-Optics Operation on March 23, 24, and 25, 1976. The second phase will take place at USA-ETL on April 20, 21 and 22, 1976. Each phase will consist of all tests, demonstrations, and deliveries as required by the contract. Details relevant to each phase follow.

The first phase of the ETP at E00 will utilize two modes of visual display and hardcopy reproduction. They are direct blowback with spatially incoherent, monochromatic light and holographic blowback with spatially coherent, monochromatic light. In both cases the light source will be an Argon laser with  $\lambda = 514.5$  nm. The use of two storage and projection techniques will permit the COR to judge their advantages and disadvantages when reduced to practice. Primary emphasis, however, will be on holographic blowback.

The specific tests, measurements, and evaluations that will comprise the ETP at E00 for both read-out modes are the following:

1. Black and white graphic materials will be projected full size from holograms not exceeding 20 mm x 20 mm onto a diffuse screen for visual display and evaluation. The same visual displays will be provided by direct blowback using original 70 mm transparencies. Hardcopy reproductions will be made on Kodak SS7 photographic film.
2. Resolving power will be measured from the full size projection and hardcopy reproduction of an array of Government-supplied USAF resolution targets.

3. Distortion will be measured and analyzed by determining the difference in coordinate values between hardcopy reproductions and the original of a standard master grid. The grid is assumed to be constructed with vertical and horizontal lines having a defined separation of 2 cm center-to-center in both orthogonal dimensions.
4. Luminance of displayed graphic inputs will be measured from the projection of selected graphic inputs.
5. Luminance uniformity will be evaluated by measuring the variation of luminance from center to edge of a constant transmittance graphic input.

The second phase of the ETP at USA-ETL will consist of deliveries and demonstrations specified in the contract and otherwise agreed upon by the COR and Program Manager. Items for delivery are 1) the Government-supplied Wray Micro Lens, 2) Government-supplied transparencies, 3) holograms of Government-supplied transparencies, 4) hardcopy reproductions made from blowbacks of Government-supplied transparencies, and 5) the 4 x 5 foot electrostatic film holder used for hardcopy reproduction. In accordance with Line Item 7 of Section F of the contract, we will provide all equipment necessary to demonstrate the full size display of graphic data. Since USA-ETL has elected to assemble a breadboard configuration similar to that available at E00, this provision is interpreted to mean only special breadboard components need be provided, such as film transparency holder, hologram mount, and Wray Micro Lens positioner, and so forth as is necessary for completion of the USA-ETL breadboard. Visual display of graphic data will be demonstrated

before the extended completion date of the contract, and assistance in breadboard and film holder setup, holographic recording, and hardcopy resources reproduction will be supplied on a level consistent with remaining contract at that time.



## SECTION 5

### TEST METHODS

This section summarizes the test methods to be used for the evaluation of Contract Line Items 4, 5, 6, 7, 8, and 10 which are defined in Section 5 and discussed in Section 6. Although most test procedures are straightforward, distortion measurement requires relatively sophisticated procedures. An outline of test methods follows:

#### Item 4

Visual inspection and measurement with a metric rule will be used to determine that the geometric constraints are satisfied.

#### Item 5

Visual inspection of the recorder/reproducer breadboard and a qualitative evaluation of full-scale projections will be utilized to demonstrate compliance with this requirement.

#### Item 6

Visual inspection of full size projections and hardcopy reproductions of USAF resolution target arrays will be used to determine if the 125 cycle/mm resolving power requirement or its equivalent is satisfied.

#### Item 7

The measurement of the geometric position of approximately 80 vertices on a hardcopy reproduction of a master grid using a Bendix Datagrid Digitizer will be used to measure distortion. The data will be analyzed by means of a computer program that generates data on point-to-point deviations, average deviations, and rms deviations from metric fidelity.

Item 8

Luminance and luminance uniformity of full size projected images will be measured with a Gamma Scientific Model 29 Autophotometer that has been calibrated to provide direct readings in footlamberts for  $\lambda = 514.5 \text{ nm}$ .

Item 10

To be jointly determined by the COR and Program Manager before initiation of the second phase of the ETP.

## SECTION 6

### ACCEPTANCE CRITERIA

This section outlines the basis upon which the requirements of Contract Line Items 4, 5, 6, 7, 8, and 10 of Section 5 are to be judged satisfactory. As this program studied new technologies and methods for the microreduction and blowback of graphic information, some flexibility in their evaluation is justified. This is reflected in the following acceptance criteria:

#### Item 4

All holograms are to be less than or equal to in area a 20 mm x 20 mm square. Six or more holograms are to be recorded on a film chip no greater than 4 x 6 inches in area.

#### Item 5

Full-scale images are to be projected in a manner suitable for both visual inspection and hardcopy reproduction from holographic storage.

#### Item 6

The resolving powers indicated by the full-scale projection of USAF resolution target arrays are to be consistent with the reproduction of 3-mil line widths; for any blowback scaling this implies Rayleigh resolution of the fifth element of Group 3 in the standard USAF resolution target, or 12.8 cycles/mm. An alternative criterion is the well-defined reproduction of all line weights and the resolution of the finest spatial details in all separates in their hardcopy reproduction form. As fidelity and cosmetic quality are critical factors, the second definition is recommended.



Item 7

The vertices of standard 2-cm master grids are to be located geometrically within a circle of radius 2-mils, centered on the vertices of the original master grids, for hardcopy reproductions obtained from full-scale blowbacks.

Item 8

The luminances of selected graphic inputs are to be 35 fL or greater in full-scale projection and as measured in the visual display mode. Scaling based on diffraction efficiency and on available laser power during the testing period may be used to determine an empirical luminance level. Luminance uniformity is to have less than 25 percent variation from the center of a constant transmittance blowback to any edge.

Item 10

Full size visual displays of graphic data are to be demonstrated at USA-ETL before end of contract. The displays are to be characterized by the same properties as those demonstrated at E00.

APPENDIX A

PART TWO

RESULTS OF EQUIPMENT TEST PLAN  
FOR  
MICROREDUCTION AND ENLARGEMENT OF  
GRAPHIC INFORMATION STUDY

Contract No. DAAG53-75-C-0155

U.S. ARMY ENGINEERING TOPOGRAPHIC  
LABORATORIES  
FORT BELVOIR, VIRGINIA

Conducted at  
Electro-Optics Department  
Harris Electronic Systems Division  
Melbourne, Florida 32901

# SECTION 1

## SYSTEM COMMENTS

Because the equipment test plan described below utilizes techniques discussed earlier in this report, those techniques will not be discussed here. For the details of the holographic Kohler illumination scheme used for all holographic recordings in this section and for the theoretical discussions of both the direct and holographic blowback techniques used, see Section II of the main body of the report. A presentation of the experimental parameters of the holographic recording method used throughout the ETP is in Paragraph 4.7.2.



## SECTION 2

### DISTORTION ANALYSIS

In accordance with the methods discussed in Section 5 of this report, holographic distortion analysis was begun using the following procedure:

- a. The hologram of the Ellerslie map series grid transparency is measured with a metric ruler.  
Measured Size: 35 mm width x 35 mm length  
Required Size: less than 20 mm width x 20 mm length
- b. The hologram above is blown back and recorded on Kodak SS7 film on the electrostatic easel.
- c. The film is processed in the Kodak Supermatic 55 Processor at a speed of 3 feet per minute.
- d. Thirteen grid coordinates are measured on the processed film on the Bendix Datagrid Digitizer (R No. 111585).
- e. The grid coordinates are processed in the H-P Model 9830 Computer to calculate distances between each of the grid coordinates.
- f. These distances are processed in the H-P Model 9830 Computer to calculate mean distortion and the standard deviation of the data from the mean when these distances are compared to those of a standard 2-cm grid.
- g. The mean distortion and standard deviation are recorded.
- h. Any mechanical adjustments necessary to bring the system into better alignment than as recorded in g. are made.

- i. Distortion minimization is completed when the standard deviation is  $\leq 0.002$  inch, taking into account a 0.0075-inch distortion due to processing.

Only one blowback turned out to be necessary to reach an acceptable distortion limit; the Bendix Datagrid Digitizer measurements of this grid are recorded in Table A-1. The initial mean distance error was 0.1254 inch, with a standard deviation of 0.0505 inch, but it was possible to scale the measurements using the computer-calculated ratio of 1.0092 between the holographic copy of the grid and the theoretical 2-cm grid. Then the resulting mean distance error was -0.0001 inch with a standard deviation of 0.0068 inch.

In the comments section of the distortion analysis work, B. R. Reddersen noted, that, with an irradiance of  $28.8 \mu\text{W}/\text{cm}^2$  available at the hardcopy easel, an exposure of only 0.25 second was necessary to expose the SS7 hardcopy film properly, for a net exposure of  $7.2 \mu\text{J}/\text{cm}^2$ . W. R. Graver added that the grid exposure was not uniform, resulting in the breaking up of the grid lines and resulting difficulty in viewing the lines when measuring coordinates for the distortion analysis in his opinion this may be due to a nonuniform ratio of the reference intensity to that of the signal in the recording of the hologram.

An additional comment must be added here that, although a 35 mm x 35 mm size was measured on this and all other holograms throughout the ETP, the actual useful area was only 21 mm x 23 mm. This discrepancy, caused by the fact that the signal beam transform is only 21 mm x 23 mm, is easily seen in amplitude holograms of a lesser K-ratio.

The set of holographic blowbacks of the Ellerslie map series was made from the above 21 mm x 23 mm holograms following the completion of this section of the ETP.

Table A-1. Holographic Grid Blowback Coordinate Measurements

Coordinate Number	Theoretical Coordinates (Inches)		Measured Coordinates (Inches)	
	x	y	x	y
1	0.000	0.000	0.000	0.000
2	0.000	8.662	0.003	8.743
3	0.000	17.323	0.011	17.474
4	-74.724	14.173	-4.755	14.312
5	-74.724	4.724	-4.760	4.770
6	-9.449	0.000	-9.528	0.013
7	-9.449	8.662	-9.525	8.759
8	-9.449	17.323	-9.518	17.500
9	-15.748	14.173	-15.877	14.326
10	-15.748	4.724	-15.888	4.781
11	-20.472	0.000	-20.662	0.013
12	-20.472	8.662	-20.650	8.766
13	-20.472	17.323	-20.641	17.505



### SECTION 3

#### RESOLUTION TARGET MEASUREMENTS

An analysis of the present system's resolution capabilities, both from holographic and direct blowbacks, was accomplished using the procedure below:

- a. Examination of the furnished resolution target 70 mm transparency.

The resolution target transparency furnished by USA-ETL is examined with the Leitz microscope R No. 223295 and the smallest resolvable group for each target is recorded. The number key for the targets is in Figure A-1.

- b. Examination of the resolution target blowback from the transparency.

The resolution target of a. is placed in the transparency holder and blown back up to approximately a 10X magnification and the smallest resolvable group for each target recorded in Table A-2.

- c. Examination of the resolution target blowback from the hologram.

1. The size of the hologram of the resolution target is measured with a metric ruler.

Measured Size: 35 mm width by 35 mm length

Required Size: Less than 20 mm width x 20 mm length

2. The hologram is reconstructed and blown back up to approximately a 10X magnification and the smallest resolvable group for each target recorded in the table below.

3. A full scale hardcopy of the holographic blowback is made on the electrostatic easel and processed in the Kodak Supermatic 55 Processor at a speed of 3 feet/minute.
4. The smallest resolvable target for each group on the hardcopy is recorded in the table below.

Both B. R. Reddersen and W. R. Graver agreed in the comments section that speckle produced major problems and that the overall signal-to-noise ratio of the holographic blowback was poor.

To analyze these results, it should be remembered that the actual useful hologram size was only 21 mm x 23 mm, as mentioned at the end of the distortion analysis portion of the ETP. Then the limiting resolution of transparency under microscopic examination must be considered: the resolution varies from an equivalent resolution of 80 cycles/mm up to 285 cycles/mm. Nevertheless, the throughput resolution, done coherently with Kohler illumination of the sort used to record the hologram, is almost a factor of two better than the holographic blowback. With a lower hologram exposure and a better resolution target transparency, however, it can be shown that a hologram of only 20 mm x 20 mm can produce the same resolution as a coherent throughput, and that both resolutions are considerably better than in this section of the ETP (see Paragraph 4-4 for a more complete evaluation of the present system's resolution capabilities).

Table A-2. Resolution Target Measurements

	Target No.								
	1	2	3	4	5	6	7	8	9
2a) Microscopic transparency evaluation: smallest group	3-6	4-6	3-1	3-6	4-3	4-4	4-5	4-3	3-1
2a) Microscopic transparency evaluation: resolution in cycles/mm	14.3	28.5	8.0	14.3	20.2	22.7	25.7	20.2	8.0
2b) Transparency blowback: smallest resolvable group	2-2	2-3	2-6	2-6	3-1	2-2	2-5	1-6	1-3
2b) Transparency blowback: resolution in cycles/mm	4.49	5.05	7.12	7.12	8.0	4.49	6.37	3.57	2.52
2c) ii. Hologram blowback: smallest resolvable group	1-1	1-1	1-6	1-6	1-6	1-2	1-6	0-3	1-1
2c) ii. Hologram blowback: resolution in cycles/mm	2.00	2.00	3.57	3.57	3.57	2.24	3.57	1.26	2.00
2c) iii. Hologram hardcopy smallest resolvable group	0-3	1-2	1-3	1-6	1-6	1-5	1-4	0-4	0-3
2c) iii. Hologram hardcopy: resolution in cycles/mm	1.26	2.24	2.52	3.57	3.57	3.18	2.88	1.41	1.26



## SECTION 4

### DISPLAYS

Black and white graphics from the Ellerslie map series of holograms were blown back for visual inspection to demonstrate the overall performance of the system in reproducing all the various kinds of graphics normally recorded as color separates. In addition, an experimental evaluation of the resolution capabilities of the system was performed using the Kohler illumination system for direct blowback, with the diffuser imaged on the aperture stop of the microreduction/enlargement lens, and using the holographic Kohler illumination method, in which the diffuser is imaged on the hologram plane. Single-wavelength and multiple wavelength illumination schemes were also compared in this study. The resulting data are recorded in Table A-3.

The main result of this analysis, as mentioned by B. R. Reddersen in the ETP comments, is that the switch from the Kohler illumination condition for holography to that for direct blowback results in great increase in resolution. Though the data does not show it here, it has also been demonstrated in Paragraph 4.7 of the main body of this report that the use of two wavelengths for hardcopy substantially reduces speckle while increasing image resolution in both coherent direct and holographic blowbacks.

Table A-3. Additional Resolution Target Measurements

CASE	Target No. From Resolution Target								
	1	2	3	4	5	6	7	8	9
a. Microscopic examination of resolution target array	3-6	4-6	3-1	3-6	4-3	4-4	4-5	4-3	3-1
b. Throughput coherent blowback, non-Kohler*	2-2	2-3	2-6	2-6	3-1	2-2	2-5	1-6	1-3
c. Holographic blowback*	1-1	1-1	1-6	1-6	1-6	1-2	1-6	0-3	1-1
d. Incoherent blowback, Kohler, multiwavelength		3-5	2-6		3-6				
e. Coherent blowback, Kohler, multiwavelength		2-6	2-5		3-4				
f. Hardcopy of d. (4880 Å and 5145 Å)					3-6				
g. Hardcopy of e. (4880 Å and 5145 Å)					3-3				
h. Coherent hardcopy from hologram, non-Kohler*	0-3	1-2	1-3	1-6	1-6	1-5	1-4	0-4	0-3
i. Throughput coherent blowback hardcopy, Kohler									
4880 Å					3-3				
5145 Å					3-3				
j. Throughput incoherent blowback hardcopy Kohler									
4880 Å					3-4				
5145 Å					3-6				

\*The diffuser was image on the hologram plane.

## SECTION 5

### LUMINANCE

A number of the Eilerslie map series transparencies and their 35 mm x 35 mm holograms were blown back to about a 10X magnification. At that point the Gamma Scientific Autophotometer Model 2900 (R No. 111639) and its related equipment (Acc. Photomultiplier, R No. 111640; Photometric Lens, R No. 222441; Scanning Eyepiece, R No. 111744) were used to measure the photometric intensities of the blowback images. The results of these measurements are recorded in Table A-4.

Several results are significant here. First of all, for approximately 30 mW of 5145 Å power available from the argon-ion laser used for these experiments, even the vegetation transparency hologram, made from a transparency with large open areas, had a range of luminance from 15.5 to 19.7 footlamberts in the three measurements taken. With additional laser power the required 35 footlamberts would be very easy to achieve. Secondly, as the intensity transmission of the transparencies goes down, the luminance goes up, as expected; for a given diffraction efficiency, the smaller the amount of clear area in a transparency, the higher the intensity in any section of the holographic blowback. Thus, the vegetation chip, with an estimated transmittance of ~40 percent, will have a markedly lower holographic intensity than that for the culture transparency (with a transmittance of ~1.4 percent), or the open water transparency (with  $I_t = \sim 1.5$  percent). Finally, there appears to be a uniform drop by a factor of six-to-eight in the signal-to-noise ratio of the throughput, blownback under the holographic Kohler condition, when compared to the holographic image.



Table A-4. Luminance Measurements

Ellerslie Chip or Hologram Subject	Intensity Transmittance of the Chip	Throughput Luminance (Footlamberts)		Holographic Blowback Luminance (Footlamberts)		Comments
		Signal	Background	Signal	Background	
Vegetation	27.5%	--	--	19.5 ± 0.6	5.8 ± 0.3	Measured in Corner 5145 Å <sup>0</sup> Reference Beam Only
Vegetation	27.5%	8.5 ± 0.3	0.49 ± 0.01	15.5 ± 0.5	5.4 ± 0.2	5145 Å <sup>0</sup> and 4880 Å <sup>0</sup> for Throughput 5145 Å <sup>0</sup> Reference Beam Only
Culture	1.1%	5.6 ± 0.2	0.104 ± 0.004	>150	16.0 ± 1	5145 Å <sup>0</sup> Throughput Beam Only 5145 Å <sup>0</sup> Reference Beam Only
Open Water	0.55%	7.8 ± 0.3	0.085 ± 0.005	>165	14. ± 1	5145 Å <sup>0</sup> Throughput Beam Only 5145 Å <sup>0</sup> Reference Beam Only
Vegetation	27.5%	--	--	19.7 ± 0.5	4.4 ± 0.1	5145 Å <sup>0</sup> Throughput Beam Only 5145 Å <sup>0</sup> Reference Beam Only
Clear Signal	100%	7.5 ± 0.4	--	--	--	

## SECTION 6

### UNIFORMITY

The vegetation transparency and its accompanying hologram were used along with a clear throughput (the "without chip" case of the uniformity data which follows) to provide blowbacks for uniformity measurements.

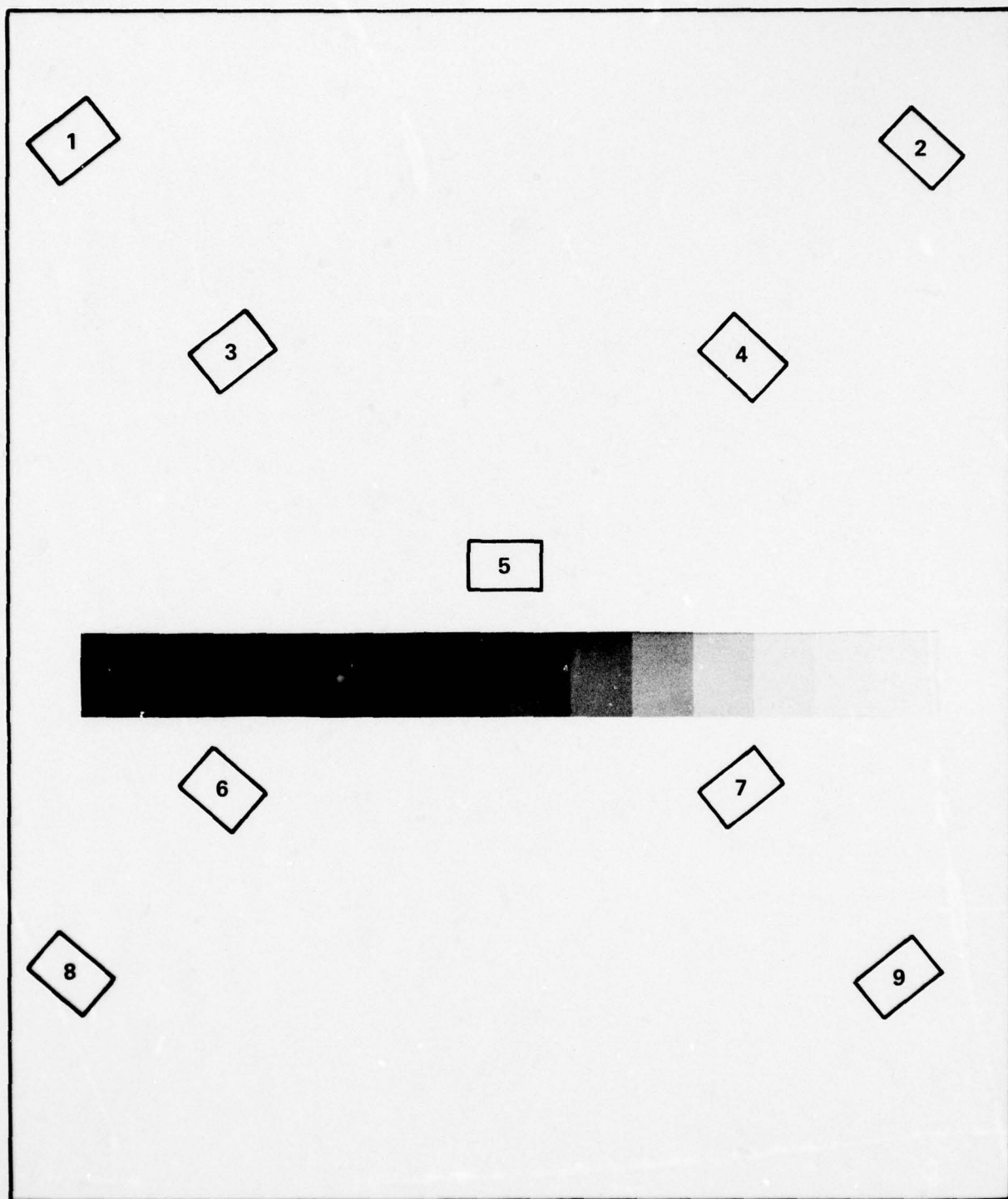
By using pieces of tape to mark the measurement locations each time, accuracy of positioning of the CR-212 power meter head was maintained to  $\pm 0.125$  inch. Data was read off from left to right and from top to bottom as recorded in Table A-5.

As the two sets of measurements of the holographic blowback show to some extent, the repeatability of the uniformity measurements was not good. During the test plan there was some difficulty in maintaining reference beam stability and uniformity, which in turn affects the blowback uniformity; this instability, as W. R. Graver mentioned in the comments section, may be due to problems with the Argon-Ion laser's pointing stability. The large increase in intensity at measurement location No. 3, as B. R. Reddersen noted in the comments, appears related to the large dark area near it. With a more uniform transform of the signal, the diffraction efficiency of the hologram would be uniformly spread across the image; as is, all the diffraction efficiency of the dark corner pours into the nearest "light" area, that of measurement area 3. Nevertheless, all the standard deviations whether from a clear signal, the vegetation throughput, or the vegetation holographic blowback measurements, are within 16.2 percent of the mean. In addition, as the holographic blowback set has shown, all the nonuniformities are within the contrast tolerance of the SS7 hardcopy film used to record the blowbacks.

Table A-5. Relative Intensities

Aperture No.	Throughput Intensity		Holographic Intensity	
	With Chip	Without Chip	Measurement No. 1	Measurement No. 2
1. Bottom	4.3	3.0	5.8	4.1
2. Bottom	4.5	2.9	5.2	3.5
3. Bottom	4.1	2.9	7.5	4.9
4. Center	4.1	2.8	5.5	3.1
5. Center	4.9	3.2	5.3	3.0
6. Center	4.3	2.9	5.3	3.8
7. Top	4.2	2.8	5.7	4.2
8. Top	4.3	2.8	5.2	3.6
9. Top	4.4	2.8	4.9	3.4
Mean	4.34	2.9	5.6	3.7
Percent change to worst variation from mean	12.9% at 4.9	10.3% at 3.2	33.9% at 7.5	32.4% at 4.9
Standard dev. from mean	0.25	0.13	0.76	0.60
Standard dev. as a percent of mean	5.65%	4.5%	13.6%	16.2%





89136-3

Figure A-1. Resolution Target Numbering Diagram

AD-A051 532

HARRIS CORP MELBOURNE FL ELECTRO-OPTICS DEPT  
MICRO-REDUCTION AND ENLARGEMENT OF GRAPHIC INFORMATION STUDY (M--ETC(U)  
DEC 77 R G ZECH, L M RALSTON, B R REDDERSEN DAA653-75-C-0155  
HESD/EOD-1624-F ETL-0063 NL

UNCLASSIFIED

5 OF 5

AD  
A051 532



END

DATE

FILMED

4-78

DDC

APPENDIX B  
SELECTED TECHNICAL REFERENCES



# Design Relationships for Holographic Memories

A. Vander Lugt

The maximum capacity of a block-oriented, random-access memory is determined primarily by the geometrical parameters of the lenses required to create a Fourier transform of a spatial bit pattern and to image the reconstructed bits onto a photodetector array. Furthermore, the maximum packing density is determined primarily by the same parameters. Several important relationships are developed that are useful in the preliminary design of holographic memories.

## I. Introduction

One important application of holography is data storage and retrieval. Holography offers the features of high storage densities, ease of readin and readout of data, a natural encoding phenomenon that makes the recorded hologram less sensitive to dust, scratches, and blemishes, reduced tolerances to mechanical motion, and so forth. The design of holographic systems useful for document storage and retrieval, random-access, block-oriented memories, or wideband recorders has generally been on an *ad hoc* basis. In this paper we show how the preliminary design of holographic memories for storing digital data can be made, based on some fundamental parameters of the major components of the system.

The major components of holographic memories are (1) a coherent light source; (2) a page composer (PC) that spatially modulates the coherent light with the data to be stored; (3) a hologram storage medium that may be partitioned into an array of hologram storage locations; (4) a device for deflecting both the signal and reference beams to a particular storage location in the hologram array and for addressing the holograms upon readout; (5) a photodetector array (PDA) for converting optical signals to electrical signals; and (6) optical elements such as lenses that are used to create the desired light distributions at various planes in the system. Some holographic memories may contain all the named components; others may contain only some of them. In this paper we concentrate on how the performance parameters of these components are related.

## II. Random Access Memories

The first holographic memory system we consider is a block-oriented, random-access memory that con-

tains all the components mentioned above; an analysis of such a memory most clearly illustrates the important relationships. If we want fast and equal access to all parts of the memory, the storage material must remain stationary; access to each stored hologram is then achieved by means of a deflection system. The basic elements of such a system are shown in Fig. 1. The electronic digital data are converted to an optical signal by a page composer (PC) that spatially modulates a coherent beam of light. The number of elements  $N$  in each direction determines the size of the page of data to be stored at each hologram location. The length of each element is  $d$ , and the ratio of the center spacing to the bit length is  $c$ . The parameters  $N$ ,  $c$ , and  $d$  completely specify the geometry of the page composer.

The light diffracted by the PC is collected by a lens and concentrated in a small region at the plane of the storage material as either a Fresnel or Fourier transform of the bit pattern. (Random phase shifters can also be used in conjunction with the page composer to reduce the dynamic range of the light distribution at the hologram plane.<sup>1,2</sup>) The light is added to a reference beam so that, after exposure and development, one element of the hologram array containing  $N^2$  bits of data is formed; the process is repeated by deflecting both the signal beam and the reference beam to each of  $N \times N$  storage locations. The length of each hologram is  $\bar{d}$ , and the ratio of the center spacing to the hologram length is  $\bar{c}$ . The parameters  $N$ ,  $\bar{c}$ , and  $\bar{d}$  completely specify the geometry of the hologram array.

In addition to creating a light distribution at plane  $P_2$  that is stored in the hologram array, the lens can be arranged to create an image of the PC at the plane of a photodetector array (PDA). The PDA must also contain  $N \times N$  photodetector elements, but the detector size and center spacing ratio may be different from those of the PC. The lens system may, therefore, have to be arranged to produce a lateral magnification  $M$  between planes  $P_1$  and  $P_3$ .

The author is with Harris Electro-Optics Center, P.O. Box 1084, Ann Arbor, Michigan 48106.

Received 20 February 1973.

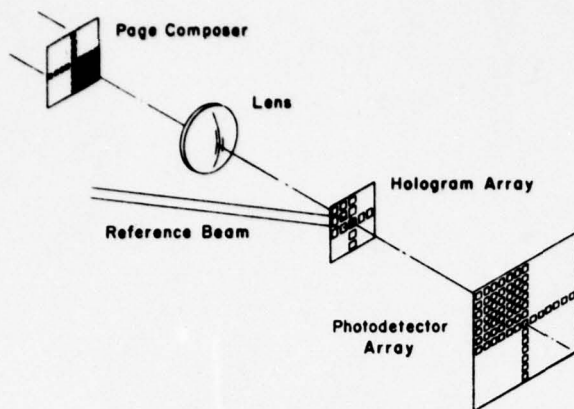


Fig. 1. Basic elements of a block-oriented, random-access holographic memory.

### A. Single Lens System

We begin the analysis by considering the geometrical relationships that must be satisfied by the PC, the lens system, the hologram array, and the PDA. We first derive the relationships for a single lens system and then expand the analysis to cover multi-lens systems. Figure 2 shows a plan view of the signal beam of the memory. We consider first a situation where the individual elements in the PC contribute light to every region of the hologram array; later we shall consider a situation where the angle of the illumination is varied to direct the signal beam to each hologram location.

The PC is placed in plane  $P_1$ , which is a distance  $l_1$  from the first principal plane of a lens having power  $K$  and an aperture ratio  $R$ . The power of a lens is the inverse focal length of the lens and the aperture ratio is the ratio of the clear diameter to the focal length of the lens. The PC is illuminated by a plane wave of monochromatic light located at  $l_1 = -\infty$ . The geometrical relationships among the various components can be established by tracing the

principal pupil ray (PPR) and the principal marginal ray (PMR) through the system. In Fig. 2, the distances and angles associated with the PPR have an overbar, e.g., the angle of the PPR is denoted by  $\bar{u}_1$ .

The aperture ratio  $R$  of the lens is given by

$$R = 2[|h| + |\bar{h}|]K, \quad (1)$$

where  $h$  and  $\bar{h}$  are the intersection heights of the PMR and the PPR at the lens. The value  $h$  indicates the minimum aperture needed to resolve an element located on the optical axis. The lens diameter must be increased by an amount  $\bar{h}$  so that elements at the edge of the PC are also resolved. Since the illumination is a plane wave propagating parallel to the optical axis, we have that  $\bar{u}_1 = 0$  and  $\bar{h} = (\sqrt{2}/2)[(N-1)cd + d]$ , but since  $N$  is large for any practical memory, we have

$$\bar{h} = \sqrt{2}Ncd/2, \quad (2)$$

where the  $\sqrt{2}$  factor accounts for the length of the diagonal of the PC relative to the length of its side. The lens aperture could be more efficiently used if the elements in the PC filled a circular region whose diameter is equal to the diagonal of the square. The gain in the number of bits that could be stored in each hologram, with no changes in the requirements on the lens, is a factor of  $\pi/2$ . Unfortunately, this format leads to a much less attractive method for loading the PC and is not consistent with the formats of available photodetector arrays. The formula for  $h$  can be most easily derived by considering the PMR angle in the image space. We have that  $h = u_2 l_2$  and that

$$u_2 = \sqrt{2Ncd}/[2(l_2 - \bar{l}_2)]. \quad (3)$$

Again, the total length of the hologram array is  $\sqrt{2}[(N-1)cd + d]$ , but since  $N$  is also large in a practical memory, Eq. (3) is a good approximation to the actual value of  $u_2$ . Since the memory must be op-

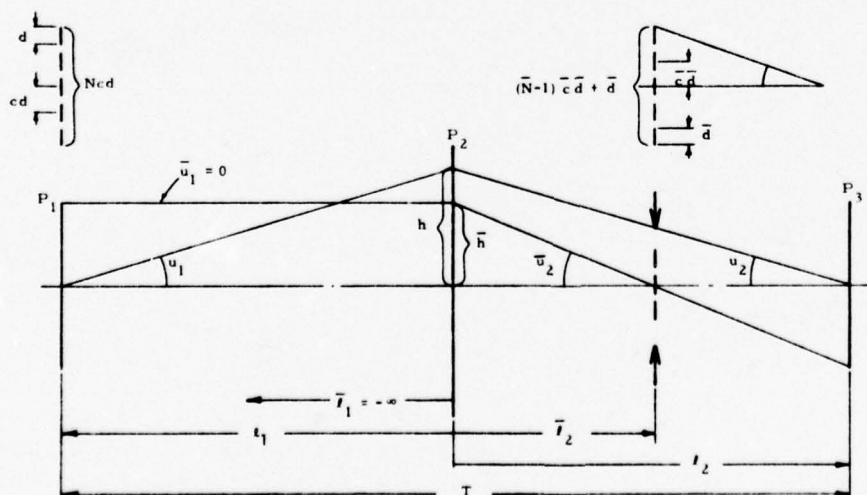


Fig. 2. Plan view of the signal beam.

erated in a space invariant mode (i.e., each bit in the BDC contributes light to each element of the hologram array), the hologram array must be placed at the exit pupil of the lens system. Since the entrance pupil is at  $l_1 = -\infty$ , the exit pupil is located at the back focal plane of the lens, i.e.,  $l_2 = 1/K$ . We can also write  $l_2$  in terms of  $K$  by introducing the magnification  $M$ :

$$l_2 = (1 - M)/K. \quad (4)$$

The value of  $h$  is then

$$h = u_2 l_2 = [\sqrt{2N\bar{c}\bar{d}}(M - 1)]/2M, \quad (5)$$

so that

$$R = 2 \left\{ \left| \frac{\sqrt{2Ncd}}{2} \right| + \left| \frac{\sqrt{2N\bar{c}\bar{d}}(M - 1)}{2M} \right| \right\} K. \quad (6)$$

The absolute value signs can be removed from the first term of Eq. (6) because  $Ncd$  is always a positive quantity. Similarly,  $N\bar{c}\bar{d}$  is a positive quantity so that

$$R = \sqrt{2Ncd}K + \sqrt{2N\bar{c}\bar{d}}K \left| \frac{M - 1}{M} \right|. \quad (7)$$

Note that if we let  $R_p = \sqrt{2Ncd}K$  and  $R_H = \sqrt{2N\bar{c}\bar{d}}K$  be the aperture ratios of the block data composer and the hologram array, Eq. (7) becomes

$$R = R_p + R_H \left| \frac{M - 1}{M} \right|. \quad (8)$$

The total capacity of the memory is  $Q^2$ , where  $Q = NN$ . By solving Eq. (7) for  $Q$ , we have

$$Q = (R - \sqrt{2Ncd}K) \frac{N}{\sqrt{2\bar{c}\bar{d}}K} \left| \frac{M}{M - 1} \right|. \quad (9)$$

We can now find the maximum value of  $Q$  with respect to any one of the parameters associated with the PC or the hologram array. We choose to use  $N$  as the appropriate parameter and find the maximum capacity by solving the equation  $\partial Q / \partial N = 0$ :

$$\frac{\partial Q}{\partial N} = \left| \frac{M}{M - 1} \right| \frac{1}{\sqrt{2\bar{c}\bar{d}}K} (R - 2\sqrt{2Ncd}K) = 0$$

or

$$R = 2\sqrt{2Ncd}K. \quad (10)$$

But, since  $R_p = \sqrt{2Ncd}K$ , we also see that  $R = 2R_p$  maximizes the capacity of the system. By substituting Eq. (10) into Eq. (9) we find that

$$Q_{\max} = \left( R^2 \left| \frac{M}{M - 1} \right| \right) / (8cd\bar{c}\bar{d}K^2). \quad (11)$$

The length  $\bar{d}$  of each hologram in the array is related to the spacing  $cd$  of each element in the PC by

$$\bar{d} = 2\lambda / cdK, \quad (12)$$

where  $\lambda$  is the wavelength of light and the factor 2 indicates that the bits are double Rayleigh resolved. Furthermore, Eq. (12) indicates that the product  $cd$  is the important parameter of the PC that determines the hologram size. For example, we may wish to illuminate the PC with an  $N \times N$  matrix of lenses so that  $d$  is very small. In this arrangement, each element of the PC contributes light to each region of the hologram array. The reconstructed bit pattern is therefore free of the speckle pattern caused by a diffuser at the PC. The required resolution at the plane of the PDA is, however, always determined by the product  $cd$ .

If we substitute Eq. (12) into Eq. (11), we find that

$$Q_{\max} = \left( R^2 \left| \frac{M}{M - 1} \right| \right) / (16\bar{c}\lambda K). \quad (13)$$

Equation (13) reveals that the maximum capacity of this system is not dependent, in the first instance, on the parameters  $N$ ,  $d$ ,  $\bar{N}$ , or  $\bar{d}$ . Instead, the capacity is determined solely by the parameters associated with the lens system. To achieve a high capacity, we want to choose a lens having a large relative aperture and a long focal length and arrange the system to give a large magnification.

The linear packing density  $\rho$  for the system shown in Fig. 2 is

$$\rho = N/\bar{d}, \quad (14)$$

and, if we substitute Eq. (12) into Eq. (14) we have

$$\begin{aligned} \rho &= NcdK/2\lambda \\ \rho &= R/4\sqrt{2\lambda} = R_p/2\sqrt{2\lambda}. \end{aligned} \quad (15)$$

We see, therefore, that the maximum packing density that can be achieved is dependent on only the aperture ratio of the PC and the wavelength of light.

The implications of Eqs. (13) and (15) are considerable. The first conclusion is that, even if we have a storage material that can store a given number of bits/cm<sup>2</sup> and produce a given SNR, the capacity of the memory cannot be made arbitrarily large simply by increasing the area of the hologram array. In fact, it may not be possible to even achieve (optically) the packing density that the storage material can support except through the use of superposition of several holograms at each storage location. Second, we see that increasing the number of bits in the PC or the number of holograms in the array does not increase the total system capacity for a given lens system. In Fig. 3 we plot the value of  $Q$  as a function of  $N$ , with  $cd$  as a parameter, for some assumed values of  $R$ ,  $M$ ,  $K$ ,  $\bar{c}$ , and  $\lambda$ . The value of  $R$  is chosen to be 0.5 (corresponding to an  $f/2$  lens). If  $R$  is much less than 0.5, the total capacity is reduced. A value of  $R = 0.5$  gives an area packing density, for  $\lambda = 500$  nm, of about  $3(10^6)$  bits/cm<sup>2</sup>. A good record-



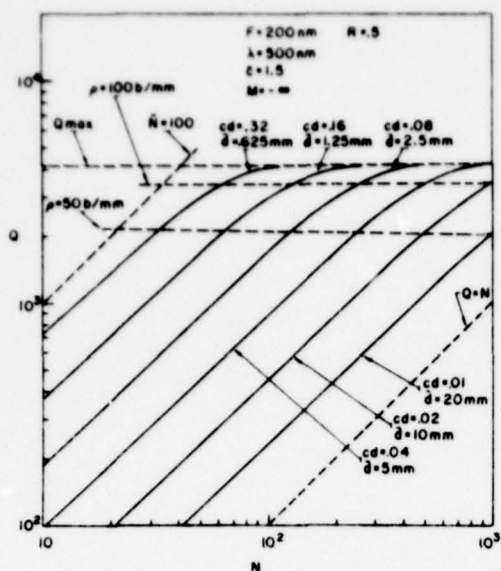


Fig. 3. Memory capacity as a function of the number of bits in the block data composer.

ing material is required at this packing density to achieve a SNR of 20 dB. Therefore, a value of  $R$  greater than 0.5 may not be useful. The value of  $M$  is set at  $-\infty$ , which implies that a second lens is needed to bring the reconstructed bit pattern to focus at a finite conjugate plane. If this lens is placed one focal length to the right of plane  $P_2$ , its aperture ratio must be equal to that of the first lens, and its focal length is chosen to give the required over-all magnification. In this manner the value of  $|M/(M-1)|$  reaches its maximum value of 1, and the system reaches its absolute maximum capacity. The value of  $c$  is set at 1.5 and is based on practical considerations governing the spacings of the holograms, and  $\lambda$  is set equal to 500 nm. The value of  $K$  is chosen, by way of example as  $0.005 \text{ mm}^{-1}$  to correspond to a 200-mm focal length lens. Since the values of all the other parameters are either fixed or cannot be varied significantly,  $K$  can be used as a scaling parameter for  $Q$ .

Also shown on the graph are dotted lines that represent bounds on the permissible solutions. If  $N = Q$ , the memory consists of a single hologram. Similarly, if  $\bar{N} = Q$  the PC is a single element; both extremes are unattractive in practice. If  $cd$  is too small, the BDC may be difficult to fabricate; if  $cd$  is too large, the hologram size may be too small. Thus, we are free to choose one of the four remaining parameters ( $N$ ,  $\bar{N}$ ,  $cd$ , or  $d$ ) to satisfy a side consideration; the values of the remaining three parameters are then fixed by the established relationships. Two dotted lines are also shown for  $\rho = 100 \text{ bits/mm}$  and  $\rho = 50 \text{ bits/mm}$ .

Equation (13) shows that the maximum capacity of the system varies inversely as the power of the lens (i.e., directly as the focal length of the lens). It

is therefore necessary to use a long focal length lens to achieve a large capacity memory. But since the capacity is even more strongly dependent on the aperture ratio, we want to maximize  $R$  without exceeding the practical limit. As the capacity increases, the physical aperture of the lens becomes very large.

From Eq. (8) we note that if  $M = -\infty$ , the aperture of the lens is equal to the sum of the diagonals of the PC and the hologram array. Furthermore, Eq. (10) indicates that when the capacity is maximized with respect to  $N$ , the two diagonals are equal in length. The system capacity could also have been maximized with respect to  $N$ ,  $d$ , or  $cd$ ; exactly the same relationships arise as can be shown by partially differentiating Eq. (9) with respect to each of the other parameters. Thus, one-half of the aperture of the lens is required to create the axial hologram, and the other half is required to form the holograms for the off-axis hologram locations. This is the basic reason why the same relationships hold whether the signal beam is directed to each hologram location or, as analyzed here, each element of the PC contributes light to all hologram locations. The proof of this statement is straightforward and can be shown by a similar line of analysis.

If we can find a way to reduce the aperture of the lens so that it is equal in length to the diagonal of the PC or the hologram array, we would expect to find that the requirements on the lens (for a given capacity) would be reduced. In a previous paper an analogous consideration was applied to optical data processing systems.<sup>3</sup> The key concept is to use more than one lens in the signal beam of the system. One lens is located near the PC to create the holograms, and one lens is located near the hologram array to image the reconstructed waveforms.

## B. Multiple Lens Systems

Figure 4 shows a plan view of a multiple lens system. The parameters associated with the PC, the hologram array, and the PDA have the same meaning as before. If we assume that  $L_1$  and  $L_2$  are thin lenses and that planes  $P_1$  and  $P_2$  are coincident with the principal planes of these lenses, we have

$$R_1 = \sqrt{2NcdK_1} \quad (16)$$

and

$$R_2 = \sqrt{2\bar{N}c\bar{d}K_2} \quad (17)$$

If we form the sum of  $R_1$  and  $R_2$ , we have

$$R_1 + R_2 = \sqrt{2NcdK_1} + \sqrt{2\bar{N}c\bar{d}K_2} \quad (18)$$

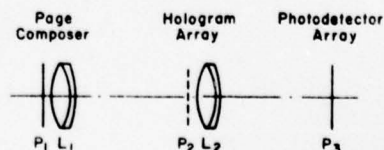


Fig. 4. Multiple-lens memory system.

which is similar to Eq. (7), except that the magnification factor is determined by the ratio of  $K_1$  to  $K_2$ . We also have

$$\bar{d} = 2\lambda/cdK_1 \quad (19)$$

and

$$\rho = N/\bar{d} = R_1/2\sqrt{2}\lambda. \quad (20)$$

From Eq. (20) we immediately note that the linear packing density is increased by a factor of 2 for the same aperture ratio of the first lens; the area packing density is therefore increased by a factor of 4. But since  $R_1 = R_P$  in this case, Eq. (20) basically reduces to Eq. (15).

If we solve Eq. (18) for  $Q$  and again maximize  $Q$  with respect to  $N$  (or any of the other three parameters), we find that

$$Q_{\max} = [(R_1 + R_2)^2]/(16\bar{c}\lambda K_2). \quad (21)$$

Equation (21) is similar to Eq. (13) except that the magnification does not appear explicitly. This means that the two-lens system permits more flexibility in choosing suitable PDA's to match practical PC parameters.

An alternative and somewhat simpler way to derive the capacity of the two-lens memory is to form the product  $R_1R_2$ :

$$R_1R_2 = 2N\bar{N}cd\bar{c}dK_1K_2. \quad (22)$$

By using the fact that  $Q = N\bar{N}$  and by using Eq. (18), we have

$$Q = (R_1R_2)/(4\lambda\bar{c}K_2). \quad (23)$$

as the capacity of the memory. If we set Eq. (23) equal to  $Q_{\max}$  as given by Eq. (21),  $R_2$  must equal  $R_1$  to achieve the maximum memory capacity. But since  $R_2 = R_H$  and  $R_1 = R_P$ , the same fundamental constraints are placed on the memory capacity by the optics. Takeda,<sup>2</sup> Mikaeliane *et al.*,<sup>4</sup> and Graf and Lang<sup>5</sup> use the first part of the optical system shown in Fig. 4 to derive similar results, but they do not show how the bits are imaged onto a PDA. Their results generally lead to an over-stated total memory capacity.

### C. Comments on the Lens Design

In the previous two sections the focal lengths and the aperture ratios of the lenses were used to develop some important restrictions on the capacity of the system. In both instances the lenses were assumed to be thin. In a practical design, each lens will become a multielement thick lens (including some negative elements to keep the sum of the powers small). If the focal length is kept fixed, distributing the elements along the axis has the effect of making the aperture ratio of each element less than that of the lens as a whole. Thus, the fabrication of a  $f/2$  lens having a large aperture becomes less difficult.

In fact, when the lenses are thickened, the difference between the single lens system and the multi-lens system becomes much less apparent. In each case the packing density is determined by the aperture ratio of the PC ( $R_P$ ). If each system is optimized for maximum capacity and if  $M = -\infty$  in the single lens case, we have that  $R = R_P + R_H = R_1 + R_2$  so that Eqs. (13) and (21) are identical. The most important conclusion to be reached, however, is that the optical design may well be the most important consideration for block-oriented, random-access memories.

It is worthwhile to review the steps to be taken in the preliminary design of a block-oriented, random-access memory. From the users viewpoint the most important memory parameters are the (1) total capacity, (2) the error rate, (3) the random access time, and (4) the input and output rates. Of these parameters, only the first two impact directly on the geometrical properties of the memory. Lee has shown that the error rate of a holographic memory is dependent on the signal-to-noise ratio (SNR) that can be produced by the recording material.<sup>6</sup> He has also shown that the SNR is given by

$$\text{SNR} \propto (DE/\phi\rho^2), \quad (24)$$

where  $DE$  is the diffraction efficiency,  $\phi$  is the Weiner spectrum of the storage material, and  $\rho^2$  is the area packing density. If the storage material is selected on the basis of exposure sensitivity, diffraction efficiency, or other characteristics, we can determine  $\rho^2$  from (24) for the SNR required to give the appropriate error rate.

The design guidelines will be given with respect to the relationships developed for the single lens memory with  $M = -\infty$ ; a similar procedure holds for the two-lens system. Using the value of  $\rho$  as established by (24) we solve Eq. (15) for  $R$ . If  $R$  is greater than 0.5, we may want to limit its value to keep the lens aberrations under control. In this case, a different storage material may be desirable, for example, one with a higher sensitivity and a correspondingly higher Weiner spectrum. If  $R$  is less than 0.5, we solve Eq. (13) for the value of  $K$  that gives the desired memory capacity.

The next step is to determine a value for  $N$ ,  $\bar{N}$ ,  $\bar{d}$ , or  $cd$ . Any one of these parameters may be set by fabrication considerations or by the performance of the deflector system. The best guideline is usually Eq. (14), which states that the linear packing density is also equal to  $N/\bar{d}$ . The maximum value of  $\bar{d}$  is often determined by the aberrations introduced by the substrate of the storage material, and the minimum value of  $\bar{d}$  is determined by the desired immunity of the holograms to dust, scratches, and blemishes, as well as by the characteristics of the reference and signal beam deflection systems. For  $R = 0.5$  and  $\lambda = 500$  nm, we find that  $\rho = 176.8$  bits/mm. If  $\bar{d} = 1$  mm, the number of bits in the PC may be too large; we see therefore that  $\bar{d}$  will be of the order of 0.7 mm, which is a reasonable compro-



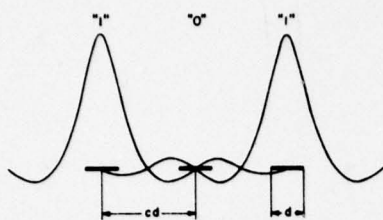


Fig. 5. PDA geometry related to reconstructed bit geometry.

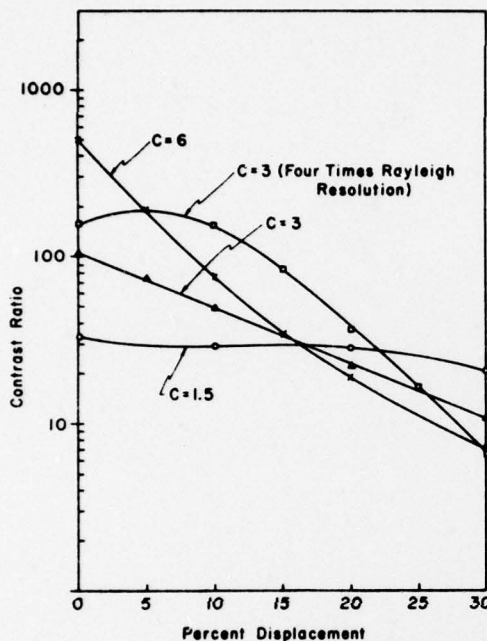


Fig. 6. Contrast ratio as a function of bit displacement for uniform illumination.

mise between the maximum and minimum values established by aberrations and blemishes.

#### D. Optical Design Considerations

In Secs. II.A and II.B we derived relationships between the major components based on Gaussian optics. In the actual design of the lenses, we must set tolerances on the accuracy of the bit locations at the PDA plane, the accuracy of the hologram location, and on the amount of phase error in the hologram recording medium. The tolerance on the bit location is dependent on the illumination of the hologram, on the size of the hologram relative to the bit size, and on the photodetector spacing ratio.

In Fig. 5 we show the relationship between the light distribution for a reconstructed bit pattern (101) to the photodetector geometry. The light representing each bit is a sinc  $x$  function, which implies that the signal, reference, and reconstruction beams are each uniform in amplitude and that the size of the hologram is sufficient to double Rayleigh resolve the bits.

In Fig. 6 we show the contrast ratio at the photodetector array plane as a function of the bit displacement, expressed as a percentage of the bit spacing.

First, we note that the contrast ratio for no displacement decreases as  $c$  decreases. Second, note that the contrast ratio varies more slowly as a function of the percentage shift as  $c$  decreases. This phenomenon can be explained by noting that if  $c$  is large, the photodetector area is relatively small, and the rapid change in contrast as the bit shifts is due mainly to a decrease in the received energy at a 1 position rather than a large increase in the received energy at a 0 position.

If the hologram size is increased so that the reconstructed bits are resolved by more than twice the Rayleigh limit the absolute contrast ratio increases for small displacements, but the contrast ratio decreases more rapidly as a function of displacement. For example, in Fig. 6, we also plot the contrast ratio for  $c = 3$  where the hologram size has been increased to provide four times Rayleigh resolution.

Since uniform illumination is not likely to occur in practice, we also performed the same calculation for two other kinds of illumination. In one instance we let the product of the signal, reference, and readout beam illumination have a  $\text{sinc}^2 x$  distribution with its first zeros at the edge of the hologram. In the second instance we let the same product be a Gaussian distribution with its  $1/e^3$  point at the edge of the hologram. In each case the hologram size was selected so that, if uniformly illuminated, it would provide double Rayleigh resolution.

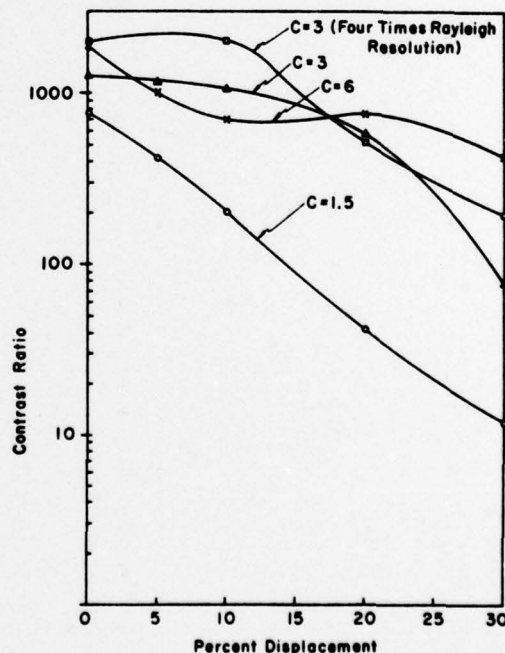


Fig. 7. Contrast ratio as a function of bit displacement for Gaussian illumination.



The contrast ratio for the  $\text{sinc}^2 x$  illumination was unacceptable, primarily because the reconstructed bits spread into adjacent "0" positions. Clearly, a larger hologram size would be required to make the contrast ratio acceptable, but at a reduction in packing density. The results for the Gaussian illumination were better than that for uniform illumination (see Fig. 7). The improvement in contrast ratio is due to the suppression of the sidelobe levels by the Gaussian weighting. A comparison of Figs. 7 and 6 shows that the contrast ratio for every value of  $c$  is better with the Gaussian illumination for all percentage displacements. In general, the contrast ratio increases as  $c$  decreases. Figure 8 shows the percentage of light collected as a function of  $c^{-1}$ . A compromise between the contrast ratio and the efficiency of the system must be made.

In the lens design, these tolerances must be met for bits reconstructed from all hologram locations. Primary aberrations such as spherical aberration, coma, astigmatism, and curvature of field are not significant except for their influence on distortion as a function of pupil (hologram) location because the relative aperture of any individual hologram is very small (typically equivalent to a  $f/150$  lens). The lens designer must, however, ensure that the percentage displacement for all bit positions, from any hologram location, is within tolerance.

The tolerance on the accuracy of the hologram position is related to considerations such as those given above. If the bundle of light rays from some elements in the PC is not centered on the desired hologram location, some of the rays will, of course, be vignetted, and the reconstructed bit will not be adequately resolved. If the elements of the PC are made smaller, the bundle of rays will increase in size so that the entire hologram is illuminated. Some light is thereby wasted, but the bundle must be larger than the hologram anyway to satisfy the illumination condition mentioned above to allow for some bit displacement. A tolerance of  $\pm 10\%$  on hologram location is generally adequate since there are guardbands between holograms, and the absolute displacement tolerance is still much larger than the absolute displacement tolerance for the bits. Nevertheless, in a memory system of this kind, pupil plane imagery cannot be neglected.

In addition to the bit displacement that may be caused by residual aberrations in the lens design, bit displacement may be caused by phase aberrations in the recording medium. Again, the most important aberration is a linear phase shift, because the aperture ratios of the individual holograms are too small for higher order terms to have much effect on the resolution of the bits.

If the slope  $g$  of the linear phase shift is  $g = \delta/\bar{d}$ , the displacement of all bits at the PDA plane is equal to  $gF$ . The percentage displacement is

$$\% \text{ displacement} = 100gF/(2\lambda F/\bar{d}) = 100g\bar{d}/2\lambda.$$

If the phase difference over the hologram aperture is

$\delta = \lambda/2$ , the bits are displaced by 25% relative to the bit spacing. We see therefore that small linear phase shifts can cause relatively large displacements. For most recording materials the linear phase variations are determined by the manufacturing process. Therefore, the maximum hologram length must be chosen to keep the displacement small.

The nature of the displacements caused by linear phase errors is different from those caused by residual lens aberrations. The displacements due to lens aberrations are usually functions of both field and aperture (i.e., both the bit position at the PDA and the hologram location). Little can be done, therefore, to compensate for these displacements except through proper lens design. The displacements due to a linear phase error over the hologram affect all the bit locations at the PDA equally. These displacements could be measured by using a separate photodetector element that receives light from an extra bit in the PC or from the directly transmitted component of the readout beam. The angle of the readout beam could be adjusted by a feedback system to compensate for such linear phase errors. Fairly large displacements could be corrected by this method.

#### E. Laser Power Requirements

We now consider the requirements on the laser power required for readin and readout. We consider first the required laser power for readout of the bits stored at each hologram location. If we want to retrieve data from the memory at an average rate of  $\nu_0$  bits/sec, we must read each hologram in a time interval of

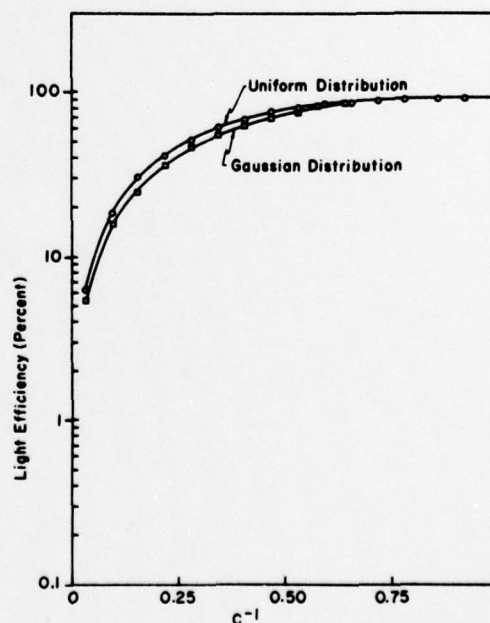


Fig. 8. Percentage light collected by a photodetector as a function of  $c^{-1}$ .

$$\tau_0 = N^2/\nu_0. \quad (25)$$

If we use a photodetector array in the charge storage mode, we must use some fraction  $\alpha$  of  $\tau_0$  for integration and the remaining time  $(1 - \alpha)\tau_0$  for sensing the electrical signal. The instantaneous readout rate may, therefore, exceed  $\nu_0$  bits/sec, but we can temporarily store the  $N^2$  bits in a buffer and transfer from the buffer at an average rate of  $\nu_0$  bits/sec.

The photodetector sensitivity is denoted as  $S$  J/bit; the laser power required for readout during the time  $\alpha\tau_0$  is

$$P_0 = SN^2/(\alpha\tau_0\eta_h\eta_0\eta_r), \quad (26)$$

where  $\eta_h$  is the diffraction efficiency of the hologram and  $\eta_0\eta_r$  is the efficiency of the optical system in the readout mode. By substituting Eq. (25) into Eq. (26), we find that

$$P_0 = S\nu_0/(\alpha\eta_h\eta_0\eta_r). \quad (27)$$

Note that the laser power required is not dependent on the number of bits stored at each hologram location. If  $N$  increases, the readout cycle time also increases so that the power required is constant. Equation (27) is valid, of course, only if the entire page of data is read out. If only a subset of the page is read and if  $\nu_0$  is the average data rate for the subset, the laser power required is increased by the ratio of the total page size to the subset size.

If  $\alpha$  is very small it may be advantageous to use a pulsed laser whose average power is  $P_0' = \alpha P_0$ . If  $\alpha$  is greater than 0.25–0.5, it may be better to use a continuous laser. As  $\alpha$  increases, however, the instantaneous readout rate increases, placing greater demands on the electrical photodetector array.

We have found that typical photodetector arrays have a sensitivity of  $S = 10^{-11}$  J/bit. If the average readout rate is  $10^6$  bits/sec and if  $\alpha = 1/2$ ,  $\eta_h = 0.01$ , and  $\eta_0\eta_r = 0.25$ , the average power requirement of a cw laser is  $P_0 = 8$  mW.

The contributing factors that determine  $\eta_0\eta_r$  are the efficiency of the beam forming optics and the beam deflector and the ratio of the photodetector area to the area of the reconstructed bits. We shall return to the latter point in Sec. II.F.

An analysis of the required laser power for readin is more complicated, because we must consider the efficiencies of more components. We begin by noting that the light intensity must be divided into two parts to provide both reference and signal beam illumination. Suppose that a fraction  $m$  of the power  $P_i$ , incident on a beam splitter, is directed into the signal beam and that a fraction  $(1 - m)P_i$  is directed into the reference beam. (We will include the losses of the beam splitter with those of other optical elements.) Through the use of beam forming optics, we can illuminate the PC in the signal beam and direct the light to an area  $\bar{d}^2$  at the plane of the hologram array. If the over-all efficiency of the signal beam optics, including the lenses and the PC, is  $\eta_s$ , the light intensity at the hologram plane due to the signal beam is  $m\eta_s P_i/\bar{d}^2$  W/cm<sup>2</sup>.

The ratio of the reference beam intensity to the signal beam intensity at the hologram array is  $Z$ . The total intensity at the hologram array is, therefore,

$$I_h = (1 + Z)m\eta_s P_i/\bar{d}^2. \quad (28)$$

When  $I_h$  is multiplied by the time interval allowed for recording, we have the exposure value for the readin. As before, we let

$$\tau_i = N^2/\nu_i, \quad (29)$$

where  $\tau_i$  is the readin cycle time and  $\nu_i$  is the average readin rate. If a fraction  $\beta$  of  $\tau_i$  is needed to load the PC, the remaining time  $(1 - \beta)\tau_i$  is available for recording the hologram.

If the sensitivity of the recording material is  $E_0$  J/cm<sup>2</sup>, we have

$$E_0 = (1 + Z)m\eta_s P_i(1 - \beta)\tau_i/\bar{d}^2 \quad (30)$$

or

$$P_i = E_0\bar{d}^2/[(1 + Z)m\eta_s(1 - \beta)\tau_i]. \quad (31)$$

By some simple algebra we can show that, to obtain a given value  $Z$  at the hologram array, the value of  $m$  is given by

$$m = \eta_r/(\eta_s Z + \eta_r), \quad (32)$$

where  $\eta_r$  is the efficiency of the reference beam optics. If we combine Eqs. (32), (31), and (29) and let  $\eta_0$  be the efficiency of the optical system from the laser to the beam splitter, we find that the laser power required during the exposure time is

$$P = \frac{E_0\nu_i(\eta_s Z + \eta_r)}{(1 + Z)\eta_r\eta_0(1 - \beta)\rho^2}. \quad (33)$$

We see that, as expected, the required power is directly proportional to  $E_0$  and  $\nu_i$  and inversely proportional to the packing density. The power is also influenced by the reference to signal beam ratio required to optimize the recording process. If  $Z$  is large and if  $\eta_s \approx \eta_r$ , we find that the laser power is nearly independent of the efficiency of the signal beam path. However, if  $\eta_s K \ll \eta_r$ , the power is highly affected by the efficiency of the signal beam and is relatively less sensitive to the efficiency of the readout beam.

Again, if  $\beta$  is small, a continuous wave laser is desirable, and if  $\beta$  is large, a pulsed laser may be more effective. The average power  $P_i$  of a pulsed laser is  $P_i' = (1 - \beta)P_i$ . Suppose that  $E_0 = 40(10^{-3})$  J/cm<sup>2</sup>,  $\beta = 1/2$ ,  $\eta_r = 0.75$ ,  $\eta_0 = 0.25$ ,  $\rho^2 = 10^6$  bits/cm<sup>2</sup>, and  $\nu_i = 10^6$  bits/sec, and that  $\eta_s K \gg \eta_r$ ; the average readin power of a cw laser is  $P_i = 425$  mW.

It is interesting to determine the conditions under which the input and output laser powers are equal, because the laser power is then used most effectively. If we equate Eqs. (27) and (33) we find that



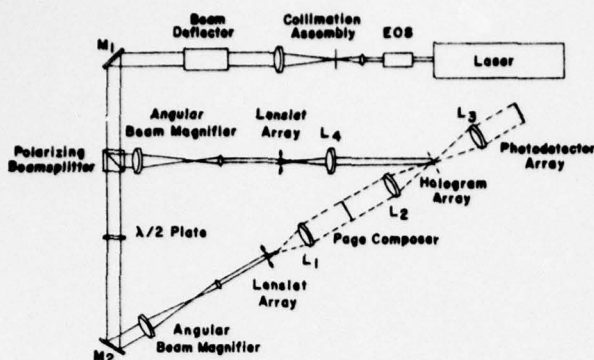


Fig. 9. Layout of a random-access read/write holographic memory.

$$\frac{S\nu_0}{\alpha\eta_h} = \frac{E_0\nu_i(\eta_s Z + \eta_r)}{(1 + Z\eta_h(1 - \beta)\rho^2)} \quad (34)$$

If  $Z$  is large and  $\eta_s Z \gg \eta_r$ , we have

$$S\nu_0/\alpha\eta_h = (E_0\nu_i)/[(1 - \beta)\rho^2]. \quad (35)$$

If, in addition,  $\alpha = \beta = 1/2$ , we find that

$$\rho^2 = (E_0\eta_h\nu_i)/S\nu_0. \quad (36)$$

We can use some values for  $E_0$ ,  $\eta_h$ , and  $S$  as in the previous calculations and show that, if the readin and readout powers are equal, the packing density must be  $\rho^2 = 40(10^6)\nu_i/\nu_0$  bits/cm<sup>2</sup>. Clearly, this packing density is much too high for the given parameters unless  $\nu_0 \approx 40\nu_i$ . In many memory applications  $\nu_0 = \nu_i$  so that equal readin and readout powers can be achieved only if  $E_0$  is reduced considerably. Equation (36) also reveals that to increase  $\eta_h$  or decrease  $S$  does not provide the expected gain (except for lower readout powers) in the total system performance unless  $\nu_0 \gg \nu_i$ .

#### F. Example of a Memory Design

We can now apply some of the principles developed previously to make a preliminary design of a random-access block-oriented holographic memory having no moving parts. Figure 9 shows one of several possible layouts for a random-access read/write memory. Light from the laser passes through an electrooptic switch that controls the plane of polarization. A collimating assembly is used to fill the aperture of an x-y beam deflector, and a polarizing beam splitter causes part of the light to be reflected into the reference beam and part to be transmitted into the signal beam. The reflected light is vertically polarized, whereas the transmitted light is horizontally polarized; a half-wave plate is therefore used in the signal beam so that both vertically polarized beams can interfere at the hologram array plane. The angular beam magnifiers are used to address lenslet arrays that are congruent to the holo-

gram array. Lens  $L_4$  collimates the light produced by one element of the reference beam lenslet array to illuminate a particular hologram location. Lens  $L_1$  collimates the light from one element of the signal beam lenslet array to illuminate the PC. Lens  $L_2$  then forms the Fourier transform of the bit pattern at the same hologram location. Lens  $L_3$  displays the reconstructed bit pattern upon readout at the PDA plane.

Suppose we want to design a  $10^8$  bit capacity memory with a random access time of  $10 \mu\text{sec}$  to any block of data. We begin by calculating the required lens focal length from Eq. (13) under the assumption that  $M = -\infty$ ,  $\hat{c} = 1.2$ , and  $\lambda = 500 \text{ nm}$ . For a given recording material we may find that a packing density of  $2(10^6)$  bits/cm<sup>2</sup> will give adequate SNR. The aperture ratio  $R$  is then computed from Eq. (15) to be  $R = 0.4$ . From Eq. (13) we find  $F = 600 \text{ mm}$ . If we use a  $128 \times 128$  element block data composer, we find from Eq. (10) that  $cd = 0.663 \text{ mm}$ , and that the length of the block data composer is  $120 \text{ mm}$ . From Eq. (12) we find that  $\bar{d} = 0.90 \text{ mm}$ , which is a convenient hologram size. As a check on the calculations we find that  $\rho^2 = (N/\bar{d})^2 = (128/0.90)^2 = 2(10^4)$  bits/mm<sup>2</sup> or  $\rho^2 = 2(10^8)$  bits/cm<sup>2</sup>.

As mentioned before, it may be preferable to divide the aperture ratio of the lens into unequal parts to make the lens design problem simpler. We can, after deciding how to partition the aperture ratio, use Eq. (8) to proceed with the calculations. Suppose that we want the aperture ratio of the page composer to be  $R_p = 0.20$  and the aperture ratio of the hologram to be  $R_H = 0.15$ . We can use Eqs. (8) and (13) to solve for  $F$  under the new conditions and find that  $F = 784 \text{ mm}$ . From Eq. (7) we find  $cd = 0.866 \text{ mm}$ , and from Eq. (12) we see that  $\bar{d}$  is again equal to  $0.90 \text{ mm}$ . Thus, the packing density is the same as before; the penalty paid for having  $R_p \neq R_H$  is that a longer focal length lens must be used.

### III. Read-Only Archival Memories

Many of the considerations given in the preceding sections also apply to read-only memories. The most significant difference is that fast random access is generally not required to all parts of the memory so that the memory material can be moved. Some of the key restrictions that apply to the random access can now be removed.

Also, since the film can be moved, we have more flexibility in choosing the hologram format. In particular, although a two-dimensional format can be used, a one-dimensional format may offer certain attractions such as the use of linear photodetector arrays. If a one-dimensional format is selected, we can generate the holograms either interferometrically (using a one-dimensional page composer) or synthetically (using an electronic hologram generator unit). The interferometric method may be preferred when the input data rate is high, whereas the synthetic method may be preferred when the data rate is low.



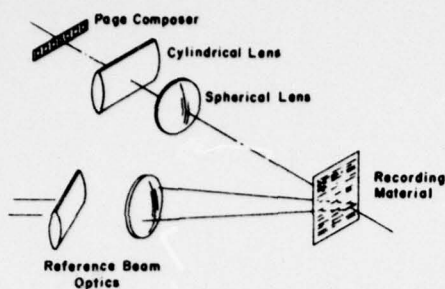


Fig. 10. Basic elements of a one-dimensional read-only memory.

#### A. One-Dimensional Interferometric Approach

The equations that govern the one-dimensional interferometric approach are similar to those developed earlier. There are some differences that are worth noting. Figure 10 shows the key elements in such a system. The cylindrical-spherical lens combination collects the light diffracted by the PC and creates a Fourier transform of length  $\bar{d}$  in the  $x$  direction and an image of length  $\delta_y$  in the  $y$  direction. To double-Rayleigh resolve the bits, the hologram length must be

$$\bar{d} = 2\lambda F_x / cd, \quad (37)$$

where  $F_x$  is the focal length of the lens system in the  $x$  direction. The packing density in the  $x$  direction is

$$\rho_x = N/\bar{d} = Ncd/2\lambda F_x.$$

The aperture  $A_x$  of the lens must be  $A_x = Ncd + \bar{d}$ , but since  $\bar{d}$  is usually very much less than  $Ncd$ , we have

$$\rho_x = R_x/2\lambda. \quad (38)$$

Again, the packing density is dependent only on the aperture ratio of the lens and the wavelength; it is not an explicit function of any of the page composer parameters. Note, too, that the packing density is a factor of  $2\sqrt{2}$  higher than in the two-dimensional approach; the factor of 2 is due to the fact that the lens need only produce an on-axis hologram, and the  $\sqrt{2}$  factor is due to the fact that the lens need only cover the length of the page composer, not the diagonal of a two-dimensional page composer.

The two-dimensional packing density is

$$\rho = \rho_x/\delta_y, \quad (39)$$

and the film velocity in the  $y$  direction is

$$V = v_i \delta_y \bar{c}_y / N$$

or

$$V = v_i \bar{c}_y / \rho \bar{d}, \quad (40)$$

where  $v_i$  is the average input data rate and  $\bar{c}_y$  is the hologram spacing ratio in the  $y$  direction. We see that we should maximize  $\rho$  to minimize the film velocity; the maximum value of  $\bar{d}$  may be constrained by the phase aberrations in the recording material.

The requirement on laser power for readin and readout is identical to those developed earlier except that  $\rho^2$  is replaced by  $\rho = \rho_x/\delta_y$  in the equation for the readout power.

#### B. One-Dimensional Synthetic Approach

One of the major components in a holographic memory that uses an electronic system to generate the hologram is the laser scanner. The sampled values of the Fourier transform of the input data are used to control a laser beam modulator; the modulated beam is scanned onto the recording material by a spinning mirror. In a typical system the number of scanned spots per hologram is  $4N$ , where  $N$  is the number of data bits recorded in a hologram.

The prime consideration in designing the laser scanner is the depth of focus of the system. The depth of focus is

$$\Delta Z = \pm(\lambda/2R^2), \quad (41)$$

where  $R$  is the ratio of the beam diameter to the focal length of the lens used in the scanner. The depth of focus is an important parameter, because it is difficult to make mechanisms that can hold film flat to within a few micrometers over a large area.

The second important parameter is the size of the scanned spots in the data direction. To double Rayleigh resolve the bits, the spacing between spots must be

$$\delta_x = 2\lambda/R. \quad (42)$$

If  $N$  bits are stored in each hologram, the length of the hologram is

$$\bar{d} = 4N\delta_x. \quad (43)$$

The packing density in the  $x$  direction is

$$\rho_x = N/\bar{d} = 1/4\delta_x = R/8\lambda. \quad (44)$$

We see that, for a given value of  $R$ , the packing density is a factor of 4 less than for the one-dimensional interferometric approach. The area packing density is

$$\rho = \rho_x/\delta_y = R/8\lambda\delta_y. \quad (45)$$

The equations for film velocity and for laser readout power are the same as those developed before. The readin power for this approach is

$$\rho = v_i E_0 / \eta_0 \rho, \quad (46)$$

where  $\eta_0$  is the over-all optical efficiency of the recording system.

### C. Example of a Memory Design

We now give an example of a one-dimensional synthetic hologram memory system. We again want to have a large value of  $R$  to give a large packing density in the  $x$  direction; but if  $R$  is too large, the depth of focus becomes too small. If  $R = 0.3$ , the packing density in the  $x$  direction is  $\rho_x = 75$  bits/mm, and the depth of focus is  $\Delta z = \pm 2.78 \mu$ . The spacing between spots is  $\delta_x = 3.34 \mu$ , and the length of the hologram, for  $N = 128$ , is  $d = 1.7$  mm.

If the width of each hologram is  $\delta_y = 10 \mu$ , the area packing density is  $0.75 (10^6)$  bits/cm<sup>2</sup>. The film velocity is calculated from Eq. (40) as  $V = 78$  n.m/sec for an input data rate of  $\nu_i = 10^6$  bits/sec. The average laser power required for readin at the same data rate is  $\rho = 1.7$  mW if the over-all optical efficiency is  $\eta_0 = 0.03$ .

### IV. Conclusions

Several authors have considered certain aspects of holographic memories and concentrated their attention on the packing density that can be achieved. First, without reference to the optical constraints, it is tempting to base a calculation of packing density on the information storage of recording materials such as photographic films (often without due consideration of what SNR is needed to obtain acceptable bit error rates). Such calculations are misleading because, as Eqs. (15) and (20) show, the packing

density is limited by the geometric constraints of the optics. If superposition of holograms is used to overcome the geometric constraints, we must carefully consider the effects of the resulting reduction in SNR and diffraction efficiency. Second, even if the optical constraints are considered, the maximum packing density that can be achieved may not be useful in practice because imaging the reconstructed bit patterns onto the PDA may then be very difficult, particularly in a block-oriented, random-access memory. In this paper we show that the system capacity, not the packing density, is of prime importance; the packing density is, however, an important tradeoff parameter (e.g., laser power requirements and SNR).

I thank many colleagues who have made contributions to the development to the ideas presented in this article. Special thanks to A. Kozma, D. E. Klingler, W. H. Lee, and H. N. Roberts. This work was funded under a contract with NASA-MSFC, contract NAS 8-26360, monitored by E. J. Reinbolt.

### References

1. C. B. Burckhardt, *Appl. Opt.* **9**, 695 (1970).
2. Y. Takeda, *Japan. J. Appl. Phys.* **11**, 656 (1972).
3. A. Vander Lugt, *Proc. IEEE* **54**, 1055 (1966).
4. A. L. Mikaelian, V. I. Babrinev, S. M. Naumov, and L. Z. Sokolova, *IEEE J. Quantum Electron* **QE-6**, 193 (1970).
5. P. Graf and M. Lang, *Appl. Opt.* **11**, 1382 (1972).
6. W. H. Lee, *J. Opt. Soc. Am.* **62**, 797 (1972).

# Packing Density in Holographic Systems

A. Vander Lugt

The holographic packing density is derived for any plane in a coherently illuminated optical system. The gain in packing density relative to the object plane is given. A two-lens optical system in which a condenser lens provides high packing densities and an imaging lens provides sufficient resolution is superior to a system in which a single lens performs both functions.

## I. Introduction

In applications such as the holographic storage and retrieval of documents, graphics, or photographs, we often want to record at that plane in the optical system where the packing density is highest. A high packing density implies a high equivalent reduction ratio, which, in combination with the other advantages of holographic storage and retrieval systems, is desirable when large data bases must be rapidly accessed. Sometimes a recording plane may be selected where the packing density is lower to achieve a higher SNR or to reduce the dynamic range of the recorded signal. We want to derive, therefore, formulas that give the packing density at any plane in the system.

Since the total information at any plane in an optical system is constant, under the constraint that there is no vignetting, the problem can be stated as finding the aperture size through which all the information passes. The packing density is then given by the ratio of the information content to the area or the length of the aperture.

An equally important consideration is to determine the maximum information capacity of a coherently illuminated optical system. We shall show, however, that systems having equally high packing densities may have quite different information capacities. Furthermore, for any system in which the object is illuminated with a plane wave and for which the information capacity is optimized, the packing density is equal at two planes in the system—the object plane and the Fourier transform plane. An increase in packing density can be achieved for a given imaging lens if the object is illuminated with a convergent wave. Formulas applicable in this case are also developed.

The author is with the Electro-Optics Operation, Harris Corporation, P.O. Box 37, Melbourne, Florida 32901.  
 Received 8 January 1975.

## II. Maximum Information Capacity

The basic analysis is carried out with respect to the optical system shown in Fig. 1. An object of height  $2\eta$  is placed a distance  $l$  from a lens having focal length  $F$ . The illumination is provided by a point source located a distance  $l$  from the lens. The image of the object is located a distance  $l'$  to the right of the lens, and the frequency plane, which is the image plane of the primary source, is located a distance  $l'$  to the right of the lens. The principal pupil ray (PPR) is denoted by  $\bar{u}$ , and the principal marginal ray (PMR) is denoted by  $u$ . The formulas that relate  $\bar{u}$  to  $\bar{u}'$  and  $u$  to  $u'$  are given by

$$\begin{aligned}\bar{u}' - \bar{u} &= \bar{h}/F \\ u' - u &= h/F\end{aligned}\quad (1)$$

where  $\bar{h}$  and  $h$  denote the intersection heights at the lens of the PPR and the PMR. As shown in the diagram,  $l$ ,  $\bar{l}$ ,  $u$ ,  $\bar{u}$ , and  $s$  are negative; all other quantities are positive.

The space bandwidth product  $\phi$  of the signal is given by the product of the length of the signal ( $2\eta$ ) and the maximum frequency content  $f$ :

$$\phi = 2\eta f. \quad (2)$$

The space bandwidth product is closely related to the information content of the signal; it denotes the number of discrete resolvable elements contained in the object. If the elements take on binary values,  $\phi$  is also equal to the information content. More generally, each element may be in one of  $N$  states (polarization, wavelength, gray scale, and so forth). The information content  $H$  is then  $H = \phi \log_2 N$ . But if we maximize either the packing density or the capacity of the system relative to the space-bandwidth product, we also maximize these quantities with respect to the information content.

We begin by maximizing the information capacity of the system when  $\bar{u} = 0$  (plane wave illumination).



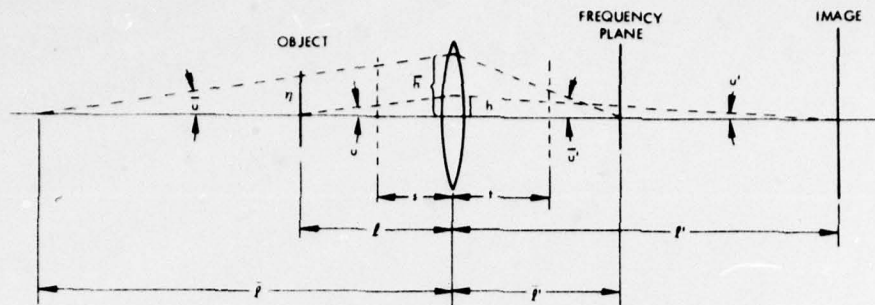


Fig. 1. Single-lens optical system.

We shall also let  $l = -F$  so that the object is placed at the front focal plane of the lens. The lens then creates an image of the object at  $l' = \infty$ , and the magnification is  $M = -\infty$ . A second lens is therefore needed to bring the image to focus at a finite conjugate distance, but the same general results also apply to the second lens. A similar analysis was used to develop relationships for the capacity of holographic memories<sup>1</sup>; as shown there,  $M = -\infty$  causes the capacity to be absolutely maximized and does not affect the generality of the results.

The aperture ratio  $R$  of the lens is defined to be the ratio of its clear aperture to its focal length. From Fig. 1 we see that the aperture ratio of the lens is

$$R = 2\{|h| + |\bar{h}|\}/F, \quad (3)$$

where  $h$  and  $\bar{h}$  are the intersections of the PMR and the PPR at the lens. But  $\bar{h} = \eta$  because  $\bar{u} = 0$ ,  $h = -ul = \lambda f/F$  because  $u = \lambda f$ , and  $l = -F$ . Thus,

$$R = 2\{|\lambda f/F| + |\eta|\}/F.$$

Since both  $\bar{h}$  and  $h$  are positive (at the lens plane), we have

$$R = (2\lambda f/F + 2\eta)/F \quad (4)$$

$$= R_t + R_o, \quad (5)$$

where  $R_t$  is the aperture ratio of the Fourier plane, and  $R_o$  is the aperture ratio of the object plane. If we multiply Eq. (4) by  $\eta$  and solve for the space-bandwidth product ( $\phi = 2\eta f$ ), we have

$$\phi = \frac{-1}{2\lambda} (4\eta^2/F - 2R\eta). \quad (6)$$

Since we want to find the aperture ratio  $R$  that will maximize the capacity of the system, we differentiate  $\phi$  with respect to  $\eta$  (or, through the substitution of related formulas, to  $f$ ):

$$\frac{\partial \phi}{\partial \eta} = \frac{-1}{2\lambda} (8\eta/F - 2R) = 0,$$

which implies that

$$R = 4\eta/F \quad (7)$$

will maximize the capacity. Note that  $R = 2R_o$ , which further implies that since  $R = R_o + R_t$ , we also have

$$R_o = R_t. \quad (8)$$

Thus, we see that one-half of the aperture ratio of the lens is needed to collect the diffracted light, and the other half is needed to collect the undiffracted light. Also, the size of the object and Fourier planes is the same.

The maximum space-bandwidth product is obtained by substituting Eq (7) into Eq. (6):

$$\phi_{\max} = \frac{R_o \eta}{\lambda}. \quad (9)$$

This result shows that the maximum space-bandwidth product is proportional to the product of the aperture ratio of the object and one-half of the number of wavelengths contained in the object. Also, Eqs. (7) and (4) imply that the highest frequency that can be transmitted through the system is given by  $f = R_o/2\lambda$ .

### III. Maximum Packing Density

We now find the formulas for the packing density at any plane in the optical system in Fig. 1. The packing density is defined as

$$\rho = \phi/D,$$

where  $D$  is the minimum aperture through which all rays from the object pass. We consider planes to the left of the lens separately from those to the right of the lens and again let  $\bar{u} = 0$ ; later we shall consider the case when  $\bar{u} \neq 0$ .

#### A. Maximum Packing Density in Object Space for $\bar{u} = 0$

If  $\bar{u} = 0$ , it is simple to find the diameter of an aperture through which all rays pass. Let  $s$  denote the distance of an arbitrary plane from the lens. Then we have

$$D = 2u(l - s) + 2\eta. \quad (10)$$

Note that  $2\eta$  is the object length, which is the minimum size of the aperture independently of the value

of  $s$  (because  $\bar{u} = 0$ ) for any spatial frequency content. The first term of Eq. (10) gives the additional aperture needed to resolve the frequencies over the entire field of the signal. Thus, the minimum aperture on the object side of the lens is  $D = 2\eta$  which occurs when  $s = l$ . The packing density is, therefore, highest at the object plane itself and is equal to

$$\rho = \frac{\phi}{D} = \frac{2\eta f}{2\eta} = f \text{ bits/mm.} \quad (11)$$

The packing density in this plane is independent of the length of the signal.

#### B. Maximum Packing Density in Image Space for $\bar{u} = 0$

We let  $t$  denote the distance to an arbitrary plane in the image space. We also make use of the transfer formulas for the ray heights above the axis:

$$\left. \begin{aligned} h_t &= h - tu' \\ \bar{h}_t &= \bar{h} - t\bar{u}' \end{aligned} \right\} \quad (12)$$

The aperture size  $D$  is given by

$$D = 2\{|h_t| + |\bar{h}_t|\}, \quad (13)$$

but, for  $0 \leq t \leq l'$ , both  $h_t$  and  $\bar{h}_t$  are positive so we can use Eqs. (12) and (13) to get

$$D = 2\{h - tu' + \bar{h} - t\bar{u}'\}; 0 \leq t \leq l'. \quad (14)$$

From Eqs. (1) and (12) we see that

$$\left. \begin{aligned} u &= -\lambda f, \\ h &= ul = -\lambda fl, \\ \bar{u} &= 0, \\ \bar{h} &= \eta - u\bar{l} = \eta, \\ u' &= h/F + u = ul/F + u = u(1 + l/F), \\ \bar{u}' &= \bar{h}/F + u = \eta/F, \end{aligned} \right\} \quad (15)$$

so that

$$D = \{-2\lambda fl + 2\lambda fl(1 + l/F) + 2\eta(1 - l/F)\} \quad (16)$$

or

$$D = \left\{ -2\lambda fl + 2\lambda fl(1 + l/F) + \frac{\phi}{f}(1 - l/F) \right\}. \quad (17)$$

By solving for  $\phi$  and forming  $\rho = \phi/D$ , we have

$$\rho = \phi/D = \frac{f}{(1 - l/F)} \left[ 1 + \frac{2\lambda fl}{D} - \frac{2l\lambda f(1 + l/F)}{D} \right] \quad (18)$$

To find the maximum value of  $\rho$ , we differentiate  $\rho$  with respect to  $t$ :

$$\begin{aligned} \frac{\partial \rho}{\partial l} &= f(1 - l/F) \left[ \frac{-2\lambda f(1 + l/F)}{D} \right] (1 - l/F)^{-2} \\ &\quad - (-f/F) \left[ 1 + \frac{2\lambda fl}{D} - \frac{2l\lambda f(1 + l/F)}{D} \right] (1 - l/F)^{-2} = 0, \end{aligned}$$

which gives

$$D = 2\lambda fF \quad (19)$$

as the minimum aperture in the image space. We now substitute Eq. (19) into Eq. (16) and find that

$$l = F. \quad (20)$$

Equation (20) shows that the minimum aperture size of  $D = 2\lambda fF$  is obtained at  $t = F$ , where  $F$  is the focal length of the lens, for all values of  $l$ . Thus, we see that for  $0 \leq t \leq l'$ , the back focal plane of the lens is the plane where the highest packing density is obtained. The packing density in this plane is

$$\rho = \phi/D = \frac{2\eta f}{2\lambda fF} = \frac{\eta}{\lambda F} \text{ bits/mm,} \quad (21)$$

which is independent of the frequency content of the signal. Note that  $2\eta/F$  is equal to the aperture ratio  $R_0$  of the object size to the focal length of the lens so that

$$\rho = (R_0/2\lambda). \quad (22)$$

It remains to be shown that no plane exists for  $l' < t < l$  at which the packing density is higher than that given by Eq. (21). In this case,  $h_t$  is negative, but, because  $D = 2\{|h_t| + |\bar{h}_t|\}$ , the same conclusion is reached, i.e., that  $t = F$  is the distance for the plane at which the maximum packing density is obtained.

It is worth noting the gain in packing density that can be achieved by operating on the image instead of the object side of the lens. The ratio of Eq. (21) to Eq. (11) is the gain  $G$ :

$$G = R_0/(2\lambda f). \quad (23)$$

Independently of the value of the object distance  $l$ , we can always choose a lens for which the object aperture ratio  $R_0$  is a constant (say, of the order of  $1/4$ ). Then  $G = 1/8\lambda f$ , which, for small values of  $f$ , is considerable. For example, if  $f = 5$  l/mm, the gain is  $G = 50$  for  $\lambda = 500$  nm. As  $f$  increases, the gain becomes smaller until, at  $f = 250$  l/mm, the gain is unity.<sup>2</sup> For higher spatial frequencies, the gain is less than one, and the object plane then becomes the one having the highest packing density.

But if the object has high spatial frequency content and a large size (i.e., a large value for  $\phi$ ), the question of system capacity becomes important. In the preceding section we showed that when the system is maximized for space-bandwidth product the size of the object and Fourier planes is equal, which is another way of stating that the gain is unity. Aside from the shift-invariant and distributive properties of holograms, there is little advantage in recording at the Fourier plane, when  $f$  is large, if we are interested in large reduction ratios.

#### IV. Divergent and Convergent Illumination Considerations

We see that the maximum space-bandwidth product, the maximum frequency, and the maximum packing density are proportional to  $R_0$ , the aperture ratio of the object. Furthermore, Eq. (5) reveals that the aperture ratio of the lens is equal to the sum of  $R_0$  and  $R_t$ . Thus, even if  $R_t$  is small, the aperture ratio of the lens must be at least equal to  $R_0$ , and to maximize  $\rho$ ,  $\phi$ , and  $f$  we must maximize  $R_0$ . Lenses with large relative apertures are, therefore, required even if the resolution requirement for imaging is low.



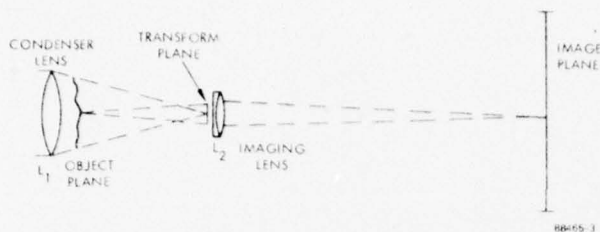


Fig. 2. Two-lens optical system.

We now show that, by using a two-lens system so that  $u \neq 0$ , we can develop more attractive systems.

If  $u$  is negative (i.e., the illumination is a diverging wave), the Fourier plane occurs between the back focal plane of the lens and the image. Both the lens aperture and the size of the Fourier plane must be increased if all rays are to be transmitted to form an accurate image. Thus, the packing density at the Fourier plane is even less for divergent illumination than for plane illumination.

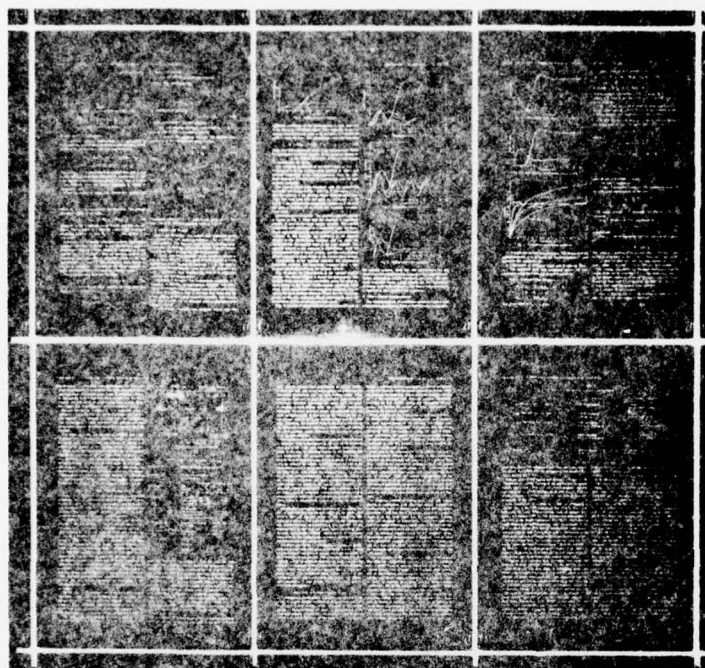


Fig. 3. Image transmitted through the two-lens system with  $R_1 = 0.5$  and  $R_2 = 0.045$ .

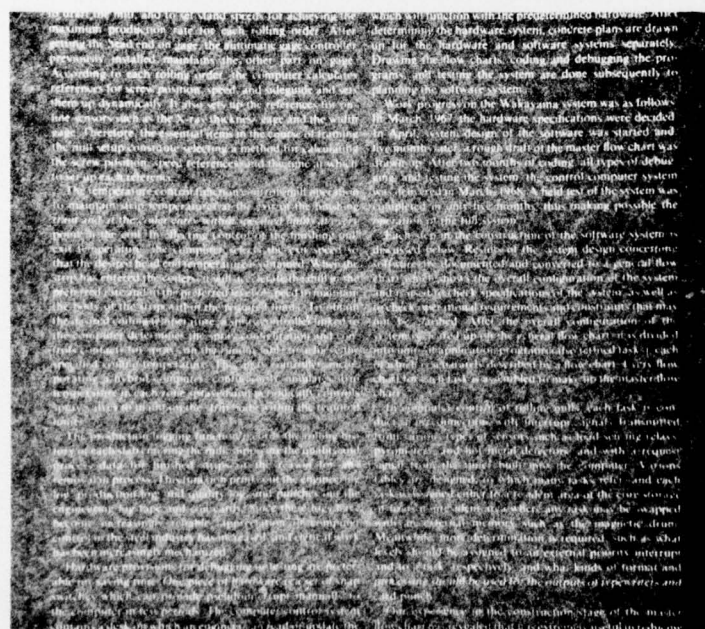


Fig. 4. Magnified portion of transmitted image.



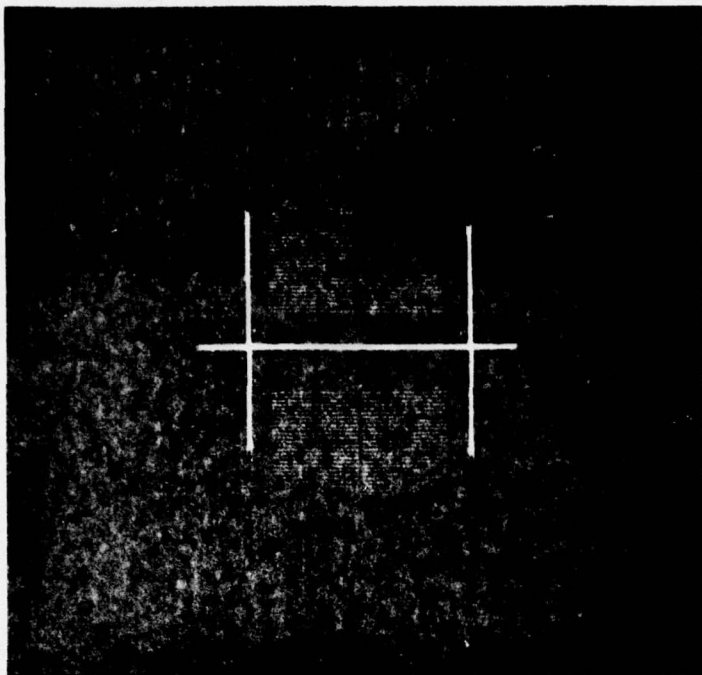


Fig. 5. Transmitted image with  $R_1 = 0.25$  and  $R_2 = 0.045$  showing partial vignetting.

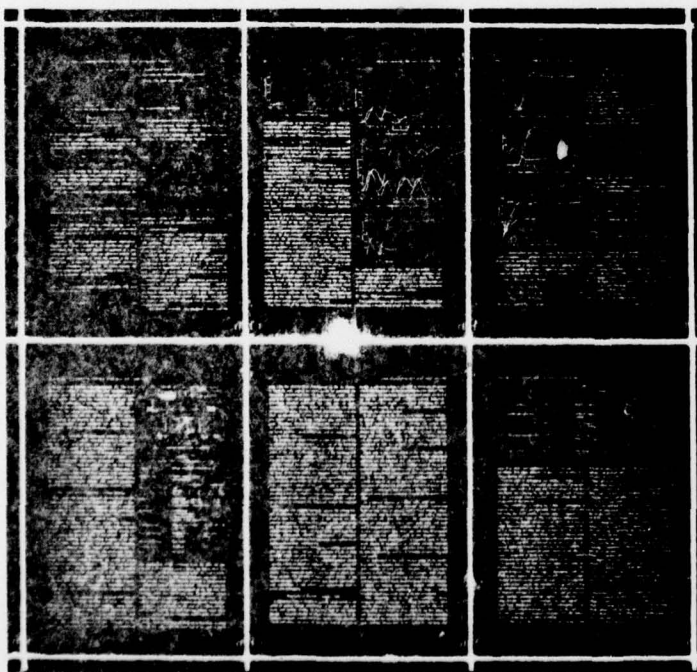


Fig. 6. Transmitted image with  $R_1 = 0.25$  and  $R_2 = 0.125$ , restoring the vignettted rays.

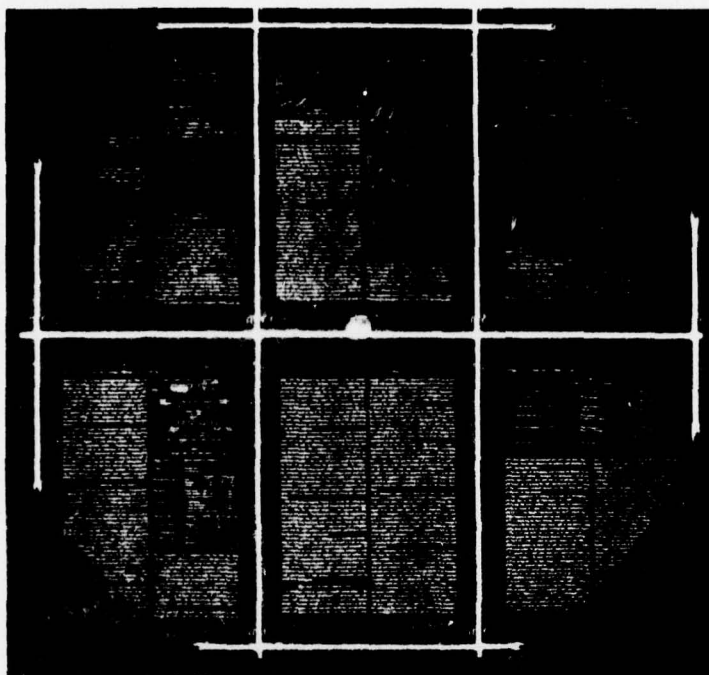


Fig. 7. Transmitted image with  $R_1 = 0$  and  $R_2 = 0.25$  showing unavoidable vignetting.

If  $\bar{u}$  is positive (a convergent illuminating wavefront), the Fourier plane occurs between the back focal plane of the lens and the object. Both the lens aperture and the Fourier plane can now be reduced without vignetting rays. As  $\bar{u}$  increases, the Fourier plane moves closer to the lens until, when  $u = 2\eta/F$  the Fourier plane coincides with the plane of the lens. Under this condition  $\bar{u} = R_0$  so that the packing density is also given by Eq. (22). We now see, however, that the lens aperture required is, from Eq. (5), given by  $R = R_t = 2\lambda f/F$  because  $\bar{h} = 0$  when  $\bar{u} = 2\eta/F$ .

This result reveals that, when  $\bar{u} = R_0$ , the packing density is equal to or greater than that at any plane on the image side of the lens, and the aperture ratio of the lens is minimized. A condenser lens is needed, of course, to produce the convergent illuminating wavefront. It is important to note that the aperture ratio of the condenser lens is independent of the frequency content of the signal and that the aperture ratio of the imaging lens is now independent of the length of the object. Furthermore, the condenser lens does not work over a finite field so that a lens corrected only for spherical aberrations can be used. By dividing the total power between the two lenses, we have arrived at a system concept that provides increased flexibility and performance (see Fig. 2).

Since the performance of the single lens system is no longer compromised by being required to perform two operations (provide high packing density as well as good imagery), we can increase the information capacity of a single lens system having a given aperture ratio. For example, previously we found that, if  $\bar{u} = 0$ , the aperture ratio of the lens is equally divided be-

tween, but equal to the sum of, the aperture ratios of the object and transform planes. For an  $f/2$  lens, we have  $R_0 = R_t = 0.25$ , which sets an upper bound on the packing density and the frequency content in the single lens system. If both lenses in the two-lens system have an aperture ratio of  $R = 0.5$ , both the packing density and the frequency content can be doubled.

A second benefit of the two-lens system becomes apparent when the frequency content is low. The condenser lens will have an aperture ratio determined by the packing density required. This ratio can now be of the order of 0.50. The imaging lens can have an aperture ratio selected to be just large enough to resolve the detail in the object. For document storage and retrieval, the imaging lens may have an aperture ratio of only  $R = 0.004$  ( $f/250$ ) which is adequate to resolve 4-l/mm detail. If we had used a one-lens system, its aperture ratio would have to be  $R = 0.504$  to achieve both the desired resolution and packing density.

Finally, the gain of the two-lens system as given by Eq. (23) is doubled because  $R_0$  can be doubled. Thus, for  $f = 5$  l/m,  $G = 100$  instead of 50, and the gain becomes unity at  $f = 500$  l/mm instead of 250 l/mm.

## V. Experimental Results

We performed some experiments that illustrate the advantages of the two-lens system approach as sketched in Fig. 2. The imaging lens is a 225-mm F. L. lens having a maximum aperture ratio of  $R_2 = 0.25$  ( $f/4$ ) and a minimum aperture ratio of  $R_2 = 0.045$

( $f/22$ ). The objective was a 34.5-mm  $\times$  33-mm transparency containing six microimages of printed text. The condenser lens was arranged to provide ratios of  $R_1 = 0.5$  ( $f/2$ ),  $R_1 = 0.25$  ( $f/4$ ), and  $R_1 = 0$  ( $f/\infty$ ). When  $R_1 = 0.5$ , the transform plane occurs on the object side of lens  $L_2$  (as shown in Fig. 2). When  $R_1 = 0$ , the transform plane occurs on the image side of lens  $L_2$  at its back focal plane (as shown in Fig. 1). When  $R_1 = 0.25$ , the transform plane is approximately halfway between the transform planes previously identified.

Figure 3 is a photograph of the image plane when  $R_1 = 0.5$  and  $R_2 = 0.45$ . The entire object field is transmitted by the system without vignetting and with good resolution as shown in Fig. 4, which is a magnified photograph of one of the pages. If  $R_1$  is reduced to 0.25, the object is vignetted as shown in Fig. 5. By increasing  $R_2$  to 0.125, the entire object field can be transmitted as shown in Fig. 6. Finally, if  $R_1 = 0$ , the object is more severely vignetted, and even if  $R_2$  is increased to its maximum value of 0.25 some vignetting is unavoidable as shown in Fig. 7. In the latter two cases the packing density is decreased because  $R_1$  is decreased, and the aberrations for lens  $L_1$  must be more fully corrected.

## VI Summary and Conclusion

The results of this analysis show that, to achieve a high effective reduction ratio in a holographic storage and retrieval system, a two-lens system is superior to a one-lens system. Packing densities and capacities can each be increased by a factor of 2, and the lens designs are considerably simplified because the requirements to achieve high packing densities and good resolution are separated. The analysis also shows that as the spatial frequency content increases, the effective reduction ratio decreases so that holographic storage and retrieval have most promise for the storage of documents, charts, and maps; it is relatively less attractive for storing photographs having fine detail (high spatial frequencies).

I thank M. O. Greer for obtaining the experimental results given in this paper.

## References

1. A. Vander Lugt, *Appl. Opt.* **12**, 1677 (1973).
2. E. G. Ramberg [*RCA Rev.* **33**, 5 (1972)] states that holography does not provide an increase over direct recording in terms of packing density. His analysis did not consider the more general case treated here wherein we show that, by using lenses, increased packing density can indeed be achieved while retaining all the benefits of holography.